Department of Chemistry

Biomarkers and their stable isotopic compositions in sulfide-rich ancient deposits related to mass extinction events

Ines Mercedes Melendez Mogollon

This thesis is presented for the Degree of
Doctor of Philosophy
of
Curtin University

March 2014

To my loved Family,

Here and there always in my heart

Declaration

To the best of my knowledge and belief this thesis contains no material previously published by any other person except where due acknowledgment has been made.

This thesis contains no material that has been accepted for the award of any other degree or diploma in any university.

Ines Melendez

Perth, March 25th 2014

Abstract

Most of the organic-matter (OM)-rich sediments are globally associated with periods in Earth's history where marine anoxia and high productivity played a critical role; limited oxygen supplies to the bottom of the water column limits microbial degradation and thus allows for the preservation and accumulation of OM; however, this condition limits the biodiversity that dwell under such environmental conditions. In anoxic water bodies, high sulfide concentrations are a product of bacterial sulfate reduction (BSR) occurring in the sediments and/or at the sediment water interface. Sulfate reducers utilize sinking organic biomass as a source of energy while producing toxic hydrogen sulfide (H_2S). Euxinic conditions are established when free H_2S reaches the chemocline (e.g. modern day inland Black Sea and Antarctic fjords). Under these conditions in the zone of light penetration (i.e. Photic Zone Euxinia- PZE) only purple sulfur bacteria (PSB) and the exclusive anaerobic green-brown sulfur bacteria (BSB) and green-green sulfur bacteria (GSB) can thrive. Therefore, the presence of toxic H_2S in the photic zone have been suggested as one of the main drivers and/or the kill mechanism for some of the major extinction events of the Phanerozoic; nevertheless, questions still remain to explain and reconstruct the way some ecosystems thrived and evolved under such toxic conditions (e.g. aftermath of the end-Permian mass extinction event).

The continued search for biomarkers and isotopic trends related to restricted but extremely specialized biota that dwelled under anoxia and/or PZE will help to establish the paleoenvironment related to the deposition of the most prolific source rocks but also the most dramatic global environmental crises. In this PhD the major focus has been orientated to elucidate and reconstruct the biogeochemical changes that occur in two particular oxygen-limited environments associated to extended periods of geological time during ecological crises. The events studied in this thesis include the end-Devonian and end-Permian events: (i) a case of unique fossil and biomolecular preservation that occur in the anoxic chemical-microenvironment associated with concretion growth during the Givetian in Western Australia, prior to the Frasnian/Famennian extinction event; (ii) a well exposed marine section spanning the entire Early-Triassic, recording environmental perturbation(s) after the major

extinction event near to the End-Permian event. In both anoxic settings, markers of Chlorobi have been identified indicating PZE conditions in these ancient seas.

The Gogo Formation is mainly composed of dark fine-grained shales, deposited under limited-oxygen conditions in the inter basin of the Devonian reef in the Canning Basin, north of Western Australia. Calcareous concretions randomly occur in the Gogo Formation in which exceptionally well-preserved fossils, including original bone and mineralized soft tissue as well as unique low-maturity biomarker and lipids, can be found. Although exceptional fossil preservation has been studied in great detail in various depositional settings using conventional approaches, organic-geochemical approaches are rarely employed. In **Chapter 2** the biogeochemical cycles leading to the exceptional preservation were investigated by reconstructing the molecular and isotopic composition of sedimentary OM within a 380 Ma old carbonate concretion. The inner part of the concretion contained phosphatized soft-tissue from an unidentified invertebrate fossil. Low thermal maturity biomarkers derived from phytoplankton and Chlorobi-derived carotenoids, were identified and quantified in the carbonate concretion with an increasing concentration towards the nucleus where the fossil is preserved.

A chemo-taxonomical approach was applied in **Chapter 2** to unequivocally identify the invertebrate as a crustacean. Based on the abundance and distribution of steranes within the sub-samples of the concretion the invertebrate was identified as a crustacean. ααα-20*R* cholestane, prevailing in the proximity of the fossil layer, is proposed here to mainly derive from the organism, whereas the remaining steranes represent a source of sterols from phytoplankton, which the organism used as its food source. A suite of biomarkers, including very low Pristane/Phytane (Pr/Ph) ratios and Chlorobi-derived aryl isoprenoids, here provide strong evidence of persistent PZE conditions at the time of fossil-decay and initial preservation. Among the aryl isoprenoids, intact isorenieratane was identified in the free extract but remarkably, it was also preserved in the sulfurized fraction. Stable isotopic values ($\delta^{13}C$ of alkanes and isoprenoids) characteristic of a consortium of sulfate reducing bacteria (SRB) promoting the growth of authigenic carbonate were also present in the sample. The presence of an active sulfur cycle in the water column of the inner reef system, including SRB and the resulting euxinia, protected the crustacean tissue and sinking OM from further decomposition and promoted the rapid encapsulation of the

organic-remains within a tight biogenic mineral matrix. These results present strong evidence of the important role of PZE during fossil (including soft tissue) and biomarker preservation.

The results presented in **Chapter 3** describe a suite of steroids preserved at an unprecedented level in the same fossil crustacean analyzed in **Chapter 2**. Intact biological sterols, including cholest-5-en-3β-ol, 24-methycholest-5-en-3β-ol and 24-ethylcholest-5-en-3β-ol, have been identified here for the first time in sediments older than Cretaceous (~125 Ma). Apart from stenols, ca. 50 of their diagenetic products previously ascribed to result from microbial conversion and progressive thermal alteration were also identified, including stanols, sterenediols, stenol-ketones, stanones, sterenes, diasterenes, steranes, diasteranes, monoaromatic and triaromatic steroids. The parallel occurrence of sterols and steranes and aromatic steroids in a concretion that has undergone the same burial history is unique. This diagenetic continuum of steroids previously presumed unfeasible is attributed to microbial-mediated and reduced sulfur catalyzed eogenetic processes.

The survival of these highly reactive steroidal compounds associated with a fossil crustacean preserved in a Devonian concretion can be attributed to a euxinic zone expanding very close to the productive surface waters, thus enabling very short travelling times of primary biomass through the oxic water column. As described in **Chapter 2** the exceptional preservation of biomass within carbonate concretions is attributed to a rapid microbially-induced mineral encapsulation during the earliest stages of diagenesis in the anoxygenic sediment/water interface. It can even be postulated that this preservation starts at the chemocline; in which the biomass is isolated from microbial degradation therefore preventing full decomposition and transformation of the original biolipids during diagenesis. Degradation-sensitive biomolecules, when embedded in the uppermost sediments became rapidly encapsulated within the carbonate concretion, protecting the organic skeletons, thus extending sterol occurrences in the geosphere by 250 Ma. The evidence provided in **Chapters 2** and **3** indicate that under exceptional conditions concretions are able to preserve biomolecules at unprecedented levels improving our understanding of taphonomic processes from an organic geochemistry perspective.

Chapter 4 applies numerous organic geochemical (biomarker and stable isotopes) and geological (sedimentology and paleontology) approaches to examine

the aftermath of one of the most prominent mass extinction events that occurred during the Phanerozoic near to the Permian/Triassic Boundary (PTB). The prolonged recovery (up to 5 Ma) of the biota and environment of the Early Triassic is not completely understood. It has been hypothesized that the pace of the recovery across the globe was not temporally synchronous. However it was markedly controlled by the paleogeographical fluctuations of the harsh environmental conditions, including anoxic water and elevated levels of free H_2S. The aim of this research project was to establish the environmental conditions that controlled the recovery in the continental margins of the Boreal Sea in the Northern hemisphere. A detailed investigation including biomarker and compound specific isotope analysis (CSIA) coupled with traditional sedimentology, paleontology and bulk isotope geochemistry ($\delta^{13}C_{carbonate}$, $\delta^{13}C_{org}$, $\delta^{34}S$, $\delta D_{kerogen}$) have been performed on samples collected from a section spanning the Early Triassic from Spitsbergen, Svalbard.

The OM found in the marine section of Svalbard is mainly a mixture of Type II and Type III kerogens, with a total organic carbon content (TOC % wt.) that fluctuates through the section, increasing preservation potential towards the end of the Early-Triassic. The relative thermal maturity of the samples is found to be in the initial stages of the oil generation window, therefore adequate to evaluate variations in biomarkers susceptible to thermal maturity. The proportion of redox sensitive compounds, such as pristane, phytane and Chlorobi-derived aryl isoprenoids, suggest persistent anoxic conditions prevailed at the time of deposition during the Induan and Smithian sub-stage of the Early Triassic; normalization of the oxygen content in the water column seems to occur toward the Spathian sub-stage.

In general, the environmental conditions in the Early Griesbachian (after the PTB) are here controlled by fluctuations of the anoxic conditions of the water column. The biomass contribution in this interval represents short periods of high algal productivity followed by increased heterotrophic reworking. The contribution of terrestrial biomass decreased towards the top of the section (Middle Triassic), suggesting the extent of the extinction on land or increasing distance to the paleoshoreline. Similar conditions occurred close to the Griesbachian-Dienerian boundary, where sea level rise might have favored the transfer of essential nutrients into ocean-surface waters stimulating primary productivity, which triggers marine anoxia through eutrophication and yields a biomass enriched in ^{13}C. The parallel

enrichment in isotopes of C and H and S of pyrite during the Dienerian also support an increase in ocean salinity and/or upwelling of warm saline bottom waters with low oxygen levels. This assemblage of geochemical features during the Dienerian is here compared to the Haline Euxinic Acidic Thermal Transgressions (HEATT) biogeochemical model described by Kidder and Worsley (2004; 2010). This model best describes the possible oceanic upwelling of warm, saline bottom waters containing low oxygen and few of the required nutrients for autotrophic organisms to survive enhancing blooms of heterotrophic communities (sulfate reducers), prasinophytes and/or halophilic archea. All of the above derived from the reoccurring volcanic activity reported for the Early Triassic.

The Olenekian stage in this section is characterized by a steady carbon isotope depletion in ^{13}C that could be related to the initial stages of recovery of the marine ecosystem but also potential incorporation of light carbon into the atmosphere (e.g. collapse of methane clathrates or reworked OM, Nabbefeld et al., 2010c). The biomarker C_{33} *n*-alkylcyclohexane was here identified and strongly increases in concentration within the Induan stage. This marker has been previously ascribed to a distinctive phytoplanktonic-acritarch related community within the P/Tr extinction interval (Grice et al., 2005a). We also showed a positive correlation of the *n*-C_{33} alkyl cyclohexane (ACH) with the regular isoprenoid *i*-C_{21} derived from halophilic bacteria, suggesting that anoxic and salinity waters higher than normal seawater levels could trigger the abundance of the ACH-C_{33} biomarker precursor. Overall, based on the comprehensive dataset established for the Early Triassic deposits of the shallow shelf deposits of the Boreal Sea, the main paleoenvironmental features of this period show several perturbations of the marine ecosystem near the paleoshorelines of the Boreal Sea, showing more stable and suitable conditions for the flourish of phototrophic organisms towards the end of the Early Triassic.

Overall, this thesis presents the successful application of integrated biomarker, elemental and molecular stable isotope approaches to reconstruct ancient marine depositional environments severely affected by ecological and paleoenvironmental perturbations.

Acknowledgements

First and foremost, I would like to thank my principal supervisor, Prof. Kliti Grice, for her constant support and guidance during this study. I would like to express my genuine gratitude for her patience, dedication, guidance and scientific encouragement throughout this work. Thanks to Kliti for giving me this splendid opportunity to come from the other side of the world and share with me her 'contagious enthusiasm' towards science and research. This journey was accompanied by multiple opportunities to present my very "lucky" crustacean organic geochemical results at conferences all over the world, thanks to the constant scientific and financial support from Prof. Grice, whom always provided the most of the opportunities presented to all of her students and staff. I also have to thank Kliti for always being considerate and thoughtful in every challenging situation especially given that 'we' -international students- have to confront when we are far away from home.

Similarly, I would like to sincerely thank my co-supervisor, Associate Prof. Kate Trinajstic for her support and always smart advice; also for providing multiple concretions of samples from the Gogo Formation and with them always providing very interesting facts. Also I Thank Kate for always being available for scientific and casual discussions during my stay at Curtin.

In this journey I had the opportunity to share ideas, knowledge and coffee with many inspiring people of the Organic Geochemistry community, their willingness to educate and share knowledge not only did it provide me with ideas to improve scientific interpretation but also inspired and really shaped my career. Without any particular order but with a lot of appreciation to all of them I would like to thanks: Prof. Rogers Summons, Prof. Simon George, A. Prof. Paul Greenwood, Dr Eric Tohver, A. Prof. Arndt Schimmelmann, Prof. Martin van Kranendonk, Prof. Richard Twitchett, Prof. Michael Böttcher, Dr. John Dodson, Dr. Andrew Murray and A. Prof. Greg Skrzypek. Special thanks also go to Prof. Dr Lorenz Schwark for his inspiring scientific discussions during his visits to Perth, for his always-honest opinions and sincere way to do research, his immeasurable knowledge and ideas are admirable.

I particularly want to thanks A. Prof. Arndt Schimmelmann for hosting me in his laboratory at Indiana University (IU), his hospitality made the trip to Indiana a very gratifying experience. I would also thank Dr Peter Sauer, for scientific discussion and D/H analyses. Sincere thanks goes to Geoff Chidlow for his invaluable technical support and wiliness to always share his knowledge giving all the GC-MS users accurate explanations.

I thank Prof. Richard Twitchett for the sedimentological analyses of the samples from Spitsbergen (**Chapter 4**) and the multiple revisions of the manuscript, always adding smart interpretation and creative ideas. At the same time I acknowledge Prof. Clinton B. Foster for providing palynological data and interpretation. Thanks to A. Prof. Greg Skrzypek and Dr Douglas Ford for their support with $\delta^{13}C$ analyses of OM and carbonates.

The most special thanks go to Anais Pagès, for sharing this journey with me, literally back-to-back, cheering each other up when needed and making life around and outside the university so much easier and pleasant. Our friendship is one of the best outcomes of this PhD. Also, very special thanks go to Dr Svenja Tulipiani, thanks for your unconditional attitude to help everyone with almost everything. Furthermore, I would like to thank all WA-OIGC colleagues (Dr Caroline Jaraula, Mojgan Ladjavardi, Dr Jeffrey Dick, Dr Robert Lockhart, Dr Lyndon Berwick, Alex Holman, Chloe Plet and Hendrik Grotheer) for always keeping an enjoyable, peaceful and harmonious work environment, for helping each other out, for inspiring scientific discussions, for the multiples coffee-tea breaks and the chats and laughs that we shared that always will be remembered. Very special thanks to Alex Holman for his great job during last minute proof reading.

I gratefully acknowledge ANSTO/AINSE (and Prof. John Dodson) for top-scholarships and the opportunity to work with such a talented team. Further, I would like to express my sincere gratitude to Curtin University for a CSIRS scholarship and the Western Australian-Organic isotope Geochemistry Centre (WA-OIGC). I also thank the ARC for funding (QEII Discovery/ DORA and a Linkage grant) awarded to Prof. Kliti Grice, Curtin University for fee waiver and EAOG for travel award.

From the bottom of my heart, I thank to Andres for patiently accompanying throughout this journey. Thanks to his love and dedication, he became my happy-place, my home. Many thanks to Vicki and Murray for opening the doors of their home and their family and becoming my Australian's parents.

Finally, thanks to all my beautiful and loved family for keeping me always in their hearts and thoughts while being so far away. To my brothers, for their unconditional support, there are no words big enough to say thank you to you two. And of course, infinite thanks to my Mom, always my rock and my wings.

Thank you all.

Primary publications

This thesis is assembled by publications, two (2) of them are published in high impact internationally recognized journals and the content of Chapter 4 has been recently submitted to an internationally recognized journal. The individual chapters are listed below.

Chapter 2

Melendez I., Grice K., Trinajstic K., Ladjavardi M., Greenwood P., Thompson K. Biomarkers reveal the role of photic zone euxinia in exceptional fossil preservation: An organic geochemical perspective. *Geology* **41**, 123-126, (2013) Impact factor 4.306.

Chapter 3

Melendez I., Grice K. and Schwark L. Exceptional preservation of Paleozoic steroids in a diagenetic continuum. *Scientific Report-Nature.* 3, 2768. doi: 10.1038/srep02768 Impact factor 5.078.

Chapter 4

Melendez I., Grice K., Twitchett R., Böttcher M.E., Schimmelmann A Episodic mayhem after the end-Permian biotic crisis in the Boreal Sea: microbial blooms during hypersaline-oxygen limited conditions Submitted. *Proceedings of the National Academy of Sciences (US)* Impact factor 9.809

Contributions of Others

The work presented in this thesis was primarily designed, experimentally executed, interpreted, and the individual manuscripts were prepared by the first author (Ines Melendez). Contributions by co-authors are described below.

Chapter 2

The analyzed carbonate concretion was collected by Tim Sendon and Kate Trinajstic. Experiments were designed by Ines Melendez and Kliti Grice and executed by Ines Melendez with technical support from Geoff Chidlow. Preliminary analyses of the concretion were made by Mojgan Ladjavardi and Katharine Thompson. Carbon isotopes analyses of carbonates and bulk OM were performed by Douglas Ford and Greg Skrzypek at the School of Plant Biology, University of Western Australia, Australia. Ines Melendez wrote the manuscript with contributions from Kliti Grice, Kate Trinajstic and Paul Greenwood. All the authors provided intellectual input in discussions. Kliti Grice provided analytical facilities except where mentioned otherwise. This research was funded by QEII and ARC Linkage/Infrastructure grants (Kliti Grice).

Chapter 3

This chapter described further analysis made in the same sample used in **Chapter 2**. Experiments were designed by Ines Melendez, Kliti Grice and Lorenz Schwark. All the sample preparation and analyses were performed by Ines Melendez. Identification of steroidal compounds was made by Ines Melendez, Lorenz Schwark and Kliti Grice (through the thesis of PhD scholar Andrew Mackenzie). All co-authors provided intellectual input in discussions and writing of the manuscript. Kliti Grice provided analytical facilities. This research was funded by QEII and ARC Linkage/Infrastructure grants (Kliti Grice).

Chapter 4

The samples were collected by Kliti Grice, Birgit Nabbefeld and Richard Twitchett during a field trip to Spitsbergen in 2007. Ines Melendez and Kliti Grice designed all experiments. Ines Melendez was responsible of the selection of samples and their preparation, including decarbonation for kerogen isolation and elemental analysis, preparations for bulk $\delta^{13}C$ analysis of OM and carbonates, organic extraction chromatographic separation, Gas Chromatography-Mass Spectrometry (GC-MS) and Gas Chromatography-Isotope Ratio Mass Spectrometry (GC-irMS) analyses. Isolation of kerogens for δD analysis was performed by Ines Melendez following methodology designed by Arndt Schimmelmann from the Department of Geological Sciences, Indiana University, USA. δD analysis of kerogens was carried out by Peter Sauer also at Indiana University, USA. Clinton Foster performed palynological analyses at Geoscience Australia. $\delta^{13}C$ analyses of OM and carbonates were performed by Douglas Ford and Greg Skrzypek at the School of Plant Biology, University of Western Australia, Australia. Kliti Grice provided analytical facilities for the remaining analyses. Ines Melendez processed and interpreted the data and wrote the manuscript. Richard Twitchett contributed to the writing and provided geological framework of the investigation. All Co-authors provided intellectual input in discussions and contributed to the writing of the manuscript. This research was funded by QEII/DORA and ARC Linkage/Infrastructure grants (Kliti Grice).

Secondary Publications

Manuscripts and abstracts based on research conducted during the preparation of this thesis.

Peer reviewed journal articles not part of thesis research

Trinajstic, K., Grice, K., Downes, P., Bottcher, M.E., **Melendez, I**., Dellwig, O., Burrow, C. and Verrall, M., 2013, Macromolecule and organ preservation in a 380 million year old actinopterygian fish from the Gogo Formation, Western Australia. *PlosOne.* In revision

Ladjavardi, M., Grice, K., Metcalfe, I., Boreham, C.J., Schimmelmann, A., Sauer, P.E., Böttcher, M.E., **Melendez, I.,** 2013, Stable isotopic proxies (molecular fossils and bulk parameters) to establish the paleoenvironmental changes spanning the Induan-Olenekian boundary in the northern onshore Perth Basin, Western Australia: Evidence for methane clathrate release in the Early Triassic. *Gondwana Research.* In revision

van Kranendonk, M.J., Schopf, J.W., Williford, K., Grice, K., Pagès, A., Kudryavtsev, A. B., Gallardo, V.A., Espinoza, C., Ushikubo, T., Kitajima, K., Lepland, A., Walter, M.R., Yamaguchi, K.E., Hegner, E., Ikehara, M., **Melendez**, **I.,** Flannery, D., Valley, J., 2014, A 2.3 Ga sulfur-cycling microfossil assemblage dating from the rise of atmospheric oxygen. *Geobiology,* Submitted.

Conference abstracts

*****Not related to PhD

Melendez, I., Grice, K., Schwark, L. An Early Diagenetic Continuum: Steroids biomarkers exceptionally preserved in the Paleozoic. "26th International Meeting of Organic Geochemistry" (IMOG), Tenerife, Spain, September 2013, Plenary

Oral Contribution, Book of Abstract (http://digital.csic.es/handle/10261/81640), Vol. 1, page. 55.

Melendez, I., Grice, K., Twichett, R., Böttcher, M.E., Schimmelmann, A. Biomarkers and Their stable isotopic composition associated with the recovery of the End-Permian mass extinction event "26th International Meeting of Organic Geochemistry" (IMOG), Tenerife, Spain, September 2013, Poster Presentation, Book of Abstract (http://digital.csic.es/handle/10261/81640), Vol. 1, page. 452.

Grice, K., Tulipani, S., Jaraula, C.M.B., **Melendez, I.,** Böttcher, M.E., Schwark, L., Foster, C.B., Twitchett, R. Consistent changes in biomarkers (microbes and flora) and stable isotopes across three major extinction events of our planet "26th International Meeting of Organic Geochemistry" (IMOG), Tenerife, Spain, September 2013, Poster Presentation, Book of Abstract (http://digital.csic.es/handle/10261/81640), Vol. 1, page. 442.

Melendez, I., Grice, K., Schwark, L. Exceptional lipid preservation in fossil from the Gogo Formation. "17th Australian Organic Geochemistry Conference" (AOGC), Sydney, Australia, December 2012, Oral presentation, Program and Abstract Book, p 77.

Grice, K., Jaraula, C.M.B., Williford, K., **Melendez, I.,** Tulipani, S**.**, Nabbefeld, Summons, R.E., Böttcher M.E., Woltering, M., Twitchett, R. Consistent changes in biomarkers (microbes & flora) & stable isotopes across several major extinction events of our planet, "34th International Geological Congress" (IGC), Brisbane, Australia, Aug 2012.

Melendez, I., Grice, K., Biomarkers and stable isotopes of euxinia and their role in fossil preservation. "American Geophysical Union (AGU) Fall Meeting" San Francisco, USA, December 2011. Oral presentation

Pages, A., Grice K., Lockhart, R., Holman, A., **Melendez, I.*,** van-Kranendonk, M., Jaraula, C. Biomarkers of sulfate reducing bacteria from a variety of different aged samples including a modern microbial mat. "American Geophysical Union (AGU) Fall Meeting" San Francisco, USA, December 2011. Oral presentation.

Grice, K., Nabbefeld, B., Maslen, E., Jaraula, C., Holman, A., **Melendez, I.,** Tulipani, S., Twitchett, R., Hays, L.E., Summons, R.E., Mella, L., Williford, K.H., McElwain, J., Böttcher, M. (2011) Exploring mass extinction events and their association with global warming events from muliproxy biomarker and isotopic approaches, "American Geophysical Union (AGU) Fall Meeting" San Francisco, USA, December 2011. Invited speaker.

Melendez, I., Grice, K., Trinajstic, K., Thompson, K., Ladjavardi, M., Schimmelmann, A., Greenwood, P. Biomarkers and stable isotopes of euxinia and their role in fossil preservation. "25th International Meeting of Organic Geochemistry" (IMOG), Interlaken, Switzerland, October 2011.Oral presentation.

Melendez, I., Grice, K., Trinajstic, K., Thompson, K., Ladjavardi, M. Biomarkers and stable isotopes of euxinia and their role in fossil preservation. "11th Australasian Environmental Isotope Conference & 4th Australasian Hydrogeology Research Conference", Cairns, Australia, oral presentation, July 2011. Oral presentation. Program and Abstract Book, p 45.

Melendez, I., Grice, K., Trinajstic, K., Thompson, K., Ladjavardi, M. Biomarkers and stable isotopes of euxinia and their role in fossil preservation. "The XVII International Congress on the Carboniferous and Permian" Perth, Australia, July 2011, Oral presentation. Program and Abstract Book, p 91.

Melendez, I., Grice, K., Trinajstic, K., Thompson, K., Ladjavardi, M. Biomarkers and stable isotopes of euxinia and their role in fossil preservation "Australian and New Zealand Society for Mass Spectrometry Conference" (ANZSMS), Perth, Australia, January 2011. Oral presentation, Abstract Book, p 62.

Melendez, I., Grice, K., Trinajstic, K., Thompson, K., Ladjavardi, M. Biomarkers and stable isotopes of euxinia and their role in fossil preservation. "Australian Organic Geochemistry Conference" (AOGC), 2010, Canberra, Australia, December 2010. Oral presentation, Abstract Book, p 31.

Table of contents

Table of Figures

Chapter 1

Chapter 2

Chapter 2 - Appendixes

Chapter 3

Chapter 3 - Appendixes

Chapter 4

Chapter 4 – Appendixes

CHAPTER 1

Introduction and Overview

Biogeochemical cycles of carbon, nitrogen, sulfur, and phosphorus are controlled by the metabolic pathways within living organisms, geological processes and chemical reactions, mobilizing them between and within the biosphere, atmosphere, hydrosphere and geosphere. Perturbations in these cycles have potentially driven the major environmental and ecological changes reported in the geologic record. By weight, carbon accounts in average for less than 0.5% of the Earth's crust, where carbonate minerals in sedimentary rocks accounts for ca. 99.9 % of the total crustal abundance. Nevertheless, one of the more important roles of carbon in nature is in the biosphere and biochemical processes, where it is responsible for all forms of life and is the most abundant element in organic compounds. The global carbon cycle is closely linked to other global cycles such as oxygen, nitrogen, and sulfur because of the important role these elements play in biological and geochemical processes.

The global carbon cycle can be subdivided in various sub-cycles, including fluxes to and from the mantle, such as CO_2 realese from e.g. volcanic activity and mid ocean ridges. However, for the purpouse of this literature overview only the main sub-cycles involving crustal Carbon are examined: the larger carbon pool in sedimentary rocks, controlled by carbonate minerals and with residence time of millions of years; and the biogeochemical part of the carbon cycle, which comprises living organisms and fossil organic matter (OM) present in sediments, water bodies and soils. These

two parts of the carbon cycle are in equilibrium with a two-way flux: (i) the incorporation of carbon into sedimentary rocks (as carbonate-C and organic carbon-OC) and in the opposite direction (ii) primarily through erosion and weathering of sedimentary rocks. Even though quantitatively the biogeochemical part of the C cycle is minor, all the OM and a large part of the carbonates originate from these biogeochemical processes.

The cycling of OC on the lithosphere involves fluxes to and from the major reservoirs (**Figure 1.1**). OM in sedimentary rocks, mainly as fossil fuels and kerogen, comprise the largest OC pool, making up approximately 99.5% of the total OC. In land surfaces the OC is mainly stored in soil and land biomass; which can be further separated into terrestrial plant tissues (woody and non-woody biomass), soil microbes, humic substances and litter. The smaller C pools are found in marine biomass as dissolved and particulate OC (DOC and POC, respectively) in seawater, in living marine organism(s) and finally in marine surface sediments. Gas hydrates are an important part of the C reservoir in the subsurface; however, the exact proportion of C stored this way has not been fully explored. In the atmosphere C is stored largely as CO_2 (99.2 %) and methane (CH_4). Burning of biomass and respiration are the main biochemical processes that incorporate CO_2 into the atmosphere. Carbon can be also incorporated into the atmosphere and oceans by released of CO_2 from the mantle by volcanic activity (Grard et al., 2005), and/or by collapse of methane chlatrates (Retallack et al., 2008) during periods of warm climate.

Photosynthesis is the most important mechanism to synthesize OM by conversion of atmospheric and aqueous CO_2 into cellular organic material, using sunlight as a source of energy. This mechanism is essentially responsible for all of the biochemical synthesis of OM (Field et al., 1998). Chemosynthesis by microbial organisms, which involves chemical energy rather than sunlight for C fixation, is a less significant mechanism and has more local importance. Equation 1.1 represents the generalized reaction for C fixation by photosynthesis in bacteria such as cyanobacteria, eukaryotic algae and higher plants in which CH_2O stands for OM in the form of carbohydrates.

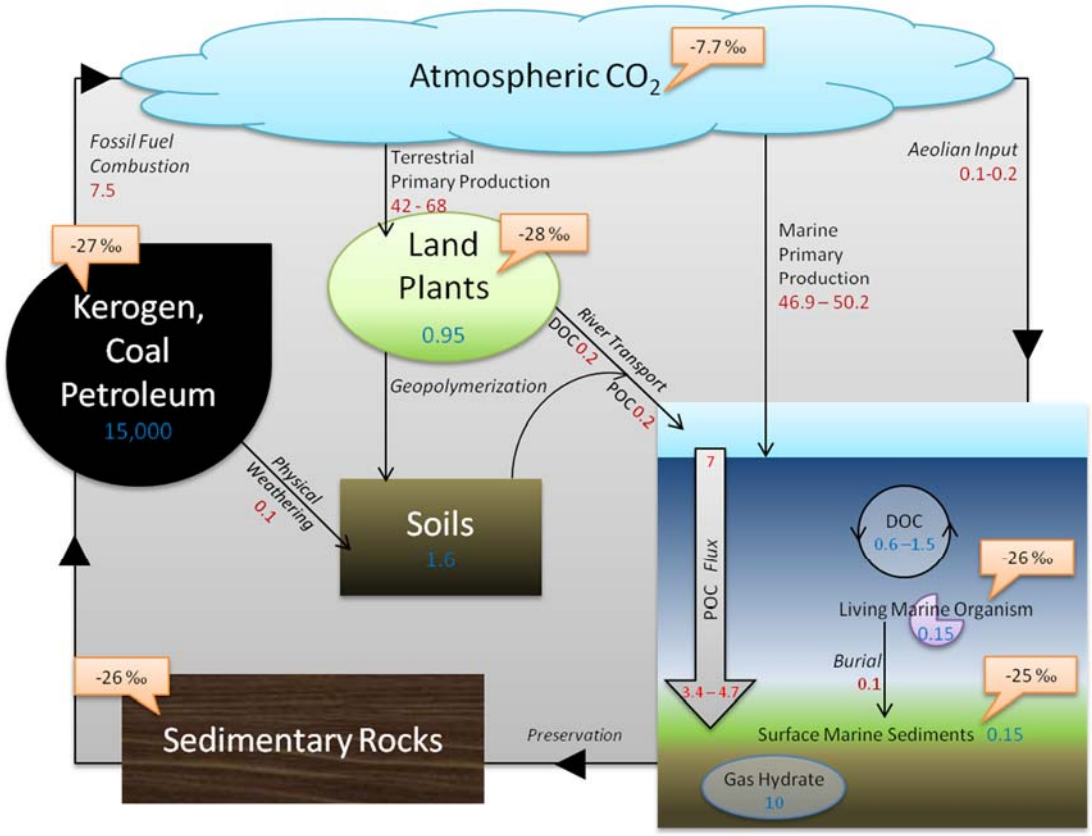

Figure 1. 1 The global OC cycle, and major reservoirs and fluxes. Values of the superficial and deep reservoirs are denoted in blue (10^{18} g C). The physical processes that allow for the C to flow between the reservoirs are italicized and described next to the arrows in the figure. Flux values are in red (10^{15} g C $Year^{-1}$). Examples of average isotopic composition of carbon ($\delta^{13}C$) in the reservoir are denoted in orange boxes. Adapted from Hedges, 1992; Reitner and Thiel, 2011; Volkman and Hutinger, 2006.

Photosynthetic organisms are found on land and in the photic zone in the water column (usually less than ~100 m). On land, the main limitation for primary production is due to the availability of water to perform photosynthesis. Also, high temperatures restrain photosynthesis by destroying or altering enzymes and cellular components of plants (Field et al., 1998). The highest gross terrestrial production and accumulation as biomass occur in the tropics, while polar regions contribute the least (Reitner and Thiel, 2011). Therefore it is likely that in the past, coals were formed in swampy areas maintained by high rainfall, similar to the tropical rain-forests where the most productive areas of land biomass are found (Killops and Killops, 2005), reflecting global patterns of temperature and precipitation.

$$2H_2O + CO_2 \xrightarrow{light} O_2 + CH_2O + H_2O \qquad (1.1)$$

In marine environments, primary production is dominated by open water (pelagic) phytoplankton, accounting for up to ca. 95% of total marine primary production. The availability of light, inorganic nutrients, particularly nitrates and phosphates, along with water temperature are the crucial factors for the effective production of biomass in water bodies. The main source of nutrients derive from run-off from land but also from vertical recycling; both usually efficiently occurring in coastal waters and upwelling zones (Killops and Killops, 2005; Peters et al., 2005). Under hypersaline conditions the diversity of primary producers is severely reduced as only a few species can adapt to such conditions. However, cyanobaterial mats have a high tolerance to hypersaline waters and can contribute with important amounts of biomass in these environments .

There are multiple sources of OM in the oceans; most of them are reliant upon the intensity of the biological pump and the proximity and magnitude of inputs from rivers, coastal erosion, and the atmosphere (Volkman and Hutzinger, 2006). However, not all the biomass, allochthonous and autochthonous, in water bodies is successfully transformed into sedimentary biomass. Actually, most of the OM produced in oxic waters by autotrophic organisms or transported from land is recycled in the water column or at the sediment-water interface, at a depth no deeper than 1000 m. Heterotrophic microbes -bacteria- in the water column are the main agent for the complex and selective processes of reworking of primary biomass, but also contribute their own remains within the euphotic zone, or secondary productivity, despite their diminutive size.

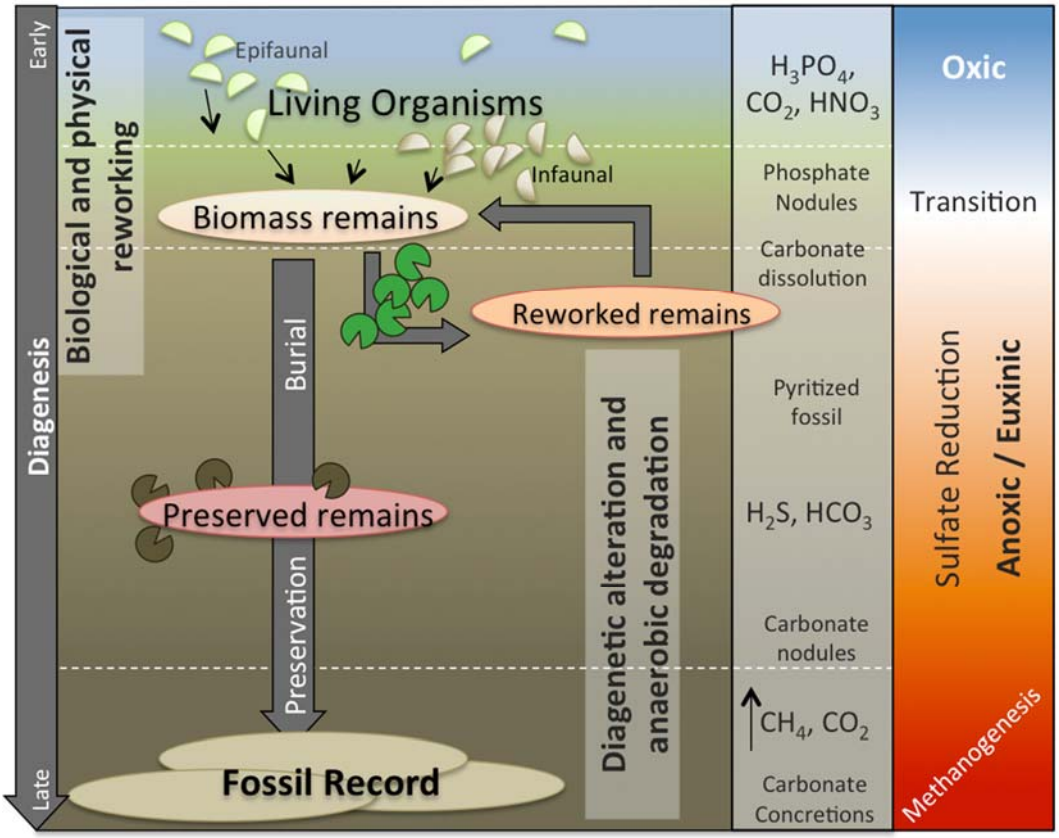

Figure 1. 2 Simplified illustration of transformation processes of OM during diagenesis in marine environments, in which oxic water column overlay the water/sediment interface. The transicion zone between oxic and anoxic zones can either be within the water column or close to the sediment-water interface. Middle columns highlight bacterially mediated diagenetic processes and products; right columns identify redox zones.

The abundance of OM deposited in sedimentary basins not only depends on the rate of primary pruduction but on the redox conditions that prevail in the water column during deposition. In oxygenated settings less than 0.1% of OM is preserved in the bottom sediments of planktonic environments. Under these conditions, most of the organic carbon from primary producers is remineralized back to carbon dioxide in the top 200 m of the water column and is returned to the hydrosphere-atmosphere system; these includes most of the functionalized biogenic compounds such as carbohydrates, proteins and nucleic acids derived from primary producers. However, the rate of preservation drastically increases in environments with limited water circulation and reduced oxygen availability. These reducing/anoxic conditions, ideal

for OM preservation, can be a result of stagnation periods, substantial inputs of OM and strong thermoclines.

Oxygen-deficient environments are more favorable for preservation of OM, in which up to 5% of the biologically produced biomass in the surface water can be incorporated into the geological record. Restricted water circulation within enclosed basins is a key factor for anoxic conditions to establish and persist trough the water body. In areas where primary production is exceptionally high and the water column is stratified, the bottom sediments and the water column –reaching even only meters off the surface- can become anoxic. In the modern oceans, the Cariaco Basin off the coast of Venezuela and the Black Sea in Europe, are examples where the water is anoxic from the seafloor to nearly the surface, due to lack of deep oxygen-rich currents that replaced the consumed oxygen in respiration by organisms (Gaines et al., 2009; Tissot and Welte, 1985). Stagnant waters in past and present oceans can be thermally and/or salinity stratified. A thermocline separates less dense warmer waters from bottom colder and less dense water bodies. Analog halocline separates salinity stratified water columns, in which less saline water (e.g. freshwater, saline) overlays more saline water (saline, hypersaline).

Once the OM has escaped the reminaeralization process can accumulate. Multiple biological, chemical and physical processes can alter the long-term fate of OM over geological time. Tectonic phases of subsidence and burial or uplift and erosion determine whether the organic content of a sediment is preserved and transformed or is eroded and oxidized (Tissot and Welte, 1985).

The earlier stage of OM preservation includes a series of microbial and thermally driven chemical changes. These transformation are known as diagenesis (Tissot and Welte, 1985; Vandenbroucke and Largeau, 2007). The organic compounds that escape the mineralization process and start diagenetic alterations can lead to the formation of macromolecular and/or aggregates via polycondensation but also can be exposed to defunctionalisation processes such as fragmentation, oxidation, reduction,

isomerization, and epimerization reactions (Brocks and Pearson, 2005; Peters et al., 2005; Tissot and Welte, 1985; Vandenbroucke and Largeau, 2007). Thruough this process more refractory biomass (e.g. pigments, lipids and structural macromolecules) become enriched and more labile molecules can be further degraded by anaerobic heterotrophic organisms such as sulfate reducers, fermenters and methanogens (e.g. Brocks and Pearson, 2005; Hedges and Keil, 1995; Hedges et al., 1997; Megonigal et al., 2004). The OM product of transformation and degradation during diagenesis is cross-linked and form kerogen, an amorphous and complex structural network of biochemical subunits (e.g. De Leeuw et al., 1991; Vanden Broucke and Largeau, 2007). During the formation of kerogen, vulcanization a reaction mediated by sulfur and polysulfides, play an important role in connecting smaller molecular units, such as lipids, to the macromolecular aggregate, thus protecting them against further structural alterations (Hebting et al., 2006; Sinninghe Damsté and De Leeuw, 1990). Increasing burial depth, and with it temperature, parts of the macromolecular structure of kerogen decomposes and favor the formation and generation of liquids and gaseous hydrocarbon (e.g. formation of Petroleum).

Over geological periods and with increasing burial depth and geothermal heat, preserved lipids within sediments will undergo structural rearrangement *via* cracking and isomerization reactions. Through reduction, elimination and aromatization the organic compounds typically will lose all of their functional groups during thermal maturation. The resultant products are geologically stable hydrocarbon skeleton. However, there is now substantial evidence that suggests under very unique environmental conditions some biolipids such as fatty acids, alcohols and sterols, and other polar structures, can be incorporated intact into the protokerogen during early stages of diagenesis and be preserved over the geological record conserving its original functionality (Melendez et al., 2013a; Melendez et al., 2013b).

Biomarkers or molecular fossil are defined as organic compounds formed during diagenesis and catagenis of OM *via* defunctionalisation, isomerization and/or

aromatization reactions. These compounds have a structural skeleton that can unambiguously be linked to its biological precursor, despite some structural alteration during diagenesis (Peters et al., 2005). These molecular fossils preserved over geological time evidence of past or even extant life and therefore are commonly used to help elucidate source of OM and to reconstruct palaeoenvironmental conditions that prevailed during sediment deposition. Multiple biological precursors for a biomarker or the presence of the biological precursor in a wide range of organisms reduced the effectiveness of some biomarkers as a tool to elucidate sources; nevertheless, along with compound specific isotope analysis (CSIA) can help to establish a more accurate interpretation (see isotope section below).

Sulfide rich enviroments: Photic zone euxinia

In present day oceans the balance between removal of sulfate by formation of sulfide minerals and the incorporation of sulfate by oxidative weathering and erosion, maintain a concentration of approximately 28,000 μmol L^{-1} of dissolve sulfate in sea water and a time of residence of ca. 8 million years (Reitner and Thiel, 2011). The occurrence of free H_2S in seawater is rare and is indicative for the activity of sulfate reducing bacteria (SRB) in the sediments and/or at the sediment/water interface. SRB are prokaryotic microorganisms that utilize sulfate as electron acceptor for anaerobic oxidation of OM, while reducing sulfate and producing sulfide (Killops and Killops, 2005; Kump et al., 2005; Peters et al., 2005; see reaction 1.2). This process accounts for the majority of the OM oxidation in marine settings.

$$2CH_2O + SO_4^{2-} \longrightarrow 2HCO_3^- + H_2S \qquad (1.2)$$

Most of the biogenic sulfide produced in marine environments is usually reoxidized at the benthic or pelagic chemocline by microbial or chemical processes, leading to the formation of intermediate sulfur species and sulfate. However, in isolated deep Fjords (e.g. Anderson et al., 1988) and in the Black Sea (e.g. Murray et al., 2007),

free H_2S reach important concentrations within the water column, as a result of intense chemical sulfate reduction in or near the sediments. High concentrations of H_2S in the ocean are described as euxinic conditions (Kump et al., 2005). Such conditions usually develop in marine settings with a stagnant water-column; however, episodically, free H_2S can extend into the zone of light penetration where photosynthesis occurs (i.e. photic zone) and photic zone euxinia (PZE) develops (Figure 1.3; e.g. Grice et al., 2005a).

Only specialized organisms can live under PZE conditions, including purple sulfur bacteria (PSB, these can also tolerate O_2), BSB and the GSB (e.g. Grice and Brocks, 2011). Green and brown-pigmented Chlorobi i.e. GSB are obligate anaerobic phototrophs, which fix CO_2 *via* anoxygenic photosynthesis utilizing H_2S generated by SRB as an electron donor (Reaction 1.3). GSB can only thrive under PZE conditions or occasionally in thick microbial mats in shallow waters (Brocks and Pearson, 2005). Since Chlorobi utilize the TCA-cycle for carbon fixation, their biolipids are enriched in ^{13}C compared to those of most other marine phytoplankton.

$$2H_2S + CO_2 \longrightarrow 2S + CH_2O + H_2O \qquad (1.3)$$

Several specific biomarkers are derived from unique carotenoids and bacteriochlorophylls in Chlorobi, which provide unequivocal evidence for PZE in the depositional environment. For example isorenieratane, palaeorenieratane, chlorobactane, specific maleimides and a suite of ^{13}C enriched aryl isoprenoids (Sinninghe Damsté and Koopmans, 1997; Grice et al., 1996a; Grice et al., 1996b; Koopmans et al., 1996; Requejo et al., 1992; Summons and Powell, 1986, 1987). Aryl isoprenoids can however also be derived from β-carotene, which is a non-specific biomarker, abundant in many organisms (e.g. Koopmans et al., 1996). Especially if no intact C_{40} carotenoids (e.g. isorenieratane) or other specific biomarkers for Chlorobi are present in the same sample. Many of the above-mentioned carotenoids and biomarkers derivatives, have been identified in past

environments, indicating definite PZE prevailed in several oceanic anoxic events (OAE) and mass extinctions around the globe (e.g. Grice et al., 2005; Hays et al., 2007; Melendez et al., 2013a; Tulipani et al., 2014; Nabbefeld et al., 2010 Pancost et al., 2004; Sinninghe Damsté and Köster, 1998).

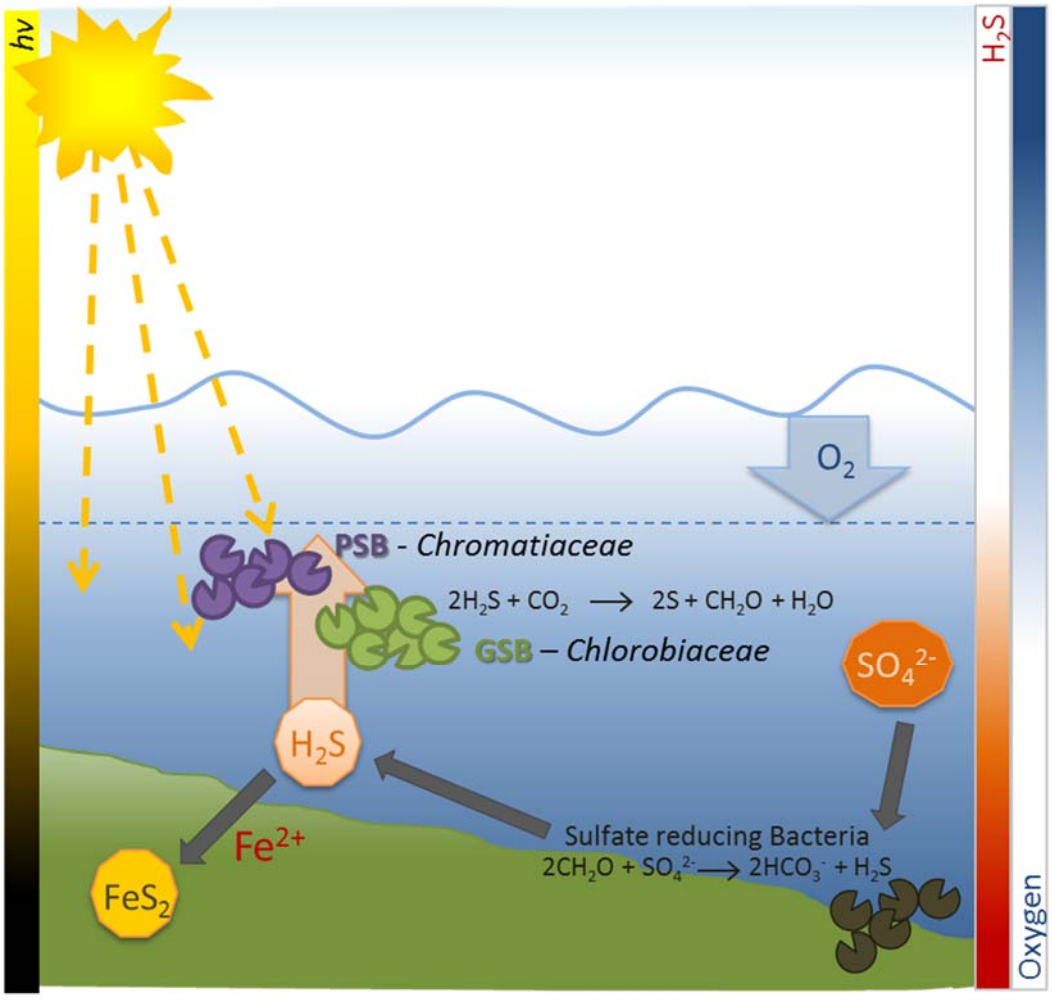

Figure 1. 3 Simplified representation of photic zone euxinic (PZE) conditions in a stratified water body and the main organisms associated with these environmental conditions.

Isotopes in organic geochemistry

Conventional biomarker analysis in ancient sedimentary sequences provides valuable information for detailed reconstructions of paleoenvironments. However, hydrocarbon profiles (e.g. *n*-alkanes, isoprenoids, and aryl isoprenoids) found in the geological record can be derived from multiple organisms that produce the same biolipids and therefore similar molecular fingerprints (Collister et al., 1994; Grice et al., 1996; Koopmans et al., 1996; Volkman et al., 1998). However, evidence of the biosynthetic pathway and source origin of OM can be preserved in the isotopic composition of their major elements (Reitner and Thiel, 2011). Stable isotope compositions of C, S, N and H in biomass (e.g. kerogen, biomarkers) can provide valuable information related to the biochemical, ecological, environmental, hydrologic, and atmospheric processes.

Table 1. 1 Stable isotopes and their natural abundances (atom %).

Carbon	*Hydrogen*	*Sulfur*	*Oxygen*	*Nitrogen*
^{12}C (98.899)	^{1}H (99.985)	^{32}S (95.018)	^{16}O (99.759)	^{14}N (99.9634)
^{13}C (1.111)	^{2}D (0.0105)	^{34}S (4.215)	^{17}O (0.0374)	^{15}N (0.3663)
			^{18}O (0.2039)	

The elements H and C are the main constituents of OM and play key roles in many biological and chemical processes on Earth. Therefore, this summary mainly focuses in the stable isotopic compositions of C and H preserved in OM. C and H have two stable isotopes (^{12}C and ^{13}C and ^{1}H and ^{2}D, respectively). The light isotopes are generally much more abundant than their heavier counterparts, for instance ^{12}C accounts for 98.899 weight % of the total carbon pool and ^{1}H accounts for 99.985 weight % (Table 1.1; Hoefs, 2009). Although, the abundance of stable isotopes remains constant, characteristic isotopic fractionations occur in nature due to physical, chemical and biological processes as a result of slightly different

physicochemical properties (e.g. bond strength) of heavier and lighter isotopes. Isotopic fractionation can occur by equilibrium isotope exchange and by kinetic processes.

Equilibrium isotope effects are defined as the fractionation processes that take place between different phases of compounds in a closed system in the state of thermodynamic equilibrium. For instance, the tendency of heavy isotopes to form stronger bonds leads to heavy isotopes being enriched in the phase with stronger intra-molecular interactions (Urey, 1947). This fractionation is temperature-dependent and operates as a reversible mechanism. In contrast, the carbon isotope fractionation that results from unidirectional kinetic isotope effects (KIE) is controlled by the slower rate of reaction for a ^{13}C-containing bond compare to the rate in an exclusively ^{12}C-containing bond. This irreversible mechanism leads to net changes in the isotopic composition of an enclosed system (Bigeleisen and Wolfsberg, 1958).

The fractionation processes that operate in OM and sedimentary carbonates produce very distinct isotopic characteristics. The isotope equilibrium exchange reactions within the multiple chemical species of the inorganic carbon system (CO_2, HCO_3^-, H_2CO_3, CO_3^{2-}) lead to an enrichment of ^{13}C in carbonates. The isotopic fractionation associated with the different species that participate in the equilibrium of the dissolve inorganic carbon (DIC) pool is only dependent on temperature, although the relative abundances of the species are strongly dependent on pH (Hoefs, 2009).

In the OC pool, kinetic isotope effects during photosynthesis favor the accumulation of the light isotope (^{12}C) in the synthesized organic material (Hayes, 1993). Fractionation processes during C fixation, include the uptake and intracellular diffusion of CO_2 and the biosynthesis of cellular components (Freeman, 2001; Hayes, 2001), are clearly dependent on the partial pressure of CO_2 (pCO_2) in the system. Pioneering investigations led by J. Hayes (1991-2002) have recognized the parameters that affect the final carbon isotope composition of naturally synthesized OM, including the isotopic composition of the C source, the C fixation pathway, isotope effects associated with metabolism and biosynthesis and the cellular C budgets. In phytoplankton and marine plants the isotopic discrimination is also

controlled by temperature, availability of $CO_{2(aq)}$, light intensity, availability of nutrients, pH and physiological factors such as cell size, cell geometry and growth rates (Hoefs, 2009; Popp et al., 1998; Schouten et al., 1998). Isotopic fractionation rates in biosynthetic organisms are higher when an unlimited access to the substrate is provided in the system; when the substrate is limited less isotopic fractionation occurs during fixation, leading to comparatively enriched biolipids (Freeman and Hayes, 1992; Takahashi et al., 1990). For example, low availability of $[CO_2]_{aq}$ during phytoplankton blooms leads to a ^{13}C enriched biomass (e.g. Pancost et al., 1997; Grice et al., 1996). Similarly, lower solubility of CO_2 in hypersaline environments will lead to ^{13}C-enrichment in organisms (Andersen et al., 2001; Grice et al., 1998; Schidlowski et al., 1994; Schidlowski et al., 1984).

Distinctive isotopic fractionation occurs in specific biosynthetic pathways used by primary producers (**Figure 1.4**); those metabolic pathways can lead to distinct isotopic values of the biomass but also between compound classes within the same organism (Zhou et al., 2010). Terrestrial plants and almost all aerobic marine primary producers fix CO_2 *via* the C3 pathway, also known as Calvin Cycle. This mechanism causes a strong isotopic fractionation that discriminates against ^{13}C, producing biomass depleted by an average of ~21 ‰ from the CO_2 source. Typically the $\delta^{13}C$ in biomass synthesized by the C3 pathway shows a clear distinction to the more ^{13}C-enriched biomass generated by plants using the C4 pathway (grasses, saltmarsh or desert plants). Carbon fixation *via* the (reductive) tricarboxylic acid (TCA)-cycle in facultatively and obligate anaerobic autotrophs, including GSB and some SRB leads to comparatively minor isotopic fractionations and ^{13}C-enriched biomass (Quandt et al., 1977; Schidlowski et al., 1994; Schidlowski et al., 1984; Scott et al., 2006).

Standards, notation and measurements

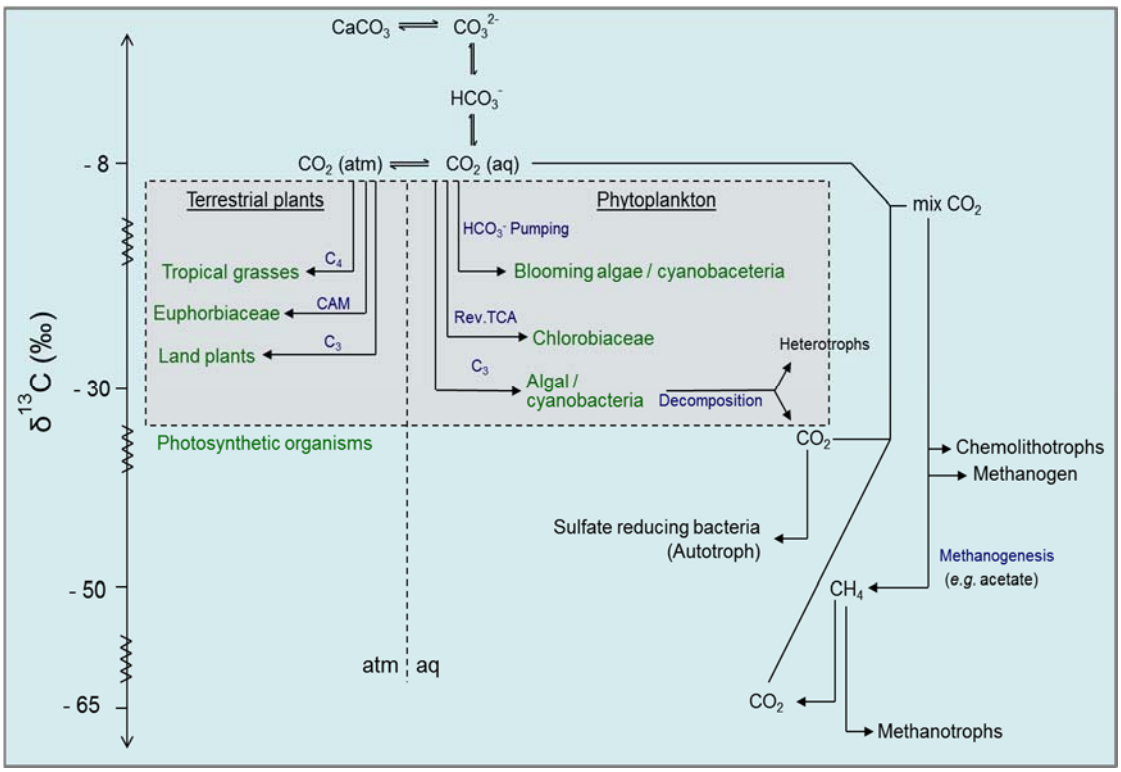

Figure 1. 4 Stable carbon isotope ratios in different primary producers (in green) associated with specific carbon fixation pathways (in blue). Adapted from Grice, 2001.

The isotopic composition of a sample does not reflect the absolute concentration of the different isotopes; instead, values are calculated as ratios of the heavier to the lighter isotopes relative to a reference standard, which have a known isotopic composition. Stable isotope compositions are expressed in the δ-notation in per mil (‰) relative to international reference materials. In the equation below, R stands for the ratio of the heavier to the lighter isotope (e.g. $^{13}C/^{12}C$).

$$\delta \text{ sample} = [(R \text{ sample} - R \text{ standard})/R \text{ standard}] \times 1000 ‰ \qquad (1.4)$$

The international standard used for $\delta^{13}C$ measurements is the marine carbonate Vienna Pee Dee Belemnite (VPDB). For δD and $\delta^{18}O$ analyses, Vienna Standard Mean Ocean Water (VSMOW) is used as an international standard. For $\delta^{34}S$ and $\delta^{14}N$ Canyon Diablo Troilite (CD) and atmospheric nitrogen are used as international standards, respectively.

Isotope ratio mass spectrometers (irMS) are the instrumentation suitable for stable isotope analyses. This instrument requires high precision and accuracy to detect minor variations in the isotope ratios of the analytes; it simultaneously monitors the abundances of selected ions at set *m/z* ratios using fixed collector cups. To make a sample amenable to irMS it is first converted into a suitable gas analyte (CO_2, N_2, SO_2 and H_2 for C, N, S and H analysis, respectively) on which the isotope ratios are measured. With $\delta^{13}C$ analysis, for example, the traces of *m/z* 44 ($^{12}CO_2$), 45 ($^{13}CO_2$) and 46 ($^{12}C^{18}O^{16}O$) are monitored. The detectors for δD-analysis are set to *m/z* of 2 (H_2) and 3 (DH) in a separate configuration of the mass spectrometer. The formation of H_3^+ as a by-product in the ion source during δD-analysis produces an isobaric interference. Appropriate H_3^+-factor correction needs to be determined and applied for appropriate correction of the measured isotope ratios (Sessions et al., 2001; Sessions et al., 1999).

For bulk $\delta^{13}C$ measurements on carbonates and OM, different preparation methods exist in order to convert the C present in the sample into CO_2. Gas is generated from carbonates mineral by selective reaction with 100% phosphoric acid at different temperatures under a helium atmosphere. The generated CO_2 is then separated from the by-product of the reaction (e.g. water) and then diverted into the irMS for the $^{13}C/^{12}C$ measurement. OM is generally oxidized at high temperatures (850–1000◦C) with an elemental analyzer (EA, for C, N and S); the CO_2 generated in this process is then transferred by a continuous flow (CF) system into the irMS.

Since the development of $\delta^{13}C$ of individual compounds (compound-specific isotope analysis - CSIA) by Matthews and Hayes (1978) and the later invention of hydrogen (H)-CSIA (Burgoyne and Hayes, 1998; Hilkert et al., 1999) the measurement of $^{13}C/^{12}C$ and $^{2}D/^{1}H$ of individual compounds in complex organic mixtures is possible (e.g., petroleum, natural gases, sediments, soils, groundwater, potable waters, and extracts from plants and other media). CSIA is performed with a continuous flow system that links a gas chromatograph (GC) to an irMS. The separation of individual compounds occurs in the GC, which is connected to a suitable interface that quantitatively converts the chromatographically separated compounds into a gas which is then transferred to the irMS. For C-CSIA the individual compounds are

converted into CO_2 and H_2O at ~850 – 940 °C in a combustion furnace containing CuO (and in some systems also NiO) as an oxidant. Water is subsequently removed by a liquid nitrogen-trap or a Nafion®-membrane. For H-CSIA, compounds are reduced to H_2, C and CO by high temperature conversion at ~1450 °C (without a catalyst using glassy carbon inside a ceramic tube) or ~1050 °C (with a chromium catalyst inside a quartz tube).

Mass extinction events

Of the total number of species that have ever lived on Earth, some 99 % are now extinct. Rates of extinction have varied over the Earth's history; however, 5 major extinction events statistically distinct from background extinction levels (**Figure 1.5**) have been identified to exceed the background extinction rates in the past 600 Ma (Raup and Sepkoski 1982). A mass extinction event is defined as an increased rate of extinction of multiple higher order taxa over a wide geographic area in a realtively short space of geological time (Bambach, 2006; Sepkoski, 1986). These extinction events have resulted in major losses of living organisms during the Ordovician, and identified close to the following age boundaries: Permian/Triassic (P/Tr), the Triassic/Jurassic (Tr/J) and the Cretaceous/Tertiary (K/T) and during the Late Devonian (Raup and Sepkoski 1982; Wiese and Reitner, 2011). Numerous hypotheses have been proposed in the literature to explain the causes that trigger mass extinctions, including catastrophic events such as extra-terrestrial impacts or extreme volcanic activity, major climatic perurbations that in conjunction with complex interactions and feedbacks with the biogeochemical cycles lead to a biological crisis. Nevertheless, the definite cause of mass extinction events remains controversial.

The Late Ordovician mass extinction was the first of the five major mass extinctions in the Phanerozic and is postulated to have occurred in two steps as a result of glaciations. The first extinction pulse was associated to a sea level regression episode, affecting the marine ecosystem by upwelling of deep oceanic toxic waters, killing up to 57 % of genera and about 85 % of marine species (Sheehan, 2001). A second extinction pulse followed the subsequent rise of sea level when the glaciation ended suddently, causing stagnation in the oceans. After these extinctions episodes the fauna took several million years to recover to pre-extinction levels (Sepkoski, 1986; Sheehan, 2001) .The upper Devonian (F/F boundary) extinction event resulted in marine faunal losses from a broad range of marine habitats. However, the timeing and causes of this mass extinction remain in debate; reduced atmospheric CO_2 and increased nutrient runoff, both related to the evolution and diversification of land

plants, have been proposed to result in global cooling and anoxia/eutrophication in the oceans (Algeo and Scheckler, 1998). Rapid sea-level change, warming and widespread marine anoxia have also been suggested (McGhee, 1996; Murphy et al., 2000; Tulipani et al., 2014).

The greatest of the 5 mass extinctions struck close to the Permian/Triassic boundary (PTB) and occur simultaneously to the Siberian Trap Large Igneous Provinces (STLIP). Evidence for a single cause creating such devastation has not been found and over the past decade debate has focused on three main geological triggers to account for the end-Permian mass extinction (i) overturn or upwelling of deep-water in a stratified, anoxic ocean; (ii) eruption of the STILP flood basalts; and the least favoured – (iii) a bolide impact. Large amounts of CO_2 and SO_2 are thought to be released from the volcanic activity causing major disturbances in the climate, either warming or cooling, but also oceanic anoxia and destabilization of gas hydrates might have played an important role (Benton and Twitchett, 2003; Wignall, 2001). Independantly of the main caused, a series of positive feedback aggravated the environmental conditions promoting changes from greenhouse-like environment to episodes of hothouse conditions (Benton and Twitchett, 2003; Kidder and Worsley, 2004; 2010).

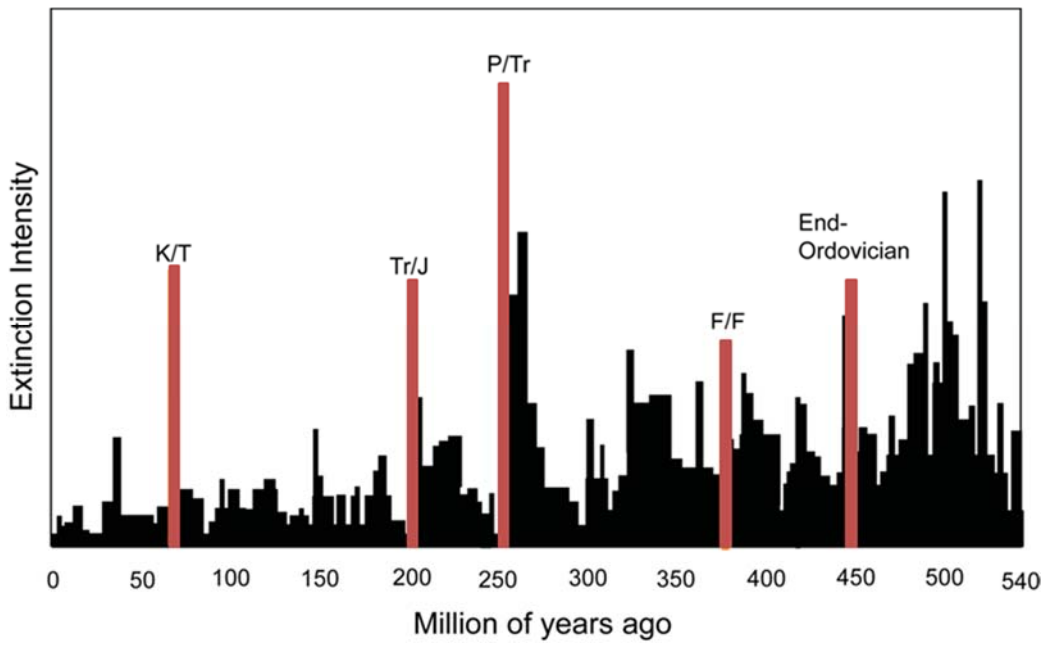

Figure 1. 5 Main mass extinction events in the Earth's history (after Bambach et al. 2006).

Devonian extinctions and the Gogo Formation

The biotic crises during the Late Devonian occurred in a series of distinctive stages, which include no less than eleven (11) global extinction events from the Givetian through Famennian culminating with the major event close to the Frasnian–Famennian (F–F) boundary, 372 Ma (McGhee, 1996; Walliser, 1996). A series of local and global environmental changes happened contemporaneous to the biotic overturn. Environmental conditions throughout the Middle and Late Devonian has been credited to rapid diversification of terrestrial plants —particularly, Archaeopteris forests— (Algeo and Scheckler, 1998). Increased population of land plants contributed to accelerate the formation of soils and modified the pattern of rock weathering, but also the diversification of terrestrial biomass acted as a C-sink, removing CO_2 from the atmosphere (Algeo and Scheckler, 2010). The removal of greenhouse gases might have favoured global cooling and drops in the sea level, contributing to the extinction of 82 % of the marine species (Algeo and Scheckler, 1998; McGhee, 1996).

Widespread anoxic/dysoxic conditions in shallow epicontinental seas have been proposed as one the major perturbations of the ecosystem in the Devonian, associated with warming and sea-level changes (Bond and Wignall, 2008). Eutrophication and the successive shortage of oxygen in shallow seas (Buggisch and Joachimski, 2006) is thought to be the result of increased OM and nutrient influx from land during the Middle and Late Devonian. Evidence of anoxic/euxinic conditions has been found to occur in different parts of the world from the Late Givetian until the early Carboniferous (e.g. Brown and Kenig, 2004; Buggisch and Joachimski, 2006; Marynowski et al., 2011; Maslen et al., 2009; Melendez et al., 2013a, 2013b; Requejo et al., 1992; Summons and Powell, 1986). Oxygen shortages along to massive burial of marine OC are associated not only to the global occurrence of black shales but are also potencial triggered for mass extinctions during this period. The intensity, nature and causes of the Late Devonian biotic crises remain in dispute; authors (e.g McGhee, 2005; Murphy et al., 2000) have also considered volcanic activity as a plausible cause for climate change and/or rapid sea-level fluctuations during this period.

What is now known as the Kimberly region was during the Devonian Period a well-exposed reef complex that extended over a marine platform of hundreds of square kilometres (**Figure 1.6**). Deposition of the reef complexes commenced in the middle Givetian and continued through the Frasnian and most of the Famennian, when an abrupt regression resulted in the exposure and erosion of the reefal platforms (Playford et al., 2009). The reef complexes are probably one of the best-preserved systems and are largely unaffected by tectonic events in the Kimberly region. A detailed review of the geology of the reef-systems in the Canning Basin is provided by Playford et al., (2009). A brief overview of the reef building systems identified in this reef complex can be summarized in two: (i) The Late-Givetian - Late-Frasnian reef-building episode in the Canning Basin comprising the Pillara sequence, and the (ii) the Famennian Nullara sequence unconformable over the Pillara sequence as a result of a significant drop in sea-level.

The Pillara sequence include sediments deposited in the platform (Pillara Formation), marginal slope facies in the Sadler Formation and the Gogo Formation, which consists of pelagic sediments accumulated in the inter-reef basin of the Pillara complex. Sediments in the The Nullara sequence primarily consists of the Windjana and Nullara Formations, which are the Famennian platform facies, the Upper-Frasnian to Middle Famennian marginal slope and basin facies from the Virgin Hills Formation (where the Frasnian-Famennian is located) and the Middle to Upper-Famennian marginal slope and basin facies of the Piker Hills and Bugle Gap Formations (Playford et al., 2009).

The Gogo Formation, deposited during the Givetian to Frasnian period, is characterized by black shales and siltstones, accumulated under low-energy anoxic to dysaerobic conditions; sporadic thinly bedded limestones and turbiditic deposits are also present (Copp, 2000). This formation is well known for the exceptionally well preserved fossils found in the Frasnian harizons, that include original bones, fully articulated fishes and also rarely preserved soft tissue (Long and Trinajstic, 2010; Trinajstic et al., 2007). This unique preservation occurs within carbonate concretions, known as ‘Gogo nodules’, which are thought to be formed by bacterial action during early diagenesis around bioclastic and organic material (Copp, 2000; Playford et al.,

2009; Playford and Wallace, 2001). Some of these nodules contain remarkably well-preserved biomolecules that can be related back to the microbial community present at the time of the concretion-formation but also directly linked to the organism preserved within the concretion (Melendez et al., 2013a; Melendez et al., 2013b). A calcareous concretion containing a well preserved invertebrate fossil was collected from Paddys Valley, an enclosed embayment in the Canning Basin, and was the object of multiple analyses during the course of this PhD, and the main findings are captured in **Chapters 2** and **3** and associated publications (Melendez et al., 2013a; Melendez et al., 2013b).

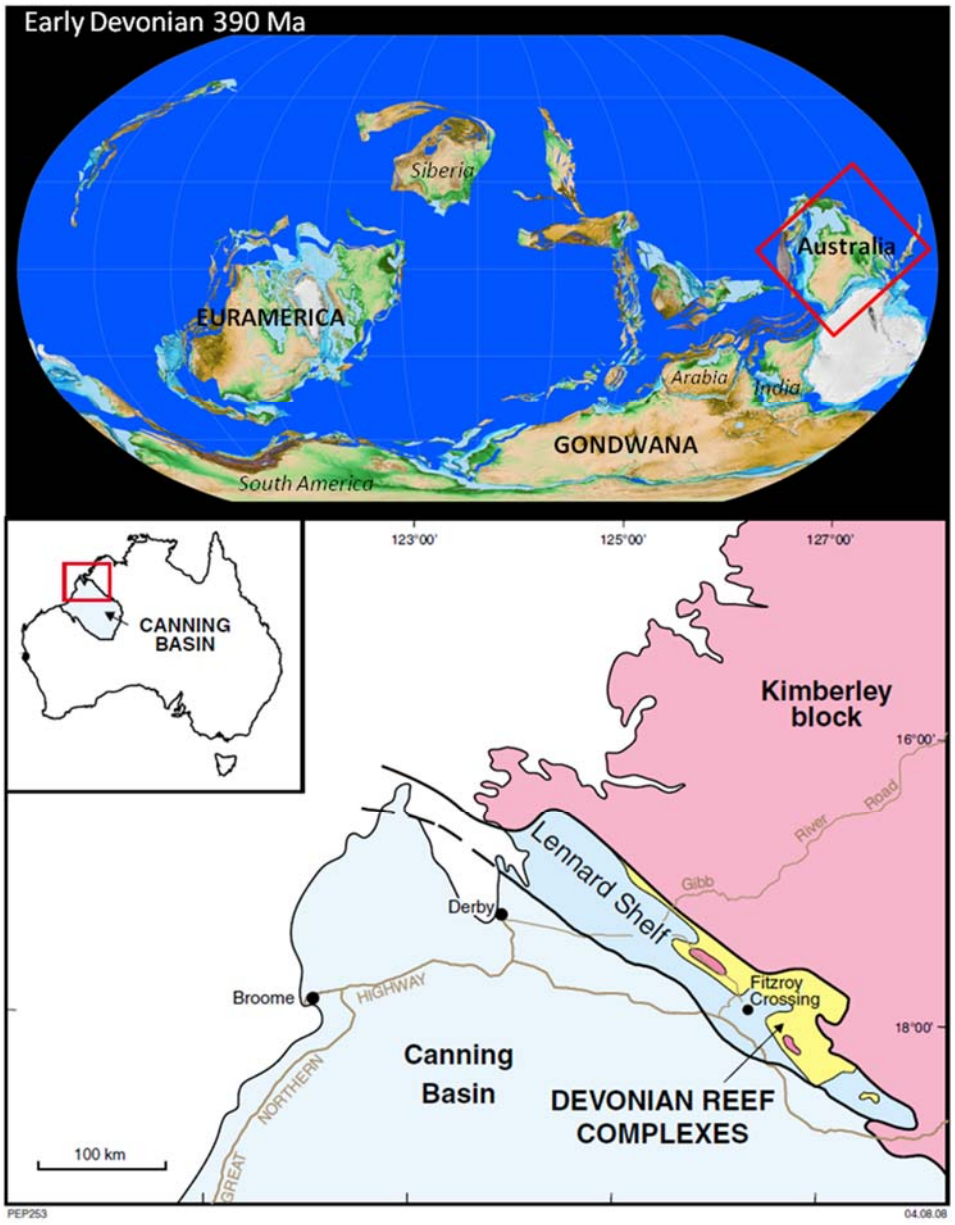

Figure 1. 6 Paleogeographic map of the Devonian world at 390 Ma. Modified after GPlates 1.4 (http://www.gplates.org/). Location of the Devonian reef complex in Western Australia (Playford et al., 2009).

Permian-Triassic Boundary (PTB)

The end-Permian extinction event (253.8–252 Ma) is by far the most dramatic and abrupt ecological crises in Earth's history and affected both the marine and terrestrial ecosystems (Benton, 1995; Benton and Twitchett, 2003). Around the PTB more than 79 % of marine invertebrate genera and ca. 95 % of the shelf biota became extinct; particularly, the marine calcified-biota with limited biological capacity to buffer themselves against changes in seawater conditions (e.g. ambient pCO_2, temperature, pH, and oxygen concentrations (Payne and Clapham, 2012). This biotic catastrophe coincided with an interval of widespread ocean anoxia and volcanic eruption that resulted in the formation of one of Earth's largest continental flood basalt provinces, the STILP.

The eruption of the STILP province is currently the most favored hypothesis to explain the extinction near the PTB. Synchronous emplacement of the STILP and the end-Permian extinction has been proposed based on radiometric dates (Kamo et al., 2006). The large magnitude of the volcanic activity was considered sufficient to disturb the atmospheric and ocean chemistry (Payne and Clapham, 2012). The release of vast amount of CO_2 and volatiles could have favoured the development of global warming (Benton and Twitchett, 2003; Wignall, 2001) leading to the melt down of gas hydrates releasing methane (Krull and Retallack, 2000). As part of the cascade effect of the volcanic activity, reduction in the ocean circulation and release of acid volatiles (e.g., CO_2 and SO_2) favor the development of global oceanic anoxia and in cases incursions of harmful H_2S into the oxygen-deficient upper water column (Grice et al., 2005; Hays et al., 2012; Kidder and Worsley, 2004; Nabbefeld et al., 2010b; Wignall and Twitchett, 1996). Global warming conditions might have also promote an increased on chemical weathering and therefore in sediment fluxes to the marine depositional environments, being this the source of nutrients to maintain high levels of productivity favoring the prevalence of ocean anoxia at that time (Algeo and Twitchett, 2010; Meyer et al., 2008).

The extinction interval can be traced around the globe; among the geological and geochemical features that characterized the extinction horizon in marine sequences

are laminated sediments, small pyrite framboids, biomarkers of Chlorobi and also C and S isotopic excursions. The occurrence of these suite of features have been proposed to be derived of intrusions of oxygen-depleted waters and also H_2S into the shallow-marine ecosystem and possibly in the deep-sea, triggering the P/Tr mass extinction (Benton and Twitchett, 2003; Chen and Benton, 2012; Grice et al., 2005; Kump et al., 2005). However, recent geochemical models suggest that atmospheric O_2 was too high to cause widespread shallow-marine anoxia/euxinia at that time (Berner, 2006). Albeit, deep ocean anoxia could have been sustained under high productivity conditions in a nutrient-rich environment (Meyer et al., 2008), these biogeochemical conditions are unlikely to be the sole cause of the biotic crises but might have worsened the environmental conditions contributing to the extinction.

Isotopic signature during the PTB

One of the most distinctive geochemical features preserved in sediments deposited at around the end-Permian, is a negative carbon isotope excursion that occur after the onset of biotic collapse. Comparable isotopic shifts are noticeable in $\delta^{13}C_{carbonate}$ and $\delta^{13}C_{org}$ records of marine and non-marine sections and can be of up to *ca.* 5 ‰ (Berner, 2002; Korte et al.,2004; Korte and Kozur, 2010). These isotope excursions have been observed in high latitudes sites, in marine sections from the equatorial Panthalassan Ocean and also multiple Paleotethyan deposits (Korte and Kozur, 2010; Krull and Retallack, 2000), suggesting a global reorganization of the C-cycle. However, the mechanism that causes the isotopic shift is probably different from the actual cause of the extinction event; most likely, is that the isotopic excurtions is a consequence of the perturbation of the global C cycle during the end-Permian. Changes in the way OC is buried and/or oxidized, is a plausible mechanism to explain the isotopic shift at that time. Increase in the amount of C released by oxidation of dead biomass but also the reduction of primary productivity in oceanic surface - dropping the amount of OM transported to the deep-waters - would be a consequence of the extinction episode (Kump et al., 2005; Meyer et al., 2008; Nabbefeld et al., 2010a). Widespread oceanic anoxia has also been reported during the PTB and, along with ocean overturning could imprint a negative shift in the isotopic record (Wignall and Twitchett, 1996). The STILP volcanism could unchain

a series of events that may account for the isotopic record; however, the actual degassing of the plume by increasing atmospheric CO_2 was not the sufficient to fully account for the isotopic excursions (Berner, 2002, 2006; Kump and Arthur, 1999). On the other hand the release of CH_4 and CO_2 as a result of thermal metamorphism of old coals derived from the STILP magmatism, could have contributed to considerable ^{13}C-depleted C that may account for the negative excursions (Korte and Kozur, 2010; Payne and Kump, 2007). High latitudes methane hydrates from sea-floor sediments and also permafrost soils might have dissociated under the warming episode of the PTB (Krull and Retallack, 2000; Retallack et al., 2011; Twitchett et al., 2001). Oxidation of that methane ($\delta^{13}C < -60$ ‰) will significantly contribute with isotopically light C, consistent with the negative C isotope signature (Berner, 2002; Krull and Retallack, 2000).

Early Triassic: Recovery of the end-Permian Extinction event

The end-Permian mass extinction event was unique not only for the extent of the biotic annihilation but also for the unusually prolonged recovery, which took most if not all of the Early Triassic. The timing and pattern of recovery remains poorly understood; recently, it has been proven that the recovery varies with depositional setting, paleoaltitud and region (Foster and Twitchett, 2014). Neverthelees, the oceanic and climatic conditions during the Early Triassic, (e.g. global warming, acid rain, ocean acidification and anoxia) also play an significant role in the timing and pattern of recovery at that time (e.g. Chen and Benton, 2012). Perhaps, the immature and primitive ecosystem that survived the extinction was not strong enough to endure the extreme environmental conditions, contributing to the slow rate of recovery. In addition to the low abundance of animals typical of the Early Triassic, the species that inhabited the recovering environment were particularly small in size (Metcalfe et al., 2011) and the taxonomic diversity was exceptionally low, while microbial structures in marine sedimentary rocks were abnormally abundant (Payne and Clapham, 2012). This biotic assemblage is a reflection of frequent episodes of low-oxygen, exceptionally high temperatures and also disruptions to primary productivity. Ultimately, the reorganization of the carbon cycle after the PTB resulted in a reduction in atmospheric O_2 levels and an increase in atmospheric CO_2

levels intensively affecting the environmental conditions for the entire Early Triassic (Berner, 2002).

After the end-Permian the STILP provinces continued active and flood basalts through coal and other OM-rich sediments are thought to occur during the Early Triassic. Massive releases of CO_2 by volcanism and volatilization of sedimentary OM, favored the development of intense global warming as well as perturbation of the ocean chemistry, including ocean acidification (Payne and Clapham, 2012; Sun et al., 2012). The incorporation of greenhouse gases during the Early Triassic was boosted with the extinction of land plants and ocean plankton and with that the loss of CO_2 drawdown. Additionally, decay of dead biomass and oxidation of CH_4 produced an important decline in atmospheric oxygen (Kidder and Worsley, 2004). The lethal effects that extreme global warming have on ocean ecosystems include: profound chemical weathering, enhanced continental erosion, sea level rise, changes in the nutrient runoff and alteration of the productivity rates, all these aggravating pre-existing ocean anoxia (Algeo et al., 2011; Algeo and Twitchett, 2010; Grasby et al., 2012; Grice et al., 2005; Metcalfe et al., 2013; Meyer et al., 2011; Nabbefeld et al., 2010b; Payne and Clapham, 2012; Payne et al., 2004; Retallack et al., 2011; Woods, 2005; Xie et al., 2010)

Evidence of extremely hot temperatures during the Early Triassic have been recently proposed by Sun et al (2012), estimating equatorial sea surface temperatures exceeding 40 °C (ca. 14 -10 °C higher than present day) during the Late Smithian Thermal Maximum and consistently higher than present day temperatures during the entire period. Such conditions would have been lethal for many forms of life. Warmer episodes during the Early Triassic correlate with the lowest levels of biodiversity in both marine and terrestrial vertebrates, suggesting the rate of recovery was controlled by the environmental conditions (Sun et al., 2012) and the capacity of an organism to survive/adapt. Along with increased temperatures, anoxia and H_2S (Grasby et al., 2012) in shallow waters, help to explain the negative and positive shifts observed in the $\delta^{13}C$ of carbonates and organic biomass after the PTB and stabilizing during the Middle Triassic (Corsetti et al., 2005; Korte and Kozur, 2010).

The isotopic excursion associated with the end-Permian extinction event has been studied worldwide, while isotopic characterization of Triassic sections has attracted less attention. A publication by Corsetti et al (2005) contains a comprehensive summary of the available isotopic data spanning the Early and Middle Triassic, showing the extraordinarily oscillatory nature of the isotopic record for that period. After the extinction event, a series of negative and positive excursions in the $\delta^{13}C_{carb}$ occurred during the Early Triassic (Payne and Kump, 2007; Payne et al., 2004). Two large positive excursions are observed near the Dienerian–Smithian and Smithian–Spathian Sub-Stage Boundaries and one in the early in the Anisian stage; also a marked negative excursion occurred during the Smithian (Corsetti et al., 2005; Korte et al., 2005; Payne et al., 2004).

Nevertheless, the exact causes of the isotopic excursions and their relationship with the rate of recovery seem to vary geographically and depend of local environmental conditions. With the aim of evaluating the paleoenvironmental conditions during the entire Early Triassic in the northern hemisphere, samples were collected from an outcrop in Svalbard spanning most of the Early Triassic and the contact with the Middle Triassic. Those samples were evaluated using "state of the art" techniques to characterize the organic content from a molecular and isotopic point of view. Results and outcomes of this part the investigation are in **Chapter 4**.

Abundant evidence of widespread anoxia during the Early Triassic implies ocean stratification/turnover at that time (Corsetti et al., 2005; Woods, 2005). Fluctuation of the oceanic redox conditions can be correlated to the variable carbon isotopic record of the Early Triassic; negative shifts in $\delta^{13}C$ of organic carbon (kerogen, $\delta^{13}C_{org}$) and carbonates ($\delta^{13}C_{carb}$) are associated with intensifying of the anoxic conditions and stratification, while positive shifts could be related to waning of the anoxia. Similarly, Payne et al (2004) suggested extraordinarily high C burial will result in positive shift of $\delta^{13}C_{carb}$, these episodes will exist at the time of low oxygen content in the surface waters and are potentially derived of increased in pCO_2 and warming; while lower burial of OC will led to the negative shifts. Fluctuation of the redox conditions in the seawater might be also related to volcanism (Grasby et al., 2012). Different scenarios have been tested by one-box ocean model by Payne and Kump

(2007) in order to constrain the carbon cycle disturbance that best explain the isotopic fluctuation during Early Triassic. Overall the authors proposed that only several pulses of C were released with different proportions of organic and mantle isotope compositions can explain the Early Triassic isotopic trends (Payne and Kump, 2007).

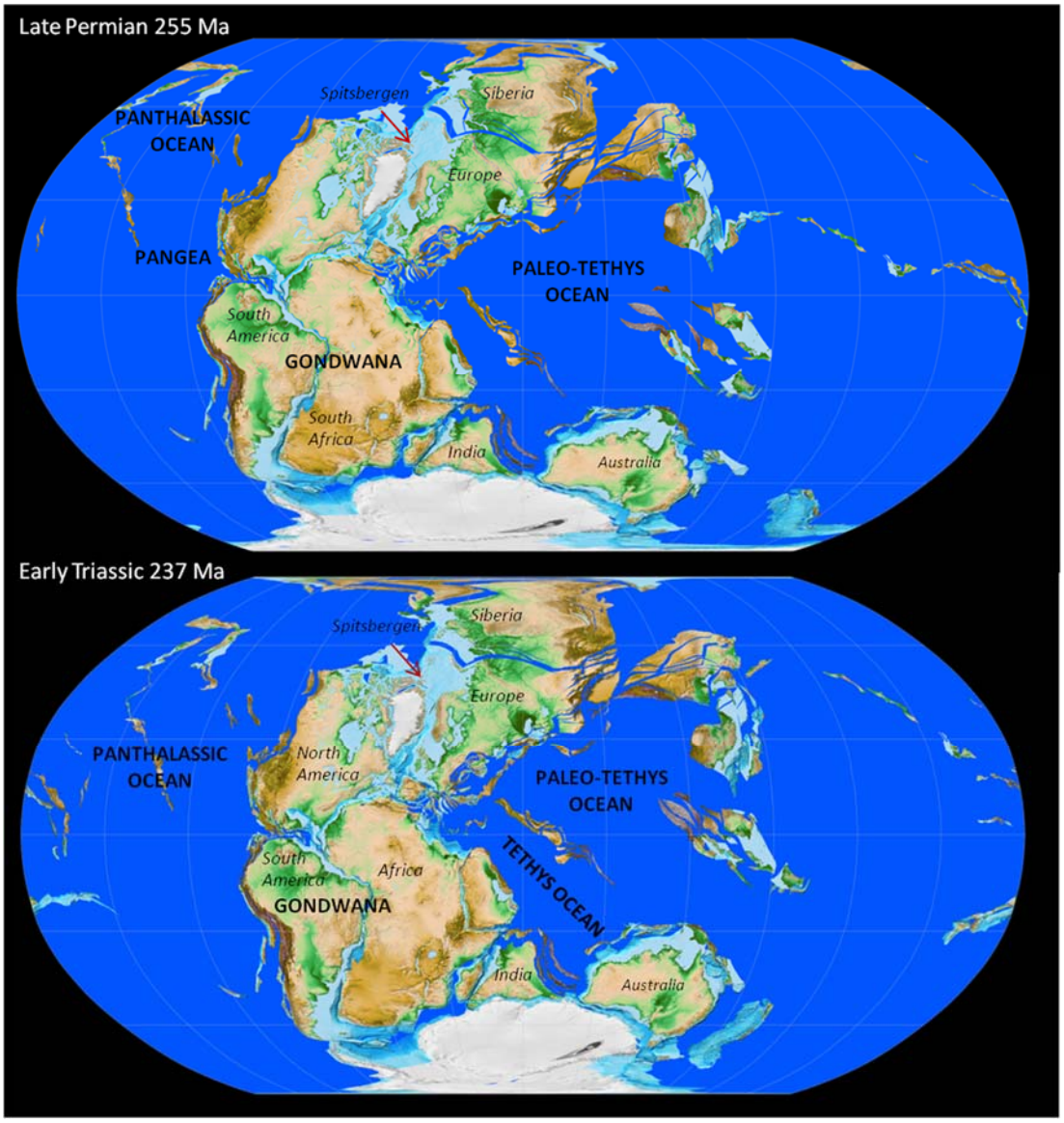

Figure 1. 7 Paleogeographic map of the End-Permain (255 Ma) and Early Triassic (237 Ma). Modified after GPlates 1.4 (http://www.gplates.org/).

Aims of this thesis

The main purpose of this PhD was to improve our understanding of the organic geochemistry of highly sulfidic microenvironments in ancient deposits, many of which have been associated with the most catastrophic biotic crises in the Phanerozoic. The major focus has been orientated to elucidate and reconstruct the biogeochemical changes that occur in oxygen-limited environments from an organic geochemistry point of view. H_2S rich environments have been important not only as a potential kill mechanism during extinction events, similar conditions have been recognized to be the setting of exceptional preservation not only for biomolecules but fossil of vertebrates and invertebrates. Sulfurization as a preservation pathway (vulcanization) have been broadly studied, however, the presence of an active sulfur cycle in the water column and the resulting euxinia play an important role in the preservation of organic-remains that requires further investigation. An organic and isotopic geochemistry approaches have been applied comprising the analyses of bulk stable isotopes ($\delta^{13}C_{org}$, $\delta^{13}C_{carbonate}$, $\delta^{34}S_{pyrite}$), identification and quantification of an ample variety of biomarkers and $\delta^{13}C$ and δD of individual hydrocarbons in two distinctive geological settings.

In order to track the paleoenvironmental and biogeochemical changes that resulted in the exceptional preservation of fossils from the Gogo Formation, multiple analyses were made in a carbonate concretion containing a well-preserved invertebrate. In **Chapter 2** biomarkers were identified and quantified from different layers of the concretion, giving a sense of redox and microbial changes through time, from the initial stage of the invertebrate encapsulation until the final stage of concretion-formation. The role of PZE in the preservation of fossils was investigated and Chlorobi-derived biomarkers were identified in the free and sulfur-bound extracts of the fossil and surrounding carbonate matrix. The association of steroids to the fossil remains gave this investigation the opportunity to narrow the identification of the fossil specimen. The isotopic characterization of hydrocarbons in the fossil and surrounding carbonate layers, allow for reconstruction of the microbial and algal community present in the water column at the time of deposition.

Chapter 3 expands on the exhaustive characterization of the carbonate concretion used in **Chapter 2**, and presents an unprecedented example of remarkable survival of biomolecules for a sample of 380 Ma old. The main goal in **Chapter 3** was to identify in a very detailed old-fashion approach all the steroidal compounds that were preserved within the total extractable biomass of the fossil and matrix (within detection limits) and establish their diagenetic relationships. In order to determine the origin/source of the intact biolipids present in the concretion quantitative analysis were made in different concentric layers of the concretion, preventing the mistaken identification of recent biomass. The potential link of the intact functionalized steroids and their diagenetic derivatives found coexisting in the same sample was investigated and compared with the diagenetic pathway of steroids from the literature back in the 1980's. The coexistence of sterols and their diagenetic transformation products (geomolecules) in a carbonate concretion allowed here for the investigation of the mechanism that explains the progressive transformations of biomarkers in the absence of elevated temperatures to drive the physicochemical reactions.

Chapter 4 aims to establish the environmental and biotic changes that surrounded the marine ecosystem following the major extinction episode at around the PTB, by a systematic and high-resolution characterization of an extended outcrop section spanning sediments from the Early Triassic from Spitsbergen, Svalbard, paleogeographically located in the shallow shelf area of the Boreal Sea. In order to improve our understanding of global paleoenvironmental conditions at this time, this part of the investigation focused on building a comprehensive dataset, comparable worldwide, in order to further explore the level of biotic stress reflected in changes to the microbial assemblage during the Early Triassic. To achieve these goals identification and quantification of biomarkers -susceptible to source and environmental conditions- along with C and H isotopic characterization of individual compounds and bulk biomass was conducted. Also, a systematic stratigraphic Rock-Eval characterization combined with palynolgical and sedimentological analyses were achieved in this study allowing for comparison between the Boreal and Tethyan regions in well-framed geological context. These results can be used to investigate different theories of e.g. algal productivity and anoxia, postulated to occur during the

recovery of the PTB extinction; contributing to a better understanding of the Early Triassic shallow marine paleoenvironment of the Boreal Sea.

In general this investigation presents the successful application of integrated biomarker and stable isotope approaches to reconstruct highly sulfidic ancient marine depositional environments as consequence of ecological and environmental perturbations.

References

Algeo, T., Scheckler, S., 2010. Land plant evolution and weathering rate changes in the Devonian. Journal of Earth Science 21, 75-78.

Algeo, T.J., Chen, Z.Q., Fraiser, M.L., Twitchett, R.J., 2011. Terrestrial–marine teleconnections in the collapse and rebuilding of Early Triassic marine ecosystems. Palaeogeography, Palaeoclimatology, Palaeoecology 308, 1-11.

Algeo, T.J., Scheckler, S.E., 1998. Terrestrial-marine teleconnections in the Devonian: links between the evolution of land plants, weathering processes, and marine anoxic events. Philosophical Transactions of the Royal Society of London. Series B: Biological Sciences 353, 113-130.

Algeo, T.J., Twitchett, R.J., 2010. Anomalous Early Triassic sediment fluxes due to elevated weathering rates and their biological consequences. Geology 38, 1023-1026.

Andersen, N., Paul, H.A., Bernasconi, S.M., McKenzie, J.A., Behrens, A., Schaeffer, P., Albrecht, P., 2001. Large and rapid climate variability during the Messinian salinity crisis: Evidence from deuterium concentrations of individual biomarkers. Geology 29, 799-802.

Anderson, L.G., Dyrssen, D., Hall, P.O.J., 1988. On the sulphur chemistry of a super-anoxic fjord, Framvaren, South Norway. Marine Chemistry 23, 283-293.

Bambach, R.K., 2006. Phanerozic Biodiversity Mass Extinctions. Annual Review of Earth and Planetary Sciences 34, 127-155.

Barnosky, A.D., Matzke, N., Tomiya, S., Wogan, G.O.U., Swartz, B., Quental, T.B., Marshall, C., McGuire, J.L., Lindsey, E.L., Maguire, K.C., Mersey, B., Ferrer, E.A., 2011. Has the Earth/'s sixth mass extinction already arrived? Nature 471, 51-57.

Brocks, J.J., Pearson, A., 2005. Building the Biomarker Tree of Life. Reviews in Mineralogy and Geochemistry 59, 233-258.

Brown, T., Kenig, F., 2004, Water column structure during deposition of Middle Devonian–Lower Mississippian black and green/gray shales of the Illinois and Michigan Basins: A biomarker approach: Palaeogeography, Palaeoclimatology, Palaeoecology, v. 215, p. 59–85.

Benton, M., 1995. Diversification and extinction in the history of life. Science 268, 52-58.

Benton, M.J., Twitchett, R.J., 2003. How to kill (almost) all life: the end-Permian extinction event. Trends in Ecology & Evolution 18, 358-365.

Berner, R.A., 2002. Examination of hypotheses for the Permo–Triassic boundary extinction by carbon cycle modeling. Proceedings of the National Academy of Sciences 99, 4172-4177.

Berner, R.A., 2006. GEOCARBSULF: A combined model for Phanerozoic atmospheric O2 and CO2. Geochimica et Cosmochimica Acta 70, 5653-5664.

Bigeleisen, J., Wolfsberg, M., 1958. Theoretical and experimental aspects of isotope effects in chemical kinetics. Advances in Chemical Physics, Volume 1, 15-76.

Bond, D.P.G., Wignall, P.B., 2008. The role of sea-level change and marine anoxia in the Frasnian–Famennian (Late Devonian) mass extinction. Palaeogeography, Palaeoclimatology, Palaeoecology 263, 107-118.

Buggisch, W., Joachimski, M.M., 2006. Carbon isotope stratigraphy of the Devonian of Central and Southern Europe. Palaeogeography, Palaeoclimatology, Palaeoecology 240, 68-88.

Burgoyne, T.W., Hayes, J.M., 1998. Quantitative production of H2 by pyrolysis of gas chromatographic effluents. Analytical Chemistry 70, 5136-5141.

Chen, Z.-Q., Benton, M.J., 2012. The timing and pattern of biotic recovery following the end-Permian mass extinction. Nature Geoscience 5, 375-383.

Collister, J.W., Lichtfouse, E., Hieshima, G., Hayes, J.M., 1994. Partial resolution of sources of n-alkanes in the saline portion of the Parachute Creek Member, Green River Formation (Piceance Creek Basin, Colorado). Organic Geochemistry 21, 645-659.

Copp, I., 2000. Subsurface Facies Analysis of Devonian Reef Complexes Lennard Shelf, Canning Basin. Western Australia: Western Australia Geological Survey.

Corsetti, F.A., Baud, A., Marenco, P.J., Richoz, S., 2005. Summary of Early Triassic carbon isotope records. Comptes Rendus Palevol 4, 473-486.

De Leeuw, J. W. D., Bergen, P. F. V., Aarssen, B. G. K. V., Gatellier, J.-P. L. A., Damsté, J. S. S., Collinson, M. E., Ambler, R. P., Macko, S., Curry, G. B., Eglinton, G., and Maxwell, J. R., 1991, Resistant Biomacromolecules as Major Contributors to Kerogen [and Discussion]: Philosophical Transactions: Biological Sciences, v. 333, no. 1268, p. 329-337.

Field, C.B., Behrenfeld, M.J., Randerson, J.T., Falkowski, P., 1998. Primary Production of the Biosphere: Integrating Terrestrial and Oceanic Components. Science 281, 237-240.

Freeman, K.H., 2001. Isotopic Biogeochemistry of Marine Organic Carbon. Reviews in Mineralogy and Geochemistry 43, 579-605.

Foster, W.J., Twitchett, R.J., 2014. Functional diversity of marine ecosystems after the Late Permian mass extinction event. Nature Geosci 7, 233-238.

Gaines, S. M., Eglinton, G., and Rullkötter, J., 2009, Echoes of life : what fossil molecules reveal about earth, New York, Oxford University Press, Inc.

Grard, A., Francois, L., Dessert, C., Dupré, B., and Godderis, Y., 2005, Basaltic volcanism and mass extinction at the Permo-Triassic boundary: environmental impact and modeling of the global carbon cycle: Earth and Planetary Science Letters, v. 234, p. 207-221.

Grasby, S.E., Beauchamp, B., Embry, a., Sanei, H., 2012. Recurrent Early Triassic ocean anoxia. Geology 41, 175-178.

Grice, K., Brocks, J.J., 2011. Biomarkers (organic, compound specific isotopes), in: Reitner, J., Thiel, V. (Eds.), Encyclopedia of Geobiology.

Grice, K., 2001. $\delta^{13}C$ as an indicator of paleoenvironments: A molecular approach, in: Unkovich, M., Pate, J., McNeill, A., Gibbs, J. (Eds.), Application of stable isotope techniques to study biological processes and functioning ecosystems. Kluwer Academic Publishers, pp. 247-281.

Grice, K., Cao, C., Love, G.D., Böttcher, M.E., Twitchett, R.J., Grosjean, E., Summons, R.E., Turgeon, S.C., Dunning, W., Jin, Y., 2005. Photic zone euxinia during the Permian-triassic superanoxic event. Science 307, 706-709.

Grice, K., Gibbison, R., Atkinson, J.E., Schwark, L., Eckardt, C.B., Maxwell, J.R., 1996a. Maleimides (1H-pyrrole-2,5-diones) as molecular indicators of anoxygenic photosynthesis in ancient water columns. Geochimica et Cosmochimica Acta 60, 3913-3924.

Grice, K., Schaeffer, P., Schwark, L., Maxwell, J.R., 1996b. Molecular indicators of palaeoenvironmental conditions in an immature Permian shale (Kupferschiefer, Lower Rhine Basin, north-west Germany) from free and S-bound lipids. Organic Geochemistry 25, 131-147.

Grice, K., Schouten, S., Nissenbaum, A., Charrach, J., Sinninghe Damsté, J.S., 1998. Isotopically heavy carbon in the C21 to C25 regular isoprenoids in halite-rich deposits from the Sdom Formation, Dead Sea Basin, Israel. Organic Geochemistry 28, 349-359.

Hayes, J.M., 1993. Factors controlling ^{13}C contents of sedimentary organic compounds: Principles and evidence. Marine Geology 113, 111-125.

Hayes, J.M., 2001. Fractionation of Carbon and Hydrogen Isotopes in Biosynthetic Processes. Reviews in Mineralogy and Geochemistry 43, 225-277.

Hays, L.E., Grice, K., Foster, C.B., Summons, R.E., 2012. Biomarker and isotopic trends in a Permian–Triassic sedimentary section at Kap Stosch, Greenland. Organic Geochemistry 43, 67-82.

Hebting, Y., Schaeffer, P., Behrens, A., Adam, P., Schmitt, G., Schneckenburger, P., Bernasconi, S.M., Albrecht, P., 2006. Biomarker Evidence for a Major Preservation Pathway of Sedimentary Organic Carbon. Science 312, 1627-1631.

Hedges, J. I., and Keil, R. G., 1995, Sedimentary organic matter preservation: an assessment and speculative synthesis.: Marine Chemistry, v. 49, p. 81-115.

Hedges, J. I., Keil, R. G., and Benner, R., 1997, What happens to terrestrial organic matter in the ocean?: Organic Geochemistry, v. 27, p. 195-212.

Hilkert, A., Douthitt, C., Schlüter, H., Brand, W., 1999. Isotope ratio monitoring gas chromatography/mass spectrometry of D/H by high temperature conversion isotope ratio mass spectrometry. Rapid Communications in Mass Spectrometry 13, 1226-1230.

Hoefs, J., 2009. Stable isotope geochemistry. 6th edition. Springer Berlin Heidelberg.

Kamo, S.L., Crowley, J., Bowring, S.A., 2006. The Permian-Triassic boundary event and eruption of the Siberian flood basalts: An inter-laboratory U–Pb dating study. Geochimica et Cosmochimica Acta 70, A303.

Kidder, D.L., Worsley, T.R., 2004. Causes and consequences of extreme Permo-Triassic warming to globally equable climate and relation to the Permo-Triassic extinction and recovery. Palaeogeography, Palaeoclimatology, Palaeoecology 203, 207-237.

Killops, S.D., Killops, V.J., 2005. Introduction to organic geochemistry. John Wiley & Sons.

Koopmans, M.P., Köster, J., Van Kaam-Peters, H.M.E., Kenig, F., Schouten, S., Hartgers, W.A., De Leeuw, J.W., Sinninghe Damsté, J.S., 1996. Diagenetic and catagenetic products of isorenieratene: Molecular indicators for photic zone anoxia. Geochimica et Cosmochimica Acta 60, 4467-4496.

Korte, C., Kozur, H., Joachimski, M., Strauss, H., Veizer, J.n., Schwark, L., 2004. Carbon, sulfur, oxygen and strontium isotope records, organic geochemistry and biostratigraphy across the Permian/Triassic boundary in Abadeh, Iran. International Journal of Earth Sciences, 565-581.

Korte, C., Kozur, H.W., 2010. Carbon-isotope stratigraphy across the Permian–Triassic boundary: A review. Journal of Asian Earth Sciences 39, 215-235.

Korte, C., Kozur, H.W., Veizer, J., 2005. $\delta^{13}C$ and $\delta^{18}O$ values of Triassic brachiopods and carbonate rocks as proxies for coeval seawater and

palaeotemperature. Palaeogeography, Palaeoclimatology, Palaeoecology 226, 287-306.

Krull, E.S., Retallack, G.J., 2000. 13 C depth profiles from paleosols across the Permian-Triassic boundary : Evidence for methane release. 1459-1472.

Kump, L.R., Arthur, M.A., 1999. Interpreting carbon-isotope excursions: carbonates and organic matter. Chemical Geology 161, 181-198.

Kump, L.R., Pavlov, A., Arthur, M.A., 2005. Massive release of hydrogen sulfide to the surface ocean and atmosphere during intervals of oceanic anoxia. Geology 33, 397-397.

Long, J.A., Trinajstic, K., 2010. The Late Devonian Gogo Formation Lägerstatte of Western Australia: Exceptional Early Vertebrate Preservation and Diversity. Annual Review of Earth and Planetary Sciences 38, 255-279.

Marynowski, L., Rakociński, M., Borcuch, E., Kremer, B., Schubert, B. A., and Jahren, A. H., 2011, Molecular and petrographic indicators of redox conditions and bacterial communities after the F/F mass extinction (Kowala, Holy Cross Mountains, Poland): Palaeogeography, Palaeoclimatology, Palaeoecology, v. 306, no. 1–2, p. 1-14.

Matthews, D., Hayes, J., 1978. Isotope-ratio-monitoring gas chromatography-mass spectrometry. Analytical Chemistry 50, 1465-1473.

McGhee, G.R., 1996. The Late Devonian Mass Extinctions: The Frasnian/Famennian Crisis. Columbia University Press.

Megonigal, J. P., Hines, M. E., and Visscher, P. T., 2004, Anaerobic metabolism: linkages to trace gases and aerobic processes, *in* WH, S., ed., Treatise on Geochemistry Volume 8, Biogeochemistry: Oxford, Elsevier-Pergamon, p. 317-424.

Melendez, I., Grice, K., Schwark, L., 2013a. Exceptional preservation of Palaeozoic steroids in a diagenetic continuum. Scientific Reports 3.

Melendez, I., Grice, K., Trinajstic, K., Ladjavardi, M., Greenwood, P., Thompson, K., 2013b. Biomarkers reveal the role of photic zone euxinia in exceptional fossil preservation: An organic geochemical perspective. Geology 41, 123-126.

Metcalfe, B., Twitchett, R.J., Price-Lloyd, N., 2011. Changes in size and growth rate of 'Lilliput' animals in the earliest Triassic. Palaeogeography, Palaeoclimatology, Palaeoecology 308, 171-180.

Metcalfe, I., Nicoll, R.S., Willink, R., Ladjavadi, M., Grice, K., 2013. Early Triassic (Induan–Olenekian) conodont biostratigraphy, global anoxia, carbon isotope excursions and environmental perturbations: New data from Western Australian Gondwana. Gondwana Research 23, 1136-1150.

Meyer, K.M., Kump, L.R., Ridgwell, A., 2008. Biogeochemical controls on photic-zone euxinia during the end-Permian mass extinction. Geology 36, 747-750.

Meyer, K.M., Yu, M., Jost, a.B., Kelley, B.M., Payne, J.L., 2011. $\delta^{13}C$ evidence that high primary productivity delayed recovery from end-Permian mass extinction. Earth and Planetary Science Letters 302, 378-384.

Murphy, A.E., Sageman, B.B., Hollander, D.J., 2000. Eutrophication by decoupling of the marine biogeochemical cycles of C, N, and P: A mechanism for the Late Devonian mass extinction. Geology 28, 427-430.

Murray, J.W., Stewart, K., Kassakian, S., Krynytzky, M., DiJulio, D., 2007. Oxic, suboxic, and anoxic conditions in the Black Sea, in: Yanko-Hombach, V., Gilbert, A.S., Panin, N., Dolukhanow, P.M. (Eds.), The black sea flood question, changes in coastline, climate and human settlement. Springer, Dordrecht.

Nabbefeld, B., Grice, K., Schimmelmann, A., Sauer, P.E., Böttcher, M.E., Twitchett, R.J., 2010a. Significance of δDkerogen, $\delta^{13}C$kerogen and $\delta^{34}S_{pyrite}$ from several Permian/Triassic (P/Tr) sections. Earth and Planetary Science Letters 295, 21-29.

Nabbefeld, B., Grice, K., Twitchett, R.J., Summons, R.E., Hays, L., Böttcher, M.E., Asif, M., 2010b. An integrated biomarker, isotopic and palaeoenvironmental study through the Late Permian event at Lusitaniadalen, Spitsbergen. Earth and Planetary Science Letters 291, 84-96.

Pancost, R.D., Crawford, N., Magness, S., Turner, A., Jenkyns, H.C., Maxwell, J.R., 2004. Further evidence for the development of photic-zone euxinic conditions during Mesozoic oceanic anoxic events. Journal of the Geological Society 161, 353-364.

Payne, J.L., Clapham, M.E., 2012. End-Permian Mass Extinction in the Oceans: An Ancient Analog for the Twenty-First Century? Annual Review of Earth and Planetary Sciences 40, 89-111.

Payne, J.L., Kump, L.R., 2007. Evidence for recurrent Early Triassic massive volcanism from quantitative interpretation of carbon isotope fluctuations. Earth and Planetary Science Letters 256, 264-277.

Payne, J.L., Lehrmann, D.J., Wei, J., Orchard, M.J., Schrag, D.P., Knoll, A.H., 2004. Large perturbations of the carbon cycle during recovery from the end-permian extinction. Science 305, 506-509.

Peters, K.E., Walters, C.C., Moldowan, J.M., 2005. The biomarker guide: Biomarkers and isotopes in the environment and human history, Second edition. Cambridge University Press, Cambridge

Playford, P.E., Hocking, R.M., Cockbain, A.E., 2009. Devonian Reef Complexes of the Canning Basin, Western Australia. Geological Survey of Western Australia Bulletin 145, 444.

Playford, P.E., Wallace, M.W., 2001. Exhalative Mineralization in Devonian Reef Complexes of the Canning Basin, Western Australia. Economic Geology 96, 1595-1610.

Popp, B.N., Laws, E.A., Bidigare, R.R., Dore, J.E., Hanson, K.L., Wakeham, S.G., 1998. Effect of phytoplankton cell geometry on carbon isotopic fractionation. Geochimica et Cosmochimica Acta 62, 69-77.

Quandt, L., Gottschalk, G., Ziegler, H., Stichler, W., 1977. Isotope discrimination by photosynthetic bacteria. FEMS Microbiology Letters 1, 125-128.

Raup, D.M., Sepkoski, J.J., 1982. Mass Extinctions in the Marine Fossil Record. Science 215, 1501-1503.

Reitner, J., & Thiel, V. (Eds.). (2011). Encyclopedia of geobiology. Springer.

Requejo, A.G., Allan, J., Creaney, S., Gray, N.R., Cole, K.S., 1992. Aryl isoprenoids and diaromatic carotenoids in Paleozoic source rocks and oils from the Western Canada and Williston Basins. Organic Geochemistry 19, 245-264.

Retallack, G.J., and Jahren, A.H., 2008, Methane release from igneous intrusion of coal during Late Permian extinction events: The Journal

Retallack, G.J., Sheldon, N.D., Carr, P.F., Fanning, M., Thompson, C.A., Williams, M.L., Jones, B.G., Hutton, A., 2011. Multiple Early Triassic greenhouse crises impeded recovery from Late Permian mass extinction. Palaeogeography, Palaeoclimatology, Palaeoecology 308, 233-251.

Schidlowski, M., Gorzawski, H., Dor, I., 1994. Carbon isotope variations in a solar pond microbial mat: Role of environmental gradients as steering variables. Geochimica et Cosmochimica Acta 58, 2289-2298.

Schidlowski, M., Matzigkeit, U., Krumbein, W.E., 1984. Superheavy organic carbon from hypersaline microbial mats. Naturwissenschaften 71, 303-308.

Schouten, S., Klein Breteler, W.C.M., Blokker, P., Schogt, N., Rijpstra, W.I.C., Grice, K., Baas, M., Sinninghe Damsté, J.S., 1998. Biosynthetic effects on the stable carbon isotopic compositions of algal lipids: implications for deciphering the carbon isotopic biomarker record. Geochimica et Cosmochimica Acta 62, 1397-1406.

Scott, J.H., O'Brien, D.M., Emerson, D., Sun, H., McDonald, G.D., Salgado, A., Fogel, M.L., 2006. An examination of the carbon isotope effects associated with amino acid biosynthesis. Astrobiology 6, 867-880.

Sepkoski Jr, J., 1986. Phanerozoic overview of mass extinction, Patterns and Processes in the History of Life. Springer, pp. 277-295.

Sessions, A.L., Burgoyne, T.W., Hayes, J.M., 2001. Correction of H3+ contributions in hydrogen isotope ratio monitoring mass spectrometry. Analytical Chemistry 73, 192-199.

Sessions, A.L., Burgoyne, T.W., Schimmelmann, A., Hayes, J.M., 1999. Fractionation of hydrogen isotopes in lipid biosynthesis. Organic Geochemistry 30, 1193-1200.

Sheehan, P.M., 2001. The late Ordovician mass extinction. Annual Review of Earth and Planetary Sciences 29, 331-364.

Sinninghe Damsté, J. S., De Leeuw, J. W., 1990. Analysis, structure and geochemical significance of organically-bound sulphur in the geosphere: State of the art and future research. Organic Geochemistry, 16, 1077-1101.

Sinninghe Damsté, J.S.S., Koopmans, M.P., 1997. The fate of carotenoids in sediments: an overview. Pure and applied chemistry 69, 2067-2074.

Sinninghe Damsté, J.S., Köster, J., 1998. A euxinic southern North Atlantic Ocean during the Cenomanian/Turonian oceanic anoxic event. Earth and Planetary Science Letters 158, 165-173.

Summons, R.E., and Powell, T.G., 1986, Chlorobiaceae in Palaeozoic seas revealed by biological markers, isotopes and geology: Nature, v. 319, p. 763–765.

Summons, R.E., Powell, T.G., 1987. Identification of aryl isoprenoids in source rocks and crude oils: biological markers for the green sulphur bacteria. Geochimica et Cosmochimica Acta 5. 557-566.

Sun, Y., Joachimski, M.M., Wignall, P.B., Yan, C., Chen, Y., Jiang, H., Wang, L., Lai, X., 2012. Lethally hot temperatures during the Early Triassic greenhouse. Science (New York, N.Y.) 338, 366-370.

Tissot, B. P. and Welte, D. H. (1984) Petroleum Formation and Occurrence. Springer-Verlag, New York.

Trinajstic, K., Marshall, C., Long, J., Bifield, K., 2007. Exceptional preservation of nerve and muscle tissues in Late Devonian placoderm fish and their evolutionary implications. Biology letters 3, 197-200.

Tulipani, S., Grice, K., Greenwood, P. F., Haines, P. W., Sauer, P. E., Schimmelmann, A., Summons, R. E., Foster, C. B., Böttcher, M. E., Playton, T., and Schwark, L., Changes of palaeoenvironmental conditions recorded in Late Devonian reef systems from the Canning Basin, Western Australia: A biomarker and stable isotope approach: Gondwana Research, (*in press*).

Twitchett, R.J., Looy, C.V., Morante, R., 2001. Rapid and synchronous collapse of marine and terrestrial ecosystems during the end-Permian biotic crisis. Geology, 351-354.

Urey, H.C., 1947. The thermodynamic properties of isotopic substances. Journal of the Chemical Society (Resumed), 562-581.

Vandenbroucke, M., and Largeau, C., 2007, Kerogen origin, evolution and structure: Organic Geochemistry, v. 38, no. 5, p. 719-833.

Volkman, J.K., Barrett, S.M., Blackburn, S.I., Mansour, M.P., Sikes, E.L., Gelin, F., 1998. Microalgal biomarkers: A review of recent research developments. Organic Geochemistry 29, 1163-1179.

Volkman, J. K. 2006. Lipid markers for marine organic matter. In Marine Organic Matter: Biomarkers, Isotopes and DNA (pp. 27-70). Springer Berlin Heidelberg.

Walliser, O., 1996. Global Events in the Devonian and Carboniferous, in: Walliser, O. (Ed.), Global Events and Event Stratigraphy in the Phanerozoic. Springer Berlin Heidelberg, pp. 225-250.

Wiese, F., Reitner, J., 2011. Critical Intervals in Earth History, in: J., R., V., T. (Eds.), Encyclopedia of Geobiology. Springer Netherlands.

Wignall, P.B., 2001. Large igneous provinces and mass extinctions. Earth-Science Reviews 53, 1-33.

Wignall, P.B., Twitchett, R.J., 1996. Oceanic Anoxia and the End Permian Mass Extinction. Science 272, 1155-1158.

Woods, A.D., 2005. Paleoceanographic and paleoclimatic context of Early Triassic time. Comptes Rendus Palevol 4, 463-472.

Xie, S., Pancost, R.D., Wang, Y., Yang, H., Wignall, P.B., Luo, G., Jia, C., Chen, L., 2010. Cyanobacterial blooms tied to volcanism during the 5 m.y. Permo-Triassic biotic crisis. Geology 38, 447-450.

Zhou, Y., Grice, K., Stuart-Williams, H., Farquhar, G.D., Hocart, C.H., Lu, H., Liu, W., 2010. Biosynthetic origin of the saw-toothed profile in $\delta^{13}C$ and $\delta^{2}H$ of n-alkanes and systematic isotopic differences between n-, iso- and anteiso-alkanes in leaf waxes of land plants. Phytochemistry 71, 388-403.

CHAPTER 2

Biomarkers reveal the role of photic zone euxinia in exceptional fossil preservation: An organic geochemical perspective

Ines Melendez, Kliti Grice, Kate Trinajstic, Mojgan Ladjavardi, Paul Greenwood and Katharine Thompson

Geology 41, 123-126, (2013)

Abstract

Photic zone euxinia (PZE) has proven important for elucidating biogeochemical changes that occur during oceanic anoxic events (OAE) including mass extinction and conditions associated with unique fossil preservation. Organic geochemical analyses of a 380 Ma invertebrate fossil including well-preserved soft tissues from the Gogo Formation of the Canning Basin, Western Australia showed biomarkers and stable isotopic values characteristic of PZE and a consortium of sulfate reducing bacteria (SRB) which lead to exceptional fossil and organic matter preservation. The carbonate concretion contained biomarkers from phytoplankton, Chlorobi and SRB with an increasing concentration toward the nucleus where the fossil is preserved. The spatial distribution of cholestane unequivocally associated with the fossilized tissue and its high relative abundance to the total steranes suggest it could be identified as a crustacean. The presence of an active sulfur cycle in this Devonian system - including sulfate reduction and the resulting euxinia - played a pivotal role in the preservation of a soft tissue body fossil and its associated low-maturity biomarker ratios.

Introduction

Photic Zone Euxinia (PZE) is defined as the presence of H_2S at the chemocline in the water column where oxygen is absent and light is available for photosynthesis by e.g. Chlorobi. Chlorobi play a prominent role in the sulfur cycle at the chemocline of stratified water columns (e.g., modern day Black Sea and Antarctic fjords) and their biomarkers provide the most direct molecular and isotopic evidence for the onset of anoxygenic photosynthesis in ancient water columns (i.e. PZE). PZE has proven important for elucidating biogeochemical changes that occur during OAEs, especially those conditions associated with the largest mass extinction event of life during the Phanerozoic (Grice et al., 2005). In addition, PZE has been reported in sediments hosting concretions with exceptionally preserved fossils (i.e., Lagerstätte) in which soft tissue is identified (e.g., Heimhofer et al., 2008; 2010; Schwark, et al., 2009). A unique set of ^{13}C-enriched biomarkers is derived from Chlorobi (often referred to as green sulfur bacteria), exclusive anaerobes which utilize H_2S during photosynthesis to fix CO_2 *via* the reversed tricarboxylic acid cycle (Summons and Powell, 1986; Hartgers et al., 1994; Grice et al., 1996; 1997; 2005). The Upper Devonian Gogo Fm. Lagerstätte of Australia preserves a unique reef fauna. It comprises a sequence of dark shales with thin beds of limestone and bedded micritic-limestone concretions and represents the basinal facies of the Devonian Reef complex. The Gogo Fm. interfingers with, and is equivalent to the Sadler Fm. marginal-slope facies, and overlies the platform facies of the Pillara Fm. (Playford et al., 2009 and references therein). A Late Givetian age, *hermanni* Zone is suggested for the lower part of the section, however, the fossil bearing nodules from the upper part of the section are well constrained to conodont zones 3-5 (Playford et al., 2009 and references therein). The exceptional three-dimensional preservation of the skeletal fossils has long been recognized but more recently soft tissues replaced by apatite have been described (Briggs et al., 2011; Long and Trinajstic, 2010). This paper investigates biogeochemical cycles leading to this exceptional preservation.

Method

A fossilized invertebrate (of unknown affinity) within a carbonate concretion was separated into 2 parts. A thin slice (ca. 5 mm thick) comprising the fossilized tissue was separated from the matrix. Additional samples were taken within the matrix, from concentric layers away from the nucleus (Fig. 2.1). All the samples were ground, organically extracted and separated by liquid chromatography into saturated, aromatic, fatty acid - methyl ester, alcohol and polars. Semi-quantitative analyses were performed in the saturated fraction and concentrations are reported in ppm (μg/g) of subsamples. Polar fractions were treated with Raney nickel to release the C-S bound compounds. Solid residues were treated with HCl (15%) to dissolve the carbonate minerals, after neutralization extraction was performed to release the carbonate-associated biomarkers. Gas chromatography –mass spectrometry (GC-MS) and Gas chromatography- isotope ratio mass spectrometry (GC-irMS) were performed on the saturated and aromatic fractions (detailed method description in the Appendix 2).

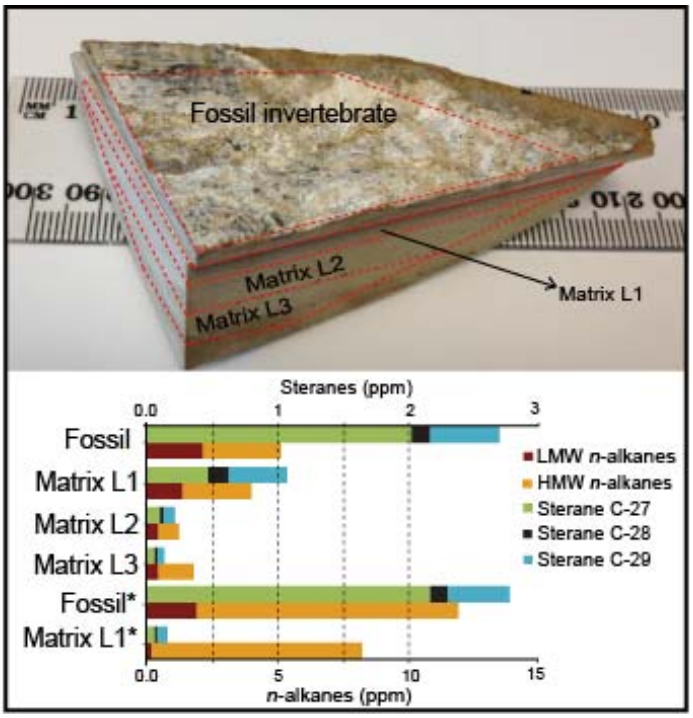

Figure 2. 1 Part of the concretion showing a thin fossil layer surrounded by a carbonate matrix. Soft tissue has been preserved as apatite and calcite. There is some staining associated with dendritic manganese. Different subsamples were taken from the concretion: fossil, and 3 different layers within the matrix. Concentrations of selected biomarkers in each layer and after decarbonation (*) are shown.

Quantification of *n*-alkanes was done in 2 ranges: low molecular weight (< C_{23}, LMW) and high molecular weight (>C_{23}, HMW).

Results and discussions

n-Alkanes, the regular isoprenoids pristane (Pr) and phytane (Ph), steranes, hopanes and components derived from Chlorobi pigments were the main compounds identified showing qualitative and quantitative (Fig. 2.1) differences in molecular composition as well as isotopic differences between the innermost (fossil) and the outermost samples of the concretion (matrix).

Relative thermal maturities of all the samples taken from the concretion were measured. The C-20 isomerization of steranes in the fossil sample is dominated by the thermally unstable biological epimer (20*R*), rather than the geologically favored *20S* configuration (Peters et al., 2005). The C_{29} 5α, 14α, 17α(H) sterane has a 20*R*/20*R*+20*S* ratio of 0.15 (note that 0.5–0.6 is at equilibrium). This data, in addition to an average ratio for 22,29,30-Trisnorneohopane (Ts) / Ts + 22,29,30-Trisnorhopane (Tm) of 0.26, the absence of diasteranes and triaromatic steroids are all consistent with relatively low thermal maturity in the preserved organic matter (OM) within the fossil. Similarly low thermal maturities have been reported previously in concretions from different geological ages and depositional settings (e.g. De Craen et al., 1999; Heimhofer et al., 2010; Pearson et al., 2005), all with relatively low concentrations of clay minerals. Isomerization reactions are reported to be catalyzed by clay minerals (see Peters et al., 2005 and references therein; Nabbefeld et al., 2010) explaining the low thermal maturities reflected by biomarkers in the carbonate concretions.

Paleoenvironmental conditions

The concretions from the Gogo Fm. are thought to have formed under anoxic conditions by the action of bacteria (Long and Trinajstic, 2010; Playford et al., 2009). The average Pr/Ph ratio of 0.5 from the fossil is consistent with anoxic conditions during the time of fossil preservation and the anoxic to dysaerobic

conditions in the Devonian paleowater of the Gogo Fm. (Playford et al., 2009). However, evidence of PZE, accounting for the fossil preservation, are provided by the identification of a suite of monoaryl, diaryl and also triaryl isoprenoids with a 2,3,6/3,4,5-trimethyl-substitution pattern (Fig. 2.2A), largely attributed to carotenoid pigments of Chlorobi. The intact biomarkers e.g., isorenieratane, renieratane and the Devonian marker, paleorenieratane (Fig. 2.2; Fig. A2.1) were also identified. These biomarkers represent direct evidence for PZE conditions also globally associated with deposition of -OM-rich sediments and mass extinction events during the Phanerozoic (Summons and Powell, 1986; Brown and Kenig, 2004; Grice et al., 2005; Marynowski et al., 2011). The extent of the PZE that accompanied the fossil preservation was evaluated based on the Aryl Isoprenoid Ratio (AIR) proposed by Schwark and Frimmel (2004) and compared with oils, which source rock have been proposed to be the anoxic muds of the Gogo Fm. (Playford et al., 2009 and references therein) and also with euxinic intervals of the Gogo Fm. from a core collected in 2010 in the Canning Basin (Tulipani et al., 2014). The plot (Fig. 2.2C) suggests anoxic conditions for all the samples evaluated, however the lowest AIR was found in the fossil, indicating persistent PZE at the time of fossil preservation and episodic PZE conditions for the deposition of the muds.

It has been previously suggested that derivatives of Chlorobi carotenoids, in particular aryl isoprenoids, can be generally formed *via* thermal-induced electrocyclic reactions (Xinke et al., 1990). However, crocetane, previously reported to be a thermal product of isorenieratane in Devonian samples (oils and sediments see Maslen et al., 2009) from the Gogo Fm. (Greenwood and Summons, 2003) is absent in the concretion. Desulfurized aryl isoprenoids were obtained from the polar fraction of the fossil and were dominated by a C_{32} triaryl isoprenoid and a limited distribution of mono and diaryl isoprenoids (Fig. 2.2B). Sulfurization of biomarkers occurs at early stages of diagenesis and given the low maturity of the sample, these Chlorobi derived biomarkers may be formed by a radical reaction at the time of deposition and/or within the chemocline, being produced by electrocyclic reactions initiated by light and not associated with sub-thermal processes (Grice et al., 1996; 1997).

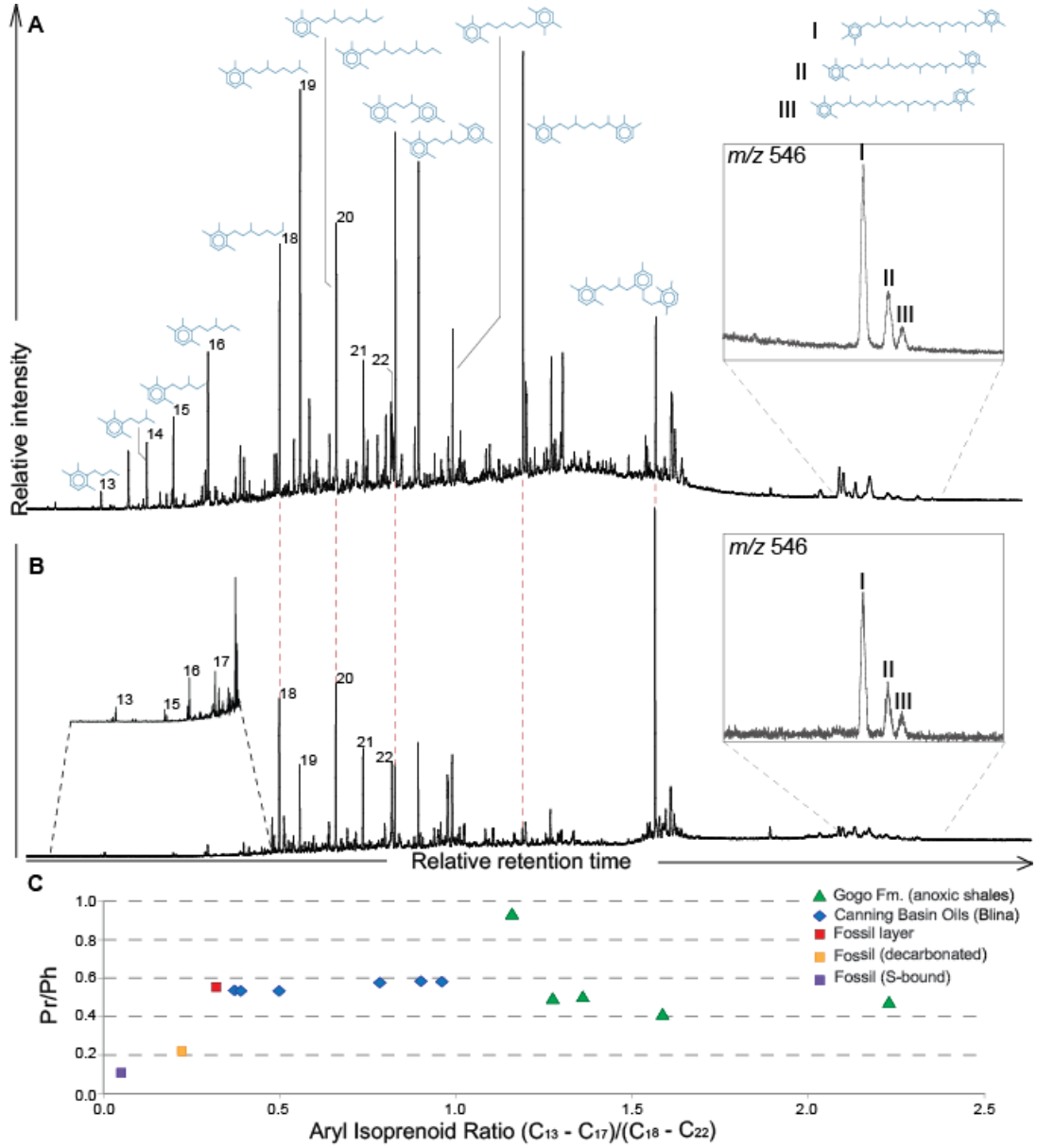

Figure 2. 2 GC-MS selected ion recording of *m/z* 133, a fragment ion characteristic for aryl isoprenoids (AI) of the aromatic hydrocarbon fraction (numbers on the chromatogram refer to numbers of carbon). Compounds were identified by comparison with typical mass spectra and standards (Supplementary information). (A) Aromatic fraction of the fossil shows a pseudo-homologous series of AI ranging from C_{13}-C_{21} with a 2, 3, 6/2, 3, 4-trimethyl substitution pattern. Diaryl (C_{21}-C_{26}) and triaryl isoprenoids (C_{32}) were also identified. The biomarkers isorenieratane (II), renieratane (III); and Devonian Chlorobi derived marker, paleorenieratane (I), were identified. (B) Aromatic fraction, released from the polar fraction of the fossil upon Raney-Nickel desulfurization, shows a similar AI distribution to (A), including the same intact carotenoids along with some aryl, diaryl and particularly abundant C_{32} triaryl isoprenoids. Sulfurization of AI proves PZE conditions occurred at the early stages of diagenesis accompanying the fossil preservation. (C) Molecular redox indicators Pr/Ph ratio against AIR, where low AIR values indicate permanent PZE whereas high values indicate episodic conditions (Schwark and Frimmel, 2004).

Preservation of OM throughout sulfurization is an important pathway under anoxic conditions caused by reactions with H_2S produced by SRB at early stages of diagenesis, especially where low iron levels occur (Sinninghe Damsté and De Leeuw, 1990). The desulfurized saturated fraction showed a typical distribution for a paleoenvironment rich in H_2S, showing abundant *n*-alkanes (C_{15} to C_{32}) with an even-over-odd carbon predominance related with microbial sources from a highly saline and carbonate-rich environment (Dembicki et al., 1976; Summons et al., 2010). Also, the Pr/Ph ratio (0.13) is consistent with the prevailing reduction of phytol to dehydrophytol under euxinic conditions at the time of sulfur incorporation of the functionalized biolipids.

Chemotaxonomy

Quantitative analyses of *n*-alkanes and steranes performed on all extracted samples (Fig. 2.1) provide a sense of spatial variation within the concretion. Overall there is a greater abundance of biomarkers towards the fossil nucleus consistent with a high phytoplanktonic input (including the crustacean's diet) at the early stage of the concretion formation. The isotopic and molecular differences found in the saturated biomarkers of the concretion arise from three possible sources (i) sinking particles derived from phytoplankton, (ii) *in situ* decomposition products of secondary OM recycled by microbial activity of SRB building the concretion and more remarkable (iii) biomolecules associated with the invertebrate preserved within the fossilized soft tissue.

Steranes are common biomarkers derived from sterols present in the lipid membrane of Eukaryotes (Peters et al., 2005). In the fossil layer, where the invertebrate tissue is preserved, cholestane is the dominant sterane (75% of total steranes) and its concentration is up to 10 times more abundant compared to the external layers of the concretion (Fig. 2.3A; Fig. 2.1; Fig. A2.2). Comparable predominance of the C_{27} sterane was found in the S-bound fraction (Fig. 2.3B) as well as in the bitumen released after decarbonation of the fossil part (results not shown). The dominance of cholestane in this concretion is unique and suggests it is indigenous to the fossil biomass making it suitable as a marker for taxonomic identification. Even though the contribution of sterols from algae and cyanobacteria

cannot be excluded in the sample, amongst extant taxa similar predominance of the C_{27} sterol has only been reported in crustaceans and certain molluscs (Kanazawa, 2001 and references therein). The absence of the shell in the sample precludes this animal from the Mollusca. We here place the unidentified invertebrate within the sub-phylum Crustacea due to the presence of segmented muscle bands, preserved as apatite and calcite (Fig. A2.3; Fig. A2.4.) and the dominance of cholestane in the fossil layer, which is a diagenetic product of the cholesterol preserved in the tissue.

Cholesterol in a crustacean is obtained from an external source of cholesterol and/or dealkylation of sterols present in their algal diet, as they cannot biosynthesize it *de novo* (Kanazawa, 2001). Herbivory studies (Grice et al., 1998) show that the $\delta^{13}C$ of cholesterol serves as a conservative marker of dietary sterols at this trophic level. For instance, the $\delta^{13}C$ value of cholestane (–30.5 ‰) in the fossil (Fig. 2.3A) represents an average of the $\delta^{13}C$ value of the sterols in the Eukaryotic community from the upper part of the water column. Cholestane is enriched by 4.0 ‰ and 3.5 ‰ compared with the average of the C_{16} to C_{19} *n*-alkanes (–34.8 ‰) and Ph (–34.0 ‰), respectively (Fig. 2.3A). These isotopic disparities are consistent with the different biosynthetic pathways for fatty acids and isoprenoids as well as their location of synthesis in phytoplankton cells (Schouten et al., 1998).

In contrast with the steranes, the long chain *n*-alkanes (>*n*-C_{22}) in the sample are widespread through the concretion and dominate the saturate fraction in both, fossil and matrix (Fig. 2.1) released after acid treatment, similar to results reported from bacterially-mediated ooids (Summons et al., 2010). Another source is proposed here for these long chain *n*-alkanes, which are relatively depleted in $\delta^{13}C$ (average –40‰) (Fig. 2.3A, 2.3C). Also, aliphatic composition are important in the diagenetic product of the biopolymer chitin in modern and fossil cuticles (Gupta et al., 2009 and references therein), but the $\delta^{13}C$ values of the aliphatic compounds reported here are inconsistent with a chitin source (Schimmelmann et al., 1986). On the other hand, the strong affinity of these ^{13}C-depleted *n*-alkanes with the carbonate minerals may be the result of autolithification from the remains of bacterial cell walls during bacterially-mediated soft tissue mineralization (Briggs, 2003).

SRB have been recognized to be strongly involved in the exceptional preservation of soft tissue by authigenic mineralization in anoxic sediments (Briggs, 2003 and references therein). Minerals such as calcite, apatite and dolomite along with pyrite (3-4 μm to 20 μm in diameter) were identified in the fossil (Appendix 2). Based on the evidence of anoxic conditions, mineral association and ^{13}C depleted long chain *n*-alkanes, SRB living at the sediment/water interface are proposed to promote the mineralization processes involved in the soft tissue preservation and contribute in the precipitation of the carbonate concretion under alkaline conditions (Londry and Des Marais, 2003; Londry et al., 2004; Marynowski et al., 2011; Ladygina et al., 2006; Briggs, 2003 and references therein). Although the $\delta^{13}C$ of the carbonate (-7.1 ‰) suggests a mixture of sources, SRB were probably fundamental at the early stages of the fossil preservation and diagenetic carbonates (Coleman, 1993; Duan et al., 1996).

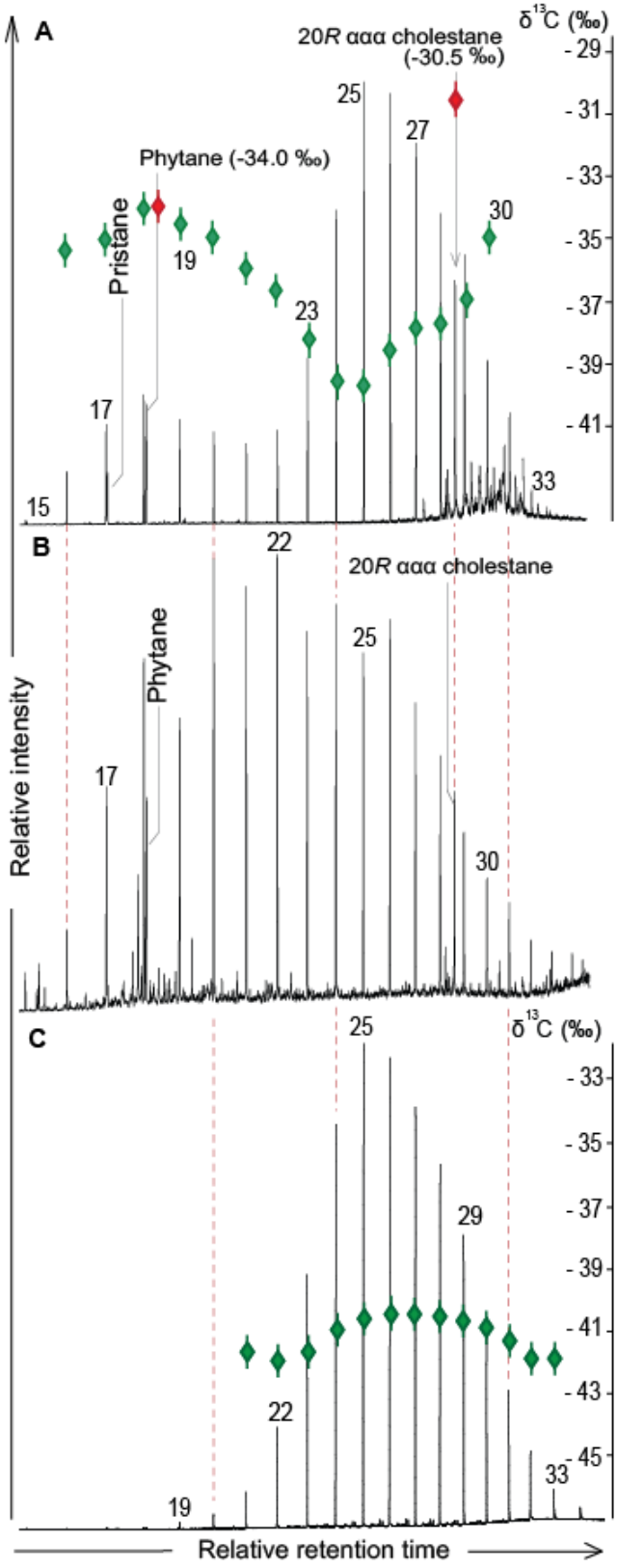

Figure 2. 3 Total ion chromatogram of GC-MS analysis and $\delta^{13}C$ of saturated hydrocarbon fraction from: (A) the extract of the fossil nucleus. N-alkanes in a bimodal distribution ($C_{15} – C_{21}$ and $C_{22} – C_{30}$) reflecting two sources. The biological stereoisomer ααα 20R cholestane was the most dominant sterane, its $\delta^{13}C$ (–30.5 ± 0.3 ‰) supports a source from algal sterol retained by the crustacean (e.g.,

Grice et al., 1998). Pristane (Pr) and phytane (Ph) show a ratio (Pr/Ph = 0.5) consistent with anoxic conditions. Ph (−34.0 ± 0.2 ‰) is ^{13}C depleted relative to cholestane by ~3‰ and both respect to the average C_{16} – C_{21} n-alkanes (−35 ‰) by up to 5‰. This isotope discrepancy reflects the biochemical pathway in Eukaryotic communities (Schouten et al., 1998). (B) Bitumen released by Raney-Nickel desulfurization of the fossil polar fraction. N-alkanes from C_{15} to C_{32} were the most abundant hydrocarbons, presenting a strong even/odd predominance. The biomarkers ααα 20*R* cholestane and Ph were abundant, indicating sulfurization of the functionalized lipids at early stages of diagenesis supporting highly euxinic conditions in the water column. (C) The extract of the carbonate matrix. Long chain n-alkanes from C_{19} to C_{34}, were dominant. Its $\delta^{13}C$ ranging from -40.5 to -42.0‰ has been attributed to remains of autolithified SRB playing a compelling role during the mineralization of the fossil tissue and concretion formation. Vertical error bars in the isotope data represent the standard deviation of at least two measurements.

Implications and Conclusions

The exceptional preservation of a set of biomarkers (phytoplanktonic, Chlorobi derived and SRB related) in the fossil points to rapid encasement of the crustacean enhanced by SRB under PZE, preventing further decomposition of the crustacean tissue and sinking OM. This work provides the first evidence of PZE playing a vital role in fossil (including soft tissue) and biomarker preservation. The presence of pyrite along with sulfurized biomarkers suggests preservation of the Crustacean occurring within the water column and/or the chemocline under persistent PZE (based on AIR). The SRB recycled the organic matter anaerobically, decreasing the alkalinity and leading to conditions that allow the carbonate concretion to accumulate. The $\delta^{13}C$ differences between cholestane, phytane and *n*-alkanes (< C_{23}) support high phytoplanktonic productivity in the upper water column (Schouten et al., 1998; Grice et al., 2005). It is likely that a phytoplankton bloom along with limited water circulation promoted the anoxic conditions and eventually the development of PZE in a stratified water body of the Devonian paleowater column.

Acknowledgments

Prof. KG and IM thank the ARC for QEII Discovery grant awarded to KG entitled: Characteristics of OM formed in toxic, sulfide-rich modern and ancient sediments for financial support and IM's PhD stipend. IM and ML acknowledge Curtin University for fee waivers and Associate/ Prof. KT for a Curtin Fellowship. Assistant/ Prof. PG thanks John de Laeter Centre for a Research Fellowship. Thanks also to Geoff Chidlow and Stephen Clayton for technical support, Prof. Tim Sendon (Australian National University) for providing the invertebrate nodule and Svenja Tulipani for providing unpublished data from core material from the Canning Basin. The authors thank anonymous reviewers for highly constructive comments.

References Cited

Briggs, D.E.G., 2003. The role of decay and mineralization in the preservation of softbodied fossils. Annual Review of Earth and Planetary Sciences 31, 275–301.

Briggs, D. E. G., Rolfe, W. D. I., Butler, P. D., Liston, J. J., and Ingham, J. K., 2011, Phyllocarid crustaceans from the Upper Devonian Gogo Formation, Western Australia: Journal of Systematic Palaeontology, v. 9, no. 3, p. 399-424, doi:10.1080/14772019.2010.493050.

Brown, T., Kenig, F., 2004, Water column structure during deposition of Middle Devonian–Lower Mississippian black and green/gray shales of the Illinois and Michigan Basins: A biomarker approach: Palaeogeography, Palaeoclimatology, Palaeoecology, v. 215, p. 59–85.

Coleman, M., 1993, Microbial processes: Controls on the shape and composition of carbonate concretions: Marine Geology, v. 113, p. 127–140, doi:10.1016/0025-3227(93)90154-N.

De Craen, M., Swennen, R., Keppens, E.M., Macaulay, C.I., and Kiriakoulakis, K., 1999, Bacterially mediated formation of carbonate concretions in the Oligocene Boom Clay of northern Belgium: Journal of Sedimentary Research, v. 69, p. 1098–1106.

Dembicki, H., Meinschein, W.G., and Hattin, D.E., 1976, Possible ecological and environmental significance of the predominance of even-carbon number C20–C30 n-alkanes: Geochimica et Cosmochimica Acta, v. 40, p. 203–208, doi:10.1016/0016-7037(76)90177-0.

Duan, W.M., Hedrick, D.B., Pye, K., Coleman, M.L., and White, D.C., 1996, A preliminary study of the geochemical and microbiological characteristics of modern sedimentary concretions: Limnology and Oceanography, v. 41, p. 1404–1414, doi:10.4319/lo.1996.41.7.1404.

Greenwood, P.F., and Summons, R.E., 2003, GC-MS detection and significance of crocetane and pentamethylicosane in sediments and crude oils: Organic Geochemistry, v. 34, p. 1211–1222, doi:10.1016/S0146-6380(03)00062-7.

Grice, K., Schaeffer, P. Schwark, L. and Maxwell, J., 1996, Molecular indicators of palaeoenvironmental conditions in an immature Permian shale (Kupferschiefer, Lower Rhine Basin, north-west Germany) from free and S-bound lipids: Organic Geochemistry v. 25, p.131-147, doi:10.1016/s0146-6380(96)00130.

Grice, K., Schaeffer, P., Schwark, L., and Maxwell, J., 1997, Changes in palaeoenvironmental conditions during deposition of the Permian Kupferschiefer (Lower Rhine Basin, north west Germany) inferred from molecular and isotopic composition of biomarker components: Organic Geochemistry, v. 26, p. 677–690, doi:10.1016/S0146-6380(97)00036-3.

Grice, K., Klein Breteler, W.C.M., Schouten, S., Grossi, V., De Leeuw, J.W., and Sinninghe Damsté, J.S., 1998, Effects of zooplankton herbivory on biomarker proxy records: Paleoceanography, v. 13, p. 686–693, doi:10.1029/98PA01871.

Grice, K., Cao, C., Love, G.D., Boettcher, M.E., Twitchett, R.J., Grosjean, E., Summons, R.E., Turgeon, S.C., Dunning, W., and Jin, Y., 2005, Photic zone euxinia during the Permian-Triassic superanoxic event: Science, v. 307, p. 706–709, doi:10.1126/science.1104323.

Gupta N., Cody, G., Tetlie, E., Briggs, D., Summons, R., 2009, Rapid incorporation of lipids into macromolecules during experimental decay of invertebrates: Initiation of geopolymer formation: Organic Geochemistry, v. 40, p. 589-594.

Hartgers, W.A., Sinninghe Damsté, J.S., Requejo, A.G., Allan, J., Hayes, J.M., Ling, Y., Xie, T.M., Primack, J., and De Leeuw, J.W., 1994, A molecular and carbon isotopic study towards the origin and diagenetic fate of diaromatic carotenoids: Organic Geochemistry, v. 22, p. 703–725, doi:10.1016/0146-6380(94)90134-1.

Heimhofer, U., Hesselbo, S.P., Pancost, R.D., Martill, D.M., Hochuli, P.A., and Guzzo, J.V.P., 2008, Evidence for photic-zone euxinia in the Early Albian Santana Formation (Araripe Basin, NE Brazil): Terra Nova, v. 20, p. 347–354, doi:10.1111/j.1365-3121.2008.00827.x.

Heimhofer, U., Schwark, L., Ariztegui, D., Martill, D.M., and Immenhauser, A., 2010, Geochemistry of fossiliferous carbonate concretions from the Cretaceous Santana Formation–assessing the role of microbial processes: EGU General Assembly: Geophysical Research Abstracts, v. 12, p. EGU9390.

Kanazawa, A., 2001, Sterols in marine invertebrates: Fisheries Science, v. 67, p. 997–1007, doi:10.1046/j.1444-2906.2001.00354.x.

Ladygina, N., Dedyukhina, E.G., and Vainshtein, M.B., 2006, A review on microbial synthesis of hydrocarbons: Process Biochemistry, v. 41, p. 1001–1014, doi:10.1016/j.procbio.2005.12.007.

Londry, K.L., and Des Marais, D.J., 2003, Stable carbon isotope fractionation by sulfate-reducing bacteria: Applied and Environmental Microbiology, v, 69, p. 2942–2949.

Londry, K.L., Jahnke, L.L., and Des Marais, D.J., 2004, Stable carbon isotope ratios of lipid biomarkers of sulfate-reducing bacteria: Applied and Environmental Microbiology, v. 70, p. 745–751, doi:10.1128/AEM.70.2.745-751.2004.

Long, J., and Trinajstic, K., 2010, The Late Devonian Gogo Formation Lagerstatte of Western Australia: Exceptional Early Vertebrate Preservation and Diversity: Annual Review of Earth and Planetary Sciences, v. 38, p. 255–279, doi:10.1146/annurev-earth-040809-152416.

Maslen, E., Grice, K., Gale, J., Hallmann, C., and Horsfield, B., 2009, Crocetane, a potential marker of photic zone euxinia in thermally mature sediments and crude oils of Devonian age: Organic Geochemistry, v. 40, p. 1–11, doi:10.1016/j.orggeochem.2008.10.005.

Marynowski, L., Rakociński, M., Borcuch, E., Kremer, B., Schubert, B. A., and Jahren, A. H., 2011, Molecular and petrographic indicators of redox conditions and bacterial communities after the F/F mass extinction (Kowala, Holy Cross Mountains, Poland): Palaeogeography, Palaeoclimatology, Palaeoecology, v. 306, no. 1–2, p. 1-14.

Nabbefeld, B., Grice, K., Schimmelmann, A., Summons, R.E., Troitzsch, A., and Twitchett, R.J., 2010, A comparison of thermal maturity parameters between freely extracted hydrocarbons (Bitumen I) and a second extract (Bitumen II) from within the kerogen matrix of Permian and Triassic sedimentary rocks: Organic Geochemistry, v. 41, p. 78–87, doi:10.1016/j.orggeochem.2009.08.004.

Pearson, M.J, Hendry, J.P., Taylor, C.W., and Russell, M.A, 2005, Fatty acids in sparry calcite fracture fills and microsparite cement of septarian diagenetic concretions, Geochimica et Cosmochimica Acta, v69, Ap 1773–1786.

Peters, K., Walters, C., and Moldowan, M., 2005, The Biomarker Guide: Cambridge, UK, Cambridge University Press, 1132 p.

Playford, P.E., Hocking, R.M., and Cockbain, A.E., 2009, Devonian reef complexes of the Canning Basin, Western Australia: Geological Survey of Western Australia: Bulletin, v. 145, p. 444.

Schouten, S., Klein Breteler, W., Blokker, P., Schogt, N., Rijpstra, W., Grice, K., Baas, M., and Sinninghe Damsté, J.S., 1998, Biosynthetic effects on the stable carbon isotopic compositions of algal lipids: Implications for deciphering the carbon isotopic biomarker record: Geochimica et Cosmochimica Acta, v. 62, p. 1397–1406, doi:10.1016/S0016-7037(98)00076-3.

Schwark, L., and Frimmel, A., 2004, Chemostratigraphy of the Posidonia Black Shale, SW-Germany: II. Assessment of extent and persistence of photic-

zone anoxia using aryl isoprenoid distributions: Chemical Geology, v. 206, no. 3–4, p. 231-248., doi: 10.1016/j.chemgeo.2003.12.008.

Schwark, L., Ferretti, A., Papazzoni, C.A., and Trevisani, E., 2009, Organic geochemistry and paleoenvironment of the Early Eocene "Pesciara di Bolca" Konservat-Lagerstätte, Italy: Palaeogeography, Palaeoclimatology, Palaeoecology, v. 273, p. 272–285, doi:10.1016/j.palaeo.2008.03.009.

Schimmelmann, A., Deniro, M., Poulicek, M., Voss-Foucart, M., Goffinet, G., Jeuniaux, C., 1986, Stable isotopic composition of chitin from arthropods recovered in archaeological contexts as palaeoenvironmental indicators: Journal of Archaeological Science, v. 13, p. 553-566.

Sinninghe Damsté, J. S., and De Leeuw, J. W., 1990, Analysis, structure and geochemical significance of organically-bound sulphur in the geosphere: State of the art and future research: Organic Geochemistry, v. 16, no. 4–6, p. 1077-1101, doi: 10.1016/0146-6380(90)90145-p.

Summons, R.E., and Powell, T.G., 1986, Chlorobiaceae in Palaeozoic seas revealed by biological markers, isotopes and geology: Nature, v. 319, p. 763–765, doi:10.1038/319763a0.

Summons R.E., Bird, L.R., Gillespie, A.L., Pruss, S.B., and Sessions, A.L., 2010, Lipid biomarkers in ooids from different locations and ages provide evidence for a common bacterial flora (invited): Fall Meeting, American Geophysical Union, San Francisco, California, 13–17 Dec.

Tulipani, S., Grice, K., Greenwood, P. F., Haines, P. W., Sauer, P. E., Schimmelmann, A., Summons, R. E., Foster, C. B., Böttcher, M. E., Playton, T., and Schwark, L., Changes of palaeoenvironmental conditions recorded in Late Devonian reef systems from the Canning Basin, Western Australia: A biomarker and stable isotope approach: Gondwana Research, (*in press*).

Xinke, Y., Pu, F., and Philp, R.P., 1990, Novels biomarkers found in South Florida Basin: Organic Geochemistry, v. 15, p. 433–438, doi:10.1016/0146-6380(90)90170-5.

Appendix 2

Materials and Methods

Sample Description

A calcareous concretion containing a well-preserved invertebrate fossil was collected from Paddy's Valley, Canning Basin, northwest Western Australia by Prof. Tim Sendon (Australian National University). These bedded carbonate concretions occur in clayey soils -derived from the rarely exposed soft shale (Playford et al., 2009). The carbonate concretion was found weathering out of the basinal black shales of the Frasnian-aged Gogo Formation, the oldest inter-reef deposited in the region. The nodules comprise thinly laminated carbonate muds.

The concretion was divided into part and counterpart and only one half used for the experiments described below. From the inner surface of the counterpart a thin slice (ca. 5 mm thick) containing most of the fossilized tissue was separated from the carbonate matrix. Concentrically away from the fossil nucleus additional samples were taken from the carbonate matrix. All the samples were analyzed using the same techniques. Procedure blanks were performed to ensure no contaminants were incorporated in the samples.

Extractions

Both fossil and carbonate concretions were weighed into a pre-extracted cellulose thimble. The extraction was performed using a pre-extracted Soxhlet extractor using a combination of dichloromethane (DCM) and methanol (CH3OH, 9:1). Activated copper turnings were added to remove elemental sulfur. The extraction was allowed to proceed for 72 hr until the solvent was clear. Excess solvent was removed from the extracts by rotary evaporation.

After the Soxhlet extraction, all sample residues were treated with hydrochloric acid (15% v/v) to remove the carbonate minerals. The de-carbonated residue was washed (x3) with pre-extracted deionized water and dried in an oven (40 ºC) overnight. After the residue was dry, each sample was extracted with a mixture of dichloromethane

(DCM) and methanol (CH3OH, 9:1) using an ultrasonic bath for 4 hours. The organic matter released after decarbonation was further separated by column chromatography as described below.

Column chromatography

The extract was separated by small columns (5.5 cm x 0.5 cm i.d.) filled with activated silica gel (120 °C, 8 hrs.). Five fractions were separated using an elution scheme of solvents of increasing polarity. Aliphatic hydrocarbons were eluted in the first fraction with hexane (1⅜ column dead volume (DV) determined empirically for each silica bed) followed by aromatic hydrocarbons in 2 DV of 4:1 hexane: DCM, ketones and fatty acid methyl esters (FAME) in 2 DV of DCM, alcohols in 2 DV of 4:1 DCM: ethyl acetate and the last polar fraction was eluted with 2 DV of DCM: methanol (7:3). The saturated and aromatic hydrocarbon fractions were reduced to near dryness with a N2 purge and the fractions analyzed by gas chromatography - mass spectrometry (GC-MS). In addition the saturated hydrocarbon fractions were analyzed by gas chromatography – isotope ratio monitoring - mass spectrometry (GC-irMS). See below for further details. Derivatization of FAME and alcohol fractions was done using 25µL of bis(trimethylsilyl)-trifluoroacetamide (BSTFA) and anhydrous pyridine. The mixture was heated up to 60-70 ºC in a sand bath for one hour and immediately after cool down analyzed by GC-MS.

Raney Nickel desulfurization

The polar fraction (ca. 5 mg) of the fossil extract was desulfurized with Raney nickel. The fraction was dissolved in a minimum amount of toluene. Raney nickel was washed with double distilled water and dry ethanol and then added to the polar fraction from the fossil extract. The mixture was stirred and refluxed under a N2 stream for 2 h. The desulfurization product was obtained by subsequent extraction with DCM and filtered over anhydrous MgSO4. The desulfurized polar fraction was further separated by column chromatography as described above. The saturated and aromatic hydrocarbon fractions were reduced to near dryness with a N2 purge and the fractions analyzed by gas chromatography - mass spectrometry (GC-MS).

GC-MS

GC-MS analyses were performed with a Hewlett Packard 6890 gas chromatograph (GC) interfaced to a Hewlett Packard 5973 mass selective detector (MSD). The aromatic and saturated hydrocarbon fractions, dissolved in *n*-hexane, were introduced via the Hewlett Packard 6890 Series Injector into the electronically pressure controlled (EPC) split/splitless injector (320 ºC) which was operated in the pulsed splitless mode. The GC was fitted with a 60 m x 0.25 mm i.d. WCOT fused silica capillary column coated with a 0.25 µm phenyl arylene polymer stationary phase (DB-5MS, J&W Scientific). The oven temperature was programmed from 40 °C to 325 °C (at 3 °C/min) with the initial and final hold times of 1 and 50 min, respectively. Ultra high purity helium was used as the carrier gas and maintained at a constant flow of 1.1 ml/min. The MSD was operated at 70 eV and the mass spectra were acquired in full scan mode, *m/z* 50-600 at ~ 4 scans per second and a source temperature of 230 °C. The aromatic hydrocarbon fractions were analyzed in full scan and selected ion-monitoring (SIM) modes. Diagenetic products of the C_{40} carotenoids of Chlorobi were analyzed by GC-MS to determine their relative retention times for the given GC conditions. Data processing was performed with the Hewlett Packard Chemstation software. Semi quantitative analyses were performed in the saturated fraction in order to estimate the relative concentration within the concretion of diagnostic compounds for this study (*n*-alkanes, pristane, phytane and staranes). Calibration curves were prepared using different standards (*n*-C_{17}, *n*-C_{25}, squalane and cholestane) ensuring a linear range within 0.2 ppm and 40 ppm. All the concentrations reported in the publication are in ppm (mg/kg) of subsample.

GC-irMS

A Micromass IsoPrime isotope ratio monitoring - mass spectrometer (irm-MS) coupled to a Hewlett Packard HP6890 gas chromatograph (60 m x 0.25 mm i.d., 0.25 µm thick DB-1 phase) was used to determine the $\delta^{13}C$ of the selected compounds in the saturated hydrocarbon fractions from the extracts obtained from the fossil and calcareous matrix. The samples were injected using pulsed splitless mode (30 seconds hold time at 15 psi above the head pressure of the column and 35 seconds

for purge). The GC oven was programmed with the same temperature ramp as the GC-MS analysis. The $\delta^{13}C$ compositions of the compounds were determined by integrating the 44, 45 and 46 mass ion currents, and are reported in parts per mil (‰) relative to the international Vienna Peedee Belemnite (VPDB) standard. Reported values are the average of at least two analyses.

Supplementary Figures

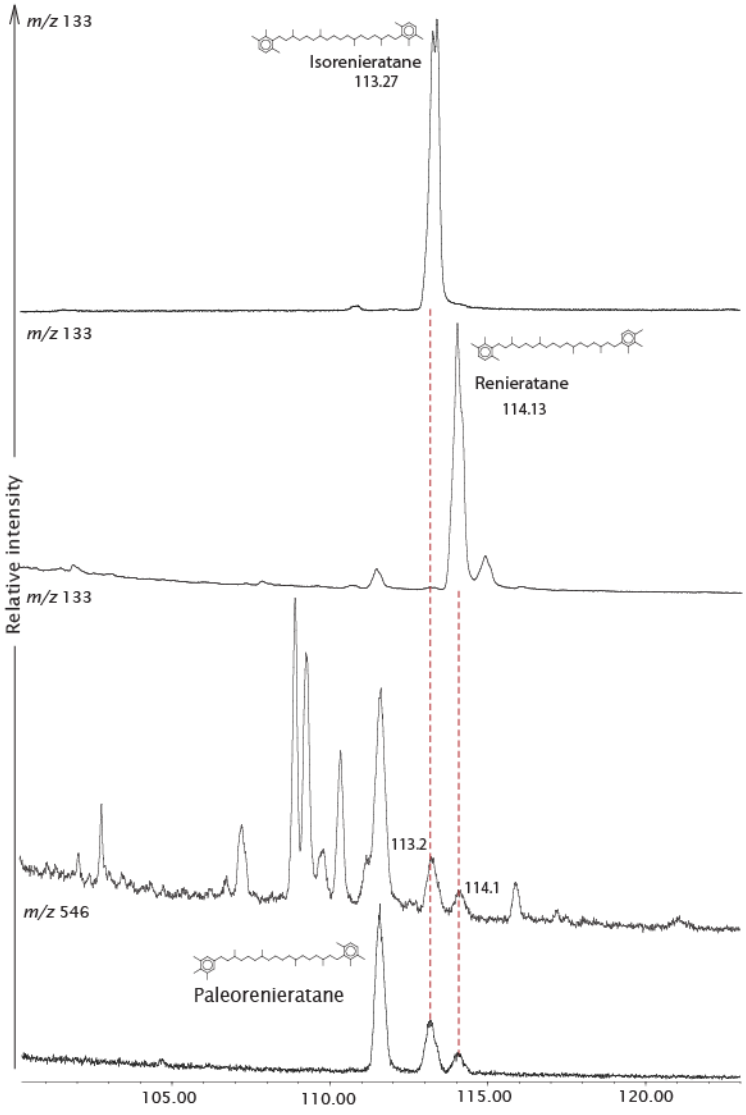

Figure A2. 1 GC-MS ion chromatogram of *m/z* 133 of standard compounds of authentic Chlorobi carotenoids (isorenieratane, Rt: 113.27 minutes and renieratane Rt: 114.13 minutes) were analyzed and their retention time and mass spectra were compared with the free and sulfur bound aromatic hydrocarbon fractions extracted from the fossil.

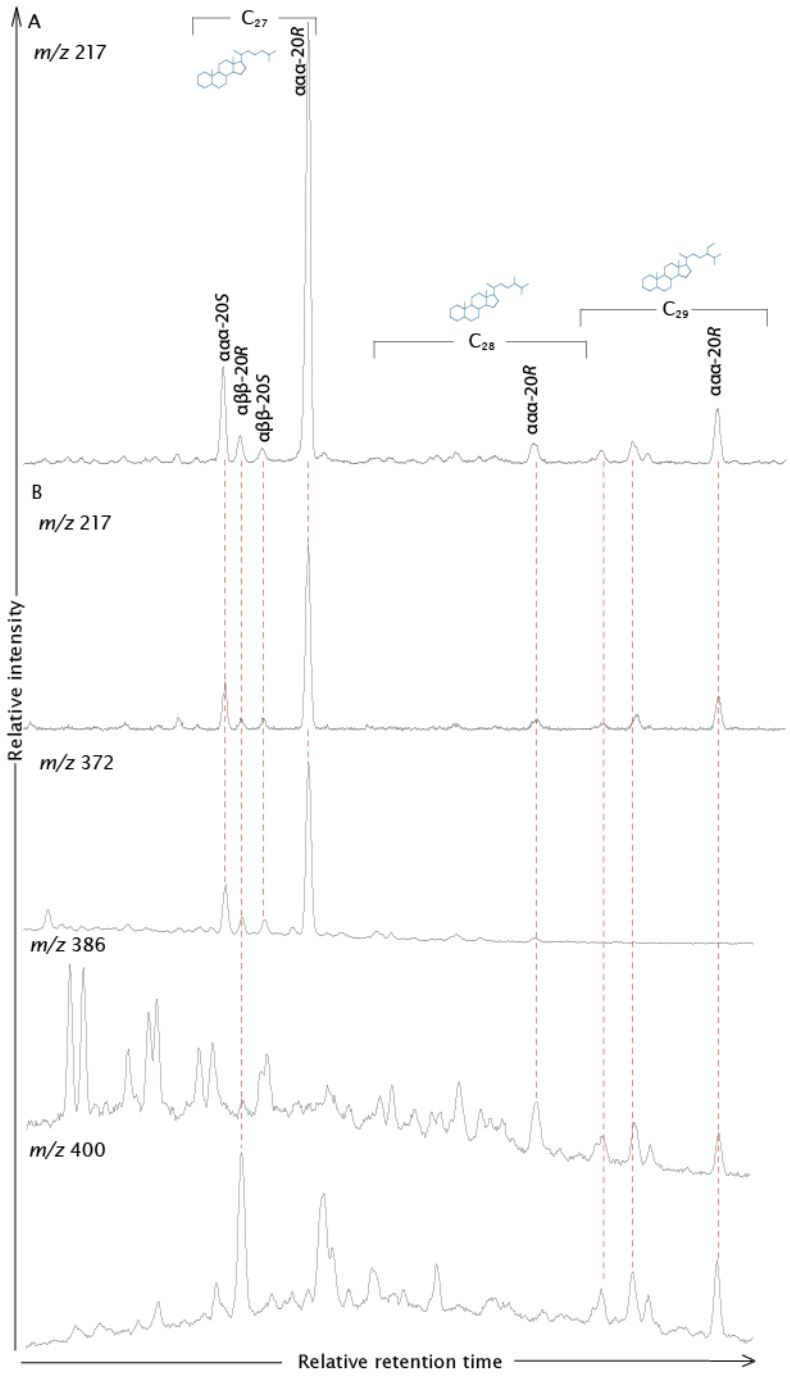

Figure A2. 2 Identification of steranes was performed by GC-MS selected ion chromatogram of the typical ions (*m/z* 217, 218) and molecular ions of the C_{27}, C_{28} and C_{29} steranes (*m/z* 372, 386 and 400). GC-MS ion chromatogram of *m/z* 217 of: A. Saturated hydrocarbons from the fossil extract B. S-bound saturated hydrocarbons released by Raney Nickel desulfurization from the polar fraction of the fossil extract.

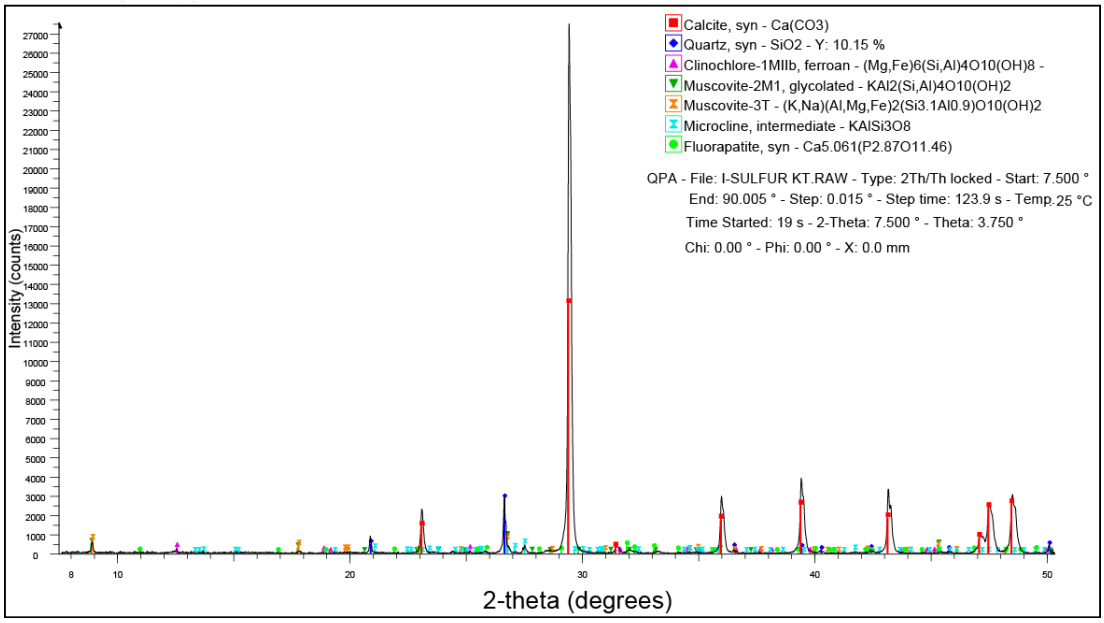

Figure A2. 3 Mineralogy of the fossil layer of the sample by X-Ray Diffraction analysis (XRD). Mineral as calcite and fluorapatite are part of the replacing minerals of the fossil tissue.

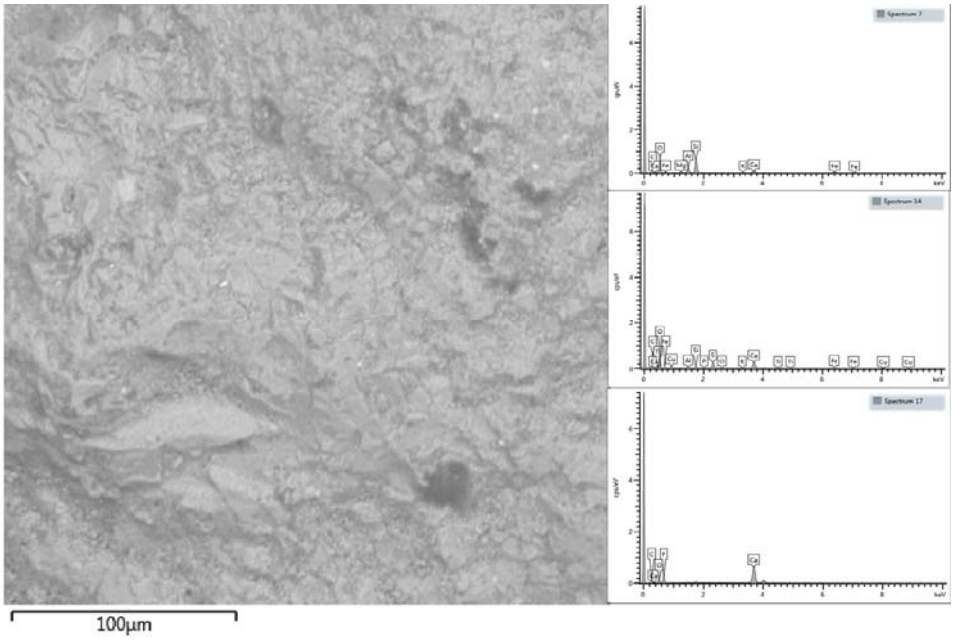

Figure A2. 4 Elemental mapping of the fossil surface by Scanning Electrom Microscopy (SEM). An association of carbon, oxygen and calcium is dominant, consistent with calcite in the fossil and concretion. Elements as Si, Al, K, Fe, Mg, Ti, P, F, and S, were also identified and corresponded with the minerals identified by XRD. Additional Fe and S were associated in aggregated from 4 to 20 µm in diameter, corresponding to pyrite.

Copyright

In compliance with Copyright regulations of The Geological Society of America©, the content of Chapter 2, previously published in the GSA Geology Journal (41(2), 123-126), have been cited throughout this thesis as Melendez et al., 2013.

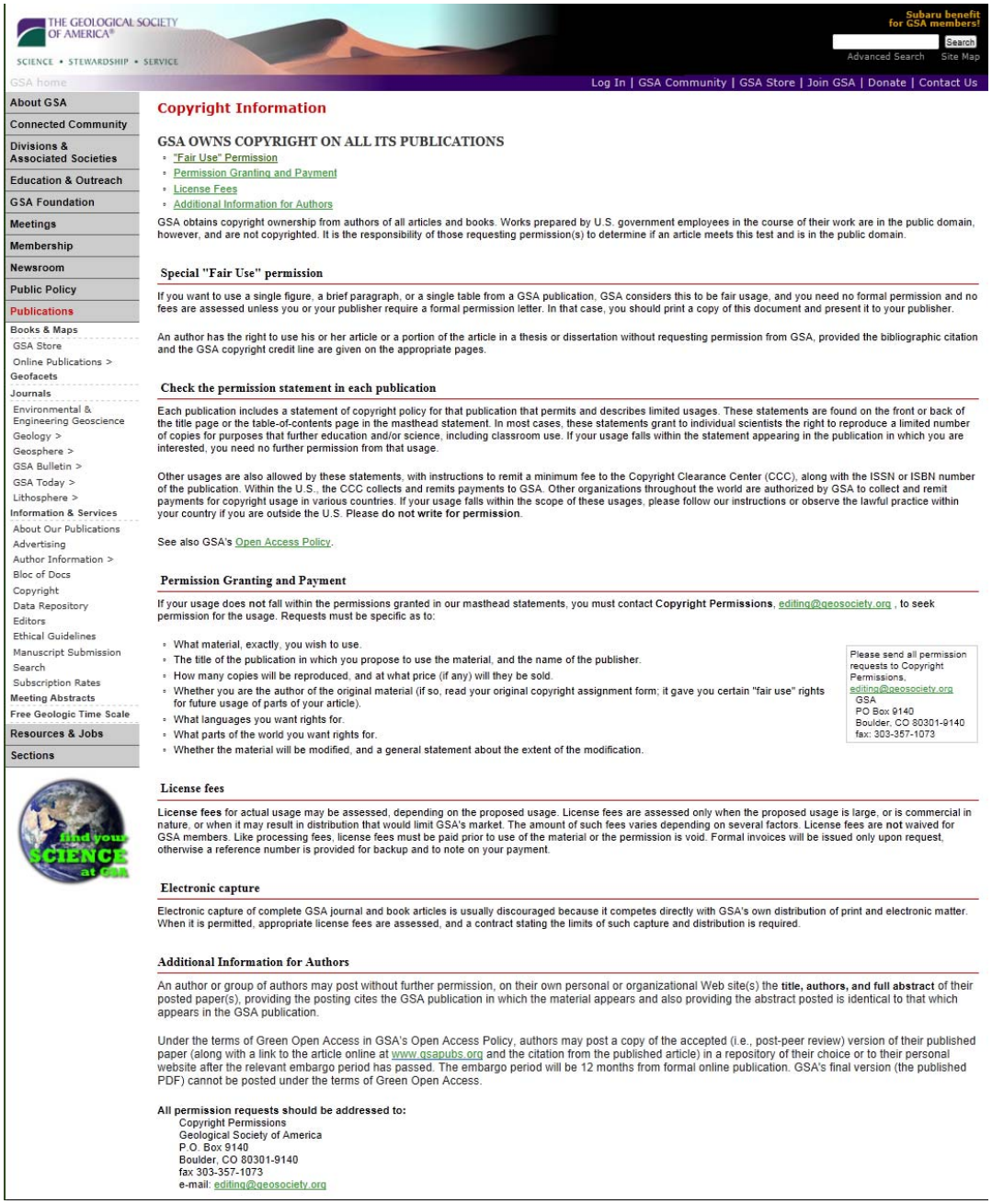

THE GEOLOGICAL SOCIETY OF AMERICA®
SCIENCE • STEWARDSHIP • SERVICE

Subaru benefit for GSA members!
Search
Advanced Search Site Map

GSA home
Log In | GSA Community | GSA Store | Join GSA | Donate | Contact Us

About GSA
Connected Community
Divisions & Associated Societies
Education & Outreach
GSA Foundation
Meetings
Membership
Newsroom
Public Policy
Publications
Books & Maps
GSA Store
Online Publications >
Geofacets
Journals
Environmental & Engineering Geoscience
Geology >
Geosphere >
GSA Bulletin >
GSA Today >
Lithosphere >
Information & Services
About Our Publications
Advertising
Author Information >
Bloc of Docs
Copyright
Data Repository
Editors
Ethical Guidelines
Manuscript Submission
Search
Subscription Rates
Meeting Abstracts
Free Geologic Time Scale
Resources & Jobs
Sections

find your SCIENCE at GSA

Copyright Information

GSA OWNS COPYRIGHT ON ALL ITS PUBLICATIONS

- "Fair Use" Permission
- Permission Granting and Payment
- License Fees
- Additional Information for Authors

GSA obtains copyright ownership from authors of all articles and books. Works prepared by U.S. government employees in the course of their work are in the public domain, however, and are not copyrighted. It is the responsibility of those requesting permission(s) to determine if an article meets this test and is in the public domain.

Special "Fair Use" permission

If you want to use a single figure, a brief paragraph, or a single table from a GSA publication, GSA considers this to be fair usage, and you need no formal permission and no fees are assessed unless you or your publisher require a formal permission letter. In that case, you should print a copy of this document and present it to your publisher.

An author has the right to use his or her article or a portion of the article in a thesis or dissertation without requesting permission from GSA, provided the bibliographic citation and the GSA copyright credit line are given on the appropriate pages.

Check the permission statement in each publication

Each publication includes a statement of copyright policy for that publication that permits and describes limited usages. These statements are found on the front or back of the title page or the table-of-contents page in the masthead statement. In most cases, these statements grant to individual scientists the right to reproduce a limited number of copies for purposes that further education and/or science, including classroom use. If your usage falls within the statement appearing in the publication in which you are interested, you need no further permission from that usage.

Other usages are also allowed by these statements, with instructions to remit a minimum fee to the Copyright Clearance Center (CCC), along with the ISSN or ISBN number of the publication. Within the U.S., the CCC collects and remits payments to GSA. Other organizations throughout the world are authorized by GSA to collect and remit payments for copyright usage in various countries. If your usage falls within the scope of these usages, please follow our instructions or observe the lawful practice within your country if you are outside the U.S. Please **do not write for permission**.

See also GSA's Open Access Policy.

Permission Granting and Payment

If your usage does **not** fall within the permissions granted in our masthead statements, you must contact **Copyright Permissions**, editing@geosociety.org , to seek permission for the usage. Requests must be specific as to:

- What material, exactly, you wish to use.
- The title of the publication in which you propose to use the material, and the name of the publisher.
- How many copies will be reproduced, and at what price (if any) will they be sold.
- Whether you are the author of the original material (if so, read your original copyright assignment form; it gave you certain "fair use" rights for future usage of parts of your article).
- What languages you want rights for.
- What parts of the world you want rights for.
- Whether the material will be modified, and a general statement about the extent of the modification.

Please send all permission requests to Copyright Permissions,
editing@geosociety.org
GSA
PO Box 9140
Boulder, CO 80301-9140
fax: 303-357-1073

License fees

License fees for actual usage may be assessed, depending on the proposed usage. License fees are assessed only when the proposed usage is large, or is commercial in nature, or when it may result in distribution that would limit GSA's market. The amount of such fees varies depending on several factors. License fees are **not** waived for GSA members. Like processing fees, license fees must be paid prior to use of the material or the permission is void. Formal invoices will be issued only upon request, otherwise a reference number is provided for backup and to note on your payment.

Electronic capture

Electronic capture of complete GSA journal and book articles is usually discouraged because it competes directly with GSA's own distribution of print and electronic matter. When it is permitted, appropriate license fees are assessed, and a contract stating the limits of such capture and distribution is required.

Additional Information for Authors

An author or group of authors may post without further permission, on their own personal or organizational Web site(s) the **title, authors, and full abstract** of their posted paper(s), providing the posting cites the GSA publication in which the material appears and also providing the abstract posted is identical to that which appears in the GSA publication.

Under the terms of Green Open Access in GSA's Open Access Policy, authors may post a copy of the accepted (i.e., post-peer review) version of their published paper (along with a link to the article online at www.gsapubs.org and the citation from the published article) in a repository of their choice or to their personal website after the relevant embargo period has passed. The embargo period will be 12 months from formal online publication. GSA's final version (the published PDF) cannot be posted under the terms of Green Open Access.

All permission requests should be addressed to:
Copyright Permissions
Geological Society of America
P.O. Box 9140
Boulder, CO 80301-9140
fax 303-357-1073
e-mail: editing@geosociety.org

CHAPTER 3

Exceptional preservation of Paleozoic steroids in a diagenetic continuum

Ines Melendez, Kliti Grice and Lorenz Schwark

SCIENTIFIC REPORTS | 3 : 2768 | DOI: 10.1038/srep02768

Abstract

The occurrence of intact sterols has been restricted to immature Cretaceous (~125 Ma) sediments with one report from the Late Jurassic (~165 Ma). Here we report the oldest occurrence of intact sterols in a Crustacean fossil preserved for ca. 380 Ma within a Devonian concretion. The exceptional preservation of the biomass is attributed to microbially induced carbonate encapsulation, preventing full decomposition and transformation thus extending sterol occurrences in the geosphere by 250 Ma. A suite of diagenetic transformation products of sterols was also identified in the concretion, demonstrating the remarkable coexistence of biomolecules and geomolecules in the same sample. Most importantly the original biolipids were found to be the most abundant steroids in the sample. We attribute the coexistence of steroids in a diagenetic continuum -ranging from stenols to triaromatic steroids- to microbially mediated eogenetic processes.

Introduction

Sterols form a specific group of triterpenoid biomolecules, generally abundant in eukaryotes where they fulfill various vital functions, including stabilization of cell membranes, signal messaging and serving as precursors to e.g. vitamins and hormones. Sterols, usually with 26 to 30 carbon atoms, possess specific structural features restricted to groups of organisms (Volkman, 1986). These biomolecules after senescence from aquatic producers undergo rapid re-mineralization under aerobic conditions in the upper water column. Only a small portion of the intact sterols produced in the euphotic zone endure eogenesis (earliest diagenesis), where microbially mediated transformations effectively yield geomolecules (Brassell et al., 1984; Gagosian et al., 1982; Peters et al., 2005; Mackenzie et al., 1982a; Mackenzie et al., 1982b). These compounds can then be related back to their natural product sterol precursors and are more stable in the geologic record. The presence of biological sterols in the rock record is limited to areas of low geothermal gradients and their preservation is enhanced by anaerobic conditions during their deposition and subsequent diagenesis, in particular, early sulfurization and reduction mediated by sulfur species (Adam et al., 2000; Hebting et al., 2006). Intact biological sterols have been observed at trace level concentrations in thermally immature marine shales (Comet et al., 1981) as old as the Upper Albian (~120Ma). In addition dinosterol and a 24-methylsterol have been reported from sediments of presumed early Jurassic age (Brassell et al., 1987). In these sediments original biolipids co-occur with a limited suite of their diagenetic derivatives, possibly due to incomplete degradation of lipids in the water column under high productivity conditions in the presence of selective microbial communities, such as sulfate reducers (Brassell et al., 1987; Comet et al., 1981).

Sterols are often recorded in petroleum as saturated and aromatic steroidal hydrocarbons and are associated with a series of complex transformations occurring during diagenesis and eventually catagenesis. The transformation of sterols during

eogenesis is controlled by microbial activity and low temperature physiochemical reactions, involving e.g.: stanols dehydration, sterenes isomerization, diasterenes and monoaromatic steranes formation and subsequent isomerization (Brassell et al., 1984; Mackenzie et al., 1982a; Mackenzie et al., 1982b). Eogenetic transformation of steroids is governed by the corresponding environmental conditions, temperature and availability of microbes and catalysts (e.g. clays and/or reduced sulfur). Additional catagenetic alteration of steroids is then attributed to thermodynamically driven abiotic physicochemical reactions with increasing temperature, causing complete aromatization, isomerization and cracking of steroids (Brassell et al., 1987; Brassell et al., 1984; Mackenzie et al., 1982a; Mackenzie et al., 1982b). At this stage functionalized steroids are expected to be completely transformed to a more stable form, thus the co-existance of sterols and their intermediate diagenetic products can only occur in immature sediments when incomplete microbial degradation has occurred (Brassell et al., 1984; Mackenzie et al., 1982a).

Recently, exceptional low thermal maturity steranes have been reported in a well preserved crustacean fossil, within a carbonate concretion from the Gogo Formation, a Devonian inter-reef deposit of the Canning Basin from the north of Western Australia (Melendez et al., 2013; Playford et al., 2009). The remarkable degree of organic matter preservation at the time of deposition of the crustacean was attributed to the occurrence of persistent euxinic conditions in the photic zone (PZE) prevailing in the ancient sea preventing aerobic degradation processes. These conditions were supported by an active consortium of sulfate reducing bacteria promoting early encapsulation of the biomass facilitating the formation of the carbonate concretion. Here we report even more outstanding preservation of biomolecules due to the observation of intact sterols in the fossilized crustacean, which are the most abundant components over other steroidal hydrocarbons (i.e. geomolecules). This is the first reported occurrence of intact biolipids co-existing with a suite of intermediate diagenetic and catagenetic counterparts preserved in Paleozoic sediments. The consecutive and complex transformations during diagenesis and catagenesis are thought to prevent the parallel occurrence of the most extreme end-members of the steroid pathway, such as functionalized steroids along

with fully aromatized counterparts. Our observations challenge this paradigm and point to microbially mediated processes yielding a variety of steroids without thermal overprinting 380Ma after their deposition.

Methods

Sample collection and preparation

The carbonate concretions used for this contribution was collected from a field trip to the Canning Basin, northern Western Australia in 2010. The sample was found weathering out of the rarely exposed basinal black shales in the Paddy's Valley, an extremely arid and remote location northwest of the basin. The concretion contains a well preserved invertebrate which based on chemo-taxonomical properties was identified as a crustacean (Melendez et al., 2013).

All the exposed surfaces of the concretion were trimmed off (ca. 10 mm) and slices orientated parallel to the fossil were taken (Fig 3.1A). The first slice (i.e. the fossil layer) contains most of the crustacean tissue. Sequential layers (Matrix-L1 and Matrix-L2) were also cut from the carbonate matrix (Fig 3.1A).

Each layer was carefully washed with deionized water in an ultrasonic bath (10 min) and dried overnight (40 °C). Further external ultrasonic washes were made using dichloromethane (DCM) and methanol (7:3) in triplicate. Cleaned samples were crushed and ground in a zirconium mill. In between each sample the mill was cleaned with solvents and annealed quartz. Organic solvent extracts were obtained by Soxhlet extraction for 72 hours with DCM-Methanol (9:1; v/v) in a pre-extracted cellulose thimble. Each extract was separated into 5 fractions by a small chromatography column (5.5 cm length x 0.5 cm i.d.) packed with activated silica gel (120 °C, 8 hour). Aliphatic hydrocarbons were eluted with 1.5 dead volumes (DV) of *n*-hexane, aromatic hydrocarbons in 2 DVs of 4:1 *n*-hexane: DCM, ketones and fatty acid methyl esters (FAMEs) in 2DVs of DCM, alcohols in 2 DVs of 4:1 DCM: ethyl acetate and the polar fraction eluted with 2 DVs of DCM: methanol (7:3). Derivatization was conducted on aliquots of the latter 3 fractions using bis

(trimethylsilyl)-trifluoroacetamide (BSTFA, 25µL) and anhydrous pyridine (25µL). The mixture was heated up to 70 ºC on a sand bath for 20 minutes and immediately after cooling analyzed by Gas Chromatography-Mass Spectrometry (GC-MS). Procedural blanks were performed to monitor laboratory contamination.

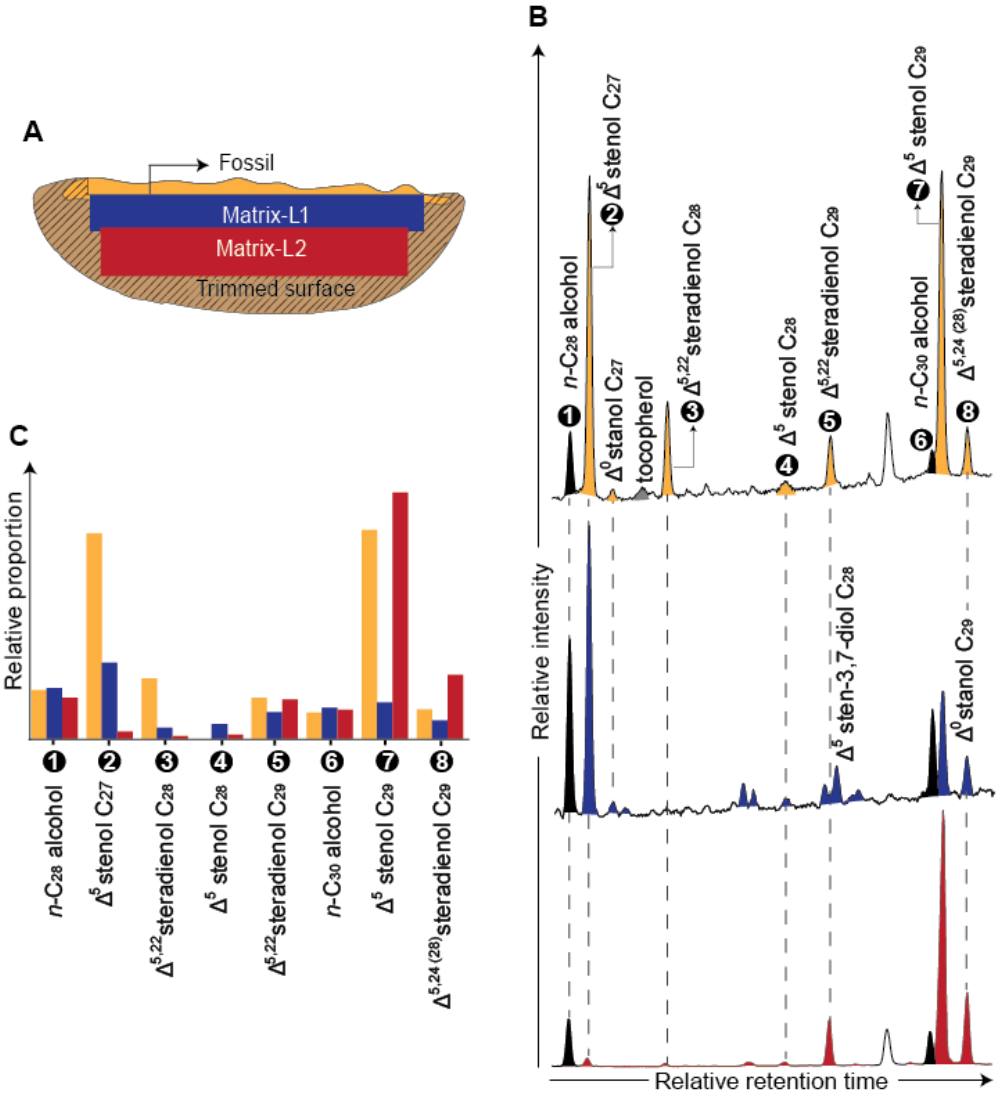

Figure 3. 1. (A) Calcareous concretion containing a well-preserved fossil from the Devonian Gogo Formation. The concretion was split into three layers concentrically away from the nucleus. (B) Partial chromatogram of the free alcohol fraction (as trimethylsilyl-ether derivatives) from the three layers depicting the first occurrence of intact sterols preserved in Paleozoic strata (see Table 3.1 and Supplementary Figs.A3.6-3.8 for detailed identification). (C) Distribution of sterols normalized to the average of C_{28} and C_{30} free *n*-alcohols reveals a dominance of C_{27}-stenols in the fossil layer ascribed to a crustacean input and decreasing proportions towards the matrix, showing elevated C_{29}-stenols derived from algal input.

Semi-quantitative analyses were performed on the total lipid extracts, separated fractions and derivatized aliquots by GC-MS using a Hewlett Packard 6890 gas chromatograph (GC) interfaced to a Hewlett Packard 5973 mass selective detector (MSD). The GC-MS was operated in a pulsed splitless mode; the injector was at 320 °C and fitted with a DB-5 capillary column (60 m x 0.25 mm i.d. x 0.25 µm film thickness). The oven temperature was programmed from 40 °C to 325 °C (at 3 °C/min) with the initial and final hold times of 1 and 50 min, respectively. Ultra high purity helium was used as the carrier gas and maintained at a constant flow of 1.1mL/min. The MSD was operated at 70 *eV* and the mass spectra were acquired in full scan mode, *m/z* 50-700 at ~ 4 scans per second and a source temperature of 230 °C.

A Thermo Finnigan Delta V mass spectrometer coupled to an Isolink GC (using the same chromatographic conditions as in the GC-MS analysis) was used to determine the $\delta^{13}C$ of selected steroids in the underivatized total extract and alcohol fractions. The $\delta^{13}C$ values of the compounds were determined by integrating the ion currents of masses 44, 45 and 46, and are reported in parts per mil (‰) relative to the international Vienna Peedee Belemnite (VPDB) standard. Reported values are the average of at least two analyses.

Results

A carbonate concretion containing a crustacean in its interior has been previously analyzed showing exceptional organic matter preservation, including low thermal maturity biomarker distribution associated with the fossilized crustacean's soft tissue (Melendez et al., 2013). Cholestane was reported to be the most dominant biomarker in this fossil and its presence was attributed to diagenetic-derivatives of cholesterol, the most abundant sterols in living crustaceans (Kanazawa, 2001; Melendez et al., 2013). Isomerization of steranes at positions C-5, C-14 and C-17 as well as at the chiral center at C-20 is concordant with the low thermal maturity of the sample investigated ($20S/(20S+20R)<0.20$). The isomerization of hopanes and hopenes in the sample (Melendez et al, 2013b) indicates slightly higher thermal maturity with side chain isomerization at the C-22 chiral center reaching unity for *S* and *R* stereoisomers.

Due to the low thermal maturity of the sample naturally occurring sterols were still present and were identified along with a suite of their diagenetic products which include stanols, sterenediols, stenol ketones, stanones, sterenes, diasterenes, diasteranes, C-ring monoaromatic and triaromatic steroids (see supplementary Figs. A3.1-A3.4); also intact straight chain fatty acids ($C_{16\text{-}18}$ and $C_{28,\ 30}$) and alcohols ($C_{28,\ 30}$) were preserved (Figs. 3.1 and 3.2). All the steroids identified (Supplementary figures for detailed identification in Appendix 3) are indigenous to the fossil and concretion and coexist, thus reflecting a diagenetic continuum. The mixture of steroids found in the sample corroborates the complex sequential biochemical transformation undergone by sterols during eogenesis (Brassell et al., 1984; Comet et al., 1981; Gagosian et al., 1982; K. E. Peters et al., 2005; Mackenzie et al., 1982a; Mackenzie et al., 1982b). The co-existence of 70 different steroidal compounds (Table 3.1) including fully aromatized steroids together with their biological precursors, exclusively found in living organisms, represents the oldest and most extensive sedimentary anachronism reported to date, challenging the paradigm that progressive steroid late dia-/catagenesis is only controlled by thermal maturation.

Exceptional preservation may add a new facet to the application of steroid based thermal maturity ratios in petroleum exploration and in reconstruction of thermal histories of sedimentary basins. Presently, co-occurrence of immature and mature biomarker signals has been attributed to i) incorporation of immature biomolecules into migrating oils (Curiale, 2002), ii) admixture of reworked mature organic matter to immature sediments (Rowland and Maxwell, 1984), or iii) charging of petroleum reservoirs from source rocks of varying maturities (Leythaeuser et al., 2007).

Exceptional preservation of Devonian sterols occurred in both the fossil and the surrounding layers of the carbonate concretion (Figs. 3.1A-C). We thus focused our investigation on the fossil layer where the highest steroid concentrations and the largest range of diagenetic derivatives were observed (Table 3.1). Within the fossil layer sterenes, steranes, diasteranes, diasterenes and monoaromatic steroids with 27 carbon atoms are up to 4 times more abundant than the C_{29} steroid analogs. The preferential preservation of C_{27} steroids towards the center of the concretion, where the fossil is preserved, suggests these originate from the crustacean, resembling the diagenetic products of sterol distributions in living crustaceans, in which cholesterol comprise more than 90% of the total steroids (Kanazawa, 2001). However, similar proportions of C_{27} and C_{29} Δ5-stenols are present in the proximity of the fossil while in the surrounding matrix the C_{29} is the most abundant. This distribution of sterols in the sample suggests a combination of sources for the intact biolipids: C_{27} steroids mainly derived from the fossil tissue (and the Crustacean's dietary products) and C_{28} and C_{29} compounds resulting from algae/phytoplankton from the upper water column. The proportion of C_{28} and C_{29} is concordant with the stage of algal evolution during the Devonian (Grantham and Wakefield, 1988; Schwark and Empt, 2006). This is in agreement with the sterane distribution ($C_{27}/C_{29} < 1$) reported for the carbonate matrix surrounding the fossil and the black shale hosting such concretions i.e. the Gogo Formation, dominated by the C_{29} steranes (see supplementary Fig A3.5) (Melendez et al., 2013).

Table 3. 1 Steroids compounds identified in the fossil layer based on their relative elution order and comparison of mass spectra with literature data (Tr: Traces). Peak numbers refer to supplementary figures available in Appendix 3.

N°	Identification	Conc. (ppb)	C_{27}/C_{29}
Steranes			
1	5α,14α,17α(H) cholestane 20*S*	413	3.7
2	5α,14β,17β(H) cholestane 20*R*		
3	5α,14β,17β(H) cholestane 20*S*	74	
4	5α,14α,17α(H) cholestane 20*R*	1503	
5	5α,14α,17α(H) 24-methylcholestane 20*S*	26	
6	5α,14β,17β(H) 24-methylcholestane 20*R*	37	
7	5α,14β,17β(H) 24-methylcholestane 20*S*	Tr	
8	5α,14α,17α(H) 24-methylcholestane 20*R*	154	
9	5α,14α,17α(H) 24-ethylcholestane 20*S*	70	
10	5α,14β,17β(H) 20*R* + 5β,14α,17α(H) 24-ethylcholestane	131	
11	5α,14β,17β(H) 24-ethylcholestane 20*S*	Tr	
12	5α,14α,17α(H) 24-ethylcholestane 20*R*	344	
Sterenes			
13	Δ^5 cholestene	112	4.0
14	Δ^5 24-ethylcholestene	28	
Diasteranes			
15	13β,17α(H) diacholestane 20*S*	127	4.6
16	13β,17α(H) diacholestane 20*R*	138	
17	13α,17β(H) diacholestane 20*S*	40	
18	13α,17β (H) diacholestane 20*R*	39	
19	13β,17α(H) 24-methyldiacholestane 20*S*	53	
20	13β,17α(H) 24-methyldiacholestane 20*R*	56	
21	13α,17β (H) 24-methyldiacholestane 20*S*	45	
22	13α,17β (H) 24-methyldiacholestane20*R*	35	
23	13β,17α(H) 24-ethyldiacholestane 20*S*	169	
24	13β,17α(H) 24-ethyldiacholestane 20*R*	75	
Diasterenes			
25	10α, $\Delta^{13(17)}$ diacholestene 20*S*	203	3.6
26	10α, $\Delta^{13(17)}$ diacholestene 20*R*	230	
27	10α, $\Delta^{13(17)}$ 24-methyldiacholestene 20*R*	229	

28	10α, $\Delta^{13(17)}$ 24-ethyldiacholestene 20*S*	Tr	
29	10α, $\Delta^{13(17)}$ 24-ethyldiacholestene 20*R*	120	
4-methylsteranes			
30	5α,14β,17β(H) 4α-methylcholestane 20*S*	27	n/a
31	5α,14β,17β(H) 4α-methylcholestane 20*R*	Tr	
32	5α,14α,17α(H) 4α-methylcholestane 20*S*	Tr	
33	5α,14α,17α(H) 4α-methylcholestane 20*R*	106	
34	5α,14β,17β(H) 4α-methyl 24-ethylcholestane 20*S*	Tr	
35	5α,14β,17β(H) 4α-methyl 24-ethylcholestane 20*R*	38	
36	5α,14α,17α(H) 4α-methyl 24-ethylcholestane 20*S*	86	
37	5α,14α,17α(H) 4α-methyl 24-ethylcholestane 20*R*	Tr	
C-ring monoaromatic steroid			
38	C_{21} 5α, 10β(CH_3)	41	2.2
39	C_{22} 5α, 10β(CH_3)	45	
40	C_{27} 5β, 10β(CH_3) 20*S*	72	
41	C_{27} 5β, 10β(CH_3) 20*R*	43	
42	C_{27} 5α, 10β(CH_3) 20*S*	Tr	
43	C_{28} 5β, 10β(CH_3) 20*S*	170	
44	C_{27} 5α, 10β(CH_3) 20*R*	78	
45	C_{28} 5a, 10β(CH_3) 20*S*	99	
46	C_{28} 5β, 10β(CH_3) 20*R*	71	
47	C_{29} 5β, 10β(CH_3) 20*S*	Tr	
48	C_{29} 5α, 10β(CH_3) 20*S*	44	
49	C_{28} 5α, 10β(CH_3) 20*R*	41	
50	C_{29} 5β, 10β(CH_3) 20*R*	Tr	
51	C_{29} 5α, 10β(CH_3) 20*R*	33	
Triaromatic steroid			
52	C_{26} 20*S*	Tr	0.5
53	C_{26} 20*R*	Tr	
54	C_{27} 20*S*	Tr	
55	C_{28} 20*S*	Tr	
56	C_{27} 20*R*	Tr	
57	C_{28} 20*R*	Tr	
Functionalized steroids			
58	cholest-5-en-3β-ol	2829	n/a
59	24-methycholest-5-en-3β-ol	590	

60	24-ethylcholest-5-en-3β-ol	4281
61	cholest-5-en-3β,7α-diol	Tr
62	24- methylcholest-5-en-3β,7α-diol	Tr
63	24-ethylcholest-5-en-3β, 7α-diol	Tr
64	Cholest-5-en-3β-ol-7-one	Tr
65	24-methylcholstenol (unknown isomer)	Tr
66	24-methycholesta-5,22-dien-3β-ol	Tr
67	24-ethycholesta-5,22-dien-3β-ol	Tr
68	24-ethycholesta-5,24 (28)-dien-3β-ol	Tr
69	5α-cholestan-3β-ol	Tr
70	5α - 24-ethylcholestan-3β-ol	Tr
71	Tocopherol acetate	Tr
72	*n*-C_{28} alcohol	Tr
73	*n*-C_{29} alcohol	Tr
74	*n*-C_{30} alcohol	Tr
75	*n*-C_{28} fatty acid	Tr
76	*n*-C_{30} fatty acid	Tr

Discussions

The distribution of the two major sterols in the sample, cholest-5-en-3β-ol ($\delta^{13}C$ of -26.8 ‰) and 24-ethylcholest-5-en-3β-ol ($\delta^{13}C$ of -30.9 ‰) and their isotopic disparity confirm the preservation of mixed eukaryotic sources in the fossil layer, i.e. crustacean tissue and that of marine biomass settling through the water column. The toxic water column (i.e. persistent PZE, see above) present at the time (Melendez et al., 2013) may have also favored the development of opportunistic blooms of prasinophycean rather than other green algae, as evident by a C_{28}/C_{29} sterane ratio of >0.4 (Grantham and Wakefield, 1988). The stable isotopic composition of cholestane ($\delta^{13}C$ of -30.5 ‰) in the fossil layer is not fully compatible with an origin exclusive from the co-existing crustacean's cholesterol (Grice et al., 1998). It is thus assumed that the cholestane in the fossil layer based on its carbon isotope signature may have also an algal or zooplanktonic contribution, also supported by the isotopic disparities between isoprenoids and *n*-alkanes found in the fossil layer (Melendez et al., 2013).

Intermediates in the earliest transformation of Δ5-stenols in the water column formed by photo-oxidation, such as cholest-5-en-3β,7α-diol, 24-ethylcholest-5-en-3β,7α-diol, 24-methylcholest-5-en-3β,7α-diol and cholest-5-en-3β-ol-7-one, were also identified in the sample. These compounds are typical rearranged products of 5α-hydroperoxides derived from photo-oxidation (type II) of Δ5-stenols in the euphotic layer of the water column (Rontani, 2001). Furthermore, trace amounts of tocopherol acetate were identified in the fossil, with the oldest occurrence of tocopherol previously reported for the Cretaceous (Dumitrescu and Brassell, 2005). The survival of these highly reactive components can be attributed to a euxinic zone expanding close to the productive surface waters, thus enabling very short transfer times of primary biomass through the oxic water column to the chemocline.

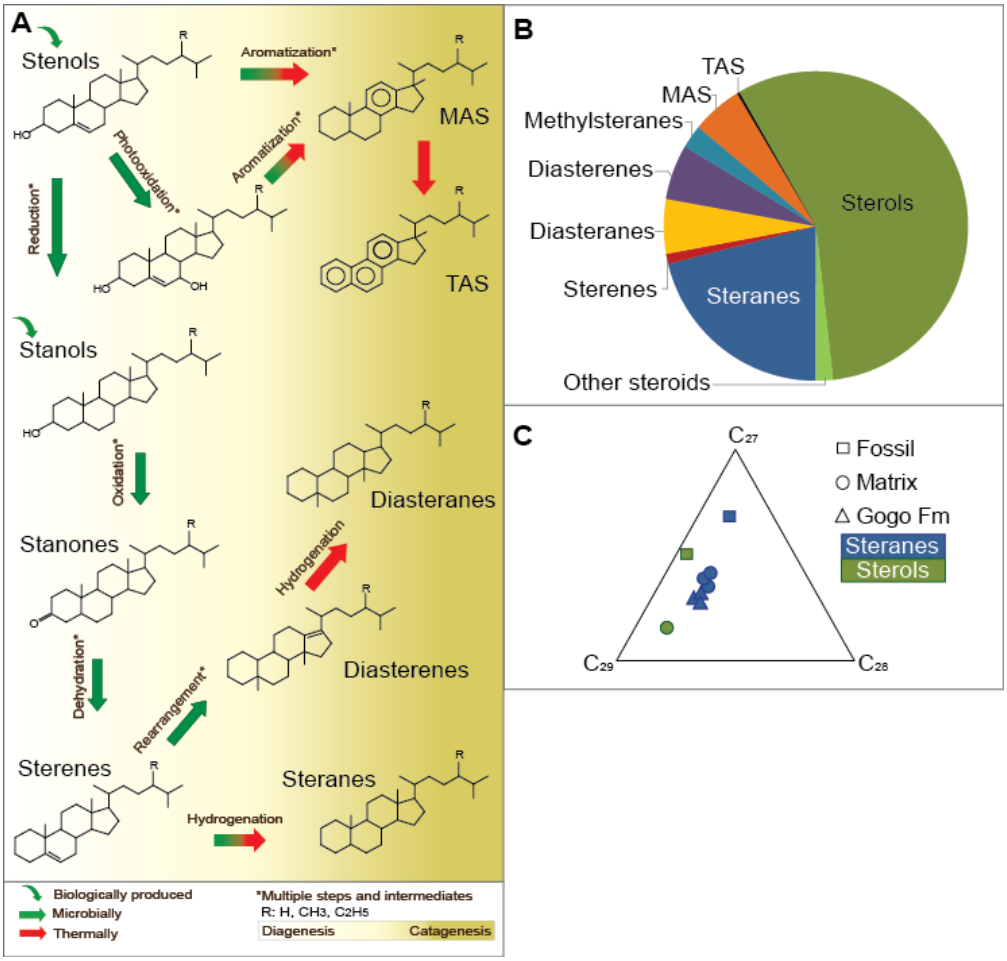

Figure 3. 2 . (A) A suite of steroids coexisting in one fossil corresponds to the assemblage of steroids generated by diagenetic (pale yellow background) and catagenetic (dark yellow background) stages of the evolutionary pathways proposed by Mackenzie et al. (3, 4). A total of 70 individual steroids, including stenols, steradienols, stanols, stanones, sterenes, steradienes, diasterenes, diasteranes, mono- and triaromatic steroids, as well as 4-methyl substituted analogues (see Table 3.1 for quantification of steroids) occur in parallel. (B) Relative proportion of compound classes within the fossil is dominated by sterols and steranes, representing the bio- and geospheric end-members of a diagenetic sequence, respectively. (C) Ternary diagram of sterols (green) and steranes (blue) differentiate the fossil from the concretion matrix and the host rock. The C_{27} dominance in the fossil layer is attributed to Crustacean tissue, whereas the matrix and host rock represent common algal input(s).

Degradation-sensitive biomolecules, when protected within organic debris embedded in the uppermost sediments became rapidly encapsulated within the carbonate concretion and were able to survive some 380 Ma. The difference in the degree of diagenetic transformation between the crustacean and the water column derived sterols is attributed to the excellent preservation of the fossil biomass protected within the crustacean's tissue (Melendez et al., 2013).

The parallel occurrence of biolipid stenols with their diagenetic geolipid derivatives including fully aromatized steroids, with the latter present in traces amounts and Δ5-stenols as the dominant compound class, in a concretion that has undergone the same geological history is exceptional. The defunctionalization of sterols to sterenes and their saturated and rearranged counterparts along with the formation of A/B-ring monoaromatic steroids is restricted to the early diagenesis zone, driven by low temperature – microbial reactions (Hussler and Albrecht, 1983; Hussler et al., 1981; Mackenzie et al., 1982a; Schüpfer et al., 2007). The later occurring early diagenetic formation of C-ring monoaromatic steroids may be initially microbially mediated but transiently continues into late diagenetic/catagenetic abiotic transformation reactions (K. E. Peters et al., 2005; Mackenzie et al., 1982a; Riolo et al., 1986). Depending on the biological precursor present and the depositional conditions prevailing, formation of specific metastable intermediates is favored during earliest diagenesis. In the Gogo concretion the lack of A-ring monoaromatic steroids and B-ring monoaromatic anthrasteroids, spirosterenes and of their presumed precursors, the 3,5-steradienes or 5,7-steradienes (Schüpfer et al., 2007) is attributed to the absence of suitable biological stenols. Although being intermediates in the steroid diagenetic continuum, monoaromatic A/B-ring steroids have been reported from sediments as old as the Cretaceous (Brassell et al., 1984; Hussler and Albrecht, 1983; Hussler et al., 1981) and spirosterenes in sediments dating to the Malmian stage (148Ma) of the Jurassic (Schwark et al., 1998). The occurrence of catagenetically formed C-ring steroids and triaromatic steroids, however, is not stratigraphically restricted with frequent reports of the stable products in Proterozoic sediments and oils (K. E. Peters et al., 2005). In contrast to early diagenesis, the full aromatization and isomerization of chiral centers in steranes and diasteranes are products of thermodynamically controlled physiochemical reactions during latest diagenesis and catagenesis (Mackenzie et al., 1982a; Mackenzie et al., 1982b). The fully aromatized steroids are considered to be of exclusively catagenetic origin (K. E. Peters et al., 2005; Mackenzie et al., 1982b) but early microbial aromatization of triterpenoids has been reported to occur widely in natural environments. Different aromatization pathways have been formulated for

higher plant triterpenoids (Le Milbeau et al., 2010) and hopanoic pentacyclic triterpenoids (Trendel et al., 1989; Wolff et al., 1989). Here we postulate that eogenetic aromatization processes involving sterols to form triaromatic steroids (Fig. 3.2A, Table 3.1) is also feasible. Disproportionation of hydrogen upon diagenetic processes within the concretion either favored the saturation of sterenes or the progressive desaturation of aromatic steroids.

The burial history of the Gogo Formation excludes temperatures in the catagenesis zone (Playford et al., 2009) and hence indicates structural rearrangement of steranes to form diasteranes and triaromatic steroids in a low thermal diagenetic regime, prior to the oil window. Abiotic mechanisms operating at low temperature cannot be excluded, especially when an active sulfur cycle was present at the time of preservation, in which a consortium of sulfate reducing and green sulfur bacteria existed in a H_2S-rich environment (Melendez et al., 2013). Evidence of anoxic-euxinic conditions has been proven for this sample, and natural vulcanization has also occurred by early sulfurization of e.g. sterols and isorenieratene derivatives previously reported in the fossil layer (Melendez et al., 2013). Elevated microbial activity along with abiotic sulfurization (Adam et al., 2000; Kohnen et al., 1993) and non-biological hydrogenation (Hebting et al., 2006) favored the preservation of abundant organic matter at early stages of diagenesis playing an important role in the reduction pathway of steroids in an oxygen depleted environment.

The co-occurrence of biomolecules and geomolecules in sediments affords extremely specific prerequisites, not only ensuing unique conditions during primary eogenesis but also after sediment emplacement with a continuation of strictly anaerobic conditions (persistent PZE) during the entire geological history. In addition, it seems to be an essential condition that anaerobic microbial processes within the lower water column and sediment may stimulate the formation of geomolecules formerly ascribed to abiotic thermally governed processes. Under certain conditions the established concept of diagenesis *versus* catagenesis as such is not applicable. Several lines of evidence provided here indicate that under exceptional conditions concretions are able to preserve biomolecules at unprecedented levels, opening a new window of opportunity to study the

distributions of biomolecules in deep time and thus offering prospects in improving our understanding of organismic evolution and past environmental conditions.

Acknowledgments

Grice and Melendez thank the Australian Research Council (ARC) for a Queen Elizabeth II Discovery grant (awarded to Grice; "Characteristics of organic matter formed in toxic, sulfide-rich modern and ancient sediments"), and for Melendez's Ph.D. stipend. Melendez acknowledges Curtin University for a fee waiver. Grice acknowledges the ARC and John de Laeter Centre for infrastructure to perform the research. Schwark acknowledges DAAD support for a sabbatical at Curtin University under DAAD-ATN Grant No. 53430494. S. Tulipani is thanked for providing a reference sample of the Gogo Formation shale, K. Trinajstic for providing the concretion and G. Chidlow for technical support.

Reference cited

Adam, P.A., Schneckenburger, P.S., Schaeffer, P.S., Albrecht, P.A., 2000. Clues to early diagenetic sulfurization processes from mild chemical cleavage of labile sulfur-rich geomacromolecules. Geochimica et Cosmochimica Acta 64, 3485-3503.

Brassell, S.C., Eglinton, G., Howell, V.J., 1987. Palaeoenvironmental assessment of marine organic-rich sediments using molecular organic geochemistry. Geological Society, London, Special Publications 26, 79-98.

Brassell, S.C., McEvoy, J., Hoffmann, C.F., Lamb, N.A., Peakman, T.M., Maxwell, J.R., 1984. Isomerisation, rearrangement and aromatisation of steroids in distinguishing early stages of diagenesis. Organic Geochemistry 6, 11-23.

Comet, P., McEvoy, J., Brassell, S., Eglinton, G., Maxwell, J., Thomson, I., 1981. Lipids of an Upper Albian limestone, Deep Sea Drilling Project Site 465. Init. Rep. DSDP 62, 923-937.

Curiale, J.A., 2002. A review of the occurrences and causes of migration-contamination in crude oil. Organic Geochemistry 33, 1389-1400.

Dumitrescu, M., Brassell, S.C., 2005. Biogeochemical assessment of sources of organic matter and paleoproductivity during the early Aptian Oceanic Anoxic Event at Shatsky Rise, ODP Leg 198. Organic Geochemistry 36, 1002-1022.

Gagosian, R.B., Smith, S.O., Nigrelli, G.E., 1982. Vertical transport of steroid alcohols and ketones measured in a sediment trap experiment in the equatorial Atlantic Ocean. Geochimica et Cosmochimica Acta 46, 1163-1172.

Grantham, P.J., Wakefield, L.L., 1988. Variations in the sterane carbon number distributions of marine source rock derived crude oils through geological time. Organic Geochemistry 12, 61-73.

Grice, K., Klein Breteler, W.C.M., Schouten, S., Grossi, V., De Leeuw, J.W., Damsté, J.S.S., 1998. Effects of zooplankton herbivory on biomarker proxy records. Paleoceanography 13, 686-693.

Hebting, Y., Schaeffer, P., Behrens, A., Adam, P., Schmitt, G., Schneckenburger, P., Bernasconi, S.M., Albrecht, P., 2006. Biomarker Evidence for a Major Preservation Pathway of Sedimentary Organic Carbon. Science 312, 1627-1631.

Hussler, G., Albrecht, P., 1983. C27-C29 Monoaromatic anthrasteroid hydrocarbons in Cretaceous black shales. Nature 304, 262-263.

Hussler, G., Chappe, B., Wehrung, P., Albrecht, P., 1981. C27-C29 ring A monoaromatic steroids in Cretaceous black shales. Nature 294, 556-558.

K. E. Peters, Walters, C.C., Moldowan, J.M., 2005. The Biomarker Guide. Cambridge University Press.

Kanazawa, A., 2001. Sterols in marine invertebrates. Fisheries Science 67, 997-1007.

Kohnen, M.E.L., Sinninghe Damsté, J.S., Baas, M., Dalen, A.C.K.-v., De Leeuw, J.W., 1993. Sulphur-bound steroid and phytane carbon skeletons in geomacromolecules: Implications for the mechanism of incorporation of sulphur into organic matter. Geochimica et Cosmochimica Acta 57, 2515-2528.

Le Milbeau, C., Schaeffer, P., Connan, J., Albrecht, P., Adam, P., 2010. Aromatized C-2 Oxygenated Triterpenoids as Indicators for a New Transformation Pathway in the Environment. Organic Letters 12, 1504-1507.

Leythaeuser, D., Keuser, C., Schwark, L., 2007. Molecular memory effects recording the accumulation history of petroleum reservoirs: A case study of the Heidrun Field, offshore Norway. Marine and Petroleum Geology 24, 199-220.

Mackenzie, A.S., Brassell, S.C., Eglinton, G., Maxwell , J.R., 1982a. Chemical fossils: the geological fate of steroids. Science 217, 491-504.

Mackenzie, A.S., Lamb, N.A., Maxwell, J.R., 1982b. Steroid hydrocarbons and the thermal history of sediments. Nature 295, 223-226.

Melendez, I., Grice, K., Trinajstic, K., Ladjavardi, M., Greenwood, P., Thompson, K., 2013. Biomarkers reveal the role of photic zone euxinia in exceptional fossil preservation: An organic geochemical perspective. Geology 41, 123-126.

Playford, P.E., Hocking, R.M., Cockbain, A.E., 2009. Devonian Reef Complexes of the Canning Basin, Western Australia. Geological Survey of Western Australia Bulletin 145, 444.

Riolo, J., Hussler, G., Albrecht, P., Connan, J., 1986. Distribution of aromatic steroids in geological samples: their evaluation as geochemical parameters. Organic Geochemistry 10, 981-990.

Rontani, J.-F., 2001. Visible light-dependent degradation of lipidic phytoplanktonic components during senescence: a review. Phytochemistry 58, 187-202.

Rowland, S.J., Maxwell, J.R., 1984. Reworked triterpenoid and steroid hydrocarbons in a recent sediment. Geochimica et Cosmochimica Acta 48, 617-624.

Schüpfer, P., Finck, Y., Houot, F., Gülaçar, F.O., 2007. Acid catalysed backbone rearrangement of cholesta-2,4,6-triene: On the origin of ring A and ring B aromatic steroids in recent sediments. Organic Geochemistry 38, 671-681.

Schwark, L., Empt, P., 2006. Sterane biomarkers as indicators of palaeozoic algal evolution and extinction events. Palaeogeography, Palaeoclimatology, Palaeoecology 240, 225-236.

Schwark, L., Vliex, M., Schaeffer, P., 1998. Geochemical characterization of Malm Zeta laminated carbonates from the Franconian Alb, SW-Germany (II). Organic Geochemistry 29, 1921-1952.

Trendel, J.M., Lohmann, F., Kintzinger, J.P., Albrecht, P., Chiarone, A., Riche, C., Cesario, M., Guilhem, J., Pascard, C., 1989. Identification of des-A-triterpenoid hydrocarbons occurring in surface sediments. Tetrahedron 45, 4457-4470.

Volkman, J.K., 1986. A review of sterol markers for marine and terrigenous organic matter. Organic Geochemistry 9, 83-99.

Wolff, G.A., Trendel, J.M., Albrecht, P., 1989. Novel Monoaromatic triterpenoid hydrocarbons occuring in sediments. Tetrahedron 45, 6721-6728.

Appendix 3

Supporting figures

Supporting figures, included in the original publication as Supporting Online Material. http://www.nature.com/doifinder/10.1038/srep02768

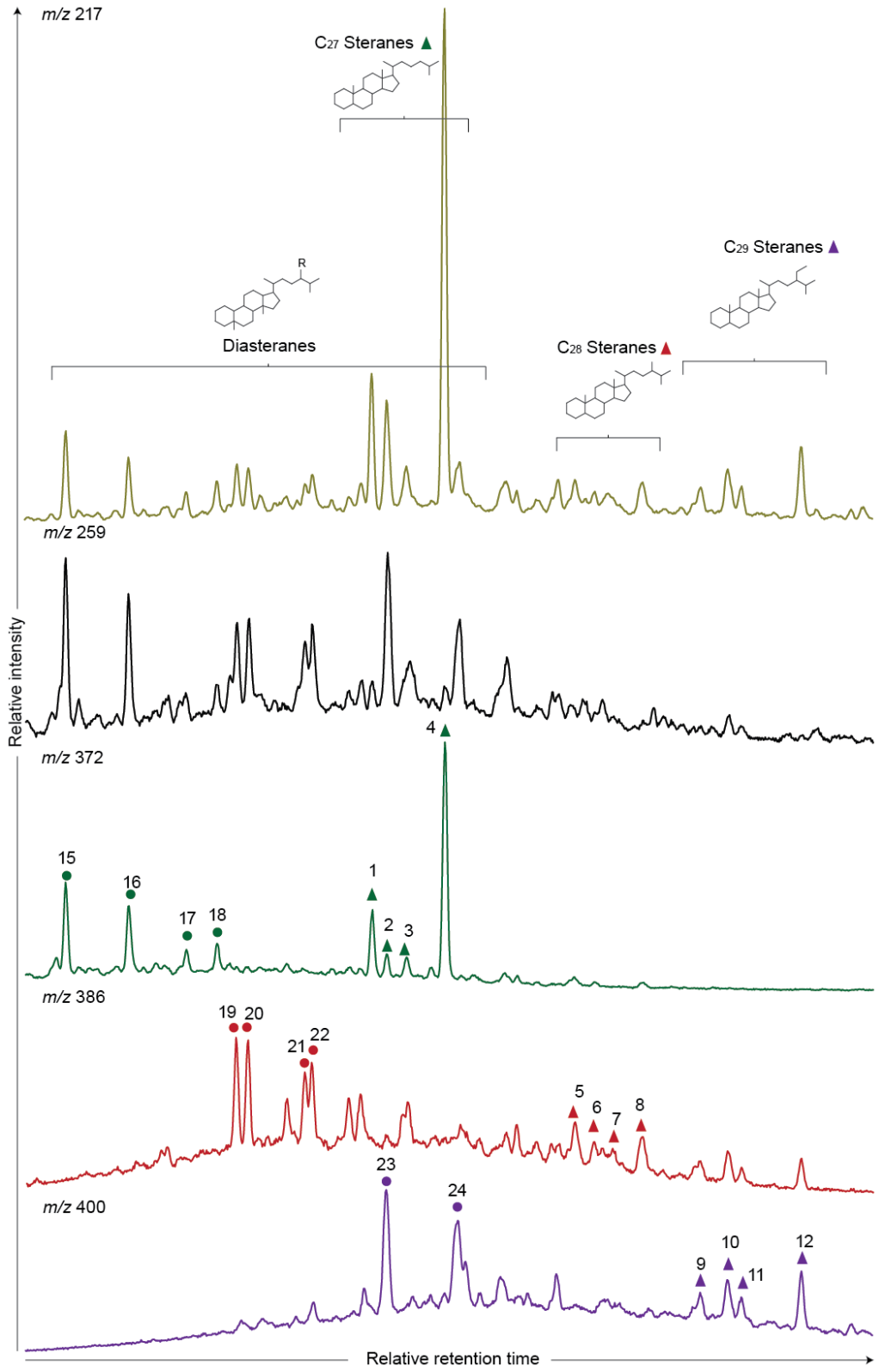

Figure A3. 1 Mass fragmentograms: *m/z* 217, 259, 372, 386 and 400, showing the distribution of steranes and diasteranes in the saturate fraction of the fossil layer (numbered peaks refer to Table 3.1). R= H, CH_3, C_2H_5.

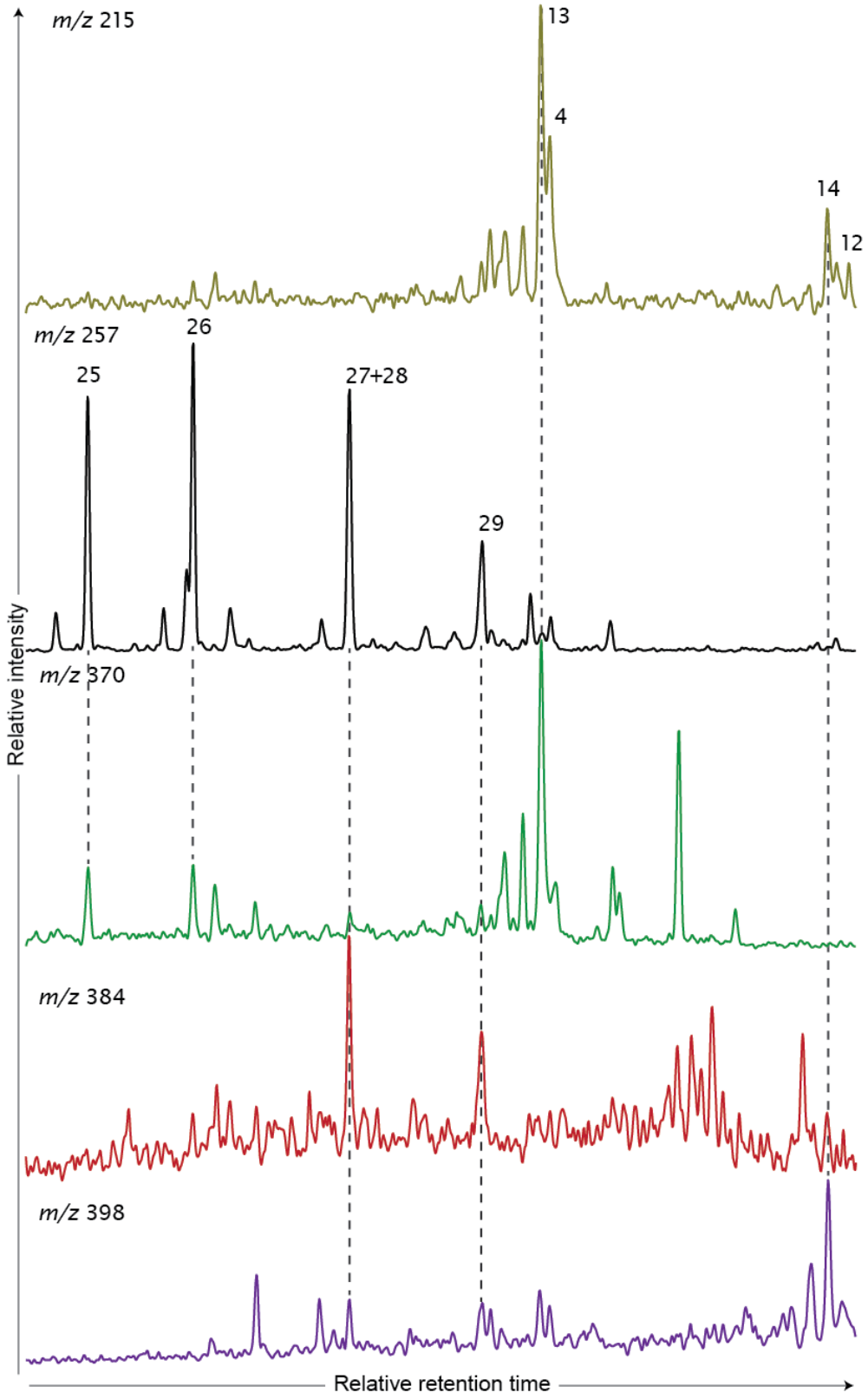

Figure A3. 2 Mass fragmentograms: *m/z* 215, 257, 370, 384 and 398, showing the distribution of sterenes and diasterenes in the saturate fraction of the fossil layer (numbered peaks refer to Table 3.1)

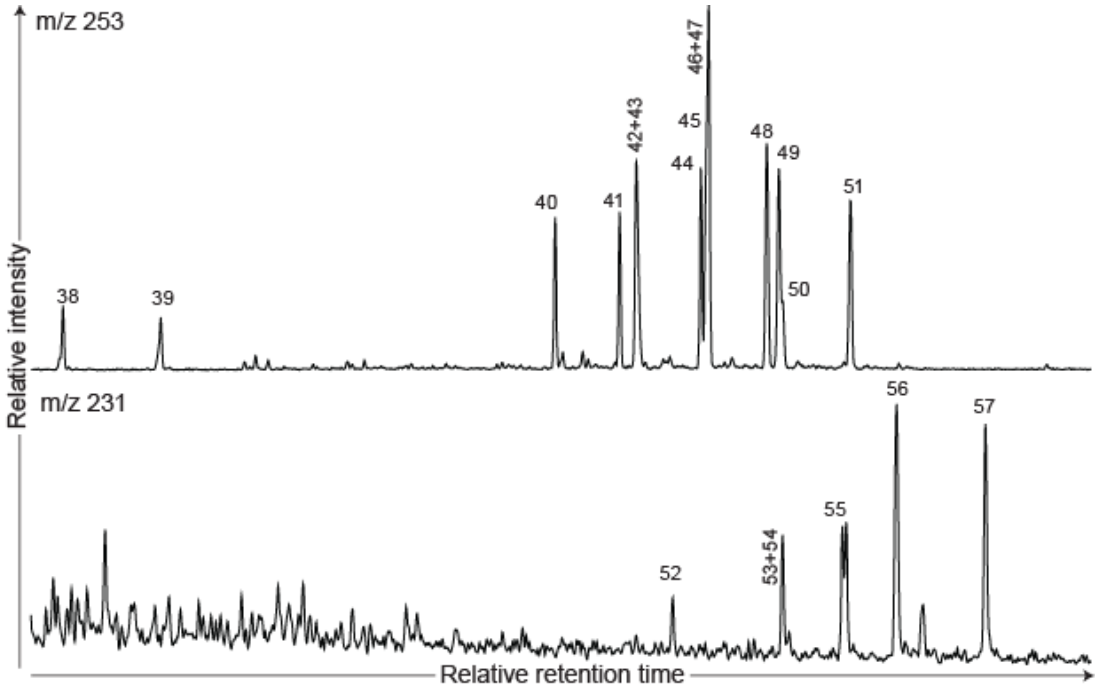

Figure A3. 3 Mass fragmentograms: *m/z* 253 and 231 of the aromatic fraction from the fossil layer, showing the distribution of mono and tri-aromatics steroids (numbered peaks refer to Table 3.1).

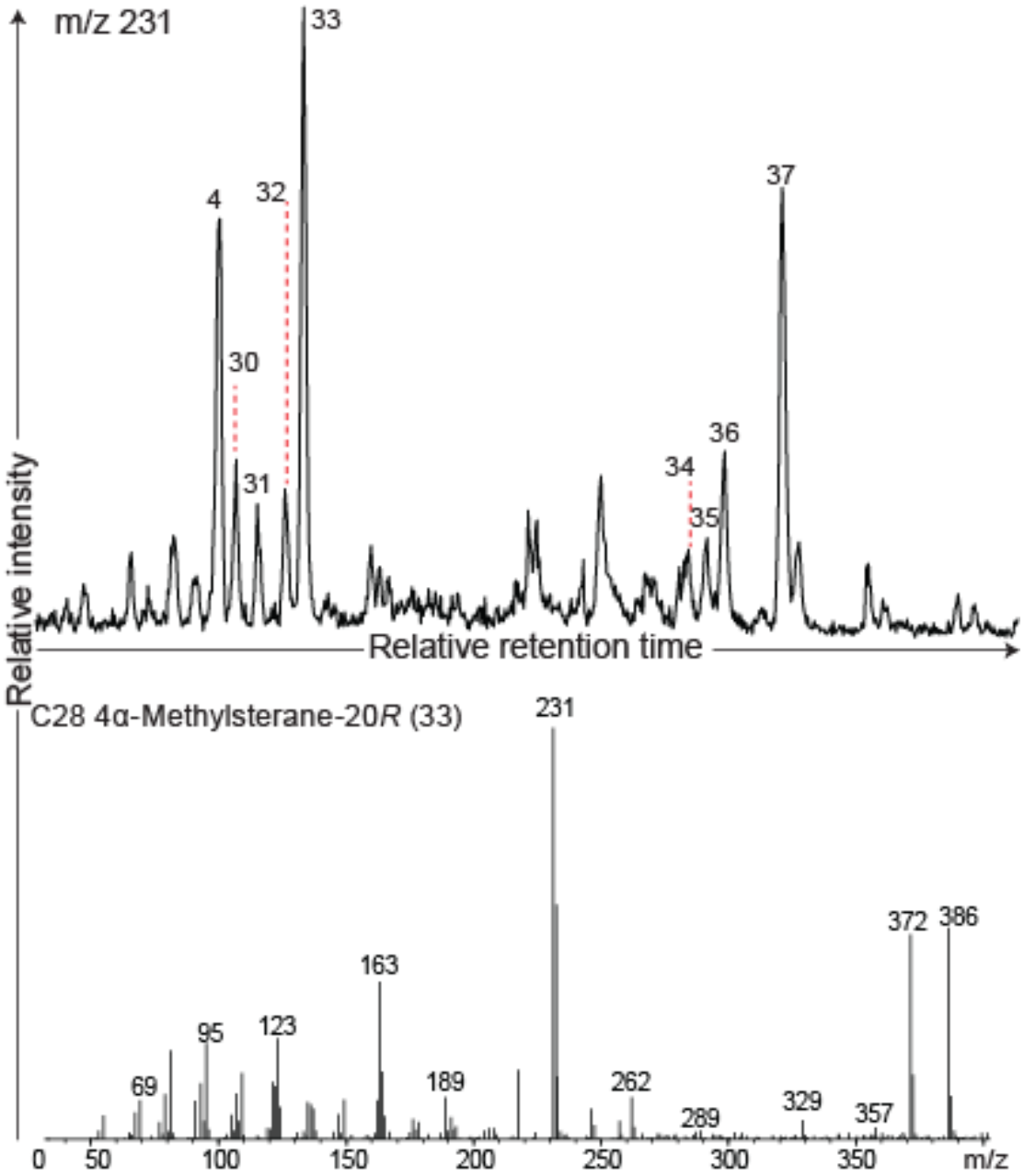

Figure A3. 4 Mass fragmentogram: *m/z* 231, showing the distribution of 4α-methylsteranes in the saturate fraction of the fossil layer (numbered peaks refer to Table 3.1) and mass spectrum of the C_{28} 4α-methylsterane-20*R* (33) confirming its identification.

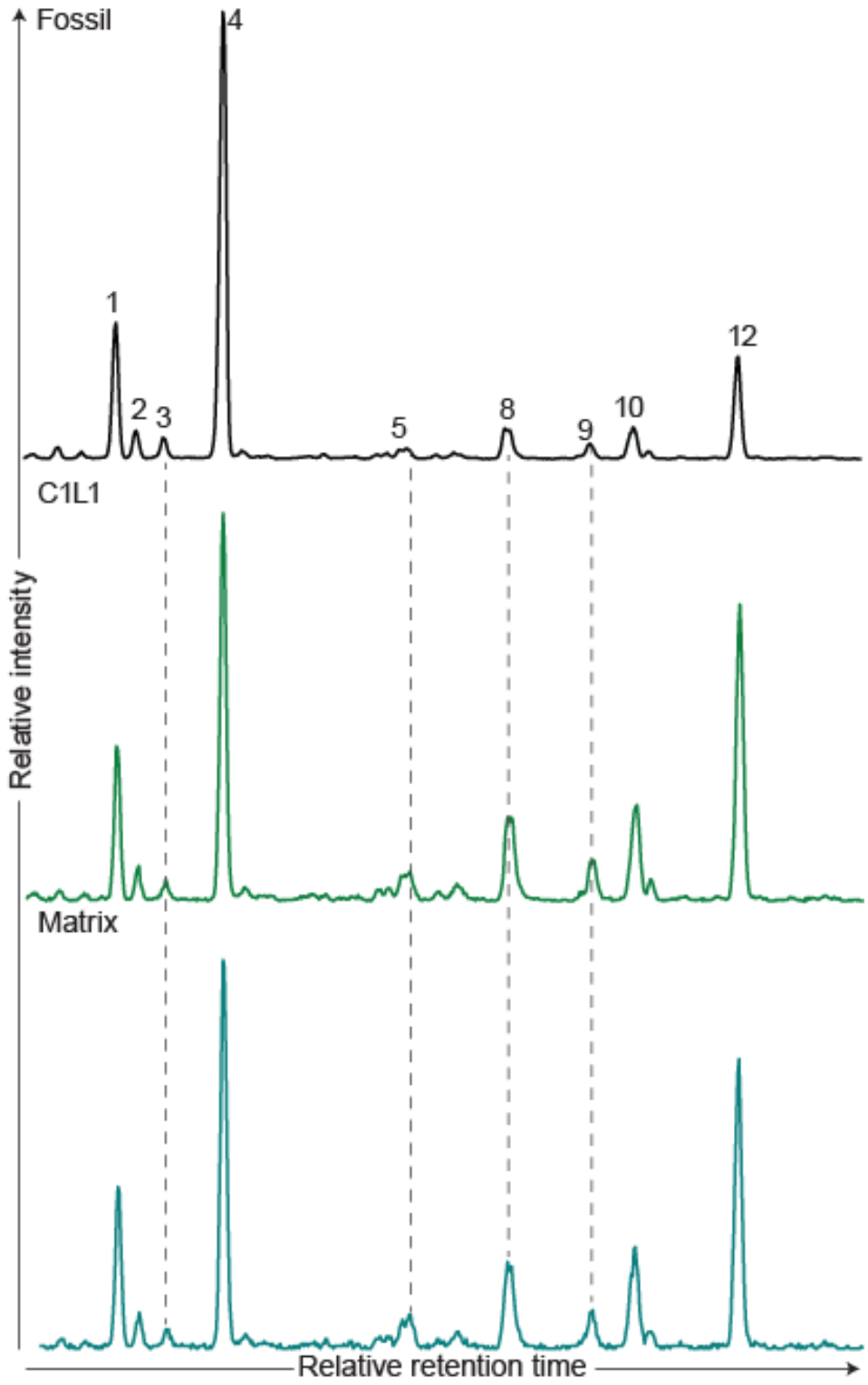

Figure A3. 5 Mass fragmentogram: *m/z* 217 of the fossil layer and subsequent matrix layers showing the variation in the distribution of steranes across the concretion (numbered peaks refer to Table 3.1).

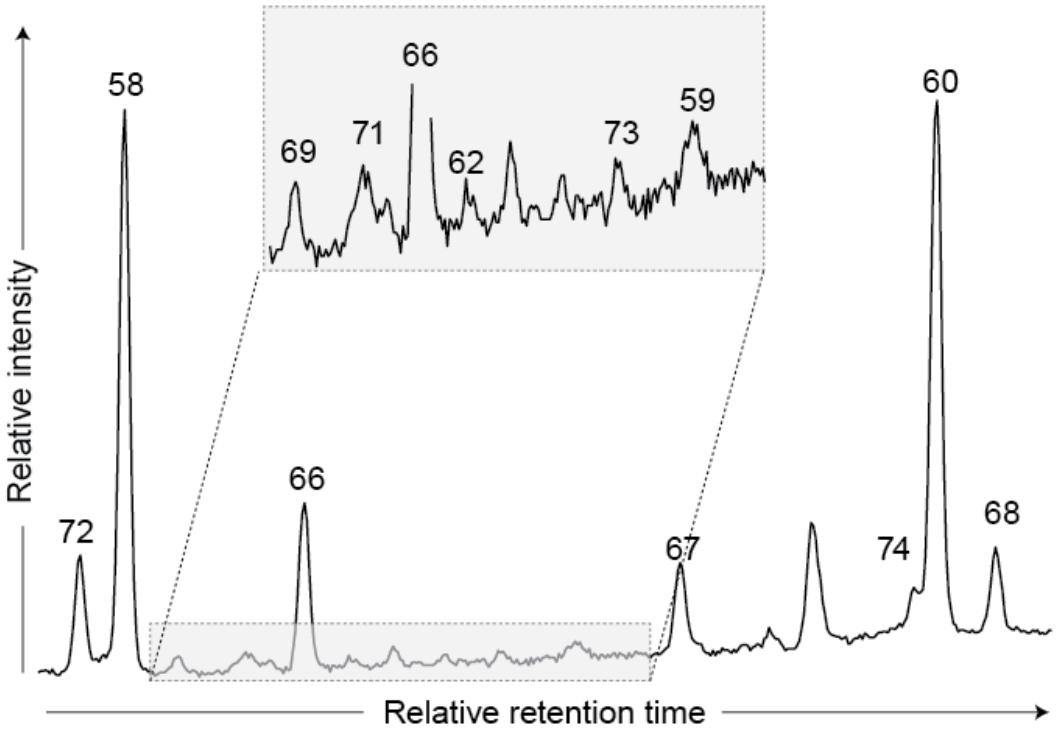

Figure A3. 6 Partial total ion chromatogram of the derivatized alcohol fraction in fossil (numbered peaks refer to Table 3.1).

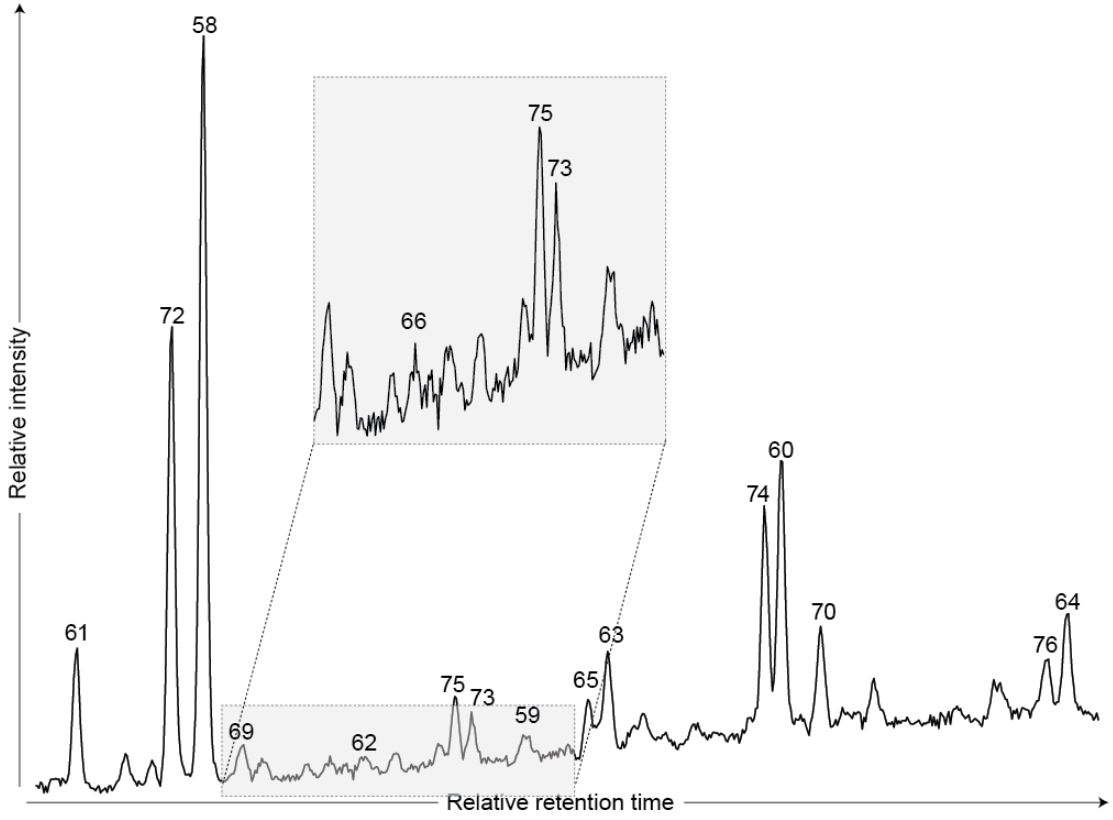

Figure A3. 7 Partial total ion chromatogram of the derivatized alcohol fraction from the matrix-L1, located underneath the fossil (numbered peaks refer to Table 3.1).

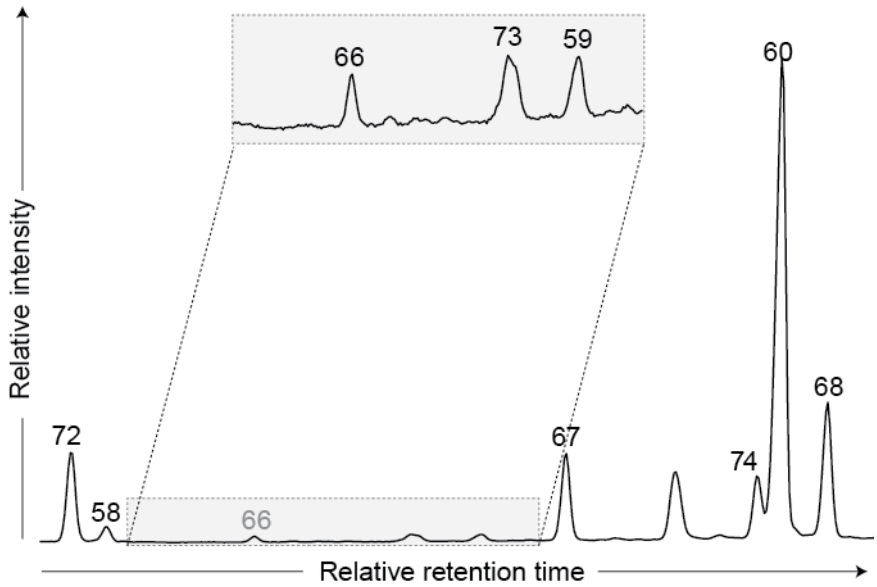

Figure A3. 8 Partial total ion chromatogram of the derivatized alcohol fraction from the matrix (numbered peaks refer to Table 3.1)

Copyright

The content of Chapter 3 has published in Scientific Reports, an online and open acces primary research publication from the Nature Publishing Group. Copyrights are retained by the authors.

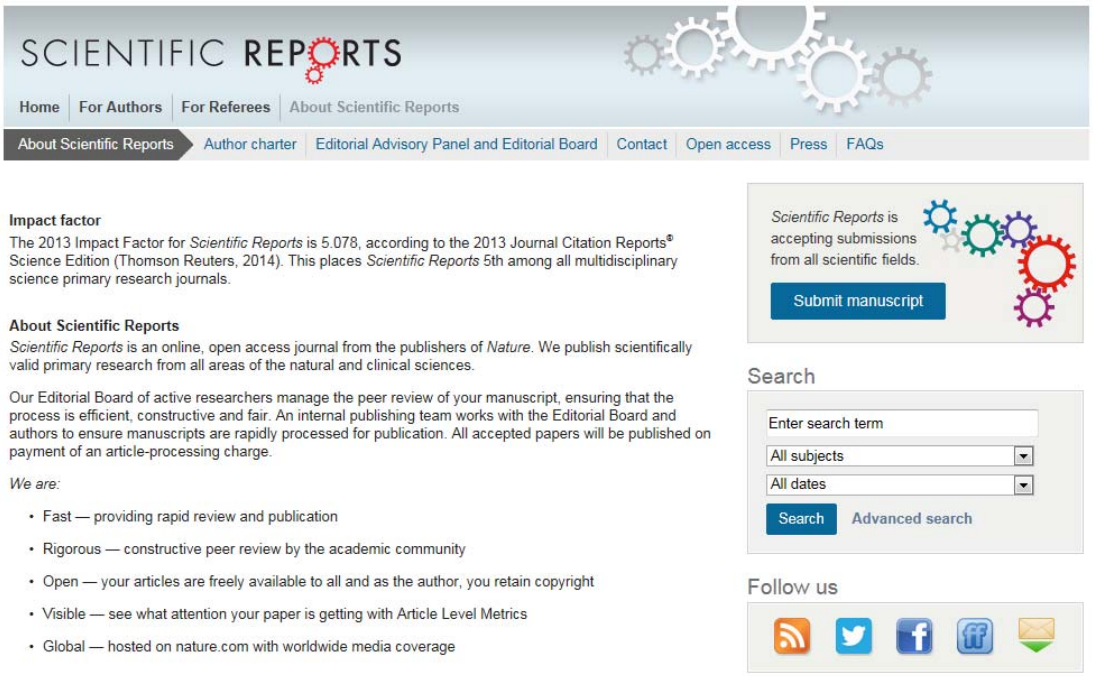

CHAPTER 4

Episodic mayhem after the end-Permian biotic crisis in the Boreal Sea: microbial blooms during hypersaline-oxygen limited conditions

Ines M. Melendez, Kliti Grice, Clinton Foster, Richard J. Twitchett

Submitted to Proceedings of the National Academy of Sciences USA

Abstract

Perturbations of the major biogeochemical cycles during the end-Permian extinction event have been thoroughly evaluated across the world, but little is known about the behavior of such cycles and how they governed the recovery of the marine and terrestrial ecosystem during the Early Triassic in the northern hemisphere. An exhaustive evaluation of an extended Early Triassic marine section of the shelf deposits from the Boreal Sea was carried out. New data for $\delta^{13}C$ and δD of bulk biomass and individual biomarkers is now available along with $\delta^{34}S_{pyrite}$ and biomarker characterization (identification and quantification) such as alkanes, isoprenoids and Chorobi-derived aryl isoprenoids and *n*-alkyl cyclohexanes. Molecular and sedimentological data show episodic anoxic/euxinic conditions during the earliest Triassic that intensified in the low Dienerian, and later declined towards the Olenekian suggesting a more oxygenated water column by the end of this period. A marked positive excursion in the $\delta^{13}C$ and δD of organic matter coincide with transgressive horizons at the Griesbachian-Dienerian boundary. These isotopic profiles and the molecular assemblages at this time suggest hothouse conditions were established causing the incursion of warm saline bottom water deficient in oxygen and nutrients, promoting eradication of photosynthetic organisms and favouring the development of opportunistic bacterial blooms, as predicted by the Haline Euxinic Acidic Thermal Transgressions (HEATT) model (Kidder and Worsley, 2004; 2010). Recurrent and massive volcanism during the early Triassic might have triggered repeated HEATT events, previously thought to occur only close to the extinction interval at the End-Permian.

Introduction

In the Phanerozoic, prior to the Permian-Triassic Boundary (PTB), over 90 % of all marine species became extinct along with major losses in land plants and animals (Benton, 1995; Benton and Twitchett, 2003). Global warming, attributed to massive emissions of CO_2 from the Siberian trap volcanism, is a widely accepted hypotheses that explain the environmental changes associated with the PTB extinction event (Benton and Twitchett, 2003; Erwin et al., 2002; Joachimski et al., 2012; Kidder and Worsley, 2004; Knoll et al., 2007). A series of cascade effects have been documented to occur following the rise of CO_2 close to the PTB, disturbing the pace of ecosystem recovery that lasted as long as the entire Early Triassic in some locations. Among the effects can be highlighted, but not limited to (i) influx of terrestrial nutrients to the oceans (ii) reduction in marine circulation and (iii) development of widespread marine anoxia including incursions of toxic H_2S extending to the chemocline (Algeo et al., 2011; Algeo and Twitchett, 2010; Grice et al., 2005a; Hays et al., 2012; Kidder and Worsley, 2004; Nabbefeld et al., 2010b; Nabbefeld et al., 2010c; Wignall and Twitchett, 1996).

Fluctuations in the carbon isotope record is documented for ~5 Ma through the Early Triassic and into the Middle Triassic (Payne and Kump, 2007; Payne et al., 2004). Modeling suggests that the prominent Early Triassic carbon isotope excursions were probably caused by a sequence of large-scale CO_2 injections from the Siberian Traps Large Igneous Province (STLIP) (Payne and Kump, 2007). However, little is known about the volumes of CO_2 released during that period and absolute dates have been shown to be inconsistent with the timing of STILP (Reichow et al., 2009). Single volcanic out-gassing and/or injection of large amounts of isotopically light methane do not fully explain the carbon isotopic records reported during the Early Triassic (Corsetti et al., 2005; Payne and Kump, 2007). Increasing microbial respiration rates and reduction of organic carbon burial are also possible explanations for the Early Triassic carbon isotope excursions. Widespread anoxia along with ocean stratification/turnover after the PTB has also been used to explain the dynamic

fluctuations of the carbon isotopic record at that time (Wignall and Twitchett, 2002). Modeling has supported a positive feedback with temperature fluctuations (Finnegan et al., 2012; Stanley, 2010). Extremely high temperatures are thought to have played a prominent role in the suppression of ecosystems in the equatorial recovery during the Early Triassic (Sun et al., 2012), however no evidence have been presented extending this hypothesis to higher latitudes.

The pace and magnitude of ecosystem recovery after the PTB vary with depositional environments, paleolatitudes and regional paleoenvironmental conditions (e.g. Foster and Twitchett, 2014; Wignall and Twitchett, 1996; Wignall and Twitchett, 2002). Particularly, variations in the intensity of the anoxic conditions seem to have a direct control over the rate of post-Permian recovery in some locations (Foster and Twitchett, 2014; Twitchett et al., 2004). Therefore, the study of local-scale sedimentary sequences of the Early Triassic is critical to improve our understanding of the ecosystem response to very specific paleoenvironmental circumstances after the PTB. This present study focuses on the environmental conditions associated with the recovery in a shallow marine environment at high latitude, involving analyses of a suite of samples (at high-resolution) collected from the Early Triassic strata from Spitsbergen, Svalbard, paleogeographically located in the Boreal Sea. This study evaluates changes in the major biogeochemical cycles affected during the PTB. Carbon burial and assemblage of microbial communities following the Late Permian extinction event are here scrutinized. A biomarker and compound specific isotope approach coupled with sedimentology, paleontology and bulk isotope geochemistry ($\delta^{13}C_{carbonate}$, $\delta^{13}C_{org}$, $\delta^{34}S$, $\delta D_{kerogen}$, $\delta^{34}S_{total\ sulfur}$, $\delta^{34}S_{pyrite}$) contribute understanding different scenarios of e.g. algal productivity, anoxic conditions, heterotrophic growths and salinity, postulated to vary after the extinction and directly affect the recovery in marine ecosystems.

Geological setting

The studied samples were collected from the type location of the Vikinghøgda Formation in central Spitsbergen and described by Mørk et al. (1999). This formation comprises, in ascending order, the Deltadalen, Lusitaniadalen and Vendomdalen members, all of which were sampled in this study, and was deposited in a marine shelf setting in the Boreal Sea, at a paleolatitude of ~45°N. The base of the Vikinghøgda Formation is defined by Mørk et al. (1999) as occurring at a 'weathering surface' within the upper two metres of a continuous succession of thickly bedded, bioturbated, shallow marine, glauconitic fine-medium sandstones. As discussed by Nabbefeld et al. (2010c), the base of the formation was originally considered to represent the PTB (Mørk et al., 1999) but combined biostratigraphy and magnetostratigraphy now shows that the boundary is located some 12 m above the base just prior to a short-duration reverse polarity interval within the local 'Vh2' magnetochron (Hounslow et al., 2008). The Deltadalen Member thus spans the Late Changhsingian to end-Induan and records the extinction horizon and latest Changhsingian transgression within the lowest few metres (Nabbefeld et al. 2010c).

Eighty-eight samples were collected in 2007 about every two metres from just above the PTB (Fig. 4.1; Fig. A4.1) in the lower Deltadalen Member to the basal Botneheia Formation (lowest Anisian). The main sections described by Mørk et al. (1999) and Hounslow et al. (2008) were logged and sampled: a lower one spanning the base of the Vikinghøgda Formation through to the basal Vendomdalen Member, mainly exposed in riverbanks around the southern flank of Vikinghøgda, and an upper one on southeast slopes of Vikinghøgda spanning the upper Vendomdalen Member and basal Botneheia Formation. Due to field constraints, ~50 m of the Vendomdalen Member were not sampled (see SOM for further details). Zonation and stratigraphy of the sampled section follows that of Hounslow et al. (2008).

The sampled portion of the Deltadalen Member comprises interbedded laminated or blocky (bioturbated) mudstones and thinly bedded, cemented siltstones and fine sandstones. The latter may be laminated, preserving parallel and ripple cross laminations, or bioturbated with low diversity assemblages of small sized

Arenicolites, *Rhizocorallium, Planolites* and, towards the upper part, *Thalassinoides,* with a maximum burrow diameter of 15 mm. The cemented silt- and sandstones are interpreted as tempestites, and this member was deposited in an offshore shelf setting mainly above storm wavebase. Ichnofabric indices of individual beds range from ii1 to ii3 (Fig. 4.2), with low values indicative of hypoxia or anoxia and/or, within the tempestites at least, relatively rapid sedimentation.

The remaining Vikinghøgda Formation was deposited in a deeper, distal offshore shelf setting and is mudstone-dominated. The Lusitaniadalen Member consists of dark grey, centimeter-bedded to laminated silty mudstones with occasional thin (typically <5 cm thick), laminated, cemented, very fine sandstones and siltstones. Early diagenetic carbonate concretion horizons are common, especially in the middle and upper parts of the member. The overlying Vendomdalen Member records the most distal deposits of the formation, and is dominated by silty, dark grey, cm-bedded to laminated mudstones, with no sandstones recorded. Horizons of carbonate concretions are common and, towards the upper part especially, thick, tabular, cemented beds, often containing ammonoids and vertebrate remains, are present. The base of the overlying Botneheia Formation is conformable and marked by ~1 m of bioturbated (ii3), thinly bedded, muddy, very fine sandstones that are capped by a 16 cm bed of small phosphatized burrows and phosphate nodules. After 7 m of poorly exposed, dark grey, cm-bedded to laminated silty mudstones, a ~1 m thick, yellow weathering, bedded, fine sandstone that is well bioturbated (ii3-4) by *Rhizocorallium*, and contains ammonoids, aulacocerids and bivalves, marks the top of the sampled section.

A detailed method description of the analyses performed on the outcrop samples is summarized in the SOM (Fig. 4.S2).

Table 4. 1 Summary of pyrolysis Rock-Eval results (TOC, T_{max}, HI, OI) and biomarker parameters. Average per stratigraphic units; the range of the measurement per stratigraphic unit is specified in red as a standard deviation.

	Facies	TOC wt.%	T_{max}	HI	OI	Ts / Ts+Tm	Ro (calc)	MPI-1	Pr / Ph	AIR	C_{33} ACH / *n*-C_{33}	TAR-HC	CPI	Kerogen type
Botneheia Formation ***Anisian*** ***n* = 4**	Deep Shelf	0.4 ±0.2	439 ±3	156 ±53	83 ±100	0.6 ±0.1	0.85 ±0.03	0.8 ±0.1	1.4 ±0.3	Nd	Nd	Nd	Nd	III
Vendomdalen Member ***Olenekian (Spathian)*** ***n* = 10**	Deep Shelf	2.9 ±1.5	440 ±2	223 ±5	12 ±5	0.60 ±0.04	0.74 ±0.01	0.57 ±0.02	1.5 ±0.1	1.6 ±0.4	Nd	0.3 ±0.1	1.18 ±0.1	II
Lusitaniadalen Member ***Olenekian (Smithian)*** ***n* = 20**	Shelf	0.7 ±0.3	441 ±2	119 ±32	41 ±32	0.78 ±0.03	0.86 ±0.03	0.76 ±0.04	1.2 ±0.1	0.6 ±0.2	2.9 ±2	0.4 ±0.1	1.08 ±0.07	II/III
Deltadalen Member ***Induan*** ***n* = 13**	Offshore shelf	0.3 ±0.2	441 ±5	120 ±84	66 ±64	0.66 ±0.1	0.86 ±0.1	0.77 ±0.1	1.3 ±0.3	0.6 ±0.4	5.2 ±4	0.98 ±0.5	1.04 ±0.06	II/III

Nd: No data; TOC (%): % Total Organic Carbon; Tmax: Maximum temperature of pyrolysis (°C); HI: Hydrogen Index (mg hydrocarbon/g TOC); OI: Oxygen Index (mg CO_2/g TOC); Ts: 18α-22,29,30-trisnorneohopane; Tm: 17α-22,29,30-trisnorhopane; Ro (calc): Ro calculated from aromatic biomarkers. MPI-1: Methyl-phenanthrene Index 1; AIR: Aryl Isoprenoid Ratio (Schwark and Frimmel, 2004); TAR-HC: Terrestrial versus aquatic hydrocarbons ratio $(C_{27} + C_{29} + C_{31})/(C_{15} + C_{17} + C_{19})$; CPI; Carbon Preferential Index.

Results and Discussion

Type and maturity of OM in the Early Triassic of the Boreal Sea

The shallowest marine deposits of the Early Triassic in this location (lower Deltadalen Member) comprise bioturbated, finely laminated sandstones of lower Induan (Griesbachian) age, with poor organic preservation (TOC < 0.58 %). The kerogen in the Deltadalen Member is a mixture of type II and III kerogens that commonly represent marine and terrigenous OM deposited in a parallic marine setting.

The overlying samples from the deeper, distal offshore shelf setting, Olenekian in age (Lusitaniadalen Member), record slightly higher TOC values (average 0.67 %) without variation in the kerogen type (II/III) respect to the earliest Triassic. A drastic change in the TOC content, reaching up to 5 %, occurs at the base of the Vendomdalen Member, towards the end of the Early Triassic. The kerogen is mainly type II, presumably derived from mixed phytoplankton, zooplankton, and bacterial debris, deposited in a distal marine setting (Lafargue et al., 1998). At the base of the Middle Triassic (Botneheia Formation) the samples show values typical of kerogen type III and TOC content of around 0.3-0.7%.

Thermal maturity of the samples was determined by Rock-Eval pyrolysis (Fig. 4.1) and estimated by biomarker ratios. According to the Tmax values the samples have nearly reached the oil window (Lafargue et al., 1998), consistent with previous studies (Mørk and Elvebakk, 1999). Maturity was also assessed from the proportion of phenanthrene and its methylated homologues (Radke et al., 1986; Radke et al., 1982). The average Methyl-Phenanthrene Index-1 (MPI-1) is consistent with early stages of oil generation. The ratio of the 18α-22, 29, 30-trisnorneohopane (Ts) and 17α-22, 29, 30-trisnorhopane (Tm) is also commonly used as a thermal maturity parameter (Ts/(Ts+Tm)). This ratio can be sensitive to clay-catalyzed reactions, therefore susceptible to lithological and redox changes (Seifert and Moldowan,

1978). The calculated Ts/(Ts+Tm) values from selected samples suggest a slightly higher maturity (average of 0.60 and 0.79 for the Lusitaniadalen Member, Table 4.1) than the values of MPI-1 and Tmax (Table 4.1). Such values for the Ts/(Ts+Tm) ratio could also be controlled by reducing conditions present in the bottom waters, and/or have been affected by coelution with C_{29} and C_{30} tricyclic terpanes.

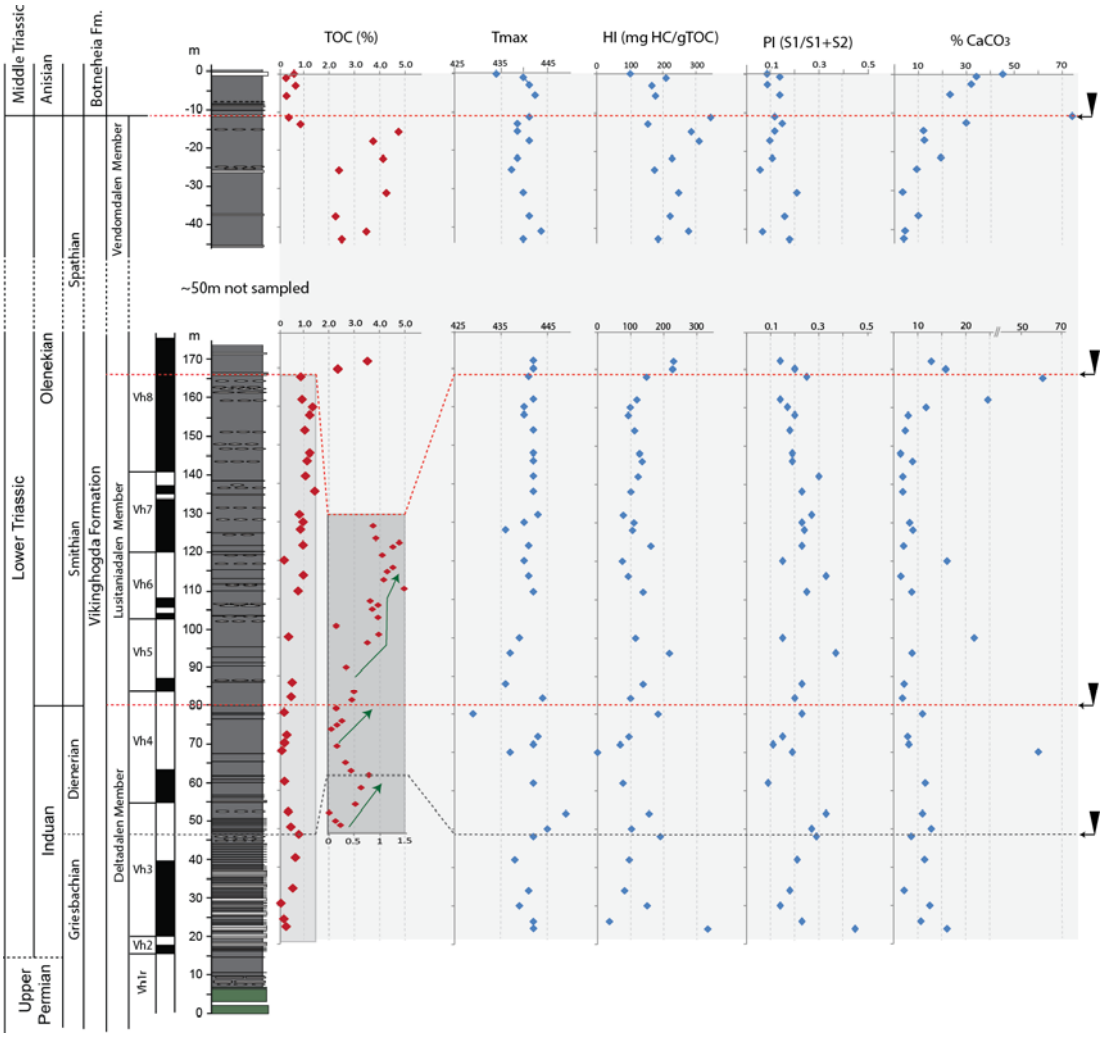

Figure 4. 1 Stratigraphic profiles of pyrolysis Rock-Eval analyses: weith percentage of Total Organic Carbon (TOC %) a close-up of the TOC data from the lowermost Triassic is noted in a dark grey box; Maximum temperature of pyrolysis (°C, Tmax); HI: Hydrogen Index (mg hydrocarbon/g TOC); PI: productivity index. % CaCO3 is determined from the total C mineral present in the sample. Black arrows refer to the base of transgressive sequences of 2nd, 3rd and 4th order, according to Hounslow et al. (2008).

Paleochanges in the Boreal Sea

Anoxic conditions are often reflected by low Pr/Ph ratios (<1.0), however, variation in the source(s) and thermal maturity of the OM can affect this ratio (Peters et al., 2005). Given that these samples have almost reached the 'oil window', high Pr/Ph values in the sequence might be slightly affected by thermal alteration. However, the general stratigraphic trend observed for this parameter reflects fluctuations in the redox conditions, as there are no significant changes in maturity through the section. Samples from the Early Triassic (Deltadalen Member) record Pr/Ph ratios ranging from 0.8 to 1.9 with the lowest values in the basal Dienerian (Figs. 2-3). The lower Pr/Ph ratios in this part of the section occur within laminated silty mudstones with low ichnofabric indices (~ ii1, Fig. 4.2), indicative of reducing conditions, possibly related to rising sea level close to the Griesbachian/Dienerian boundary. In contrast, the higher Pr/Ph ratios (1.3 – 1.9) at the top of the Dienerian are associated with well-bioturbated mudstones, as expected. However, apparently laminated and anoxic strata throughout the Olenekian record unexpectedly high Pr/Ph ratios between 1.0 and 1.5, similar to those in the bioturbated sandstones of the lower Induan. Thus, throughout most of the studied section, the Pr/Ph ratios do not reflect anoxic/euxinic conditions as recorded in late Permian and earliest Triassic section within the Boreal Sea region (Dustira et al., 2013; Hays et al., 2007; Hays et al., 2012; Nabbefeld et al., 2010c; Wignall and Twitchett, 1996).

The presence of cleaved aryl isoprenoids (Fig. 4.2), which can be direct evidence of diagenetic transformation of the intact Chlorobi derived carotenoids is, however, an excellent indicator of the extent of reducing conditions within the photic zone (e.g Grice et al 2005a). Biomarkers derived from carotenoids and bacteriochlorophylls of Chlorobi, such as ^{13}C-rich isorenieratane and methyl-*iso*butyl maleimide, respectively, provide unequivocal evidence for PZE in marine settings (Grice et al., 2005a; Grice et al., 1996; Koopmans et al., 1996; Requejo et al., 1992; Summons and Powell, 1986, 1987). A series of monoaryl and diaryl isoprenoids with a 2,3,6-trimethyl-substitution pattern were identified and quantified through the section (Fig. 4.2). These compounds were more abundant in the Lower Triassic, especially

Griesbachian and lower Smithian. These aryl-isoprenoids can be formed *via* thermally induced electrocyclic reactions (Xinke et al., 1990), consistent with the thermal maturity of this section. Also, trace amounts of crocetane (Barber et al., 2001; Greenwood and Summons, 2003), a thermal degradation product of isorenieratane (Maslen et al., 2009), was identified in the lower part of the Vikinghøgda Formation (20 – 80 m, Fig. 4.2) but non-existent in the upper Smithian (also consistent with a significantly lower abundance of aryl isoprenoids). This compound has been identified in anoxic environments showing an important depletion in ^{13}C (e.g. $\delta^{13}C$ of up to -120 ‰), from methanotrophics organisms (e.g. (Thiel et al., 1999); However, the $\delta^{13}C$ of the co-eluting Ph and crocetane is up to 3‰ more enriched with respect to Pr, endorsing in part a thermal source of crocetane from, for example, isorenieratane, rather than a methanotropich source (Fig. 4.4).

The temporal extent of the anoxic/euxinic conditions in the paleowater column was assessed by combining Pr/Ph ratio and Aryl Isoprenoid Ratio (AIR) of each sample (Fig. 4.3. Schwark and Frimmel, 2004). The relationship of these proxies suggests persistent anoxic conditions during the Induan and early Olenekian. In contrast, in the upper part of the Olenekian (Spathian, Vendomdalen Member), the concentration of aryl isoprenoids decreased (Fig. 4.2) and their distributions shifted towards a dominance of the shorter chain analogues (Fig. 4.3), suggesting shorter/weaker periods of anoxia. Thus, in this location, it would appear that in general, the intensity and duration of benthic hypoxia decreases from the PTB (Nabbefeld et al., 2010c) through the Early Triassic, turning to well oxygenated/mixed water column close to the later Olenekian.

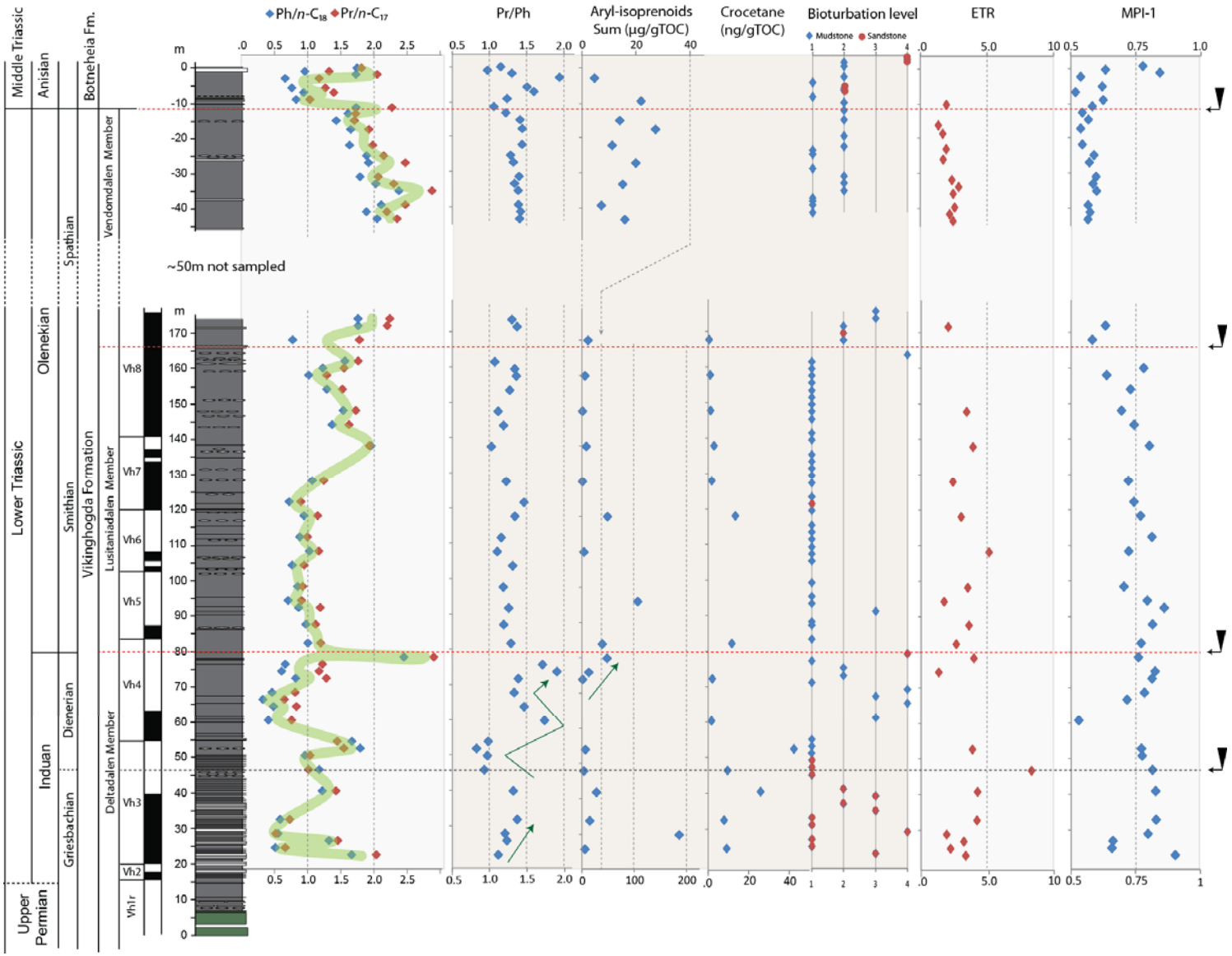
Middle Triassic
Lower Triassic
Upper Permian
Anisian
Olenekian
Induan
Griesbachian
Dienerian
Smithian
Spathian
Botneheia Fm.
Vikinghogda Formation
Vendomdalen Member
Lusitaniadalen Member
Deltadalen Member
Vh8
Vh7
Vh6
Vh5
Vh4
Vh3
Vh2
Vh1r
Ph/n-C18 Pr/n-C17
Pr/Ph
Aryl-isoprenoids Sum (µg/gTOC)
Crocetane (ng/gTOC)
Bioturbation level
Mudstone Sandstone
ETR
MPI-1
m
~50m not sampled

Figure 4. 2 Stratigraphic variability of biomarker parameters in the Lower Triassic. Bioturbation level (observations are related to the presence of infauna, and hence used as a proxy for oxygen levels. Mudrocks: 1) laminated – no infauna/ no oxygen; 2) wispy/partially laminated - presence of meio/microfauna; 3) blocky – thoroughly bioturbated by meio/microfauna, or possibly macrofauna; 4) bioturbated – presence of burrows of macrofauna. Sandstone bioturbation (macrofauna) is based on ichnofabric index from 1) laminated - no bioturbation to 4) bioturbated. Black arrows in the Bioturbation column refer to the base of transgressive sequences of 2nd, 3rd and 4th order, according to Hounslow et al. (2008).

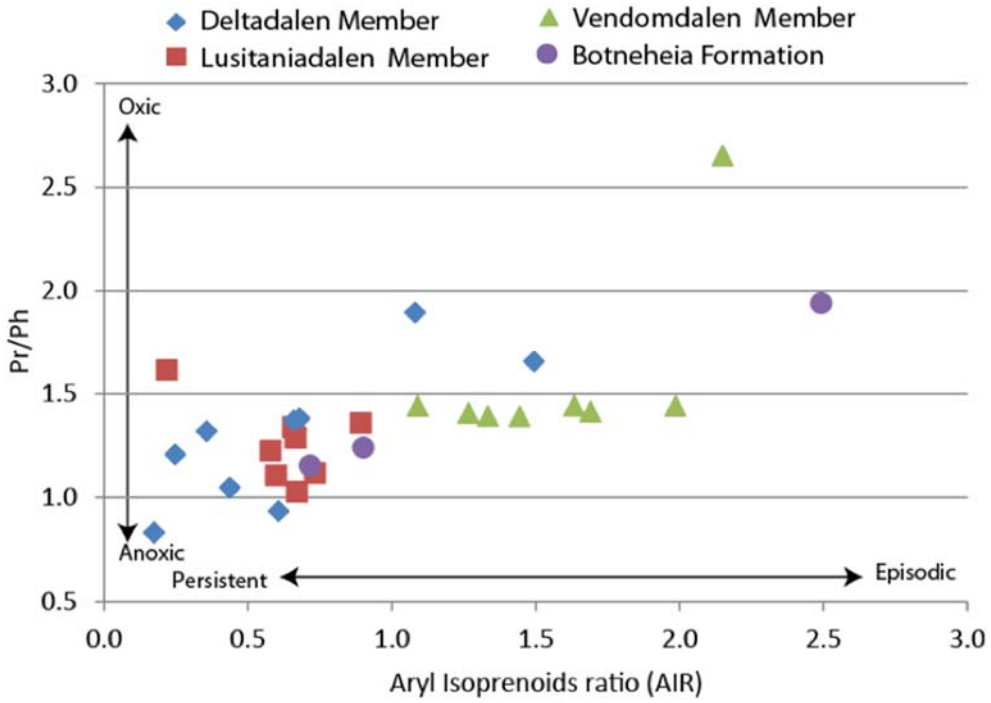

Figure 4. 3 Crossplot of Pr/Ph ratios and Aryl Isoprenoid Ratios (AIR). AIR (C_{13} - C_{17})/ (C_{18} - C_{22}) increase with thermally induced cleaved products from the aryl isoprenoids. Low AIR values indicate long-lived and permanent PZE whereas, high values indicate episodic PZE. The purple circle in the upper right corner of the figure is a bioturbated sample. The green triangle with the highest Pr/Ph is also bioturbated.

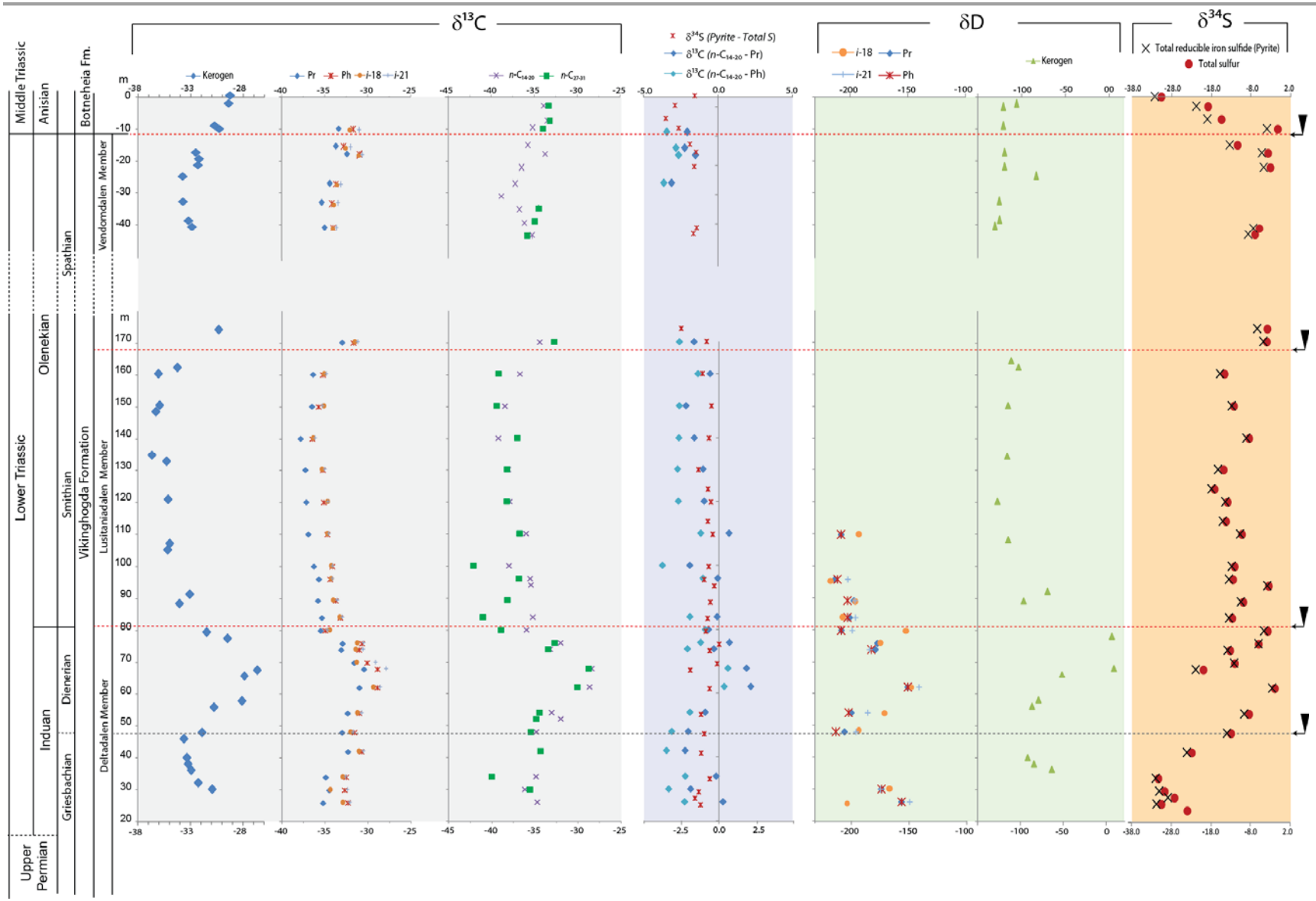
δ13C
δ34S (Pyrite - Total S)
δ13C (n-C14-20 - Pr)
δ13C (n-C14-20 - Ph)
δD
δ34S
Kerogen
Pr
Ph
i-18
i-21
n-C14-20
n-C27-31
Total reducible iron sulfide (Pyrite)
Total sulfur
m
Middle Triassic
Lower Triassic
Upper Permian
Anisian
Olenekian
Induan
Griesbachian
Dienerian
Smithian
Spathian
Botneheia Fm.
Vikinghogda Formation
Vendomdalen Member
Lusitaniadalen Member
Deltadalen Member

Figure 4. 4 Stable isotope compositions for the Early Triassic in Deltadalen, Spitsbergen. $\delta^{13}C$ and $\delta^{18}O$ of total carbonates, $\delta^{13}C$ of kerogen and individual hydrocarbons. δD was measured for purified kerogen and also the regular isoprenoids. $\delta^{34}S_{pyrite}$ as a measurement of the $\delta^{34}S$ of total reducible sulfur is ploted alongside $\delta^{34}S$ of total sulfur. Arrows represent the base of transgressive sequences of 2nd, 3rd and 4th order; according to Hounslow et al. (2008). For detailed method descriptions see the SOM.

Isotopic changes in the Boreal Sea after the PTB

Isotopic excursions are recorded globally from the latest Permian through the Early Triassic, reflecting perturbations of the global carbon cycle that spanned some 5 Ma after the main extinction event (Payne and Kump, 2007; Payne et al., 2004; Tong et al., 2007). In this investigation we focus on the isotopic variations ($\delta^{13}C$ and δD) recorded in organic remains, including kerogen and individual hydrocarbons, a powerful tool susceptible to changes in the source of biomass, environmental conditions at the time of deposition but also physiological factors such as cell size and growth rate (Popp et al., 1998); Measurments of $\delta^{34}S$ were carried out to investigate the extend of perturbations of the sulfur cycle reported to occur during the P/Tr extinction event. Globally, excursions in $\delta^{34}S$ of sulfide minerals around the P/Tr boundary have been associated to changes in sulfur burial and/or redox conditions (Grice et al., 2005a). The δD of OM is particularly associated to the depositional paleolatitude/paleoclimate of the original depositional environment where the OM was biosynthesized and hydrogen exchange with meteoric/seawater waters takes place (Andersen et al., 2001; Dawson et al., 2004; Sachse et al., 2012). However, isotopic composition ($\delta^{13}C$ and δD) of fossil OM is also sensitive to thermal alteration. As previously discussed, the constant maturity throughout the section has barely reached the initial stages of oil generation. Therefore, the isotopic changes discussed in this section reflect not only variations in the global carbon reservoir but also differences in the type of OM present during the Early Triassic in the Boreal waters.

Values of $\delta^{13}C_{org}$ range from -30.92 to -33.62 ‰ in the lowest interval of the Early Triassic (Griesbachian); followed by an important isotope enrichment into the Dienerian,

reaching the heavier isotopic value of the entire section at around 65 m in the mid-Dienerian (-26.64 ‰, Fig. 4.4). The $\delta^{13}C_{org}$ becomes more negative through the upper Dienerian and into the Smithian (minimum of -36.04 ‰); with a positive excursion (possible) at the Smithian/Spathian boundary (Fig. 4.4). Interestingly, the $\delta^{13}C$ of individual hydrocarbons in the study section follow a very similar trend to the $\delta^{13}C_{org}$, yet the absolute values are systematically depleted in ^{13}C with respect to the total biomass (Fig. 4.4); concordant with the differences found elsewhere for kerogen in the Phanerozoic (Hayes, 1993; Hayes et al., 1999).

The $\delta^{13}C_{org}$ in the lower part of the Early Triassic (Griesbachian; at around 28 m, Fig. 4.4), is comparable to pre-extinction values reported in a nearby location (Nabbefeld et al., 2010a; Nabbefeld et al., 2010c), showing carbon isotope composition returned to more positive pre-extinction values within the Early Induan period, in less than 0.3 Ma after the PTB. However, multiple isotopic variations are recorded in the following 5 Ma. Through the upper Griesbachian a ca. 3 ‰ negative excursion can be attributed to change in source of biomass, significantly diminishing terrestrial/higher plant-biomass towards the Griesbachian/Dienerian boundary.

In the Dienerian, a significant positive shift in $\delta^{13}C_{org}$ of up to 5 ‰ occurs in between two distinctive transgressive episodes. However, this event is not synchronous with the proposed global positive excursion (4 ‰ in the $\delta^{13}C_{org}$) reported at the Induan/Olenekian Boundary for the Global Stratotype Section and Point (GSSP) in Southern China and also in sections from India, Italy and Western Australia (Corsetti et al., 2005; Metcalfe et al., 2013). It is possible this isotopic excursion is not globally synchronous, or perhaps more work is needed to identify possible unrecognized problems with stratigraphic correlation between these regions.

The Dienerian positive enrichment in this section is observed in the $\delta^{13}C$ and δD of individual hydrocarbons and total biomass (kerogen; Fig. 4.4); but no significant changes in biomarker distributions within this interval are observed to relate with

variation in the source of OM. Thus, the parallel isotopic enrichment in C and D is most likely a consequence of climatically driven hydrologic perturbation; perhaps increase in atmospheric CO_2 from protracted volcanic events (Payne and Kump, 2007). Intensification of anoxic conditions into the photic zone (PZE) is also a plausible mechanism to explain the positive excursion. At the base of the Dienerian low AIR and low Pr/Ph ratios occur in parallel to above background concentrations of crocetane (Fig. 4.2-4.3). Under these conditions an increase in organic carbon burial driven by high algal productivity and high nutrient influx will yield biomass enriched in ^{13}C due to faster than normal growth rates (Popp et al., 1998). Additionally, predominant biomass deposition from organism, such as cyanobacteria and Chlorobi-related, with kinetic carbon isotopic fractionation relatively small compared to that of algae, could contribute to heavy biomass and the positive signature in OM.

Paired enrichment in the δD and $\delta^{13}C$ of OM is characteristic of hypersaline environments (Grice et al., 1998; Schidlowski et al., 1994). The δD enrichment in OM can be associated with warm climate, in which the loss of isotopically light water *via* evaporation of seawater leads to hypersaline D-enriched marine environment (Andersen et al., 2001); however, no evidence of additional warming during the Dienerian has been reported in climate studies of the tropical Tethyan region (Sun et al., 2012) and there is no paleotemperature record for the northern paleolatitudes. It is possible that this data set provides indications of a regional warming of the Boreal Ocean during the Dienerian. Alternatively, it also may indicate that local or regional seawater salinity was higher at this time, providing the first evidence of warm, saline-rich bottom waters as predicted by Kidder and Worsley (2010) in their HEATT model. Isotopic enrichment in the Dienerian might have been caused by algal or bacteria blooms, perhaps triggered by the upwelling of anoxic and saline-rich deep-water (Andersen et al., 2001; Grice et al., 1998; Kidder and Worsley, 2004; Kidder and Worsley, 2010; Schidlowski et al., 1994).

Following the isotopic enrichment, over the entire Smithian a progressive negative excursion of ca. 6 ‰ in the $\delta^{13}C_{org}$ and $\delta^{13}C$ of individual hydrocarbons is recorded (Fig.

4.4). Different hypotheses may explain this, including: (i) a source of light carbon such as methane and/or CO_2 from the weathering of coal (Retallack et al., 2011) and/or (ii) recovery of the marine ecosystem (Tong et al., 2005; Tong et al., 2007); alternatively (iii) this isotopic shift could be related to the sedimentation rates and progressive deepening of the basin through the Smithian. This isotopic record of biomass may simply be reflecting an increasing distance from the paleoshoreline. In the Smithian the most negative $\delta^{13}C_{org}$ and $\delta^{13}C$ of individual compounds are reached below the Smithian/Spathian boundary, followed by a single measurement that reflects a possible positive excursion (Fig. 4.4). Likewise, the positive shift in $\delta^{13}C_{org}$ at the Spathian/Anisian boundary (Fig. 4.4) probably reflects a change in kerogen type (from types II/III to III).

$\delta^{34}S$ in the total sedimentary sulfur and in the total reducible inorganic sulfur (TRIS), which is essentially pyrite minerals, were determined on 37 samples spanning the Early Triassic in the studied location. $\delta^{34}S_{pyrite}$ values vary between −32.3 ‰ and −2.5, showing series of isotopic shift that coincide with the major isotopic changes noted for OM ($\delta^{13}C$ and δD). Nabbefeld et al., (2010a; 2010c) recorded a negative shift of ca. 18.6‰ during the end-Permian extinction event in Spitsbergen. Their data show a general negative trend from −13.6‰ before the marine ecosystem collapse towards −32.2‰ after the main event (Nabbefeld et al., 2010c). Similarly, the early Griesbachian at the base of the sampled section, show a negative shift on the $\delta^{34}S_{pyrite}$, comparable to Nabbefeld et al., (2010a; 2010c) and attributed to changes in the sulfur cycle as a consequence of global warming and the resulting massive H_2S outgassing from the deep ocean (Maruoka et al., 2003; Kaiho et al., 2006a; 2006b; 2012). However, overturn of stagnant euxinic deep oceans could result in a similar isotopic trend (Kajiwara et al. 1994, Knoll et al. 1996).

Around mid-Griesbachian, or ca. 0.5 Ma after the main extinction event, a significant shift in the $\delta^{34}S_{pyrite}$, from -31.9 to a maximum of -2.5 is noted. This positive excursion occurs in paralleled to the positive excursion observed on $\delta^{13}C$ and δD of total OM and

biomarkers, however $\delta^{34}S_{pyrite}$ positive shift culminate earlier and is followed by a series of less drastic but rapid negative shifts thereafter. The overall positive shift in $\delta^{34}S_{pyrite}$ could be related to a change from well-oxygenated bottom waters to fluctuating low oxygen (dysoxic to possibly euxinic) conditions during the Dienerian in the waters of the Boreal Sea (Fenton et al., 2007). This result is in agreement with the parallel isotopic enrichment in C and D and its previously discussed interpretation, supporting here the plausible occurrence of algal or bacteria blooms, perhaps triggered by the upwelling of anoxic and saline-rich deep-water.

Several minor excursions of $\delta^{34}S_{pyrite}$ are observed throughout the Dienerian period and into the Smithian. In this interval, the most enriched $\delta^{34}S_{pyrite}$ values could be explained by input from detrital pyrite as they coincide with the base of transgressive sequences identified by Houslow et al (2008). At the top of the studied section, the $\delta^{34}S_{pyrite}$ shift toward more negative values consistent with increased of bacterially derived sedimentary sulphides and overall deepening of the depositional environment.

Globally occurring isotopic excursions in $\delta^{34}S$ of sulfide minerals close to the P/Tr boundary are associated, but no restricted to changes in sulfur burial and/or redox conditions, but also changes in quality of OM could affect overall sulfur isotope discrimination. (Grice et al., 2005a, Fenton et al. 2007, Kajiwara et al., 1994; Korte et al., 2004; Kaiho et al., 2006a, 2006b, 2012; Nabbefeld et al., 2010c). However, we here show that the isotope excurtion that accompanied the main extinction events persisted trought the entire early triassic, demostrating perturbations of the main biogeochemical cycles throughout.

Molecular fingerprints of microbial changes during the Early Triassic

Substantive paleoenvironmental changes associated with the Late Permian extinction event have been identified in the Boreal Sea, including the collapse of the marine and terrestrial ecosystems (Twitchett et al., 2001), transgression, phytoplanktonic blooms driven by an elevated nutrient supply, and anoxic conditions with episodes of PZE (Hays et al., 2007; Hays et al., 2012; Hounslow et al., 2008; Looy et al., 2001; Nabbefeld et al., 2010c; Wignall and Twitchett, 1996).

In most of the samples from the lower Griesbachian the distribution of *n*-alkanes ranges between *n*-C_{14} and *n*-C_{35}, peaking at around *n*-C_{17} and *n*-C_{27} (Fig. 4.5), indicating a mixture of sources, (i.e. aquatic organisms and plant waxes; Fig. 4.5-4.6), which is consistent with common spinose acritarchs (*Michrystridium spp.*), woody fragments and gymnosperm pollen grains, identified in the palynological samples of this interval (below 30 m). Around 30 m above the base of the section, the concentration of *n*-alkanes (Fig. 4.6) reaches a maximum and the distribution is dominated by the *n*-C_{27} alkane with a slight odd-over-even predominance in the higher carbon range (average CPI≥1), typical of plant waxes. At this level (ca. 28 m) the location was at its closest proximity to vegetated landmasses, perhaps due to delta progradation or sea level fall, in which a greater influx of terrestrial biomass into the marine ecosystem is observed due to elevated rainfall and runoff. Sedimentological data indicate that the fine sands interlayering cemented silts were deposited under storm conditions; in this high energy regime the seaward transport of terrestrial vegetation is likely. This interpretation is supported by a sharp increase in the concentration of aromatic compounds potentially derived from land plants (e.g. dibenzothiophene, coronene and pyrene). These compounds can be transported by run-off of fire-revaged denudated slopes into marine depositional environments, indicating episodes of wildfires (Fenton et al., 2007; Nabbefeld et al., 2010b; Nabbefeld et al., 2010c). Following this episode, a moderate decrease of the abundance of aromatic compounds is noted parallel to the negative shift

of $\delta^{13}C_{org}$ towards the Griesbachian/Dienerian boundary (Fig. A4.5), where Hounslow et al. (2008) placed the base of a transgressive sequence.

Primarily an algal and/or land plant contribution can be assumed for most of the Early Triassic samples, based on the isotopic composition of isoprenoids which usually are 1 ‰ to 3 ‰ heavier compare to the *n*-alkanes (Fig. 4.4) for these organisms (Hayes, 1993; Schouten et al., 1998). However, during the Dienerian, synchronous with the major positive excursions in $\delta^{13}C_{org}$ and δD, the *n*-alkanes are enriched in ^{13}C relative to the regular isoprenoids Pr and Ph (Fig. 4.4). At the same time, high proportions of the isoprenoids Pr and Ph relative to the *n*-alkanes C_{17} and C_{18}, respectively, suggest the major source of OM during the Dienerian in the waters of the Boreal Sea derived from heterotrophic bacteria (Grice et al., 2005a); perhaps more non-photoautotrophs (e.g. sulfate reducers) due to the lack of competition from photoautotrophs. Overall, ^{13}C-enriched biomass derived from non-photo autotrophic bacteria led to a positive carbon excursion at that time. This decline in photoautotrophic biomass may have been triggered by hostile oceanic conditions, such as upwelling of warm, saline bottom waters containing low oxygen and few nutrients.

At the top of the Induan Stage (at 75 m; Fig 5) *n*-alkanes from C_{14} to C_{36} have a strong even-over-odd predominance in the *n*-C_{18} to *n*-C_{26} interval, with a high abundance of regular isoprenoids respect to *n*-alkanes. Similar fingerprints to the one identified at this stratigraphic level have been reported in both aerobic and anaerobic bacteria consortium (e.g. sulfate-reducers) in highly saline/carbonate environments, reinforcing the idea of bacterial blooms at this time (Dembicki and Meinschein, 1976; Logan et al., 1999; Melendez et al., 2013; Nishimura and Baker, 1986).

Above the Induan-Olenekian boundary, through the Lusitaniadalen Member and into the Middle Triassic, the *n*-alkanes show a normal distribution peaking at *n*-C_{17} without an odd-over-even predominance of carbon numbers (Fig. 4.5). Average values of 0.4 for the common ratio used to express the proportion of terrigenous vs. aquatic input (TAR),

suggest a dominant contribution from algae and bacteria in a marine environment. A predominance of photosynthetic organisms is supported by the systematic increase of the ratio (Pr + Ph)/(*n*-C_{17} + *n*-C_{18}) towards the top of the Smithian (Fig. 4.3); comparable with the negative trend observed in the $\delta^{13}C_{org}$ for this section. The Vendomdalen Member was deposited in a distal shelf environment in which short chain *n*-alkanes are dominant, with a higher proportion of *n*-C_{17} and *n*-C_{18} characteristic of photosynthetic algae input (TAR ~0.2).

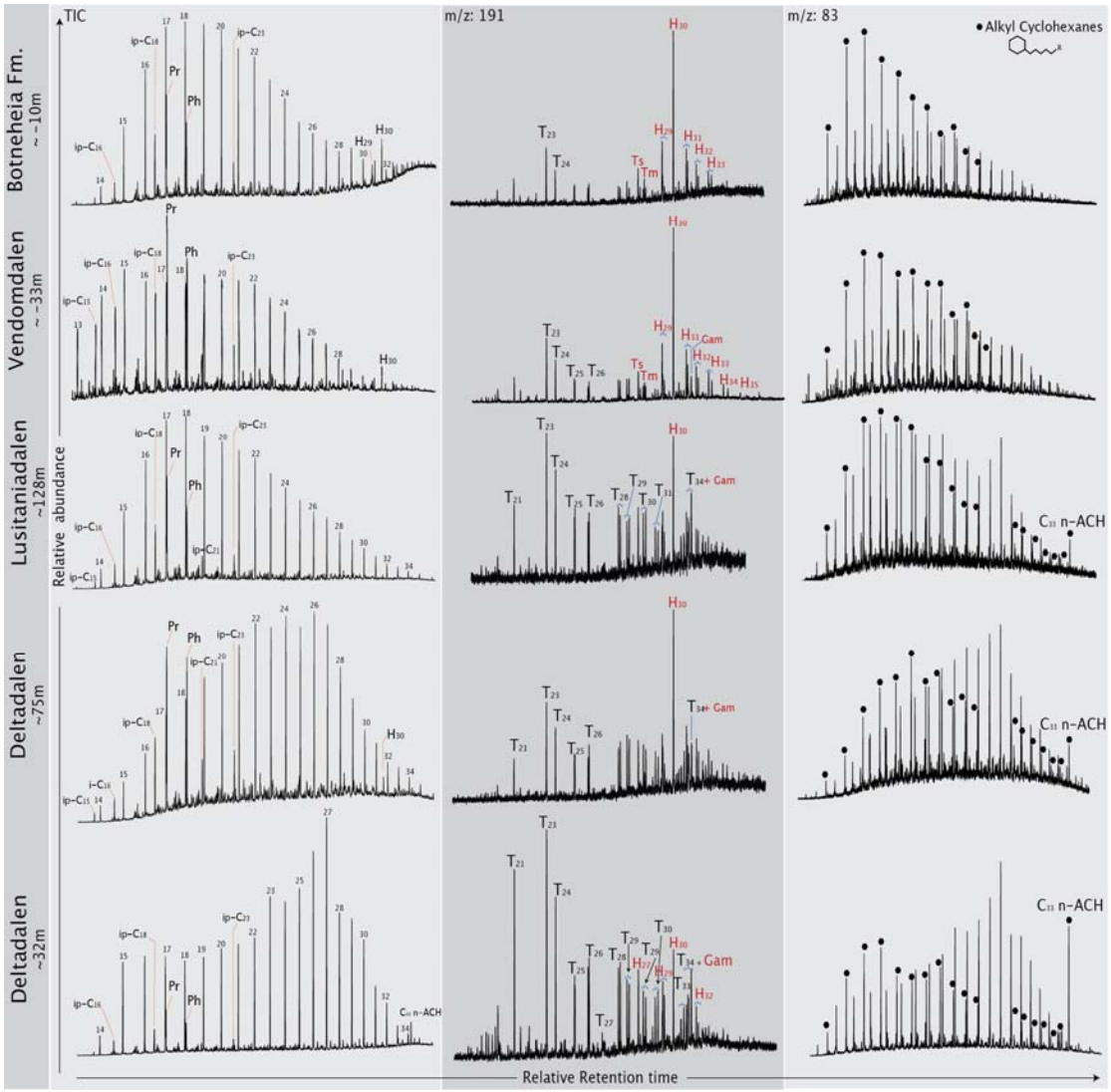

Figure 4. 5 Molecular fingerprint of representative samples of each stratigraphic unit from the Early Triassic of Spitsbergen. In the first column Total Ion Chromatograms (TIC) are observed and numbers indicate carbon number of *n*-alkanes. Regular isoprenoids are identified with the symbol *ip*-C (subscripts indicating carbon number); Pr: Pristane; Ph: Phytane. The second column displays the *m/z* 191 of selected samples allowed for the identification of tricyclic terpanes (T; subscript indicating carbon number) and also pentacyclic Hopanes (H; subscript indicating carbon number); Gam: Gammacerane. In the last column ion/mass chromatograms (*m/z* 83) show the distribution of alkanes and *n*-alkyl cyclohexanes (identified with black circles); the relative abundance of the C_{33} *n*-ACH can be noticed in samples from the Deltadalen and Lusitaniadalen Members.

The concentration of tricyclic terpanes fluctuates throughout the section, along with minor concentrations of hopanes and steranes (Fig 5-6). Tricyclic terpanes are common in Phanerozoic oils and rock extracts (Brocks and Pearson, 2005; Peters et al., 2005), and have been attributed to *Tasmanites* and prasinophyte algae (De Grande et al., 1993; Dutta et al., 2006; Simoneit et al., 1990). From the Griesbachian to the Smithian, the terpane/hopane ratio oscillates from 0.7 to a maximum of 13.6 at the Griesbachian-Dienerian boundary; but the proportion of tricyclic terpanes is normally higher than the hopanes (see *m/z* 191, Fig. 4.5). However, in the Spathian uppermost interval of the Vendomdalen Member hopanes became more abundant (terpane/hopane ratios shift from 0.2 to 0.7), dominated by the C_{30} hopane. *Tasmanites* remains have only been identified from the latest Olenekian in the studied section (Mørk and Elvebakk, 1999), which may indicate that the tricyclic terpanes potentially derive from a different algal source, at least in the Induan sediments. Here we propose prasinophytes -unicellular green algae- as the most likely source of tricyclic terpanes and C_{28} steranes, since they are commonly associated with nutrient-rich marine environments at high-latitudes and are able to thrive under stressful environmental conditions (Schwark and Empt, 2006).

In most of the Smithian samples, marine OM is more abundant and terrestrial OM becomes scarce. This is consistent with the carbon isotope record and the absence of sandstones, indicative of a deepening of the basin (i.e. relative sea level rise) and/or increased distance from the paleoshoreline. Based on the proportion of hopanes and steranes in the Smithian samples (Fig. 4.6), an increase in the relative contribution of algae and less heterotrophic recycling of OM is proposed; potentially indicative of normalization/improvement of the water chemistry at that time (Chen et al., 2011; Peters et al., 2005).

C_{33} Alkylcyclohexane: a potential salinity indicator

N-alkylcyclohexanes (*n*-ACH) are recorded within the Induan and Smithian. Their abundances (C_{14} to C_{31} *n*-ACH) follow a similar trend to the *n*-alkanes, suggesting a

common phytoplanktonic source maximizing in the lower carbon number range (Figs. 5-6). The C_{33} *n*-alkylcyclohexane (C_{33} *n*-ACH) first appears within the extinction interval, prior to the PTB, and extends into the Early Triassic (Grice et al., 2005b; Hays et al., 2012; Nabbefeld et al., 2010c). The distribution of C_{33} *n*-ACH in East Greenland closely matches that of the spinose acritarchs *Michrystridium* and *Veryhachium* (Stancliffe and Sarjeant, 1994); and so it has been ascribed to phytoplanktonic taxa that survived during the unusual environmental conditions in the latest Permian (Grice et al., 2005b). Species assigned to both genera occur within palynological assemblages throughout the studied section (See appendix 4).

The C_{20} and C_{25} regular isoprenoids are biomarkers of the ether-bound membrane lipids of haloarchea (Grice et al., 1998), which particularly bloom under hypersaline conditions above normal seawater. In most of the samples analyzed the *i*-C_{21} and *i*-C_{23} biomarkers were present and were also isotopically enriched in ^{13}C compared to Pr (Fig. 4.3, 4.5, 4.6) consistent with a haloarchea contribution. Particularly in the Griesbachian, the concentration of regular isoprenoids is very high, possibly related to the upwelling of warm saline bottom waters (e.g. Kidder and Worsley, 2004; 2010) and the development of important haloarchea communities.

A significant correlation was found between the abundance of the regular isoprenoid *i*-C_{21} and of C_{33} *n*-ACH (R^2: 0.83), suggesting that the parent organisms shared similar environmental tolerances. Thus, anoxic conditions and marginally higher than normal salinity may have triggered the radiation of the C_{33} *n*-ACH parent organism and/or are the optimum conditions for their preservation. During the Early Triassic in Spitsbergen, three stratigraphic levels (the mid-Griesbachian, the Induan/Olenekian Boundary and the mid-Smithian; Fig 5-6) show relatively higher concentrations of C_{33} *n*-ACH, compared to its immediate shorter analogue (C_{32} *n*-ACH); at these stratigraphic levels higher abundances of other biomarkers are also noted and appear to coincide with transgressive event and sea level rise, and might be indicative of minor environmental crises.

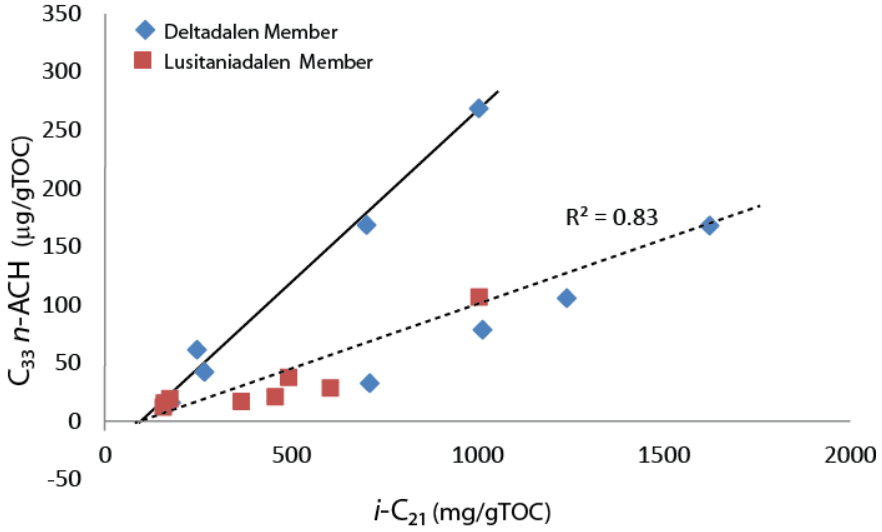

Figure 4. 6 Crossplot of the concentration of C_{33}-ACH and the *i*-C_{21}.

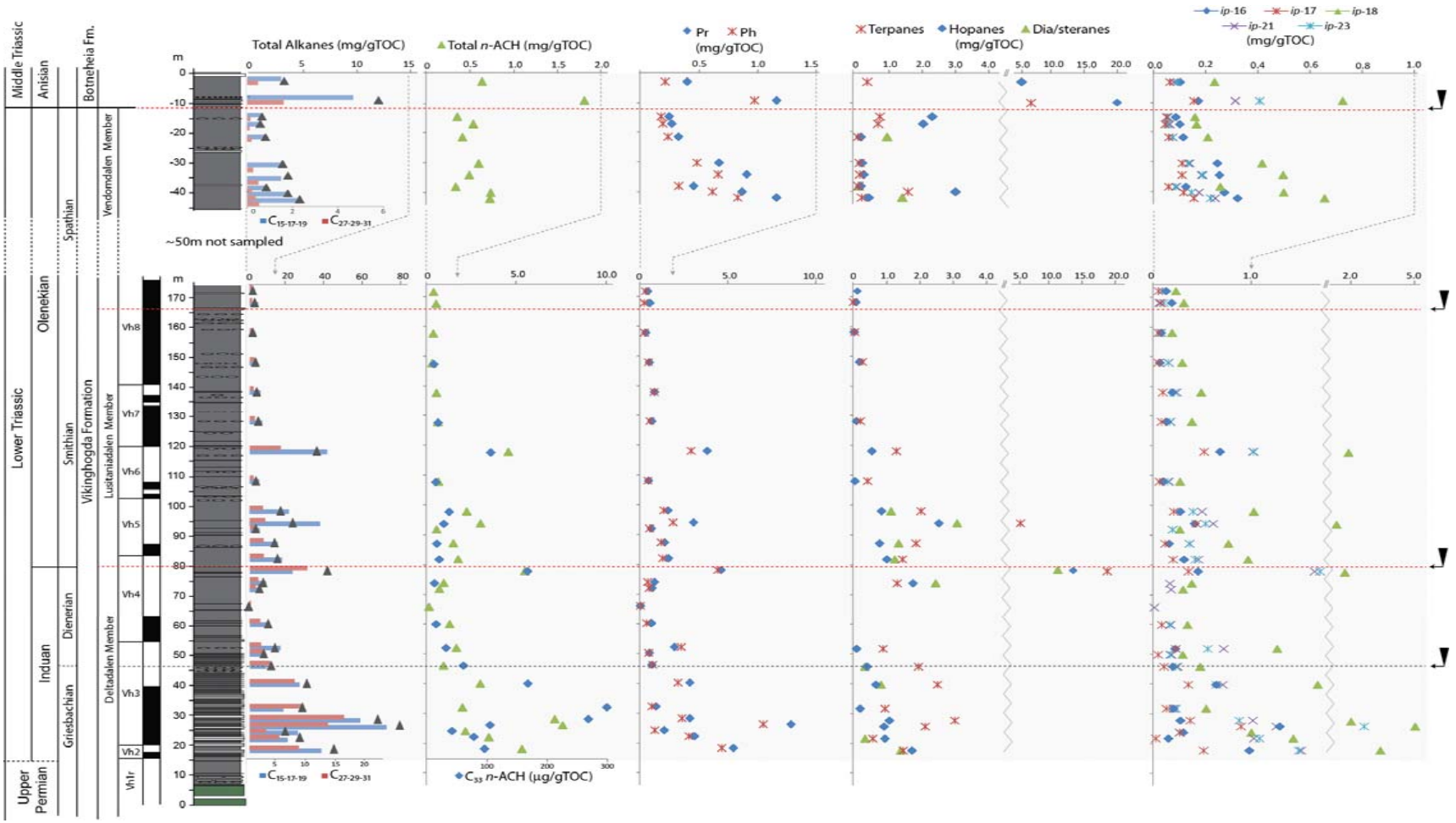

Figure 4. 7 Abundances of dominant biomarkers throughout the studied section. Total *n*-alkanes and sum of short chain *n*-alkanes in blue (*n*-$C_{15\text{-}17\text{-}19}$) and sum of long chain in red (*n*-$C_{27\text{-}29\text{-}31}$); ACH: *n*-alkylcyclohexane and C_{33}-*n*-ACH; Dia/steranes: total abundance of steranes and rearranged diasteranes; Regular isoprenoids (*i*-$C_{16\text{-}17\text{-}18\text{-}21\text{-}23}$). Arrows represent the base of transgressive sequences of 2nd, 3rd and 4th order, according to Hounslow et al. (2008).

Summary and conclusions

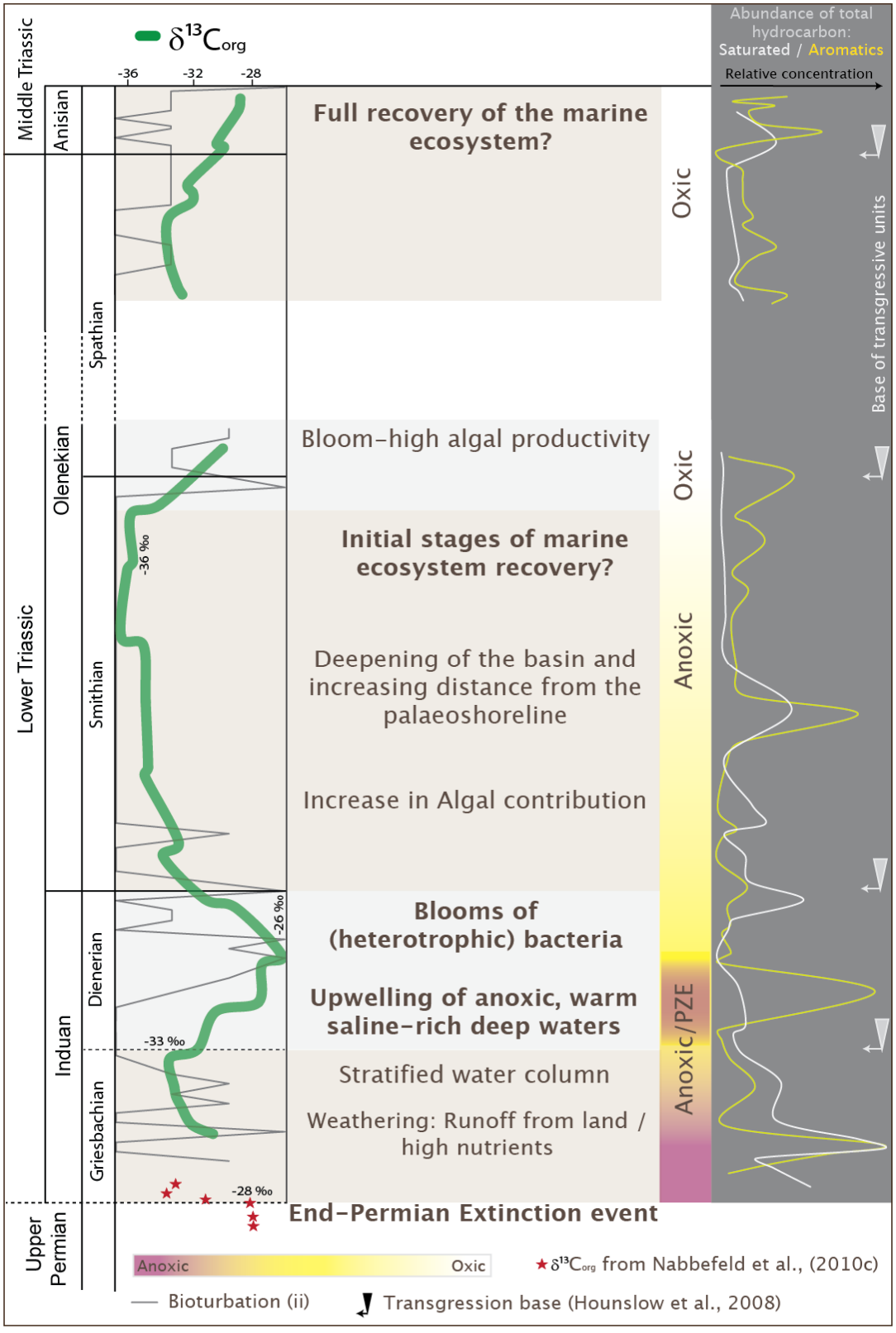

Figure 4. 8 Proposed series of events that followed the mass extinction event in PTB in the Boreal Sea. In this summary plot, the main events have been identified based on the isotopic composition of carbon and deuterium in OM as well as the molecular fingerprint. In the left hand side of the figures relative abundance of the total saturated and aromatic biomarkers is plotted.

Following the extinction event the late Permian Boreal Sea was characterized by a waxing and waning of PZE and high algal productivity (Nabbefeld et al., 2010c). Our study reveals that after the PTB intermittent anoxic/euxinic conditions continued through the earliest Triassic. The most intense and persistent anoxic/euxinic conditions during the Early Triassic were mostly confined to the Induan, with a marked decline towards the mid-Olenekian and into the Middle Triassic, where Chlorobi-derived biomarkers are rarely preserved. Within the anoxic shallow waters of the Griesbachian the relatively shallow conditions and high runoff are reflected in a temporary increase of terrestrial-derived biomass. Following, an increasing distance to the shoreline and the forthcoming change in biomass contribution is concordant with a steady negative excursion in the $\delta^{13}C$ of total biomass finishing at the Griesbachian-Dienerian boundary.

The base of a marine transgression at the Griesbachian-Dienerian boundary in the Boreal Sea coincides with a high-extended terpane ratio (ETR > 5), indicative of upwelling and/or the transgression itself, but also with biomarkers indicative of stratified water column with extreme PZE conditions (Fig. 4.8). The molecular and isotopic fingerprints of individual hydrocarbons through the Dienerian support cosmopolitan bacterial blooms, with little evidence of algal contribution at this time. These conditions in the Boreal Sea during the Dienerian might have been caused by abnormal transfer of essential nutrients into ocean-surface waters stimulating fast growth of primary producers, leading to eutrophication and biomass enriched in ^{13}C, explaining the temporary positive shift of nearly 7‰ in $\delta^{13}C_{org}$ observed at the base of the Dienerian.

The significant positive enrichment described in the $\delta^{13}C$ of OM during the Dienerian is synchronous with a positive shift in δD of individual biomarkers and of the total biomass. This parallel isotopic enrichment is characteristic of higher saline

environments in warm-hothouse conditions. Exceptionally high temperatures have been reported to occur in the tropical equatorial seas within the Griesbachian (~252.1Ma) and late in the Smithian, but have not been demonstrated into the Dienerian at high latitudes. An increase in salinity and water temperature might be better explained by the presence of warm, saline-rich bottom waters as proposed by Kidder and Worsley (2004; 2010) in their Haline Euxinic Acidic Thermal Transgressions (HEATT) models. The incursions of warm saline bottom water deficient in oxygen and nutrients might have led to the annihilation of photosynthetic organisms at this time and may have resulted in the development of blooms of opportunistic heterotrophic communities (sulfate reducers), prasinophytes and halophilic archea. Overall, our hypothesis of chaotic environmental conditions during the Dienerian is comparable to the low gradient of functional diversity found in the tropics and northern region at the same time (Foster and Twitchett, 2014), supporting the cosmopolitan nature of the fauna and the complexity of the global Induan environmental conditions (Benton and Twitchett, 2003). Nevertheless, a local reconstrucction of the ecological diversity and functional diversity needs further investigation, to compare with the global trends.

After the blooming episode in the mid-Dienerian, deepening of the depositional environment, and sea-level rise, seems to control the isotopic composition of biomass. Within a period of ca. 2 Ma the carbon isotopic composition of kerogen shifts over 10 ‰ towards more negative values. Along this negative trend photosynthetic organisms start to flourish, reflected in the biomarker distributions at this time. Possibly, not only a deeper ecosystem but also the re-establishment of greenhouse conditions allowed for the initial stage of ecosystem recovery. Nevertheless, weathering of coal and/or released of methane clathrates derived from the hothouse conditions established prior to the Dienerian might count as a source of light carbon that gets incorporated into the carbon cycle during the Early Triassic.

The set of geochemical and geological features found in the Early Triassic sediments from the shelf deposits of Spistbergen, are an outcome of the complexity of the local environmental conditions during that period, including: water chemistry, temperature and water depth; but also, several changes in the microbial assemblage and ecological richness are shown to occur along this period (Foster and Twitchett,

2014); therefore, the importance of local scale investigations in order to reconstruct the biological diversity after the extinction event.

Reference list

Algeo, T. J., Chen, Z. Q., Fraiser, M. L., and Twitchett, R. J., 2011, Terrestrial–marine teleconnections in the collapse and rebuilding of Early Triassic marine ecosystems: Palaeogeography, Palaeoclimatology, Palaeoecology, v. 308, no. 1–2, p. 1-11.

Algeo, T. J., and Twitchett, R. J., 2010, Anomalous Early Triassic sediment fluxes due to elevated weathering rates and their biological consequences: Geology, v. 38, p. 1023-1026.

Andersen, N., Paul, H. A., Bernasconi, S. M., McKenzie, J. A., Behrens, A., Schaeffer, P., and Albrecht, P., 2001, Large and rapid climate variability during the Messinian salinity crisis: Evidence from deuterium concentrations of individual biomarkers: Geology, v. 29, no. 9, p. 799-802.

Barber, C. J., Bastow, T. P., Grice, K., Alexander, R., and Kagi, R. I., 2001, Analysis of crocetane in crude oils and sediments: novel stationary phases for use in GC–MS: Organic Geochemistry, v. 32, no. 5, p. 765-769.

Benton, M., 1995, Diversification and extinction in the history of life: Science, v. 268, no. 5207, p. 52-58.

Benton, M. J., and Twitchett, R. J., 2003, How to kill (almost) all life: the end-Permian extinction event: Trends in Ecology & Evolution, v. 18, no. 7, p. 358-365.

Brocks, J. J., and Pearson, A., 2005, Building the Biomarker Tree of Life: Reviews in Mineralogy and Geochemistry, v. 59, no. 1, p. 233-258.

Chen, L., Wang, Y., Xie, S., Kershaw, S., Dong, M., Yang, H., Liu, H., and Algeo, T. J., 2011, Molecular records of microbialites following the end-Permian mass extinction in Chongyang, Hubei Province, South China: Palaeogeography, Palaeoclimatology, Palaeoecology, v. 308, no. 1–2, p. 151-159.

Corsetti, F. A., Baud, A., Marenco, P. J., and Richoz, S., 2005, Summary of Early Triassic carbon isotope records: Comptes Rendus Palevol, v. 4, no. 6-7, p. 473-486.

Dawson, D., Grice, K., Wang, S. X., Alexander, R., and Radke, J., 2004, Stable hydrogen isotopic composition of hydrocarbons in torbanites (Late Carboniferous to Late Permian) deposited under various climatic conditions: Organic Geochemistry, v. 35, no. 2, p. 189-197.

De Grande, S., Aquino Neto, F. R., Mello, M. R., Grande, S. M. B. D. E., and Neto, F. R. A., 1993, Extended tricyclic terpanes in sediments and petroleums, v. 20, p. 1039-1047.

Dembicki, H., and Meinschein, W. G., 1976, Possible ecological and environmental significance of the predominance of even-carbon number C2O-C3O n-alkanes: Geochimica et Cosmochimica Acta, v. 40, p. 203-208.

Dustira, A. M., Wignall, P. B., Joachimski, M., Blomeier, D., Hartkopf-Fröder, C., and Bond, D. P. G., 2013, Gradual onset of anoxia across the Permian–Triassic Boundary in Svalbard, Norway: Palaeogeography, Palaeoclimatology, Palaeoecology, v. 374, p. 303-313.

Dutta, S., Greenwood, P. F., Brocke, R., Schaefer, R. G., and Mann, U., 2006, New insights into the relationship between Tasmanites and tricyclic terpenoids: Organic Geochemistry, v. 37, p. 117-127.

Erwin, D. H., Bowring, S. A., and Yugan, J., 2002, End-Permian mass extinctions : A review: Geological Society of America Special Paper, v. 356, p. 363-383.

Fenton, S., Grice, K., Twitchett, R. J., Böttcher, M. E., Looy, C. V., and Nabbefeld, B., 2007, Changes in biomarker abundances and sulfur isotopes of pyrite across the Permian–Triassic (P/Tr) Schuchert Dal section (East Greenland): Earth and Planetary Science Letters, v. 262, no. 1–2, p. 230-239.

Finnegan, S., Fike, D. A., Jones, D., and Woodward, F. W., 2012, A Temperature-Dependent Positive Feedback on the Magnitude of Carbon Isotope Excursions: Geoscience Canada, v. 39, p. 122-131.

Foster, W. J., and Twitchett, R. J., 2014, Functional diversity of marine ecosystems after the Late Permian mass extinction event: Nature Geosci, v. 7, no. 3, p. 233-238.

Greenwood, P. F., and Summons, R. E., 2003, GC–MS detection and significance of crocetane and pentamethylicosane in sediments and crude oils: Organic Geochemistry, v. 34, no. 8, p. 1211-1222.

Grice, K., Cao, C., Love, G. D., Böttcher, M. E., Twitchett, R. J., Grosjean, E., Summons, R. E., Turgeon, S. C., Dunning, W., and Jin, Y., 2005a, Photic zone euxinia during the Permian-triassic superanoxic event: Science, v. 307, no. 5710, p. 706-709.

Grice, K., Schaeffer, P., Schwark, L., and Maxwell, J. R., 1996, Molecular indicators of palaeoenvironmental conditions in an immature Permian shale (Kupferschiefer, Lower Rhine Basin, north-west Germany) from free and S-bound lipids: Organic Geochemistry, v. 25, no. 3–4, p. 131-147.

Grice, K., Schouten, S., Nissenbaum, A., Charrach, J., and Sinninghe Damsté, J. S., 1998, Isotopically heavy carbon in the C21 to C25 regular isoprenoids in halite-rich deposits from the Sdom Formation, Dead Sea Basin, Israel: Organic Geochemistry, v. 28, no. 6, p. 349-359.

Grice, K., Twitchett, R. J., Alexander, R., Foster, C. B., and Looy, C., 2005b, A potential biomarker for the Permian–Triassic ecological crisis: Earth and Planetary Science Letters, v. 236, no. 1–2, p. 315-321.

Hayes, J. M., 1993, Factors controlling ^{13}C contents of sedimentary organic compounds: Principles and evidence: Marine Geology, v. 113, no. 1-2, p. 111-125.

Hayes, J. M., Strauss, H., and Kaufman, A. J., 1999, The abundance of ^{13}C in marine organic matter and isotopic fractionation in the global biogeochemical cycle of carbon during the past 800 Ma: Chemical Geology, v. 161, p. 103-125.

Hays, L. E., Beatty, T., Henderson, C. M., Love, G. D., and Summons, R. E., 2007, Evidence for photic zone euxinia through the end-Permian mass extinction in the Panthalassic Ocean (Peace River Basin, Western Canada): Palaeoworld, v. 16, no. 1–3, p. 39-50.

Hays, L. E., Grice, K., Foster, C. B., and Summons, R. E., 2012, Biomarker and isotopic trends in a Permian–Triassic sedimentary section at Kap Stosch, Greenland: Organic Geochemistry, v. 43, no. 0, p. 67-82.

Hounslow, M. W., Peters, C., Mørk, A., Weitschat, W., and Vigran, J. O., 2008, Biomagnetostratigraphy of the Vikinghøgda Formation , Svalbard (Arctic Norway), and the geomagnetic polarity timescale for the Lower Triassic, p. 1305-1325.

Joachimski, M. M., Lai, X., Shen, S., Jiang, H., Luo, G., Chen, B., Chen, J., and Sun, Y., 2012, Climate warming in the latest Permian and the Permian-Triassic mass extinction: Geology, v. 40, p. 195-198.

Kajiwara, Y., Yamakita, S., Ishida, K., Ishiga, H., and Imai, A., 1994, Development of a largely anoxic stratified ocean and its temporary massive mixing at the Permian/Triassic boundary supported by the sulfur isotopic record: Palaeogeography, Palaeoclimatology, Palaeoecology, v. 111, no. 3–4, p. 367-379.

Kaiho, K., Chen, Z.-Q., Kawahata, H., Kajiwara, Y., and Sato, H., 2006a, Close-up of the end-Permian mass extinction horizon recorded in the Meishan section, South China: Sedimentary, elemental, and biotic characterization and a negative shift of sulfate sulfur isotope ratio: Palaeogeography, Palaeoclimatology, Palaeoecology, v. 239, no. 3–4, p. 396-405.

Kaiho, K., Kajiwara, Y., Chen, Z.-Q., and Gorjan, P., 2006b, A sulfur isotope event at the end of the Permian: Chemical Geology, v. 235, no. 1–2, p. 33-47.

Kaiho, K., Oba, M., Fukuda, Y., Ito, K., Ariyoshi, S., Gorjan, P., Riu, Y., Takahashi, S., Chen, Z.-Q., Tong, J., Yamakita, S., 2012. Changes in depth-transect redox conditions spanning the end-Permian mass extinction and their impact on the marine extinction: Evidence from biomarkers and sulfur isotopes. Global and Planetary Change 94-95, 20-32.

Kidder, D. L., and Worsley, T. R., 2004, Causes and consequences of extreme Permo-Triassic warming to globally equable climate and relation to the Permo-Triassic extinction and recovery: Palaeogeography, Palaeoclimatology, Palaeoecology, v. 203, no. 3–4, p. 207-237.

Kidder, D. L., and Worsley, T. R., 2010, Phanerozoic large igneous provinces (LIPs), HEATT (haline euxinic acidic thermal transgression) episodes, and mass extinctions: Palaeogeography, Palaeoclimatology, Palaeoecology, v. 295, no. 1, p. 162-191.

Knoll, A. H., Bambach, R. K., Canfield, D. E., and Grotzinger, J. P., 1996, Comparative Earth History and Late Permian Mass Extinction: Science, v. 273, no. 5274, p. 452-457.

Knoll, A. H., Bambach, R. K., Payne, J. L., Pruss, S., and Fischer, W. W., 2007, Paleophysiology and end-Permian mass extinction: Earth and Planetary Science Letters, v. 256, no. 3-4, p. 295-313.

Koopmans, M. P., Köster, J., Van Kaam-Peters, H. M. E., Kenig, F., Schouten, S., Hartgers, W. A., De Leeuw, J. W., and Sinninghe Damsté, J. S., 1996, Diagenetic and catagenetic products of isorenieratene: Molecular indicators for photic zone anoxia: Geochimica et Cosmochimica Acta, v. 60, no. 22, p. 4467-4496.

Lafargue, E., Marquis, F., and Pillot, D., 1998, Rock-Eval 6 applications in hydrocarbon exploration, production, and soil contamination studies: Oil & Gas Science and Technology, v. 53, no. 4, p. 421-437.

Logan, G. a., Calver, C. R., Gorjan, P., Summons, R. E., Hayes, J. M., and Walter, M. R., 1999, Terminal Proterozoic mid-shelf benthic microbial mats in the Centralian Superbasin and their environmental significance: Geochimica et Cosmochimica Acta, v. 63, no. 9, p. 1345-1358.

Looy, C. V., Twitchett, R. J., Dilcher, D. L., Van Konijnenburg-Van Cittert, J. H. A., and Visscher, H., 2001, Life in the end-Permian dead zone: Proceedings of the National Academy of Sciences, v. 98, no. 14, p. 7879-7883.

Maruoka, T., Koeberl, C., Hancox, P. J., and Reimold, W. U., 2003, Sulfur geochemistry across a terrestrial Permian–Triassic boundary section in the Karoo Basin, South Africa: Earth and Planetary Science Letters, v. 206, no. 1–2, p. 101-117.

Maslen, E., Grice, K., Gale, J. D., Hallmann, C., and Horsfield, B., 2009, Crocetane: A potential marker of photic zone euxinia in thermally mature sediments and crude oils of Devonian age: Organic Geochemistry, v. 40, no. 1, p. 1-11.

Melendez, I., Grice, K., Trinajstic, K., Ladjavardi, M., Greenwood, P., and Thompson, K., 2013, Biomarkers reveal the role of photic zone euxinia in exceptional fossil preservation: An organic geochemical perspective: Geology, v. 41, no. 2, p. 123-126.

Metcalfe, I., Nicoll, R. S., Willink, R., Ladjavadi, M., and Grice, K., 2013, Early Triassic (Induan–Olenekian) conodont biostratigraphy, global anoxia, carbon isotope excursions and environmental perturbations: New data from Western Australian Gondwana: Gondwana Research, v. 23, no. 3, p. 1136-1150.

Mørk, A., and Elvebakk, G., 1999, The type section of the Vikinghogda Formation: a new Lower Triassic unit in central and eastern Svalbard: Polar ….

Nabbefeld, B., Grice, K., Schimmelmann, A., Sauer, P. E., Böttcher, M. E., and Twitchett, R. J., 2010a, Significance of δDkerogen, $\delta^{13}C_{kerogen}$ and $\delta^{34}S_{pyrite}$ from several Permian/Triassic (P/Tr) sections: Earth and Planetary Science Letters, v. 295, p. 21-29.

Nabbefeld, B., Grice, K., Summons, R. E., Hays, L. E., and Cao, C., 2010b, Significance of polycyclic aromatic hydrocarbons (PAHs) in Permian/Triassic boundary sections: Applied Geochemistry, v. 25, no. 9, p. 1374-1382.

Nabbefeld, B., Grice, K., Twitchett, R. J., Summons, R. E., Hays, L., Böttcher, M. E., and Asif, M., 2010c, An integrated biomarker, isotopic and palaeoenvironmental study through the Late Permian event at Lusitaniadalen, Spitsbergen: Earth and Planetary Science Letters, v. 291, no. 1–4, p. 84-96.

Nishimura, M., and Baker, E., 1986, Possible origin of n-alkanes with a remarkable even-to-odd predominance in recent marine sediments: Geochimica et Cosmochimica Acta, v. 50, p. 299-305.

Payne, J. L., and Kump, L. R., 2007, Evidence for recurrent Early Triassic massive volcanism from quantitative interpretation of carbon isotope fluctuations: Earth and Planetary Science Letters, v. 256, no. 1–2, p. 264-277.

Payne, J. L., Lehrmann, D. J., Wei, J., Orchard, M. J., Schrag, D. P., and Knoll, A. H., 2004, Large perturbations of the carbon cycle during recovery from the end-permian extinction: Science, v. 305, no. 5683, p. 506-509.

Peters, K. E., Walters, C. C., and Moldowan, J. M., 2005, The biomarker guide: Biomarkers and isotopes in the environment and human history, Cambridge Cambridge University Press, 1155 p.:

Popp, B. N., Laws, E. A., Bidigare, R. R., Dore, J. E., Hanson, K. L., and Wakeham, S. G., 1998, Effect of phytoplankton cell geometry on carbon isotopic fractionation: Geochimica et Cosmochimica Acta, v. 62, no. 1, p. 69-77.

Radke, M., Welte, D. H., and Willsch, H., 1986, Maturity parameters based on aromatic hydrocarbons: Influence of the organic matter type: Organic Geochemistry, v. 10, no. 1–3, p. 51-63.

Radke, M., Willsch, H., Leythaeuser, D., and Teichmüller, M., 1982, Aromatic components of coal: relation of distribution pattern to rank: Geochimica et Cosmochimica Acta, v. 46, no. 10, p. 1831-1848.

Reichow, M. K., Pringle, M. S., Al'Mukhamedov, A. I., Allen, M. B., Andreichev, V. L., Buslov, M. M., Davies, C. E., Fedoseev, G. S., Fitton, J. G., Inger, S., Medvedev, A. Y., Mitchell, C., Puchkov, V. N., Safanova, I. Y., Scott, R. A., and Saunders, A. D., 2009, The timing and extent of the eruption of the Siberian Traps large igneous province: implications for the end-Permian environmental crisis: Earth and Planetary Science Letters, v. 277, p. 9-20.

Requejo, A. G., Allan, J., Creaney, S., Gray, N. R., and Cole, K. S., 1992, Aryl isoprenoids and diaromatic carotenoids in Paleozoic source rocks and oils from the Western Canada and Williston Basins: Organic Geochemistry, v. 19, no. 1–3, p. 245-264.

Retallack, G. J., Sheldon, N. D., Carr, P. F., Fanning, M., Thompson, C. A., Williams, M. L., Jones, B. G., and Hutton, A., 2011, Multiple Early Triassic greenhouse crises impeded recovery from Late Permian mass extinction: Palaeogeography, Palaeoclimatology, Palaeoecology, v. 308, no. 1–2, p. 233-251.

Sachse, D., Billault, I., Bowen, G. J., Chikaraishi, Y., Dawson, T. E., Feakins, S. J., Freeman, K. H., Magill, C. R., McInerney, F. A., van der Meer, M. T. J., Polissar, P., Robins, R. J., Sachs, J. P., Schmidt, H.-L., Sessions, A. L., White, J. W. C., West, J. B., and Kahmen, A., 2012, Molecular Paleohydrology: Interpreting the Hydrogen-Isotopic Composition of Lipid Biomarkers from Photosynthesizing Organisms: Annual Review of Earth and Planetary Sciences, v. 40, no. 1, p. 221-249.

Schidlowski, M., Gorzawski, H., and Dor, I., 1994, Carbon isotope variations in a solar pond microbial mat: Role of environmental gradients as steering variables: Geochimica et Cosmochimica Acta, v. 58, no. 10, p. 2289-2298.

Schouten, S., Klein Breteler, W. C. M., Blokker, P., Schogt, N., Rijpstra, W. I. C., Grice, K., Baas, M., and Sinninghe Damsté, J. S., 1998, Biosynthetic effects on the stable carbon isotopic compositions of algal lipids: implications for deciphering the carbon isotopic biomarker record: Geochimica et Cosmochimica Acta, v. 62, no. 8, p. 1397-1406.

Schwark, L., and Empt, P., 2006, Sterane biomarkers as indicators of palaeozoic algal evolution and extinction events: Palaeogeography, Palaeoclimatology, Palaeoecology, v. 240, no. 1–2, p. 225-236.

Schwark, L., and Frimmel, A., 2004, Chemostratigraphy of the Posidonia Black Shale, SW-Germany: II. Assessment of extent and persistence of photic-zone anoxia using aryl isoprenoid distributions: Chemical Geology, v. 206, no. 3–4, p. 231-248.

Seifert, W. K., and Moldowan, M. J., 1978, Applications of steranes, terpanes and monoaromatics to the maturation, migration and source of crude oils: Geochimica et Cosmochimica Acta, v. 42, no. 1, p. 77-95.

Simoneit, B. R. T., Leif, R. N., Radler De Aquino Neto, F., Almeida Azevedo, D., Pinto, A. C., and Albrecht, P., 1990, On the presence of tricyclic terpane hydrocarbons in permian tasmanite algae: Die Naturwissenschaften, v. 77, no. 8, p. 380-383.

Stancliffe, R. P. W., and Sarjeant, W. A. S., 1994, The acritarch genus Veryhachium Deunff 1954, emend; Sarjeant and Stancliffe 1994; a taxonomic restudy and a reassessment of its constituent species: Micropaleontology, v. 40, no. 3, p. 223-241.

Stanley, S. M., 2010, Relation of Phanerozoic stable isotope excursions to climate, bacterial metabolism, and major extinctions.: Proceedings of the National Academy of Sciences of the United States of America, v. 107, p. 19185-19189.

Summons, R. E., and Powell, T. G., 1986, Chlorobiaceae in Palaeozoic seas revealed by biological markers, isotopes and geology: Nature.

Summons, R. E., and Powell, T. G., 1987, Identification of aryl isoprenoids in source rocks and crude oils: biological markers for the green sulphur bacteria: Geochimica et Cosmochimica Acta, v. 5.

Sun, Y., Joachimski, M. M., Wignall, P. B., Yan, C., Chen, Y., Jiang, H., Wang, L., and Lai, X., 2012, Lethally hot temperatures during the Early Triassic greenhouse.: Science (New York, N.Y.), v. 338, p. 366-370.

Thiel, V., Peckmann, J., Seifert, R., Wehrung, P., Reitner, J., and Michaelis, W., 1999, Highly isotopically depleted isoprenoids: molecular markers for ancient methane venting: Geochimica et Cosmochimica Acta, v. 63, no. 23, p. 3959-3966.

Thomas, B. M., Willink, R. J., Grice, K., Twitchett, R. J., Purcell, R. R., Archbold, N. W., George, a. D., Tye, S., Alexander, R., Foster, C. B., and Barber, C. J., 2004, Unique marine Permian-Triassic boundary section from Western Australia: Australian Journal of Earth Sciences, v. 51, no. 3, p. 423-430.

Tong, J., Hansen, H., Zhao, L., and Zuo, J., 2005, High-resolution Induan-Olenekian boundary sequence in Chaohu, Anhui Province: Science in China Series D: Earth Sciences, v. 48, no. 3, p. 291-297.

Tong, J., Zhang, S., Zuo, J., and Xiong, X., 2007, Events during Early Triassic recovery from the end-Permian extinction: Global and Planetary Change, v. 55, no. 1-3, p. 66-80.

Twitchett, R. J., Looy, C. V., and Morante, R., 2001, Rapid and synchronous collapse of marine and terrestrial ecosystems during the end-Permian biotic crisis: Geology, no. 4, p. 351-354.

Wignall, P. B., and Twitchett, R. J., 1996, Oceanic Anoxia and the End Permian Mass Extinction: Science, v. 272, no. 5265, p. 1155-1158.

Wignall, P. B., and Twitchett, R. J., 2002, Extent, duration, and nature of the Permian-Triassic superanoxic event: SPECIAL PAPERS-GEOLOGICAL SOCIETY OF AMERICA, p. 395-414.

Xinke, Y., Pu, F., and Philp, R. P., 1990, LLNovel Biomarker found in South Florida Basin: Organic Geochemistry, v. 15, no. 4, p. 433-438.

Appendix 4

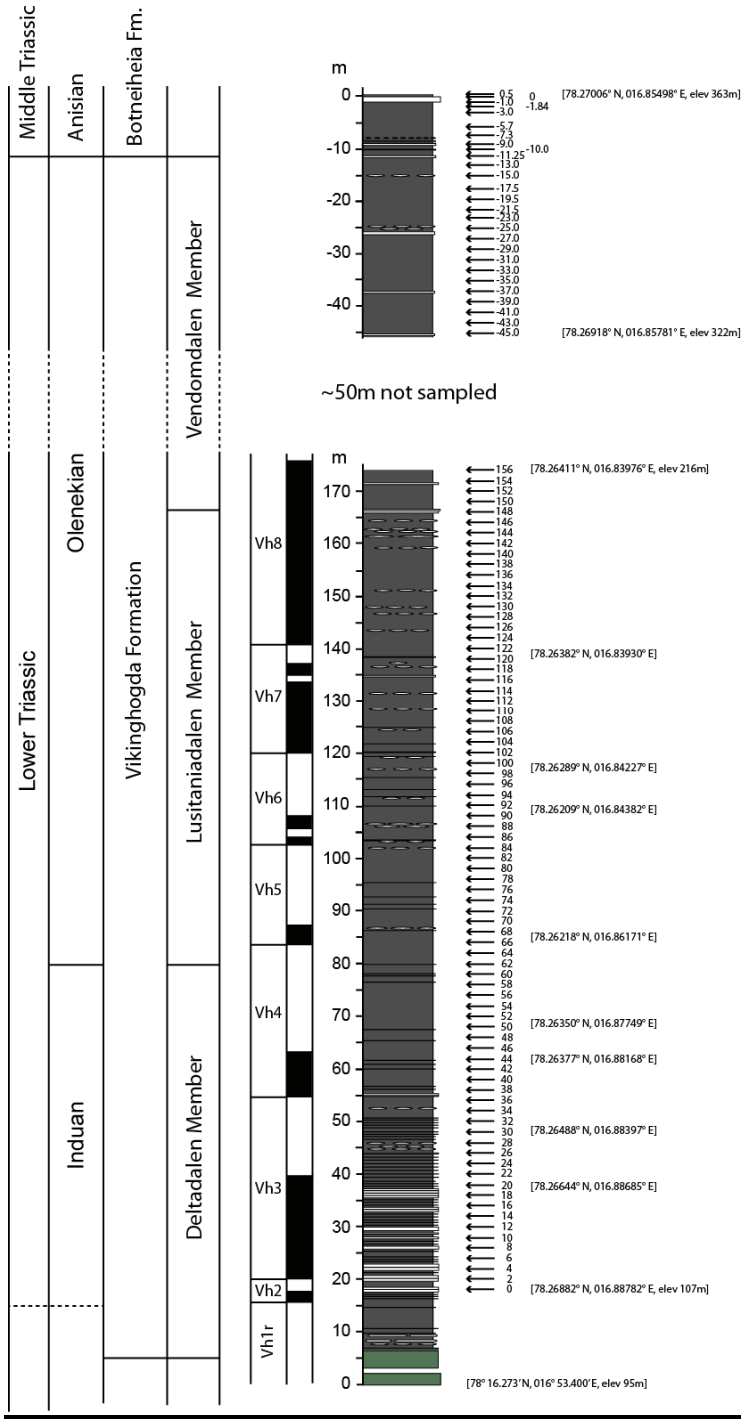

Figure A4. 1 Stratigraphic position and coordinates of samples collected in Spitsbergen in 2007.

Methods description

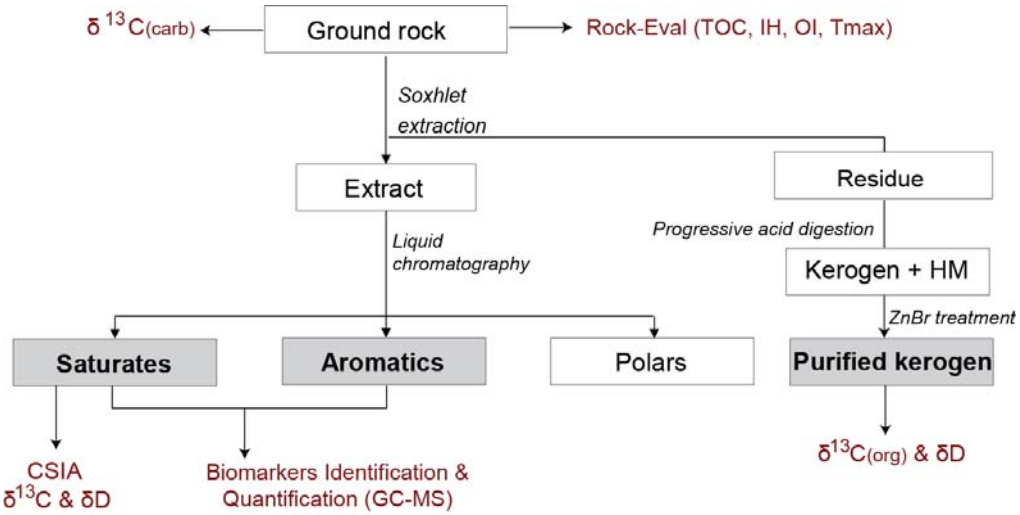

Figure A4. 2 Schematic overview of the methodologies used to separate and analyzed the samples. Within the boxes the name of fraction or sample is identified. In red font the analysis conducted in the corresponding part of the samples and in italic-black font the separation technic.

The outcrop samples (Fig. A4.1) were carefully pre-cleaned multiple times with deionized water, followed by solvents (dichloromethane: DCM and methanol: MeOH, 7:3) in an ultrasonic bath, to remove any modern contamination. Procedural blanks were performed throughout the entire analytical protocol (Fig. A4.1). After cleaning, samples were pulverized in a zirconium mill. Aliquots of the pulverized samples were pyrolysed using a Rock Eval 6 instrument (Lafargue et al., 1998) and also for determination of isotopic composition of carbonates. The $\delta^{13}C$ and $\delta^{18}O$ signatures of the carbonate minerals were determined by using a GasBench II coupled with Delta XL Mass Spectrometer (Thermo-Fisher Scientific). Three-point normalization was used in order to reduce raw values to the international scale (Paul D. and Skrzypek G., 2007; Skrzypek G., 2013). The international standards provided by IAEA: L-SVEC, NBS19 and NBS18 were used and all $\delta^{13}C$ and $\delta^{18}O$ values are given in parts per mil (‰) with respect to the international Vienna Peedee Belemnite (VPDB) standard.

The powdered samples were extracted for 72 hr. using a pre-extracted cellulose thimble in a Soxhlet apparatus, utilizing a solvent mixture of DCM and MeOH mixture (7:3 v/v) together with activated copper (to remove elemental sulfur) to yield

bitumen. The bitumen was concentrated by removing the solvent under a nitrogen purge. Each extract was separated into 3 fractions by small-scale column chromatography (5.5 cm x 0.5 cm i.d.), using activated silica gel (120 °C, 8 hr.) as a stationary phase. Aliphatic hydrocarbons (saturated) were eluted with 1.5 dead volumes (DV) of *n*-hexane, aromatic hydrocarbons with 2 DV of 4:1 *n*-hexane: DCM and the polar fraction were eluted with 2 DV of DCM: MeOH (7:3). Aliphatic and aromatic hydrocarbon fractions were analyzed by Gas Chromatography–Mass Spectrometry (GC-MS), whilst Compound Specific Isotope Analysis (CSIA) was performed on selected saturated fractions (Fig. 1).

Semi-quantitative analyses were performed on each aliphatic and aromatic fraction by GC-MS using a Hewlett Packard 6890 GC interfaced to a Hewlett Packard 5973 mass selective detector (MSD). The GC-MS was operated in a pulsed splitless mode; the injector was kept at 320 °C and fitted with a DB-5 capillary column (60 m x 0.25 mm i.d. x 0.25 µm film thickness). The oven temperature was programmed from 40 °C to 325 °C (at 3 °C/min) with initial and final hold times of 1 and 50 min, respectively. Ultra high pure helium was used as the carrier gas and maintained at a constant flow of 1.1mL/min. The MSD was operated at 70 eV and the mass spectra were acquired in full scan mode, *m*/*z* 50-700 at ~ 4 scans per second and a source temperature of 230 °C. A Thermo Finnigan DeltaV mass spectrometer coupled to an Isolink GC (using the same chromatographic conditions as in the GC-MS analyses) was used to determine the $\delta^{13}C$ values of selected biomarkers, which are reported in parts per mil (‰) relative to VPDB. Reported values are the average of at least three analyses.

Kerogen was isolated using a sequence of acid treatments HCl-HF–HF (Holman et al., 2012; Nabbefeld et al., 2010a; Nabbefeld et al., 2010b). The rock-powder residue after Soxhlet extraction was decarbonated with 1 M HCl. After drying, the samples were digested with a mixture of concentrated HF (48%) and an equal volume of Milli-Q purified water in pre-cleaned polyethylene centrifuge vials. The vials were left (2 h) in an ice bath and were regularly shaken. The liquid was decanted and a second acid/water mixture was added and left (3–4 h) at room temperature. After acid digestion the sample was washed (3×) with Milli-Q water to remove any

residual acid. Heavy mineral separation was performed using pre-extracted (dichloromethane) aqueous zinc bromide solution ($ZnBr_2$). The remaining sample was washed several times with slightly acidified water and finally freeze-dried.

Values of $\delta^{13}C_{org}$ and δD were determined from the purified kerogen fraction. Samples were analyzed for $\delta^{13}C_{org}$ using a continuous flow system consisting of a Delta V Plus mass spectrometer connected with a Thermo Flush 1112 via Conflo IV (Thermo-Finnigan/Germany). All the values are reported in per mil [‰, VPDB] according to delta notation, with an external error of analyses (1 standard deviation) no greater than 0.10 ‰. Description of the analytical technique for EA can be found in e.g. Skrzypek and Paul (2006).

δD of purified kerogen was determined considering the amount of labile hydrogen and its contribution to the total measurement (Schimmelmann et al., 2006). Two aliquots of each kerogen (0.5–0.8 mg) were weighed into silver capsules and placed into the carousel-equilibration chambers. Each set of aliquots was purged for several hours with dry N_2 until equilibration (temperature of 115 °C). The samples were then equilibrated with two isotopically distinct water vapors (>6 h): D-depleted water from Saskatoon, Canada (δDw = − 136‰), and with D-enriched water (δDw = 1173‰). The steam was subsequently replaced by a dry N_2 gas (>4 h, 115 °C) to dry the samples. The analyses were made in a Costech elemental analyzer (EA, 1410 °C, He 90 mL/min) coupled to an ir-MS, Thermo Finnigan Delta Plus XP. TCEA measurements of δD of non-exchangeable hydrogen in kerogen are reproducible within +/- 3‰. Values of δD were calculated by comparison of sample gases with peaks of H_2 reference gas, and were anchored to the VSMOW scale by comparison with the IAEA polyethylene foil (IAEA-CH-7; δD = −100.3‰; Sauer et al., 2009).

Sulfur isotope analyses were performed in the Department of Biogeochemistry from Max Planck Institute for Marine Microbiology, Bremen, Germany under the supervision of Dr. Michael Böttcher. Pulverized sediments were treated with hot acidic chromium (II) chloride solution ($Cr(II)Cl_2$) to extract the total reducible sulfur. The H_2S produced was trapped quantitatively as ZnS in a zinc acetate-bearing trap and the concentration of dissolved sulfide was measured yielding the total reducible inorganic sulfur (TRIS, essentially pyrite) content of the sample. Following, the

resulting ZnS was filtered and mixed with $AgNO_3$ solution and converted into Ag_2S, then washed with NH3-containing water and dried. Samples were combusted with V_2O_5 added as a catalyst in Sn cups in a Thermo Flash elemental analyser coupled via Thermo Conflo split interface to a Thermo Finnigan Mat 253 gas mass spectrometer. Sulfur isotope ratios ($^{34}S/^{32}S$) are reported in conventional δ-notation with a precision of approximately ± 0.3‰, and were calibrated versus the Vienna Cañon Diablo Troilite (VCDT) using the international reference materials IAEA-S-1, -2 and -3.

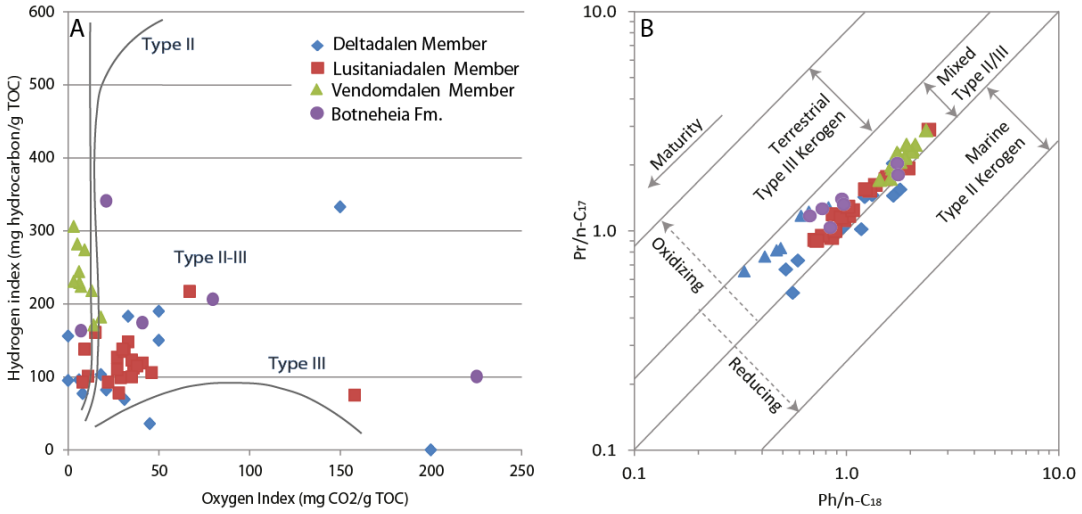

Figure A4. 3 A) Pseudo van Krevelen diagram showing kerogen type in the studied samples. B) Plot of Pr/*n*-C_{17} Vs. Ph/*n*-C_{18}, indicative of type of OM, redox condition and maturity; fields defined by Hunt, 1995. Blue symbols represent samples from the Deltadalen Member, and the blue-triangles represents the samples only from the Dienerian interval.

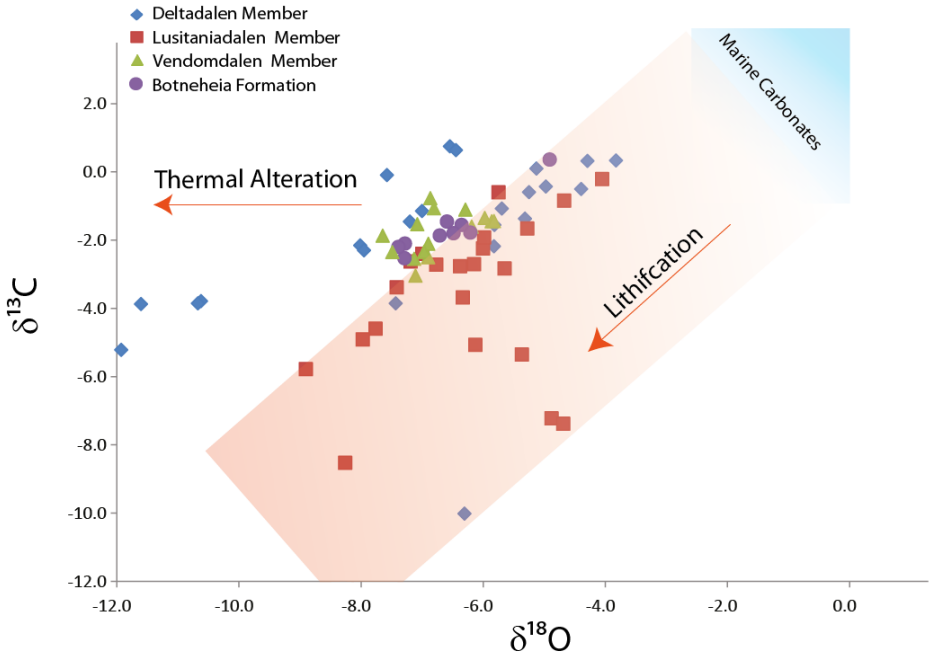

Figure A4. 4 Crossplot of $\delta^{13}C$ (‰) and $\delta^{18}O$ (‰) of carbonate mineral in the samples, showing a very good correlation indicative of alteration during diagenesis.

Palynology

Table S 1. Palynological descriptions. ND: Not Determined.

No	Rock Unit	Age - Stage	Kerogen slide (un sieved)	Kerogen color/visual strew mount	Palynomorph yield (+ 5 microns sieved fraction)	spore/pollen/ acritarch preservation	Palynological identifications	Organic maturity (acritarch/ miospore color)
12	Deltadalen Member	Induan	Abundant structured plant tissue; framboidal pyrite common	very pale yellow	few identifiable spores and pollen; sheets of cuticle - like organic matter common	poor	? Bisaccate pollen, ?Lunatisporites sp. - heavily imprinted by pyrite crystals; fungal hyphae, Cycadopites sp., Punctatisporites sp.	oil window
14			very finely comminuted organic matter; rare dark woody debris (lath-like and equi dimensional),pollen grains, and framboidal pyrite	Overall pale brown/yellowish brown; very finely comminuted organic matter; rare dark woody debris (lath-like),pollen grains, and framboidal pyrite	abundant organic tissue (very broken up), spinose acritarchs (Michrystridium spp.) common, equidimensional woody fragments, very rare striate bisaccate gymnosperm pollen, very rare lycopod spores	very poor	spinose acritarchs (Michrystridium spp.) common, equidimensional woody fragments, very rare striate bisaccate gymnosperm pollen, very rare lycopod spores	oil window (acritarchs light/dark brown [?evidence of reworking]
16			no kerogen slide	no kerogen slide	low yield; black equidimensional and long laths of woody debris (vessels and tracheids)	very poor	*Michrystridium* sp.; gymnosperm pollen, *Striatopodocarpites* sp. indet.,?*Chordasporites* sp.;lycopod tetrad, cuticle fragments	mature
26			no kerogen slide	virtually barren	virtually barren, structured organic tissue, spore tetrad	very poor	?*Leiotriletes* sp., lycopod spore tetrad	ND
28			very finely comminuted organic matter; spinose acritarchs (*Veryhachium* sp.) rare, rare angular, dark brown woody fragments; pyrite framboids present	light brown	abundant organic tissue	very poor	small thin walled, very poorly preserved, corroded leiospheres, spinose acritarchs (*Michrystridium* spp., *Veryhachium* sp.);exinal fragments with cubic pyrite crystal imprints, black equidimensional wooody fragments including tracheids	mature
30			no kerogen slide	ND	very low - black equidimensional woody fragments; organic tissue embedded with pyrite framboids	very poor	plant cuticle, structured organic matter, spinose acritarch (*Micrhystridium* spp.)	mature - below oil window

32			very finely comminuted organic matter; very few equidimensional woody tissue fragments, spinose acritarchs (*Michrystridium* sp.) with crystal pyrite imprints, some framboids	very pale yellow - almost colourless	abundant	very poor	Spinose acritarchs most common [*Michrystridium* spp., *Veryhachium* sp.) sheet-like organic tissue, rare tracheidal woody tissue	mature
34	Deltadalen Member	Induan	as above	pale brown	abundant	very poor	Spinose acritarchs most common (*Michrystridium* sp, vesicle wall imprinted by cubic pyrite crystals, *Veryhachium* sp.); exinal fragments; Rare land plant debris: lycopod spore ?*Aratrisporites* sp., ?saccate pollen	oil mature
46			more angular, dark brown/black woody debris than #28 (above) within finely comminuted organics; poorly preserved spores and pollen and fair to poorly preserved acritarchs present		Abundant	poor-fair	predominantly spinose acritarchs (~ 95% *Michrystridium* spp., *Veryhachium* sp.); Land plant input represented by rare striate gymnosperm pollen (detached corpus); *Cycadopites*? sp., spores indet., tracheidal material	mature
56			as #46 above together with large plant tissue fragments	pale brown	high	poor	Less diverse spinose acritarchs (compare #46; *Michrystridium* spp.); more land plant debris represented by woody tissue, tracheids (common), cuticle fragment with stomata *Cycadopites*? sp., trilete spore with cubic pyrite crystal imprints.	mature
64	Lusitaniadalen Member	Olenekian	finely comminuted organic , with rare larger tissue fragments, and small brown/black angular woody fragments	light brown	abundant, very fragmentary organic matter	poor	Spinose acritarchs (*Michrystridium* spp.); land plant debris, tracheids common, *Cycadopites* sp., ?lycopod spore	mature
-9			no kerogen slide	dark brown (acritarchs)	very low	very poor	*Veryhachium* sp. (globose form) of Mørk et al., 1999 common and distinctive; *Punctatisporites* sp., gymnosperm pollen (very dark)	mature; ?gas window (acritarchs dark brown)
-17.5		Olenekian	sheet-like degraded organic tissue, few spores, and rarer equidimensional woody fragments	pale brown	moderate	poor	Very few if any spinose acritarchs; gymnosperm pollen (striate and non-striate), triletes spore ?*Verrucosisporites* sp.	ND

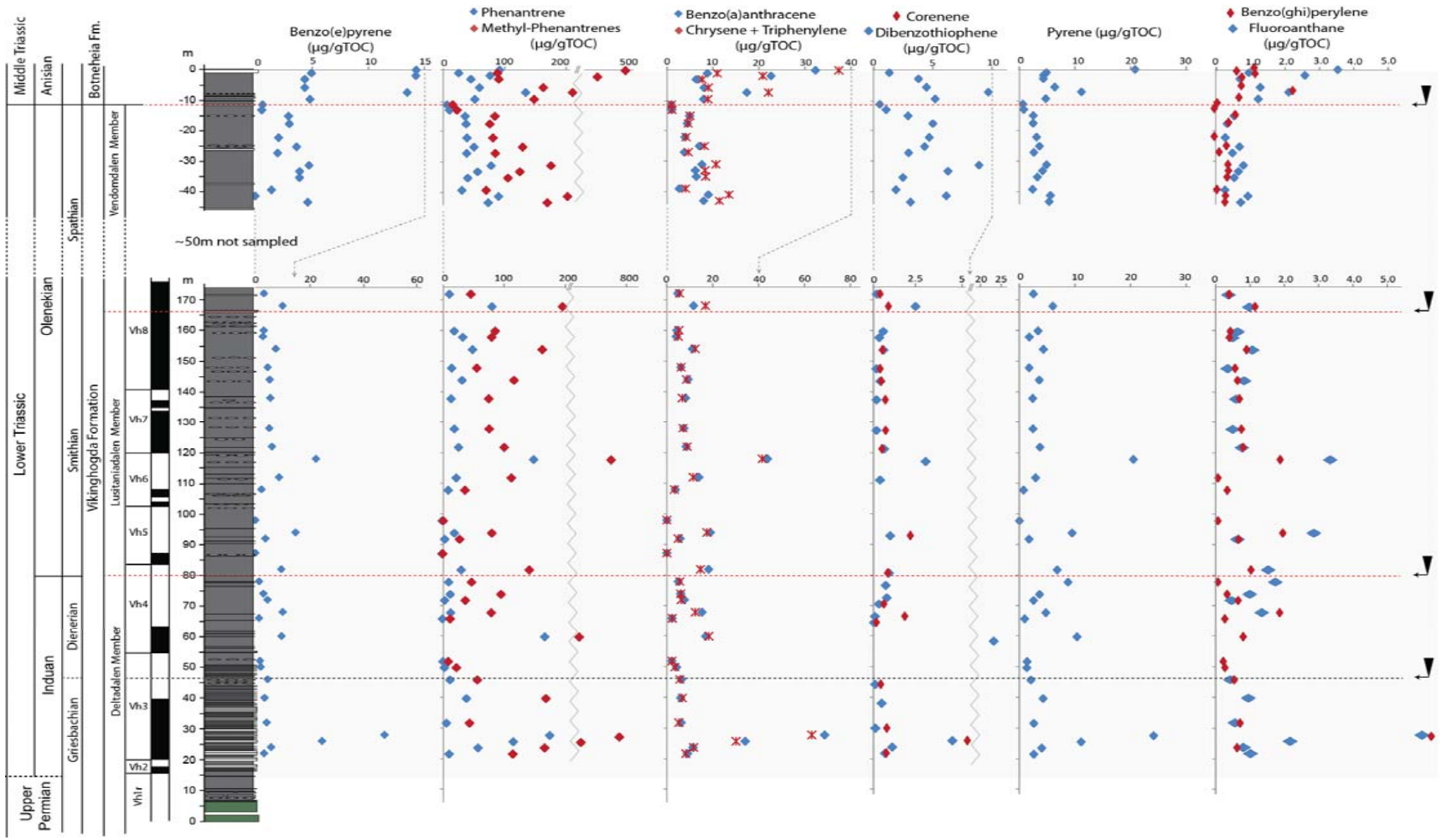

Figure A4. 5 Stratigraphic concentration of aromatic compounds, expressed in µg of compound per g of total organic carbon (TOC). Black arrows refer to the base of transgressive sequences of 2nd, 3rd and 4th order, according to Hounslow et al. (2008). Most of the spikes in concentration of aromatic compounds occur following a transgressive event, suggesting a common land-derived origin.

Supplementary References

Holman, A.I., Grice, K., Jaraula, C.M.B., Schimmelmann, A., Brocks, J.J., 2012. Efficiency of extraction of polycyclic aromatic hydrocarbons from the Paleoproterozoic Here's Your Chance Pb/Zn/Ag ore deposit and implications for a study of Bitumen II. Organic Geochemistry 52, 81-87.

Nabbefeld, B., Grice, K., Schimmelmann, A., Sauer, P.E., Böttcher, M.E., Twitchett, R.J., 2010a. Significance of δDkerogen, $\delta^{13}C_{kerogen}$ and $\delta^{34}S_{pyrite}$ from several Permian/Triassic (P/Tr) sections. Earth and Planetary Science Letters 295, 21-29.

Nabbefeld, B., Grice, K., Schimmelmann, A., Summons, R.E., Troitzsch, A., and Twitchett, R.J., 2010d, A comparison of thermal maturity parameters between freely extracted hydrocarbons (Bitumen I) and a second extract (Bitumen II) from within the kerogen matrix of Permian and Triassic sedimentary rocks: Organic Geochemistry, v. 41, p. 78–87.

Lafargue, E., Marquis, F., Pillot, D., 1998. Rock-Eval 6 Applications in Hydrocarbon Exploration, Production, and Soil Contamination Studies. Revue de l'institut francais du petrole 53, 421-437.

Paul D., Skrzypek G., 2007, Assessment of Carbonate-Phosphoric Acid Analytical Technique Performed using GasBench II in Continuous Flow Isotope Ratio Mass Spectrometry, International Journal of Mass Spectrometry 262: 180-186

Sauer, P.E., Schimmelmann, A., Sessions, A.L., Topalov, K. 2009. Simplified batch equilibration for D/H determination of non-exchangeable hydrogen in solid organic material. Rapid Commun. Mass Spectrom., 23: 949–956

Skrzypek G., 2013, Normalization procedures and reference material selection in stable HCNOS isotope analyses – an overview. Analytical and Bioanalytical Chemistry 405: 2815-2823.

Skrzypek G., Paul D., 2006, $\delta^{13}C$ Analyses of Calcium Carbonate: Comparison between the GasBench and Elemental Analyzer Techniques. Rapid Commun. Mass Spectrom. 20: 2915-2920.

Schimmelmann, A., Sessions, A.L., Mastalerz M. 2006. Hydrogen isotopic (D/H) composition of organic matter during diagenesis and thermal maturation Annu. Rev. Earth Planet. Sci., 34: 501–533.

CHAPTER 5

Conclusions and Outlook

Integration of a comprehensive biomarker dataset along with numerous stable isotope measurements (bulk and of individual compounds) were the main tools used in this PhD to provide an exhaustive insight into the biogeochemical processes that occur in distinctive environments with highly sulfide conditions.

A contemporary analog of sulfide rich environment is found in the inland Black Sea, where extensive anoxic/euxinic conditions are present at the bottom of the stratified water body; while the top layer is well oxygenated. However, episodic incursions of free H_2S into the photic zone of the Black Sea represent a modern example of PZE conditions. This environment is one of the best representations, along with Fjords and restricted lakes, of aquatic settings in which accumulation and preservation of OM is enhanced due to the poorly oxygenated waters. A great variety of geochemical evidence has been postulated suggesting that these types of settings were more common and widespread in past marine environments than present day. Sulfide-rich conditions in the photic zone are not the most suitable environments for a great variety of biota to dwell in, and have been acknowledged as one of the drivers of the extinction events associated with the PTB and its subsequent delayed recovery (Grice

et al., 2005a). Similarly, in the waters of the Devonian reefs systems in Western Australia, PZE has been also identified during the biotic stress of the Late Devonian extinctions (Tulipani et al., 2014).

In the present study two separate episodes of marine anoxia have been associated with two major biological crisis events (end-Devonian and end-Permian) but also to a case of unique preservation of marine biomass. Paradoxically, toxic H_2S in modern and past environments represent a threat to the life of many organisms; however, during the course of this investigation we have successfully demonstrated the role of H_2S in OM and soft tissue preservation within the earliest stages of deposition and in the water column (eogenesis). Therefore, the investigation of this phenomenon in deep time has an enormous significance for the evolution of life throughout Earth's history, particularly during and/or after mass extinction events; Nonetheless, the implication that evolution of life during euxinic conditions might provide useful insight into the evolution and devolpmet of early life because of the occurrence of anoxic condition through early Earth history.

Enhanced preservation of biomass under anoxic/euxinic conditions

Remains of past life on Earth can be preserved in the rock record as morphological and molecular (biomarker) fossils. In present and past environments the role of oxygen-limited conditions and the depth of the chemocline in the water column are probably influencing the extent of exceptional preservation. Within the Gogo Formation, located in the Canning Basin, north-west of Western Australia, multiple examples of remarkable preservation of reef-fauna and immature biomarkers are documented. This geological entity was deposited at around the Givetian to Frasnian period within the suboxic-anoxic waters of the inner reef basin system, forming the source rocks for the high-quality oils in the Canning Basin. The exceptional preservation of reef-fauna found in the Gogo Formation occurs within microbially formed carbonate nodules and ranges from original bones up to mineralized soft tissues including muscle bundles, nerve cells and umbilical structures. This type of exceptional preservation is thought to derive from a combination of rapid burial and

cementation within a relatively tectonically stable environment (Long and Trinajstic, 2010). Nevertheless, a precise biogeochemical-model that enlightens the way this preservation process occurs, remains unclear. In order to elucidate the palaeoenvironmental conditions and the microbial assemblages associated with the carbonate precipitation and consequent encapsulation of very delicate organic remains was described in **Chapter 2** and **Chapter 3**. A systematic organic geochemical approach was undertaken for the first time in order to characterize the biomarkers and biomolecules and their $\delta^{13}C$ values preserved within the tissue of an invertebrate fossil from the Gogo Formation.

In the examined carbonate concretion from the Gogo Formation more than 160 lipids (including saturated, aromatic and functionalized lipids) were identified and quantified based in their mass spectra, relative retention times and comparison with authentic standards, showing variable distributions and concentrations within the concretion; remarkably, the majority of compounds were strongly associated with the nucleus of the fossil concretion (**Chapters 2** and **3**). Remarkably, the concretion contained less than 0.2 % of TOC, compared to the majority of previous investigations; in which samples with very good OM preservation have TOC greater than 5 % and up to 50 %.

The most abundant non-functionalized lipids were the *n*-alkanes, regular isoprenoids -pristane (Pr) and phytane (Ph)-, steranes, hopanes and a suite of monoaryl, diaryl and triaryl isoprenoids with a 2,3,6/3,4,5-trimethyl-substitution pattern. However, differences in the molecular distribution as well as isotopic composition were observed between the biomarkers associated with the fossil tissue, where high phytoplanktonic input (including the crustacean's diet) was observed, in contrast to the more organic-lean external carbonaceous layers of the concretion (matrix), reflecting changes in the preferential preservation of biomass during the initial stages of concretion formation.

Cholestane (with a $\delta^{13}C$ value of -30.5 ‰) dominated by the ααα–20*R* biological steroisomer (least thermal stable configuration), was by far the most abundant saturated biomarker in the fossilized invertebrate (**Chapter 2**). This isomeric configuration is directly derived from functionalized steroids present in living

organisms; therefore its presence in a sample for some 380 Ma reflects a remarkable degree of preservation without thermal overprinting. The unequivocal association of the C_{27} steranes in the fossil tissue suggest these compounds represent the molecular remains of the living invertebrate. The abundance of cholestane with respect to other steranes is comparable to the sterol distribution in modern crustaceans (e.g. Kanasawa, 1990), helping to narrow the identification of the investigated fossil to a crustacean. This is the first time that biomarker and isotopic geochemisty has been applied to a Devonian fossil, demonstrating the utility of this powerful technique in molecular taphonomy.

Further investigations (**Chapter 3**) confirmed the presence not only of steranes but also intact functionalised dietary steroids (e.g. sterols and methyl sterols) exclusively found in living organisms, demonstrating the unique preservation at a molecular level in this carbonate concretion. The occurrence of intact sterols had been restricted to immature Cretaceous and Late Jurassic (~165Ma) sediments, extending the survival of intact sterols by more than 200 Ma. The most abundant compounds found in the concretion were cholest-5-en-3β-ol ($\delta^{13}C$ of -26.8 ‰) and 24-ethylcholest-5-en-3β-ol ($\delta^{13}C$ of -30.9 ‰), corroborating the preservation of biomass derived from the crustacean tissue and phytoplanktonic input direct from the water column.

The remarkable degree of preservation was elucidated and described in **Chapter 2** based on the abundance and distribution of compounds derived from the carotenoid pigments of Chlorobi. Biomarkers such as the intact isorenieratane, renieratane and the Devonian marker paleorenieratane, along with a series of monoaryl, diaryl and also triaryl isoprenoids with a 2,3,6/3,4,5-trimethyl-substitution pattern, were identified exclusively in the fossil layer (c.f. Grice et al., 1996; 1997; 2005; Koopmans et al., 1996). Some of these compounds are direct evidence of PZE conditions and an active sulfur cycle in the Devonian waters at the time of preservation (cf. Tulipani et al., 2014). The distribution of aryl isoprenoids (Schwark and Frimmel, 2004) in the concretion and within the anoxic shales of the Gogo Formation, indicates that more persistent PZE was associated with the formation of the concretion, while periodic PZE conditions prevailed in the water column during the entire deposition of the Gogo Formation (equivalent to the Duvernay Formation of the Western Canada Sedimentary Basin; Tulipani et al., 2014). Sulfate reduction is

here described as a key factor part of the active sulfur cycle that surrounded the fossil at that time, but not only as the source of free H_2S in the water column but also to promote the growth of authigenic carbonate around the decaying crustacean, providing a physical barrier that encapsulates the organic remains within the concretion preventing further heterotrophic decomposition (**Chapter 2**).

Evidence of free H_2S at early stages of diagenesis is observed in the abundance of S-bound biomarkers, which remarkably show a very similar distribution to the free saturated fraction. The sulfur-bound biomarkers support the hypothesis of very rapid encapsulation of the biomass and preservation through sulfurization during eogenesis and into earliest stages of diagenesis. Preservation of this very immature molecular signature along with extremely reactive compounds (**Chapter 3**), such as photo-oxidation products of Δ^5-stenols (e.g. cholest-5-en-3β,7α-diol, 24-ethylcholest-5-en-3β,7α-diol, 24-methylcholest-5-en-3β,7α-diol and cholest-5-en-3β-ol-7-one), formed very early on in the photic zone of the water column, can here only be explained by intense H_2S production that expanded close to the surface waters, shortening the travelling time of biomass and preventing its degradation in the oxic part of the water column. Phytoplanktonic blooms along with limited water circulation are here proposed as the cause of the stratified water column that subsequently developed in anoxic-bottom waters and persistent PZE.

In addition to the intact biolipids (e.g sterols and methyl-sterols) a suite of steroidal diagenetic transformation products were found to coexist in the same sample (**Chapter 3**). These compounds range from the most abundant and biologically derived stenols to the end member of the diagenetic pathway, fully aromatized steroids. The complex mixture of steroids associated with the organic-rich fossil layer of the concretion corroborates the sequential biochemical transformation undergone by sterols at early stages of diagenesis proposed in the early 80's (Mackenzie et al., 1982). However, the parallel co-occurrence of the most extreme end-members of the steroid pathway challenges the traditional paradigm of how steroids are transformed by thermal processes during diagenesis and catagenesis. As proposed in **Chapter 3** the coexistence of steroids in a diagenetic continuum responds to the intense microbial activity that mediates the transformations during eogenesis. This exceptionally well preserved suite of steroids in a diagenetic

continuum derived from the rapid and progressive mineral encapsulation that prevent further alteration of the crustacean biomass promoting its preservation.

Overall, **Chapters 2** and **Chapters 3** provide a valuable contribution, not only to the organic geochemistry community but also other to disciplines demonstrating that biomarker records encapsulated in unique mineral fabrics can be extremely useful to evaluate biological and chemical conditions during highly sulfidic environments due to the enhanced preservation of OM. Furthermore the successfully applied methodology presented in this work can be extended to other geological periods as well as poorly understood microbially-derived mineral fabrics, offering significant promise to investigate biolipids in deep time in association with the evolution of early life.

Environmental changes after the end-Permian extinction event

The end-Permian extinction event is known as one of the greatest ecological crises on Earth, in which a large portion of both marine and terrestrial biota became extinct (Benton, 1995; Benton and Twitchett, 2003). The environmental conditions that surrounded such a catastrophe have been a centre of multiple investigations worldwide. Changes in *p*CO2, temperature, pH, along with widespread ocean anoxia and massive volcanic activity associated with the Siberian traps, are some of the mechanisms proposed to initiate the biotic annihilation. The PTB is well exposed in the marine shelf deposits of central Spitsbergen, where this investigation is focused. Paleoenvironmental, sedimentological and isotopic reconstruction of the extinction horizon have been well documented for this location (Dustira et al., 2013; Nabbefeld et al., 2010b; Wignall et al., 1998; Wignall and Twitchett, 1996). However, systematic characterization of the sediments that comprised the Early to Middle Triassic in this region has not been evaluated, and therefore the environmental conditions that followed the major extinction event and eventually developed conditions suitable for the ecosystem to recover remains unclear. In order to examine the aftermath of one of the most prominent mass extinction events, a multidisciplinary study, including identification and quantification of numerous biomarkers, stable isotope measurements (C and H) in bulk biomass and individual compounds (CSIA) along with detailed sedimentological and paleontological data,

was undertaken for the first time on a extended Early Triassic marine section from central Spitsbergen, (**Chapter 4**).

Several lines of evidence have been outlined in **Chapter 4** to suggest protracted perturbations of the ecosystem in the Boreal Sea, where multiples transgression-regression cycles are recorded in the Early Triassic sedimentary deposits. Due to the sea level fluctuations during this period the abundances of saturated and aromatic hydrocarbons in the Early Triassic of Svalbard mainly reflect changes in lithofacies and the proximity to the paleoshoreline and/or water depth. For example, the abundance of aromatic compounds, mainly derived from the alteration of terrestrial biomass, is enlarged at the onset of transgression, and is then followed by a subsequent decrease. This pattern in the abundance of land plant biomarkers probably reflects initial flooding of coastal areas and the increasing distance to land during the transgression. Nevertheless, the proportion within saturated hydrocarbons, despite the similar pattern in concentrations to the aromatic compounds, allows for recognition of variations in the main marine biomass contributions (e.g. heterotroph/autotrophs and/or algal/bacteria-derived biomass). Similarly, the unique dataset obtained in this PhD research shows a greater utility of biomarkers and their individual stable isotopes to establish different episodes of hothouse and greenhouse conditions within the Early Triassic of the northern hemisphere (Boreal Sea).

The general trend of biomarkers and sedimentological data indicative of hypoxic, anoxic and/or euxinic conditions in the Boreal Sea after the PTB show episodic intensification of deep-water anoxia and PZE conditions during the lower part of Early Triassic. However, a marked decline of the Chorobi-derived biomarkers towards the end of this period and into the Middle Triassic is observed, suggesting oxygenation of the bottom waters. This finding contrasts the worldwide anoxia during the main phase of the mass extinction event that occurred earlier (Grice et al., 2005a; Kump et al., 2005; Nabbefeld et al., 2010c; Summons and Powell, 1986; Wignall and Twitchett, 1996) and suggests better water circulation and homogenization is likely have recovered by the end of the Early Triassic in the northern hemisphere.

The immediate aftermath of the PTB in this location, spanning Griesbachian sediments in age, was part of one of the transgressive-regressive systems of this

period. The biomarkers represent a mixture of aquatic biomass and plant wax remains, suggesting delta progradation, sea level fall and or stormy conditions enhancing runoff of terrestrial biomass that is transported up to the shallow shelf deposits. Towards the end of this period, the marine-algal biomass was dominant, supporting the end of the transgressive cycle.

At around the Griesbachian-Dienerian boundary, a large synchronous isotopic enrichment commences for the $\delta^{13}C$ and δD of OM. Molecular evidence of intensified anoxia along with blooms of heterotrophic bacteria and/or non-photoautotrophic organisms (e.g. sulfate reducers) is proposed to control the deposition of OM in the Dienerian period. The OM type might be controlled by oceanic upwelling of warm, saline bottom waters containing low oxygen and nutrients for phototrophic organisms to thrive, leading to opportunistic blooms (e.g. sulfate reducers, prasinophytes and halophilic archaea). This assemblage of geochemical features during the Dienerian is comparable to the biogeochemical model described by Kidder and Worsley (2004; 2010) to occur during the major extinction events; by which HEATT was triggered by volcanic activity; for the first time reported to occur after the extinction horizon. Perhaps, the recurrence of HEATT events in this period might delay the recovery of the ecosystem but also could be responsible for a secondary extinction (after PTB) in some organisms.

After the marked perturbation during the Induan Stage, deepening of the basin in this area of the Boreal Sea is probably reflected in the steady negative carbon isotopic shift of over 10 ‰ in the $\delta^{13}C$ of bulk OM within 2 Ma, likely related to the re-flourishment of the algae and other photosynthetic communities. However, after the hothouse conditions during the Dienerian, weathering of coal and/or release of methane from collapse of gas clathrates cannot be ruled out. There is also the possibility that this $\delta^{13}C$ negative excurtion could partly reflect widespread combustion of OM, consistent with the hothouse condition postulated during the Dienerian. Certainly, the environmental conditions towards the end of the Early Triassic seem to be less harmful and more appealing for the marine ecosystem to recover and blossom.

An important outcome of this investigation requires further work to validate the relationship between the organism responsible for the C_{33} *n*-ACH and halophilic archael markers. Previously, C_{33} *n*-ACH was ascribed to the onset of the marine extinction horizons (Grice et al., 2005b); here an excellent correlation exists with the abundance of the regular isoprenoid *i*-C_{21}, a halophilic archea-marker; suggesting optimum conditions for the radiation and/or preservation of both, the C_{33} *n*-ACH parent organism and those for haloarchea. The concentration of these biomarkers is enhanced through the section and correlate with initial stages of the marine transgression and the abundances of certain acritachs. Perhaps, hypersaline environment and reducing conditions favour the growth of the C_{33} *n*-ACH parent organism.

Limitations and Outlook

Limitations during the analysis of geological samples are constantly present and uncertainties always have to be considered. Particularly, when paleoenvironmental interpretations are made based on biomarker distributions, using traditional techniques such as GC-MS and GC-irMS, co-elution, identification and quantification are always challenging. Nevertheless, the applicability and advantage of molecular geochemistry in assessing past environment is not questionable. Overall, the outcomes of the present research project can be used as a frame work for future multidisciplinary investigations in order to help establish the link between different parts of the biogeochemical cycles within the same regions.

Particularly, the methodological approach to investigate past environment is a critical aspect that determines the outcomes of such investigation. For instance, the *old-fashion* methodological approach described and used in **Chapter 2** and **Chapter 3**, in which a single sample is investigated thoroughly, is probably no longer a common approach used in modern organic geochemistry. This traditional scientific method along with a remarkable improvement in the sensitivity and resolution of the analytical techniques was used for the first time in a carbonate concretion from the Devonian Gogo Formation, allowing for the identification of compounds and compound classes that were thought to be no longer existent in the sample according to the samples' thermal history and age. In contrast, due to the optimization in sample processing times and sophisticated statistical tools, analysis of multiple samples using several techniques is the current trend. However; the resulting large volume of data requires a comprehensive integration and depuration of valid and questionable results. During this research, both approaches were considered and applied in different geological context, demonstrating that both are equally relevant and even complementary when reconstructing past environments.

The investigation of multiple carbonate concretions, with and without fossil in their interior, from different ages and environmental context, is crucial to understand the scale and potential of these microenvironments as exceptional archives of molecular history. Similarly, the use of techniques with more sensitive detection limits and

better chromatographical resolution, such as GC-GC-TOFMS or GC-GC-FID, is vital while investigating fossil remains. Moreover, integration of *state of the art* high resolution imaging techniques, traditionally used for the identification and characterization of well preserved fossils in paleontology, along with geochemical molecular characterization could be the future to link geomolecules with fossil identity.

On the other hand, the characterization of an extended Early Triassic sedimentary section does not fully answer the entire questions about the ecosystem recovery after the PTB. Perhaps investigating the molecular remains preserved in fossils of that period (some preserved in nodules and concretions) could help better establish the environmental conditions at that time. Also, the application of a statistical approach that integrates biomarkers and isotope results with the paleontological data that records the biodiversity changes after the PTB is important to consider for future work. One opportunity to explore the recovery of the mass extinction in the Boreal Sea is in the application of chemostratigraphy in parallel to the biomarker and isotope characterization. The link between inorganic and organic approaches in such environments could be useful to explain the water chemistry that initiates the blooms of some organisms and the annihilation of others.

BIBLIOGRAPHY

"Every reasonable effort has been made to acknowledge the owners of copyright material. I would be pleased to hear from any copyright owner who has been omitted or incorrectly acknowledged"

Adam, P. A., Schneckenburger, P. S., Schaeffer, P. S., and Albrecht, P. A., 2000, Clues to early diagenetic sulfurization processes from mild chemical cleavage of labile sulfur-rich geomacromolecules. Geochimica et Cosmochimica Acta 64, 3485-3503.

Algeo, T. J., Scheckler, S., 2010. Land plant evolution and weathering rate changes in the Devonian. Journal of Earth Science 21, 75-78.

Algeo, T. J., Chen, Z.Q., Fraiser, M.L., Twitchett, R.J., 2011. Terrestrial–marine teleconnections in the collapse and rebuilding of Early Triassic marine ecosystems. Palaeogeography, Palaeoclimatology, Palaeoecology 308, 1-11.

Algeo, T. J., Scheckler, S.E., 1998. Terrestrial-marine teleconnections in the Devonian: links between the evolution of land plants, weathering processes, and marine anoxic events. Philosophical Transactions of the Royal Society of London. Series B. Biological Sciences 353, 113-130.

Algeo, T. J., Twitchett, R.J., 2010. Anomalous Early Triassic sediment fluxes due to elevated weathering rates and their biological consequences. Geology 38, 1023-1026.

Andersen, N., Paul, H.A., Bernasconi, S.M., McKenzie, J.A., Behrens, A., Schaeffer, P., Albrecht, P., 2001. Large and rapid climate variability during the Messinian salinity crisis: Evidence from deuterium concentrations of individual biomarkers. Geology 29, 799-802.

Anderson, L.G., Dyrssen, D., Hall, P.O.J., 1988. On the sulphur chemistry of a super-anoxic fjord, Framvaren, South Norway. Marine Chemistry 23, 283-293.

Bambach, R.K., 2006. Phanerozic Biodiversity Mass Extinctions. Annual Review of Earth and Planetary Sciences 34, 127-155.

Barber, C.J., Bastow, T.P., Grice, K., Alexander, R., Kagi, R.I., 2001. Analysis of crocetane in crude oils and sediments: novel stationary phases for use in GC–MS. Organic Geochemistry 32, 765-769.

Barnosky, A.D., Matzke, N., Tomiya, S., Wogan, G.O.U., Swartz, B., Quental, T.B., Marshall, C., McGuire, J.L., Lindsey, E.L., Maguire, K.C., Mersey, B., Ferrer, E.A., 2011. Has the Earth/'s sixth mass extinction already arrived? Nature 471, 51-57.

Benton, M., 1995. Diversification and extinction in the history of life. Science 268, 52-58.

Benton, M.J., Twitchett, R.J., 2003. How to kill (almost) all life: the end-Permian extinction event. Trends in Ecology & Evolution 18, 358-365.

Berner, R.A., 2002. Examination of hypotheses for the Permo–Triassic boundary extinction by carbon cycle modeling. Proceedings of the National Academy of Sciences 99, 4172-4177.

Berner, R.A., 2006. GEOCARBSULF: A combined model for Phanerozoic atmospheric O2 and CO2. Geochimica et Cosmochimica Acta 70, 5653-5664.

Bigeleisen, J., Wolfsberg, M., 1958. Theoretical and experimental aspects of isotope effects in chemical kinetics. Advances in Chemical Physics 1, 15-76.

Bond, D.P.G., Wignall, P.B., 2008. The role of sea-level change and marine anoxia in the Frasnian–Famennian (Late Devonian) mass extinction. Palaeogeography, Palaeoclimatology, Palaeoecology 263, 107-118.

Brassell, S. C., Eglinton, G., and Howell, V. J., 1987, Palaeoenvironmental assessment of marine organic-rich sediments using molecular organic geochemistry. Geological Society, London, Special Publications, v. 26, no. 1, p. 79-98.

Brassell, S. C., McEvoy, J., Hoffmann, C. F., Lamb, N. A., Peakman, T. M., and Maxwell, J. R., 1984, Isomerisation, rearrangement and aromatisation of

steroids in distinguishing early stages of diagenesis. Organic Geochemistry, v. 6, no. 0, p. 11-23.

Briggs, D. E. G., Rolfe, W. D. I., Butler, P. D., Liston, J. J., and Ingham, J. K., 2011. Phyllocarid crustaceans from the Upper Devonian Gogo Formation, Western Australia. Journal of Systematic Palaeontology 9, 399-424.

Briggs, D.E.G., 2003. The role of decay and mineralization in the preservation of soft bodied fossils. Annual Review of Earth and Planetary Sciences 31, 275–301.

Brocks, J.J., Pearson, A., 2005. Building the Biomarker Tree of Life. Reviews in Mineralogy and Geochemistry 59, 233-258.

Brown, T., Kenig, F., 2004. Water column structure during deposition of Middle Devonian–Lower Mississippian black and green/gray shales of the Illinois and Michigan Basins: A biomarker approach. Palaeogeography, Palaeoclimatology, Palaeoecology 215, 59–85.

Buggisch, W., Joachimski, M.M., 2006. Carbon isotope stratigraphy of the Devonian of Central and Southern Europe. Palaeogeography, Palaeoclimatology, Palaeoecology 240, 68-88.

Burgoyne, T.W., Hayes, J.M., 1998. Quantitative production of H_2 by pyrolysis of gas chromatographic effluents. Analytical Chemistry 70, 5136-5141.

Chen, Z.-Q., Benton, M.J., 2012. The timing and pattern of biotic recovery following the end-Permian mass extinction. Nature Geoscience 5, 375-383.

Clarkson, M.O., Richoz, S., Wood, R.a., Maurer, F., Krystyn, L., McGurty, D.J., Astratti, D., 2013. A new high-resolution $\delta^{13}C$ record for the Early Triassic: Insights from the Arabian Platform. Gondwana Research 24, 233-242.

Coleman, M., 1993. Microbial processes: Controls on the shape and composition of carbonate concretions. Marine Geology 113, 127–140.

Collister, J.W., Lichtfouse, E., Hieshima, G., Hayes, J.M., 1994. Partial resolution of sources of n-alkanes in the saline portion of the Parachute Creek Member, Green River Formation (Piceance Creek Basin, Colorado). Organic Geochemistry 21, 645-659.

Comet, P., McEvoy, J., Brassell, S., Eglinton, G., Maxwell, J., and Thomson, I., 1981. Lipids of an Upper Albian limestone, Deep Sea Drilling Project Site 465. Initial Report DSDP 62, 923-937.

Copp, I., 2000. Subsurface Facies Analysis of Devonian Reef Complexes Lennard Shelf, Canning Basin. Western Australia: Western Australia Geological Survey.

Corsetti, F.A., Baud, A., Marenco, P.J., Richoz, S., 2005. Summary of Early Triassic carbon isotope records. Comptes Rendus Palevol 4, 473-486.

Curiale, J. A., 2002. A review of the occurrences and causes of migration-contamination in crude oil. Organic Geochemistry 33, 1389-1400.

Dawson, D., Grice, K., Wang, S.X., Alexander, R., Radke, J., 2004, Stable hydrogen isotopic composition of hydrocarbons in torbanites (Late Carboniferous to Late Permian) deposited under various climatic conditions. Organic Geochemistry 35, 189-197.

De Craen, M., Swennen, R., Keppens, E.M., Macaulay, C.I., and Kiriakoulakis, K., 1999. Bacterially mediated formation of carbonate concretions in the Oligocene Boom Clay of northern Belgium. Journal of Sedimentary Research 69, 1098–1106.

De Grande, S., Aquino Neto, F.R., Mello, M.R., Grande, S.M.B.D.E., Neto, F.R.A., 1993. Extended tricyclic terpanes in sediments and petroleums. 20, 1039-1047.

De Leeuw, J. W. D., Bergen, P. F. V., Aarssen, B. G. K. V., Gatellier, J.-P. L. A., Damsté, J. S. S., Collinson, M. E., Ambler, R. P., Macko, S., Curry, G. B., Eglinton, G., and Maxwell, J. R., 1991, Resistant Biomacromolecules as Major Contributors to Kerogen [and Discussion]: Philosophical Transactions: Biological Sciences, v. 333, no. 1268, p. 329-337.

Dembick Jr, H., Meinschein, W.G., 1976. Possible ecological and environmental significance of the predominance of even-carbon number C2O-C3O n-alkanes. Geochimica et Cosmochimica Acta 40, 203-208.

Duan, W.M., Hedrick, D.B., Pye, K., Coleman, M.L., and White, D.C., 1996. A preliminary study of the geochemical and microbiological characteristics of

modern sedimentary concretions. Limnology and Oceanography 41, 1404–1414.

Dumitrescu, M., and Brassell, S. C., 2005. Biogeochemical assessment of sources of organic matter and paleoproductivity during the early Aptian Oceanic Anoxic Event at Shatsky Rise, ODP Leg 198. Organic Geochemistry 36, 1002-1022.

Dustira, A.M., Wignall, P.B., Joachimski, M., Blomeier, D., Hartkopf-Fröder, C., Bond, D.P.G., 2013. Gradual onset of anoxia across the Permian–Triassic Boundary in Svalbard, Norway. Palaeogeography, Palaeoclimatology, Palaeoecology 374, 303-313.

Dutta, S., Greenwood, P.F., Brocke, R., Schaefer, R.G., Mann, U., 2006. New insights into the relationship between Tasmanites and tricyclic terpenoids. Organic Geochemistry 37, 117-127.

Erwin, D.H., Bowring, S.A., Yugan, J., 2002. End-Permian mass extinctions : A review. Geological Society of America Special Paper 356, 363-383.

Fenton, S., Grice, K., Twitchett, R.J., Böttcher, M.E., Looy, C.V., Nabbefeld, B., 2007. Changes in biomarker abundances and sulfur isotopes of pyrite across the Permian–Triassic (P/Tr) Schuchert Dal section (East Greenland). Earth and Planetary Science Letters 262, 230-239.

Field, C.B., Behrenfeld, M.J., Randerson, J.T., Falkowski, P., 1998. Primary Production of the Biosphere: Integrating Terrestrial and Oceanic Components. Science 281, 237-240.

Finnegan, S., Fike, D.A., Jones, D., Woodward, F.W., 2012. A Temperature-Dependent Positive Feedback on the Magnitude of Carbon Isotope Excursions. Geoscience Canada 39, 122-131.

Freeman, K.H., 2001. Isotopic Biogeochemistry of Marine Organic Carbon. Reviews in Mineralogy and Geochemistry 43, 579-605.

Foster, W.J., Twitchett, R.J., 2014. Functional diversity of marine ecosystems after the Late Permian mass extinction event. Nature Geoscience 7, 233-238.

Gaines, S. M., Eglinton, G., and Rullkötter, J., 2009, Echoes of life : what fossil molecules reveal about earth, New York, Oxford University Press, Inc.

Gagosian, R. B., Smith, S. O., and Nigrelli, G. E., 1982. Vertical transport of steroid alcohols and ketones measured in a sediment trap experiment in the equatorial Atlantic Ocean. Geochimica et Cosmochimica Acta 46, 1163-1172.

Galfetti, T., Hochuli, P.a., Brayard, A., Bucher, H., Weissert, H., Vigran, J.O., 2007. Smithian-Spathian boundary event: Evidence for global climatic change in the wake of the end-Permian biotic crisis. Geology 35, 291.

Grantham, P. J., and Wakefield, L. L., 1988. Variations in the sterane carbon number distributions of marine source rock derived crude oils through geological time. Organic Geochemistry 12, 61-73.

Grard, A., Francois, L., Dessert, C., Dupré, B., and Godderis, Y., 2005, Basaltic volcanism and mass extinction at the Permo-Triassic boundary: environmental impact and modeling of the global carbon cycle: Earth and Planetary Science Letters, v. 234, p. 207-221.

Grasby, S.E., Beauchamp, B., Embry, a., Sanei, H., 2012. Recurrent Early Triassic ocean anoxia. Geology 41, 175-178.

Greenwood, P.F., Summons, R.E., 2003. GC–MS detection and significance of crocetane and pentamethylicosane in sediments and crude oils. Organic Geochemistry 34, 1211-1222.

Grice, K., Brocks, J.J., 2011. Biomarkers (organic, compound specific isotopes), in: Reitner, J., Thiel, V. (Eds.), Encyclopedia of Geobiology.

Grice, K., Cao, C., Love, G.D., Böttcher, M.E., Twitchett, R.J., Grosjean, E., Summons, R.E., Turgeon, S.C., Dunning, W., Jin, Y., 2005a. Photic zone euxinia during the Permian-triassic superanoxic event. Science 307, 706-709.

Grice, K., Klein Breteler, W.C.M., Schouten, S., Grossi, V., De Leeuw, J.W., and Sinninghe Damsté, J.S., 1998. Effects of zooplankton herbivory on biomarker proxy records. Paleoceanography 13, 686–693.

Grice, K., Gibbison, R., Atkinson, J.E., Schwark, L., Eckardt, C.B., Maxwell, J.R., 1996a. Maleimides (1H-pyrrole-2,5-diones) as molecular indicators of anoxygenic photosynthesis in ancient water columns. Geochimica et Cosmochimica Acta 60, 3913-3924.

Grice, K., Schaeffer, P., Schwark, L., Maxwell, J.R., 1996b. Molecular indicators of palaeoenvironmental conditions in an immature Permian shale (Kupferschiefer, Lower Rhine Basin, north-west Germany) from free and S-bound lipids. Organic Geochemistry 25, 131-147.

Grice, K., Schaeffer, P., Schwark, L., and Maxwell, J., 1997. Changes in palaeoenvironmental conditions during deposition of the Permian Kupferschiefer (Lower Rhine Basin, north west Germany) inferred from molecular and isotopic composition of biomarker components. Organic Geochemistry 26, 677–690.

Grice, K., Schouten, S., Nissenbaum, A., Charrach, J., Sinninghe Damsté, J.S., 1998. Isotopically heavy carbon in the C21 to C25 regular isoprenoids in halite-rich deposits from the Sdom Formation, Dead Sea Basin, Israel. Organic Geochemistry 28, 349-359.

Grice, K., Twitchett, R.J., Alexander, R., Foster, C.B., Looy, C., 2005b. A potential biomarker for the Permian–Triassic ecological crisis. Earth and Planetary Science Letters 236, 315-321.

Gupta N., Cody, G., Tetlie, E., Briggs, D., Summons, R., 2009. Rapid incorporation of lipids into macromolecules during experimental decay of invertebrates. Initiation of geopolymer formation. Organic Geochemistry 40, 589-594.

Hartgers, W.A., Sinninghe Damsté, J.S., Requejo, A.G., Allan, J., Hayes, J.M., Ling, Y., Xie, T.M., Primack, J., De Leeuw, J.W., 1994. A molecular and carbon isotopic study towards the origin and diagenetic fate of diaromatic carotenoids. Organic Geochemistry 22, 703–725.

Hayes, J. M., 1993. Factors controlling ^{13}C contents of sedimentary organic compounds: Principles and evidence. Marine Geology 113, 111-125.

Hayes, J. M., 2001. Fractionation of Carbon and Hydrogen Isotopes in Biosynthetic Processes. Reviews in Mineralogy and Geochemistry 43, 225-277.

Hayes, J. M., Strauss, H., Kaufman, A.J., 1999. The abundance of ^{13}C in marine organic matter and isotopic fractionation in the global biogeochemical cycle of carbon during the past 800 Ma. Chemical Geology 161, 103-125.

Hays, L. E., Beatty, T., Henderson, C.M., Love, G.D., Summons, R.E., 2007. Evidence for photic zone euxinia through the end-Permian mass extinction in the Panthalassic Ocean (Peace River Basin, Western Canada). Palaeoworld 16, 39-50.

Hays, L. E., Grice, K., Foster, C.B., Summons, R.E., 2012. Biomarker and isotopic trends in a Permian–Triassic sedimentary section at Kap Stosch, Greenland. Organic Geochemistry 43, 67-82.

Hebting, Y., Schaeffer, P., Behrens, A., Adam, P., Schmitt, G., Schneckenburger, P., Bernasconi, S. M., Albrecht, P., 2006. Biomarker Evidence for a Major Preservation Pathway of Sedimentary Organic Carbon. Science 312, 1627-1631.

Hedges, J. I., Keil, R. G., 1995, Sedimentary organic matter preservation: an assessment and speculative synthesis.: Marine Chemistry, v. 49, p. 81-115.

Hedges, J. I., Keil, R. G., Benner, R., 1997, What happens to terrestrial organic matter in the ocean?: Organic Geochemistry, v. 27, p. 195-212.

Heimhofer, U., Hesselbo, S.P., Pancost, R.D., Martill, D.M., Hochuli, P.A., Guzzo, J.V.P., 2008. Evidence for photic-zone euxinia in the Early Albian Santana Formation (Araripe Basin, NE Brazil). Terra Nova 20, 347–354.

Heimhofer, U., Schwark, L., Ariztegui, D., Martill, D.M., Immenhauser, A., 2010. Geochemistry of fossiliferous carbonate concretions from the Cretaceous Santana Formation–assessing the role of microbial processes. EGU General Assembly: Geophysical Research Abstracts 12, p. EGU9390.

Hermann, E., Hochuli, P.a., Méhay, S., Bucher, H., Brühwiler, T., Ware, D., Hautmann, M., Roohi, G., ur-Rehman, K., Yaseen, A., 2011. Organic matter and palaeoenvironmental signals during the Early Triassic biotic recovery: The Salt Range and Surghar Range records. Sedimentary Geology 234, 19-41.

Hilkert, A., Douthitt, C., Schlüter, H., Brand, W., 1999. Isotope ratio monitoring gas chromatography/mass spectrometry of D/H by high temperature conversion isotope ratio mass spectrometry. Rapid Communications in Mass Spectrometry 13, 1226-1230.

Hoefs, J., 2009. Stable isotope geochemistry. 6th edition. Springer Berlin Heidelberg

Holman, A.I., Grice, K., Jaraula, C.M.B., Schimmelmann, A., Brocks, J.J., 2012. Efficiency of extraction of polycyclic aromatic hydrocarbons from the Paleoproterozoic Here's Your Chance Pb/Zn/Ag ore deposit and implications for a study of Bitumen II. Organic Geochemistry 52, 81-87.

Horacek, M., Brandner, R., Abart, R., 2007a. Carbon isotope record of the P/T boundary and the Lower Triassic in the Southern Alps: Evidence for rapid changes in storage of organic carbon. Palaeogeography, Palaeoclimatology, Palaeoecology 252, 347-354.

Horacek, M., Richoz, S., Brandner, R., Krystyn, L., Spötl, C., 2007b. Evidence for recurrent changes in Lower Triassic oceanic circulation of the Tethys: The $\delta^{13}C$ record from marine sections in Iran. Palaeogeography, Palaeoclimatology, Palaeoecology 252, 355-369.

Hounslow, M.W., Peters, C., Mørk, A., Weitschat, W., Vigran, J.O., 2008. Biomagnetostratigraphy of the Vikinghøgda Formation , Svalbard (Arctic Norway), and the geomagnetic polarity timescale for the Lower Triassic. 1305-1325.

Hussler, G., Albrecht, P., 1983. C_{27}-C_{29} Monoaromatic anthrasteroid hydrocarbons in Cretaceous black shales. Nature 304, 262-263.

Hussler, G., Chappe, B., Wehrung, P., Albrecht, P., 1981. C_{27}-C_{29} ring A monoaromatic steroids in Cretaceous black shales. Nature 294, 556-558.

Joachimski, M.M., Lai, X., Shen, S., Jiang, H., Luo, G., Chen, B., Chen, J., Sun, Y., 2012. Climate warming in the latest Permian and the Permian-Triassic mass extinction. Geology 40, 195-198.

Kajiwara, Y., Yamakita, S., Ishida, K., Ishiga, H., and Imai, A., 1994, Development of a largely anoxic stratified ocean and its temporary massive mixing at the Permian/Triassic boundary supported by the sulfur isotopic record:

Palaeogeography, Palaeoclimatology, Palaeoecology, v. 111, no. 3–4, p. 367-379.

Kaiho, K., Chen, Z.-Q., Kawahata, H., Kajiwara, Y., and Sato, H., 2006a, Close-up of the end-Permian mass extinction horizon recorded in the Meishan section, South China: Sedimentary, elemental, and biotic characterization and a negative shift of sulfate sulfur isotope ratio: Palaeogeography, Palaeoclimatology, Palaeoecology, v. 239, no. 3–4, p. 396-405.

Kaiho, K., Kajiwara, Y., Chen, Z.-Q., and Gorjan, P., 2006b, A sulfur isotope event at the end of the Permian: Chemical Geology, v. 235, no. 1–2, p. 33-47.

Kaiho, K., Oba, M., Fukuda, Y., Ito, K., Ariyoshi, S., Gorjan, P., Riu, Y., Takahashi, S., Chen, Z.-Q., Tong, J., Yamakita, S., 2012. Changes in depth-transect redox conditions spanning the end-Permian mass extinction and their impact on the marine extinction: Evidence from biomarkers and sulfur isotopes. Global and Planetary Change 94-95, 20-32.

Kamo, S.L., Crowley, J., Bowring, S.A., 2006. The Permian-Triassic boundary event and eruption of the Siberian flood basalts: An inter-laboratory U–Pb dating study. Geochimica et Cosmochimica Acta 70, A303.

Kanazawa, A., 2001. Sterols in marine invertebrates. Fisheries Science 67, 997–1007.

Kidder, D.L., Worsley, T.R., 2004. Causes and consequences of extreme Permo-Triassic warming to globally equable climate and relation to the Permo-Triassic extinction and recovery. Palaeogeography, Palaeoclimatology, Palaeoecology 203, 207-237.

Kidder, D.L., Worsley, T.R., 2010. Phanerozoic large igneous provinces (LIPs), HEATT (haline euxinic acidic thermal transgression) episodes, and mass extinctions. Palaeogeography, Palaeoclimatology, Palaeoecology 295, 162-191.

Killops, S.D., Killops, V.J., 2005. Introduction to organic geochemistry. John Wiley & Sons.

Knoll, A. H., Bambach, R. K., Canfield, D. E., and Grotzinger, J. P., 1996, Comparative Earth History and Late Permian Mass Extinction: Science, v. 273, no. 5274, p. 452-457.

Knoll, A.H., Bambach, R.K., Payne, J.L., Pruss, S., Fischer, W.W., 2007. Paleophysiology and end-Permian mass extinction. Earth and Planetary Science Letters 256, 295-313.

Kohnen, M. E. L., Sinninghe Damsté, J. S., Baas, M., Dalen, A. C. K., De Leeuw, J. W., 1993. Sulphur-bound steroid and phytane carbon skeletons in geomacromolecules: Implications for the mechanism of incorporation of sulphur into organic matter. Geochimica et Cosmochimica Acta 57, 2515-2528.

Koopmans, M.P., Köster, J., Van Kaam-Peters, H.M.E., Kenig, F., Schouten, S., Hartgers, W.A., De Leeuw, J.W., Sinninghe Damsté, J.S., 1996. Diagenetic and catagenetic products of isorenieratene: Molecular indicators for photic zone anoxia. Geochimica et Cosmochimica Acta 60, 4467-4496.

Korte, C., Kozur, H., Joachimski, M., Strauss, H., Veizer, J.n., Schwark, L., 2004. Carbon, sulfur, oxygen and strontium isotope records, organic geochemistry and biostratigraphy across the Permian/Triassic boundary in Abadeh, Iran. International Journal of Earth Sciences, 565-581.

Korte, C., Kozur, H.W., 2010. Carbon-isotope stratigraphy across the Permian–Triassic boundary: A review. Journal of Asian Earth Sciences 39, 215-235.

Korte, C., Kozur, H.W., Veizer, J., 2005. $\delta^{13}C$ and $\delta^{18}O$ values of Triassic brachiopods and carbonate rocks as proxies for coeval seawater and palaeotemperature. Palaeogeography, Palaeoclimatology, Palaeoecology 226, 287-306.

Krull, E.S., Retallack, G.J., 2000. $\delta^{13}C$ depth profiles from paleosols across the Permian-Triassic boundary: Evidence for methane release. Geological Society of America Bulletin 112, 1459-1472.

Kump, L.R., Arthur, M.A., 1999. Interpreting carbon-isotope excursions: carbonates and organic matter. Chemical Geology 161, 181-198.

Kump, L.R., Pavlov, A., Arthur, M. A., 2005. Massive release of hydrogen sulfide to the surface ocean and atmosphere during intervals of oceanic anoxia. Geology 33, 397-397.

Ladygina, N., Dedyukhina, E.G., and Vainshtein, M.B., 2006. A review on microbial synthesis of hydrocarbons. Process Biochemistry 41, 1001–1014.

Lafargue, E., Marquis, F., Pillot, D., 1998. Rock-Eval 6 Applications in Hydrocarbon Exploration, Production, and Soil Contamination Studies. Revue de l'institut francais du petrole 53, 421-437.

Le Milbeau, C., Schaeffer, P., Connan, J., Albrecht, P., Adam, P., 2010. Aromatized C-2 Oxygenated Triterpenoids as Indicators for a New Transformation Pathway in the Environment. Organic Letters 12, 1504-1507.

Lehrmann, D.J., Ramezani, J., Bowring, S.a., Martin, M.W., Montgomery, P., Enos, P., Payne, J.L., Orchard, M.J., Hongmei, W., Jiayong, W., 2006. Timing of recovery from the end-Permian extinction: Geochronologic and biostratigraphic constraints from south China. Geology 34, 1053.

Leythaeuser, D., Keuser, C., Schwark, L., 2007. Molecular memory effects recording the accumulation history of petroleum reservoirs: A case study of the Heidrun Field, offshore Norway. Marine and Petroleum Geology 24, 199-220.

Logan, G.a., Calver, C.R., Gorjan, P., Summons, R.E., Hayes, J.M., Walter, M.R., 1999. Terminal Proterozoic mid-shelf benthic microbial mats in the Centralian Superbasin and their environmental significance. Geochimica et Cosmochimica Acta 63, 1345-1358.

Londry, K.L., Des Marais, D.J., 2003. Stable carbon isotope fractionation by sulfate-reducing bacteria. Applied and Environmental Microbiology 69, 2942–2949.

Londry, K.L., Jahnke, L.L., Des Marais, D.J., 2004. Stable carbon isotope ratios of lipid biomarkers of sulfate-reducing bacteria. Applied and Environmental Microbiology 70, 745–751.

Long, J., Trinajstic, K., 2010. The Late Devonian Gogo Formation Lagerstatte of Western Australia: Exceptional Early Vertebrate Preservation and Diversity: Annual Review of Earth and Planetary Sciences 38, 255–279.

Looy, C.V., Twitchett, R.J., Dilcher, D.L., Van Konijnenburg-Van Cittert, J.H.A., Visscher, H., 2001. Life in the end-Permian dead zone. Proceedings of the National Academy of Sciences 98, 7879-7883.

Mackenzie, A. S., Brassell, S. C., Eglinton, G., Maxwell , J. R., 1982a. Chemical fossils: the geological fate of steroids. Science 217, 491-504.

Mackenzie, A. S., Lamb, N. A., Maxwell, J. R., 1982b. Steroid hydrocarbons and the thermal history of sediments. Nature 295, 223-226.

Maruoka, T., Koeberl, C., Hancox, P. J., and Reimold, W. U., 2003, Sulfur geochemistry across a terrestrial Permian–Triassic boundary section in the Karoo Basin, South Africa: Earth and Planetary Science Letters, v. 206, no. 1–2, p. 101-117.

Marynowski, L., Rakociński, M., Borcuch, E., Kremer, B., Schubert, B. A., Jahren, A. H., 2011. Molecular and petrographic indicators of redox conditions and bacterial communities after the F/F mass extinction (Kowala, Holy Cross Mountains, Poland). Palaeogeography, Palaeoclimatology, Palaeoecology 306, 1-14.

Maslen, E., Grice, K., Gale, J., Hallmann, C., Horsfield, B., 2009. Crocetane, a potential marker of photic zone euxinia in thermally mature sediments and crude oils of Devonian age. Organic Geochemistry 40, 1–11.

Matthews, D., Hayes, J., 1978. Isotope-ratio-monitoring gas chromatography-mass spectrometry. Analytical Chemistry 50, 1465-1473.

McGhee, G.R., 1996. The Late Devonian Mass Extinctions: The Frasnian/Famennian Crisis. Columbia University Press.

Megonigal, J. P., Hines, M. E., and Visscher, P. T., 2004, Anaerobic metabolism: linkages to trace gases and aerobic processes, *in* WH, S., ed., Treatise on Geochemistry Volume 8, Biogeochemistry: Oxford, Elsevier-Pergamon, p. 317-424.

Melendez, I., Grice, K., Schwark, L., 2013a. Exceptional preservation of Palaeozoic steroids in a diagenetic continuum. Scientific Reports 3.

Melendez, I., Grice, K., Trinajstic, K., Ladjavardi, M., Greenwood, P., Thompson, K., 2013b. Biomarkers reveal the role of photic zone euxinia in exceptional fossil preservation: An organic geochemical perspective. Geology 41, 123-126.

Metcalfe, B., Twitchett, R.J., Price-Lloyd, N., 2011. Changes in size and growth rate of 'Lilliput' animals in the earliest Triassic. Palaeogeography, Palaeoclimatology, Palaeoecology 308, 171-180.

Metcalfe, I., Nicoll, R.S., Willink, R., Ladjavadi, M., Grice, K., 2013. Early Triassic (Induan–Olenekian) conodont biostratigraphy, global anoxia, carbon isotope excursions and environmental perturbations: New data from Western Australian Gondwana. Gondwana Research 23, 1136-1150.

Meyer, K.M., Kump, L.R., Ridgwell, A., 2008. Biogeochemical controls on photic-zone euxinia during the end-Permian mass extinction. Geology 36, 747-750.

Meyer, K.M., Yu, M., Jost, a.B., Kelley, B.M., Payne, J.L., 2011. $\delta^{13}C$ evidence that high primary productivity delayed recovery from end-Permian mass extinction. Earth and Planetary Science Letters 302, 378-384.

Mørk, A., Elvebakk, G., 1999. The type section of the Vikinghogda Formation: a new Lower Triassic unit in central and eastern Svalbard. Polar Research 18, 51-82.

Murphy, A.E., Sageman, B.B., Hollander, D.J., 2000. Eutrophication by decoupling of the marine biogeochemical cycles of C, N, and P: A mechanism for the Late Devonian mass extinction. Geology 28, 427-430.

Murray, J.W., Stewart, K., Kassakian, S., Krynytzky, M., DiJulio, D., 2007. Oxic, suboxic, and anoxic conditions in the Black Sea, in: Yanko-Hombach, V., Gilbert, A.S., Panin, N., Dolukhanow, P.M. (Eds.), The black sea flood question, changes in coastline, climate and human settlement. Springer, Dordrecht.

Nabbefeld, B., Grice, K., Schimmelmann, A., Sauer, P.E., Böttcher, M.E., Twitchett, R.J., 2010a. Significance of $\delta D_{kerogen}$, $\delta^{13}C_{kerogen}$ and $\delta^{34}S_{pyrite}$ from several

Permian/Triassic (P/Tr) sections. Earth and Planetary Science Letters 295, 21-29.

Nabbefeld, B., Grice, K., Schimmelmann, A., Summons, R.E., Troitzsch, A., Twitchett, R.J., 2010d. A comparison of thermal maturity parameters between freely extracted hydrocarbons (Bitumen I) and a second extract (Bitumen II) from within the kerogen matrix of Permian and Triassic sedimentary rocks. Organic Geochemistry 41, 78–87.

Nabbefeld, B., Grice, K., Summons, R.E., Hays, L.E., Cao, C., 2010b. Significance of polycyclic aromatic hydrocarbons (PAHs) in Permian/Triassic boundary sections. Applied Geochemistry 25, 1374-1382.

Nabbefeld, B., Grice, K., Twitchett, R.J., Summons, R.E., Hays, L., Böttcher, M.E., Asif, M., 2010c. An integrated biomarker, isotopic and palaeoenvironmental study through the Late Permian event at Lusitaniadalen, Spitsbergen. Earth and Planetary Science Letters 291, 84-96.

Nishimura, M., Baker, E., 1986. Possible origin of n-alkanes with a remarkable even-to-odd predominance in recent marine sediments. Geochimica et Cosmochimica Acta 50, 299-305.

Pancost, R.D., Crawford, N., Magness, S., Turner, A., Jenkyns, H.C., Maxwell, J.R., 2004. Further evidence for the development of photic-zone euxinic conditions during Mesozoic oceanic anoxic events. Journal of the Geological Society 161, 353-364.

Paul D., Skrzypek G., 2007, Assessment of Carbonate-Phosphoric Acid Analytical Technique Performed using GasBench II in Continuous Flow Isotope Ratio Mass Spectrometry, International Journal of Mass Spectrometry 262: 180-186

Payne, J.L., Clapham, M.E., 2012. End-Permian Mass Extinction in the Oceans: An Ancient Analog for the Twenty-First Century? Annual Review of Earth and Planetary Sciences 40, 89-111.

Payne, J.L., Kump, L.R., 2007. Evidence for recurrent Early Triassic massive volcanism from quantitative interpretation of carbon isotope fluctuations. Earth and Planetary Science Letters 256, 264-277.

Payne, J.L., Lehrmann, D.J., Wei, J., Orchard, M.J., Schrag, D.P., Knoll, A.H., 2004. Large perturbations of the carbon cycle during recovery from the end-permian extinction. Science 305, 506-509.

Pearson, M.J, Hendry, J.P., Taylor, C.W., Russell, M.A, 2005. Fatty acids in sparry calcite fracture fills and microsparite cement of septarian diagenetic concretions. Geochimica et Cosmochimica Acta 69, 1773–1786.

Peters, K., Walters, C., and Moldowan, M., 2005, The Biomarker Guide: Cambridge, UK, Cambridge University Press, 1132 p.

Peters, K.E., Walters, C.C., Moldowan, J.M., 2005. The biomarker guide: Biomarkers and isostopes in the environment and human history, Second edition ed. Cambridge University Press, Cambridge

Playford, P.E., Hocking, R.M., Cockbain, A.E., 2009. Devonian Reef Complexes of the Canning Basin, Western Australia. Geological Survey of Western Australia Bulletin 145, 444.

Playford, P.E., Wallace, M.W., 2001. Exhalative Mineralization in Devonian Reef Complexes of the Canning Basin, Western Australia. Economic Geology 96, 1595-1610.

Popp, B.N., Laws, E.A., Bidigare, R.R., Dore, J.E., Hanson, K.L., Wakeham, S.G., 1998. Effect of phytoplankton cell geometry on carbon isotopic fractionation. Geochimica et Cosmochimica Acta 62, 69-77.

Pruss, S.B., Bottjer, D.J., 2005. The reorganization of reef communities following the end-Permian mass extinction. Comptes Rendus Palevol 4, 553-568.

Quandt, L., Gottschalk, G., Ziegler, H., Stichler, W., 1977. Isotope discrimination by photosynthetic bacteria. FEMS Microbiology Letters 1, 125-128.

Radke, M., Welte, D.H., Willsch, H., 1986. Maturity parameters based on aromatic hydrocarbons: Influence of the organic matter type. Organic Geochemistry 10, 51-63.

Radke, M., Willsch, H., Leythaeuser, D., Jillich, D.-., Germany, W., 1982. Aromatic components of coal: relation of distribution pattern to rank. 1831-1848.

Rampino, M.R., Caldeira, K., 2005. Major perturbation of ocean chemistry and a 'Strangelove Ocean' after the end-Permian mass extinction. Terra Nova 17, 554-559.

Reichow, M.K., Pringle, M.S., Al'Mukhamedov, A.I., Allen, M.B., Andreichev, V.L., Buslov, M.M., Davies, C.E., Fedoseev, G.S., Fitton, J.G., Inger, S., Medvedev, A.Y., Mitchell, C., Puchkov, V.N., Safanova, I.Y., Scott, R.A., Saunders, A.D., 2009. The timing and extent of the eruption of the Siberian Traps large igneous province: implications for the end-Permian environmental crisis. Earth and Planetary Science Letters 277, 9-20.

Raup, D.M., Sepkoski, J.J., 1982. Mass Extinctions in the Marine Fossil Record. Science 215, 1501-1503.

Reitner, J., & Thiel, V. (Eds.). (2011). *Encyclopedia of geobiology*. Springer.

Requejo, A.G., Allan, J., Creaney, S., Gray, N.R., Cole, K.S., 1992. Aryl isoprenoids and diaromatic carotenoids in Paleozoic source rocks and oils from the Western Canada and Williston Basins. Organic Geochemistry 19, 245-264.

Retallack, G.J., Sheldon, N.D., Carr, P.F., Fanning, M., Thompson, C.A., Williams, M.L., Jones, B.G., Hutton, A., 2011. Multiple Early Triassic greenhouse crises impeded recovery from Late Permian mass extinction. Palaeogeography, Palaeoclimatology, Palaeoecology 308, 233-251.

Riolo, J., Hussler, G., Albrecht, P., Connan, J., 1986. Distribution of aromatic steroids in geological samples: their evaluation as geochemical parameters: Organic Geochemistry 10, 981-990.

Rontani, J.-F., 2001. Visible light-dependent degradation of lipidic phytoplanktonic components during senescence: a review. Phytochemistry 58, 187-202.

Rowland, S. J., Maxwell, J. R., 1984. Reworked triterpenoid and steroid hydrocarbons in a recent sediment. Geochimica et Cosmochimica Acta 48, 617-624.

Sachse, D., Billault, I., Bowen, G.J., Chikaraishi, Y., Dawson, T.E., Feakins, S.J., Freeman, K.H., Magill, C.R., McInerney, F.A., van der Meer, M.T.J., Polissar, P., Robins, R.J., Sachs, J.P., Schmidt, H.-L., Sessions, A.L., White, J.W.C., West, J.B., Kahmen, A., 2012. Molecular Paleohydrology:

Interpreting the Hydrogen-Isotopic Composition of Lipid Biomarkers from Photosynthesizing Organisms. Annual Review of Earth and Planetary Sciences 40, 221-249.

Sauer, P.E., Schimmelmann, A., Sessions, A.L., Topalov, K, 2009. Simplified batch equilibration for D/H determination of non-exchangeable hydrogen in solid organic material. Rapid Communication in Mass Spectrometry 23, 949–956.

Schidlowski, M., Gorzawski, H., Dor, I., 1994. Carbon isotope variations in a solar pond microbial mat: Role of environmental gradients as steering variables. Geochimica et Cosmochimica Acta 58, 2289-2298.

Schidlowski, M., Matzigkeit, U., Krumbein, W.E., 1984. Superheavy organic carbon from hypersaline microbial mats. Naturwissenschaften 71, 303-308.

Schimmelmann, A., Deniro, M., Poulicek, M., Voss-Foucart, M., Goffinet, G., Jeuniaux, C., 1986. Stable isotopic composition of chitin from arthropods recovered in archaeological contexts as palaeoenvironmental indicators. Journal of Archaeological Science 13, 553-566.

Schimmelmann, A.L. Sessions, M. Mastalerz 2006. Hydrogen isotopic (D/H) composition of organic matter during diagenesis and thermal maturation Annu. Rev. Earth Planet. Sci. 34, 501–533.

Schouten, S., Klein Breteler, W., Blokker, P., Schogt, N., Rijpstra, W., Grice, K., Baas, M., Sinninghe Damsté, J.S., 1998. Biosynthetic effects on the stable carbon isotopic compositions of algal lipids: Implications for deciphering the carbon isotopic biomarker record: Geochimica et Cosmochimica Acta 62, 1397–1406.

Schüpfer, P., Finck, Y., Houot, F., and Gülaçar, F. O., 2007. Acid catalysed backbone rearrangement of cholesta-2,4,6-triene: On the origin of ring A and ring B aromatic steroids in recent sediments. Organic Geochemistry 38, 671-681.

Schwark, L., Empt, P., 2006. Sterane biomarkers as indicators of palaeozoic algal evolution and extinction events. Palaeogeography, Palaeoclimatology, Palaeoecology 240, 225-236.

Schwark, L., Ferretti, A., Papazzoni, C.A., Trevisani, E., 2009. Organic geochemistry and paleoenvironment of the Early Eocene "Pesciara di Bolca" Konservat-Lagerstätte, Italy. Palaeogeography, Palaeoclimatology, Palaeoecology 273, 272–285..

Schwark, L., Frimmel, A., 2004. Chemostratigraphy of the Posidonia Black Shale, SW-Germany: II. Assessment of extent and persistence of photic-zone anoxia using aryl isoprenoid distributions. Chemical Geology 206, 231-248.

Schwark, L., Vliex, M., and Schaeffer, P., 1998. Geochemical characterization of Malm Zeta laminated carbonates from the Franconian Alb, SW-Germany (II). Organic Geochemistry 29, 1921-1952.

Scott, J.H., O'Brien, D.M., Emerson, D., Sun, H., McDonald, G.D., Salgado, A., Fogel, M.L., 2006. An examination of the carbon isotope effects associated with amino acid biosynthesis. Astrobiology 6, 867-880.

Sepkoski Jr, J., 1986. Phanerozoic overview of mass extinction, Patterns and Processes in the History of Life. Springer, pp. 277-295.

Sessions, A.L., Burgoyne, T.W., Hayes, J.M., 2001. Correction of H3+ contributions in hydrogen isotope ratio monitoring mass spectrometry. Analytical Chemistry 73, 192-199.

Sessions, A.L., Burgoyne, T.W., Schimmelmann, A., Hayes, J.M., 1999. Fractionation of hydrogen isotopes in lipid biosynthesis. Organic Geochemistry 30, 1193-1200.

Sheehan, P.M., 2001. The late Ordovician mass extinction. Annual Review of Earth and Planetary Sciences 29, 331-364.

Simoneit, B.R.T., Leif, R.N., Radler De Aquino Neto, F., Almeida Azevedo, D., Pinto, A.C., Albrecht, P., 1990. On the presence of tricyclic terpane hydrocarbons in permian tasmanite algae. Naturwissenschaften 77, 380-383.

Sinninghe Damsté, J.S.S., Koopmans, M.P., 1997. The fate of carotenoids in sediments: an overview. Pure and applied chemistry 69, 2067-2074.

Sinninghe Damsté, J.S., Köster, J., 1998. A euxinic southern North Atlantic Ocean during the Cenomanian/Turonian oceanic anoxic event. Earth and Planetary Science Letters 158, 165-173.

Sinninghe Damsté, J. S., De Leeuw, J. W., 1990. Analysis, structure and geochemical significance of organically-bound sulphur in the geosphere: State of the art and future research. Organic Geochemistry, 16, 1077-1101.

Skrzypek G., 2013. Normalization procedures and reference material selection in stable HCNOS isotope analyses: an overview. Analytical and Bioanalytical Chemistry 405, 2815-2823.

Skrzypek G., Paul D., 2006, $\delta^{13}C$ Analyses of Calcium Carbonate: Comparison between the GasBench and Elemental Analyzer Techniques. Rapid Communication in Mass Spectrometry 20, 2915-2920.

Stancliffe, R.P.W., Sarjeant, W.A.S., 1994. The acritarch genus Veryhachium Deunff 1954, emend; Sarjeant and Stancliffe 1994; a taxonomic restudy and a reassessment of its constituent species. Micropaleontology 40, 223-241.

Stanley, S.M., 2010. Relation of Phanerozoic stable isotope excursions to climate, bacterial metabolism, and major extinctions. Proceedings of the National Academy of Sciences of the United States of America 107, 19185-19189.

Summons R.E., Bird, L.R., Gillespie, A.L., Pruss, S.B., and Sessions, A.L., 2010, Lipid biomarkers in ooids from different locations and ages provide evidence for a common bacterial flora (invited): Fall Meeting, American Geophysical Union, San Francisco, California, 13–17 Dec.

Summons, R.E., Powell, T.G., 1986. Chlorobiaceae in Palaeozoic seas revealed by biological markers, isotopes and geology. Nature.

Summons, R.E., Powell, T.G., 1987. Identification of aryl isoprenoids in source rocks and crude oils: biological markers for the green sulphur bacteria. Geochimica et Cosmochimica Acta 5, 557-566.

Sun, Y., Joachimski, M.M., Wignall, P.B., Yan, C., Chen, Y., Jiang, H., Wang, L., Lai, X., 2012. Lethally hot temperatures during the Early Triassic greenhouse. Science 338, 366-370.

Takahashi, S., Kaiho, K., Hori, R.S., Gorjan, P., Watanabe, T., Yamakita, S., Aita, Y., Takemura, A., Spörli, K.B., Kakegawa, T., Oba, M., 2013. Sulfur isotope profiles in the pelagic Panthalassic deep sea during the Permian–Triassic transition. Global and Planetary Change 105, 68-78.

Thomas, B.M., Willink, R.J., Grice, K., Twitchett, R.J., Purcell, R.R., Archbold, N.W., George, a.D., Tye, S., Alexander, R., Foster, C.B., Barber, C.J., 2004. Unique marine Permian-Triassic boundary section from Western Australia. Australian Journal of Earth Sciences 51, 423-430.

Tissot, B. P. and Welte, D. H. (1984) Petroleum Formation and Occurrence. Springer-Verlag, New York.

Tong, J., Hansen, H., Zhao, L., Zuo, J., 2005. High-resolution Induan-Olenekian boundary sequence in Chaohu, Anhui Province. Sci. China Ser. D-Earth Sci. 48, 291-297.

Tong, J., Zhang, S., Zuo, J., Xiong, X., 2007. Events during Early Triassic recovery from the end-Permian extinction. Global and Planetary Change 55, 66-80.

Trendel, J. M., Lohmann, F., Kintzinger, J. P., Albrecht, P., Chiarone, A., Riche, C., Cesario, M., Guilhem, J., Pascard, C., 1989. Identification of des-A-triterpenoid hydrocarbons occurring in surface sediments. Tetrahedron 45, 4457-4470.

Trinajstic, K., Marshall, C., Long, J., Bifield, K., 2007. Exceptional preservation of nerve and muscle tissues in Late Devonian placoderm fish and their evolutionary implications. Biology letters 3, 197-200.

Tulipani, S., Grice, K., Greenwood, P. F., Haines, P. W., Sauer, P. E., Schimmelmann, A., Summons, R. E., Foster, C. B., Böttcher, M. E., Playton, T., and Schwark, L., Changes of palaeoenvironmental conditions recorded in Late Devonian reef systems from the Canning Basin, Western Australia: A biomarker and stable isotope approach: Gondwana Research, (*in press*).

Twitchett, R.J., Looy, C.V., Morante, R., 2001. Rapid and synchronous collapse of marine and terrestrial ecosystems during the end-Permian biotic crisis. Geology, 351-354.

Urey, H.C., 1947. The thermodynamic properties of isotopic substances. Journal of the Chemical Society (Resumed), 562-581.

Vandenbroucke, M., and Largeau, C., 2007, Kerogen origin, evolution and structure: Organic Geochemistry, v. 38, no. 5, p. 719-833.

Volkman, J. K., 1986. A review of sterol markers for marine and terrigenous organic matter. Organic Geochemistry 9, 83-99.

Volkman, J.K., Barrett, S.M., Blackburn, S.I., Mansour, M.P., Sikes, E.L., Gelin, F., 1998. Microalgal biomarkers: A review of recent research developments. Organic Geochemistry 29, 1163-1179.

Volkman, J.K., Hutzinger, O., 2006. The handbook of environmental chemistry.

Walliser, O., 1996. Global Events in the Devonian and Carboniferous, in: Walliser, O. (Ed.), Global Events and Event Stratigraphy in the Phanerozoic. Springer Berlin Heidelberg, pp. 225-250.

Wiese, F., Reitner, J., 2011. Critical Intervals in Earth History, in: J., R., V., T. (Eds.), Encyclopedia of Geobiology. Springer Netherlands.

Wignall, P.B., 2001. Large igneous provinces and mass extinctions. Earth-Science Reviews 53, 1-33.

Wignall, P.B., Twitchett, R.J., 1996. Oceanic Anoxia and the End Permian Mass Extinction. Science 272, 1155-1158.

Wignall, P.B., Twitchett, R.J., 2002. Extent, duration, and nature of the Permian-Triassic superanoxic event. Special Papers Geological Society of America, 395-414

Wolff, G. A., Trendel, J. M., Albrecht, P., 1989. Novel Monoaromatic triterpenoid hydrocarbons occuring in sediments. Tetrahedron 45, 6721-6728.

Woods, A.D., 2005. Paleoceanographic and paleoclimatic context of Early Triassic time. Comptes Rendus Palevol 4, 463-472.

Xie, S., Pancost, R.D., Wang, Y., Yang, H., Wignall, P.B., Luo, G., Jia, C., Chen, L., 2010. Cyanobacterial blooms tied to volcanism during the 5 m.y. Permo-Triassic biotic crisis. Geology 38, 447-450.

Xinke, Y., Pu, F., Philp, R.P., 1990. LLNovel Biomarker found in South Florida Basin. Organic Geochemistry 15, 433-438.

Zhou, Y., Grice, K., Stuart-Williams, H., Farquhar, G.D., Hocart, C.H., Lu, H., Liu, W., 2010. Biosynthetic origin of the saw-toothed profile in δ^{13C} and $\delta^{2}H$ of n-alkanes and systematic isotopic differences between n-, iso- and anteiso-alkanes in leaf waxes of land plants. Phytochemistry 71, 388-403.